# *Kinetics of the Reaction between Copper(II)-Ethylenediaminetetra-acetate Complex and Cyanide*

By Nobuyuki TANAKA, Minoru KAMADA and Teisuke MURAYAMA

(Received May 8, 1958)

There have been a number of papers in which the kinetic studies of oxidation-reduction reactions involving metal complexes were dealt with. F. R. Duke and W. G. Courtney[1] studied the reduction of copper(II)-ammine complex with the cyanide ion in solutions containing ammonia in high concentrations, and found that the reaction is of first order on the concentration of the copper(II)-ammine complex and fourth order on that of the cyanide. From the results, they proposed the formation of an activated complex with four cyanides co-ordinated.

Ishibashi, Fujinaga and Sato[2] observed the reduction of copper(II) in the solution containing sodium ethylenediaminetetraacetate (EDTA) and potassium cyanide by following with time the decrease of the polarographic diffusion current due to the copper(II)-EDTA complex. They showed a current-time curve in their paper, but gave no details on the kinetics.

The present investigation was undertaken in order to know the effect of the nature of ligands on the reaction kinetics involving the complex. The kinetics of the reaction of copper(II)-EDTA complex with cyanide is presented in this paper. The second-order dependence on the concentration of copper(II)-EDTA complex clearly indicates that the reduction of the copper(II)-EDTA complex with cyanide ion takes place through reaction paths different from that for the copper(II)-ammine complex.

## Experimental

**Reagents.**—A 0.1 M cupric sulfate solution was prepared by dissolving cupric sulfate which had been purified by recrystallization of the guaranteed reagent, and was standardized by electrogravimetry at a constant potential with the aid of a Yanagimoto automatic potentiostat. Disodium ethylenediaminetetraacetate of guaranteed reagent grade was purified by recrystallization[3] and dissolved in distilled water for a 0.1 M stock solution, the concentration of which was standardized amperometrically against the standardized cupric solution[4]. A stock solution of potassium cyanide was made up by dissolving the guaranteed reagent, its concentration being determined by Liebig and Denigès' method[5] whenever it was used. Sodium carbonate and sodium bicarbonate used for carbonate-bicarbonate buffers and all other chemicals used were of analytical reagent grade.

**Apparatus and Procedure.**—The rate of the reactions between the Cu(II)-EDTA complex and the cyanide ion was followed by measuring the change of the polarographic diffusion current of the complex as a function of time. The current-time curves were obtained with a Shimadzu pen-recording polarograph Model RP-2 using a dropping mercury electrode as an indicator electrode. The cell was connected with the saturated calomel electrode (S.C.E.) through a Hume and Harris' type salt bridge[6]. When no contamination of the chloride ion was desirable, the intermediate agar plug saturated with potassium chloride was replaced by the one prepared with nearly 1 M potassium nitrate. The dropping mercury electrode used had an $m$ value of 1.69 mg./sec. and a drop time of 4.78 sec., being measured in undeaerated 0.1 M potassium nitrate solution with open circuit at 50 cm. of mercury column at 25°C.

The measurements were made in carbonate-bicarbonate buffers of pH 10 at 25.0°C, unless otherwise stated. The ionic strength was adjusted to be 0.5 with potassium nitrate. Gelatin was added as maximum suppressor by 0.002% in concentration. The pH of the solution was measured with a Hitachi Model EHP-1 pH-meter, immediately after the measurement of the current-time curves, within the accuracy of 0.02 pH unit.

The reaction was initiated by adding a known amount of air-free potassium cyanide solution into the deaerated reaction mixture with the aid of a calibrated syringe at a rate of 1 ml. per second. The solution was thoroughly stirred by

1) F. R. Duke and W. G. Courtney, *J. Phys. Chem.*, **56**, 19 (1952).
2) M. Ishibashi, T. Fujinaga and M. Sato, *J. Chem. Soc. Japan, Pure Chem. Sec.* (*Nippon Kagaku Zassi*), **77**, 696 (1956).
3) W. J. Blaedel and H. T. Knight, *Anal. Chem.*, **26**, 741 (1954).
4) N. Tanaka, M. Kodama, M. Sasaki and M. Sugino, *Japan Analyst* (*Bunseki Kagaku*), **6**, 86 (1957).
5) I. M. Kolthoff and V. A. Stenger, "Volumetric Analysis," Vol. II, Interscience Publishers, N. Y. (1947), p. 282.
6) D. N. Hume and W. E. Harris, *Ind. Eng. Chem., Anal. Ed.*, **15**, 465 (1943).

bubbling pure nitrogen gas rapidly for 10 seconds. With this technique, the reproducible current-time curves were obtained from 20 seconds after the initiation of the reaction.

## Results and Discussion

**The Current-Voltage Curves of the Cu(II)-EDTA Complex in the Absence and the Presence of Potassium Cyanide at pH 10.**—Polarographic behavior of the Cu(II)-EDTA complex has been reported by several researchers[7-10]. In Fig. 1 are shown typical examples of the current-voltage curves of 1 mM of Cu(II)-EDTA complex which were obtained in carbonate buffer of pH 10.0 containing 9 mM of EDTA in the absence and the presence of potassium cyanide.

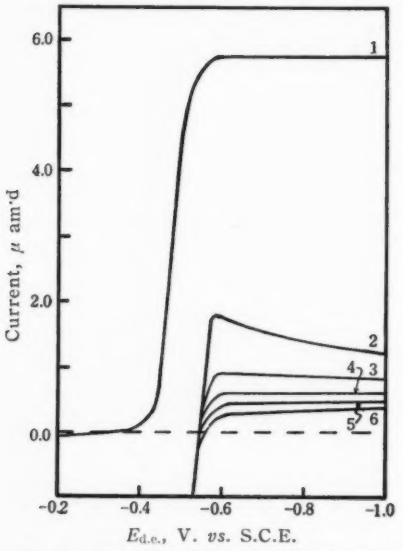


Fig. 1. Current-voltage curves of copper(II)-EDTA complex obtained in buffer of pH 10 ($\mu$=0.5) before and after the addition of potassium cyanide: curve 1, obtained with the solution containing $0.97\times10^{-3}$ M $CuY^{2-}$, $8.07\times10^{-3}$ M unchelated EDTA and 0.002% gelatin; curves 2 to 6, recorded successively after the addition of $3.80\times10^{-2}$ M KCN to the solution of curve 1.

In the absence of cyanide, the Cu(II)-EDTA complex gave a well-defined wave with the half-wave potential of −0.46 V. *vs.* S.C.E. and $i_d/C$ of 5.90 $\mu$ amp./mM (at −0.74 V. *vs.* S.C.E.) under the experimental condition. (Curve 1). Upon the addition of cyanide whose concentration was greater than the stoichiometric ratio for the Cu(II)-cyanide reaction, the diffusion current of Cu(II)-EDTA complex decreased suddenly to a half of the original magnitude and then gradually to the value of the residual current. Curves 2 to 6 show the current-voltage curves of Cu(II)-EDTA complex which were successively recorded after the addition of potassium cyanide.

The value of $i_d/C$ for Cu(II)-EDTA complex in the presence of excessive cyanide was determined to be 2.95 $\mu$ amp./mM by measuring the diffusion currents at −0.74 volt *vs.* S.C.E. with time and by extrapolating those values to zero time. It is interesting to note that the diffusion current of Cu(II)-EDTA complex obtained in the presence of cyanide was a half of that obtained in the absence of cyanide.

Absorptions of Cu(II)-EDTA complex were measured with a Hitachi EPU-2 spectrophotometer in carbonate buffer of pH 10. The absorption maximum was found at 730 m$\mu$, which was slightly different from the value given by Bennett and Schmidt[11]. They stated that the absorption spectra of the chelate at pH 8 and pH 12.5 were similar, both showing a peak at 680 m$\mu$, but they gave no information about the composition of the solution measured. Absorption spectra of the complex were also measured after the addition of potassium cyanide. The absorption maximum was found to shift slightly to shorter wave lengths. From this fact and the statement of Duke and Courtney[12], it was reasonably assumed that the Cu(II) could be represented by the total copper concentration present in the form of Cu(II)-EDTA complex.

From this observation, it may be concluded that a one-electrotron reduction of Cu(II)-EDTA complex occurs in the solution containing cyanide ions. The cupric copper was reduced with one-electron transfer to the cuprous copper, which reacted immediately with the cyanide ion to form a very stable cuprous cyanide complex. The latter gives no polarographic wave at potentials less negative than the decomposition potentials of alkali metal

7) R. L. Pecsok, *Anal. Chem.*, **25**, 561 (1953).
8) K. Bril and P. Krumholz, *J. Phys. Chem.*, **58**, 339 (1954).
9) W. Furness, P. Crawshaw and W. C. Davies, *Analyst*, **74**, 629 (1949).
10) T. Yoshino, *J, Chem. Soc. Japan, Pure Chem. Sec.* (*Nippon Kagaku Zassi*), **78**, 131 (1957).
11) M. C. Bennett and N. O. Schmidt, *Trans. Faraday Soc.*, **51**, 1412 (1955).
12) I. M. Kolthoff and J. J. Lingane, "Polarography," Vol. 2, Interscience Publishers, New York (1952), p. 494.

ions[12]. The rate of the chemical reaction between cuprous copper and cyanide ion may be much faster than that of the electrochemical reduction of cuprous copper to copper amalgam.

**The Reaction Kinetics.**—The diffusion current-time relations were obtained at various concentrations of cupric copper, cyanide and EDTA. Typical examples are given in Fig. 2.

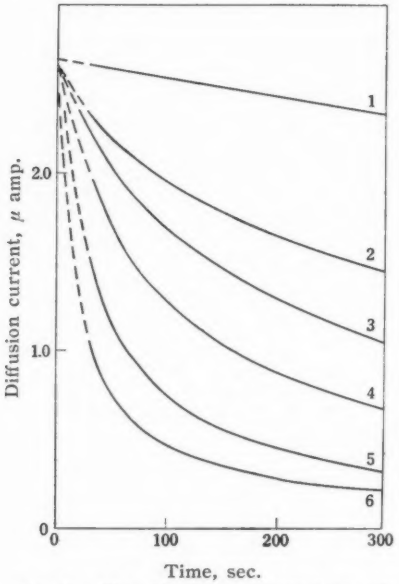


Fig. 2. The diffusion current-time relation of the reaction between $CuY^{2-}$ and $CN^-$, measured at −0.74 volt *vs.* S.C.E. in buffer of pH 9.95 of ionic strength 0.5 at 25°C. The initial concentration: $CuY^{2-}$, $0.969\times10^{-3}$ M; unchelated EDTA, $8.069\times10^{-3}$ M. The concentration of KCN added: 1, $1.88\times10^{-2}$ M; 2, $2.84\times10^{-2}$ M; 3, $3.31\times10^{-2}$ M; 4, $3.78\times10^{-2}$ M; 5, $4.73\times10^{-2}$ M; 6, $5.65\times10^{-2}$ M.

Two reaction mechanisms were assumed and compared with experimental results. Mechanism A:

$$2\,CuY^{2-} \underset{k_2}{\overset{k_1}{\rightleftharpoons}} CuYCu + Y^{4-} \text{ (rapid)} \quad (1)$$

$$CuYCu + n\,CN^- \xrightarrow{k_3} Cu(CN)_n^{2-n} + CuY^{2-} \text{ (slow)} \quad (2)$$

$$Cu(CN)_n^{2-n} \longrightarrow Cu(I)\text{-cyano complex} + 1/2(CN)_2 \text{ (rapid)} \quad (3)$$

The rate of the decrease of $CuY^{2-}$ concentration may be written as

$$-\frac{d[CuY^{2-}]}{dt} = \frac{k_1k_3[CuY^{2-}]^2[CN^-]^n}{k_2[Y^{4-}]+k_3[CN^-]^n} \quad (4)$$

If the condition, $k_2[Y^{4-}] \gg k_3[CN^-]^n$, is fulfilled, eq. 4 can be simplified as

$$-\frac{d[CuY^{2-}]}{dt} = \frac{k_1k_3}{k_2}\frac{[CuY^{2-}]^2[CN^-]^n}{[Y^{4-}]} \quad (5)$$

Mechanism B:

$$CuY^{2-} \underset{k_2'}{\overset{k_1'}{\rightleftharpoons}} Cu^{2+} + Y^{4-} \text{ (rapid)} \quad (6)$$

$$Cu^{2+} + n'CN^- \xrightarrow{k_3'} Cu(CN)_{n'}^{2-n'} \text{ (slow)} \quad (7)$$

$$Cu(CN)_{n'}^{2-n'} \longrightarrow Cu(I)\text{-cyano complex} + 1/2(CN)_2 \text{ (rapid)} \quad (8)$$

The rate of the decrease of $CuY^{2-}$ concentration can be derived as

$$-\frac{d[CuY^{2-}]}{dt} = \frac{k_1'k_3'}{k_2'}\frac{[CuY^{2-}][CN^-]^{n'}}{[Y^{4-}]} \quad (9)$$

In mechanisms A and B, the difference is in the reaction orders on the concentrations of the $CuY^{2-}$ and the cyanide ion. Therefore, the reaction rate can be written in general as

$$-\frac{d[CuY^{2-}]}{dt} = \frac{k_1k_3}{k_2}\frac{[CuY^{2-}]^m[CN^-]^n}{[Y^{4-}]} \quad (10)$$

In the reaction mixture of pH 10, the Cu(II)-EDTA complex exists only in the form of $CuY^{2-}$. The formation of $CuY(OH)^{3-}$ is considered to be negligible[11]. On the other hand, the cyanide exists in the forms of cyanide ion $CN^-$ and hydrogen cyanide HCN at pH 10, and the unchelated ethylenediaminetetra-acetate, in the forms of $HY^{3-}$ and $Y^{4-}$ ions. The concentration of $CN^-$, therefore, was calculated from the total concentration of free cyanide and the dissociation constant of hydrogen cyanide, and that of $Y^{4-}$, from the total concentration of unchelated EDTA and the fourth dissociation constant of EDTA. The value of $4\times10^{-10}$ was used for $K_{HCN}$[13] and the activity coefficient of cyanide ion, $f_{CN^-}$, at the given ionic strength was estimated. The fourth dissociation constant of EDTA used in this calculation was $10^{-9.53}$ which is the hybrid constant obtained by Carini and Martell[14] at ionic strength 0.5 at 25°C. The concentration of each species at a given time was calculated from the stoichiometric relation,

13) W. M. Latimer, "Oxidation Potentials," Prentice-Hall, Inc., New York (1952), p. 137.
14) F. F. Carini and A. E. Martell, *J. Am. Chem. Soc.*, **74**, 5745 (1952).

$$CuY^{2-} + 4\ CN^- = Cu(CN)_3^{2-} + 1/2(CN)_2 + Y^{4-}$$

and the observed concentration of $CuY^{2-}$.

Eq. 10 can be rewritten as

$$\log\left(-\frac{d[CuY^{2-}]}{dt}\right) + \log[Y^{4-}] - m\log[CuY^{2-}] = \log\frac{k_1k_3}{k_2} + n\log[CN^-] \quad (11)$$

If the reaction proceeded through mechanism A or B, a plot of the left-hand side of eq. 11 against $\log[CN^-]$ should give a straight line with slope of $n$, when $m$ in the left-hand side of eq. 11 is 2 for mechanism A and 1 for mechanism B. This relation was examined by introducing $[CuY^{2-}]$, $[Y^{4-}]$, $[CN^-]$ and $-\frac{d[CuY^{2-}]}{dt}$ at $t=120$(sec.) on the concentration-time curves obtained with varied concentrations of cyanide but at the constant initial concentrations of $CuY^{2-}$ and EDTA. As seen in Fig. 3, eq. 11 is satisfied when $m$ is 2, the plot of the left-hand side of eq. 11 against $\log[CN^-]_{t=120}$ giving a straight line with a slope of 4.1 (A in Fig. 3). The corresponding plot with $m=1$, on the other hand, gave no straight line (B in Fig. 3). This is a clear indication of the fact that mechanism B does not explain the reaction kinetics.

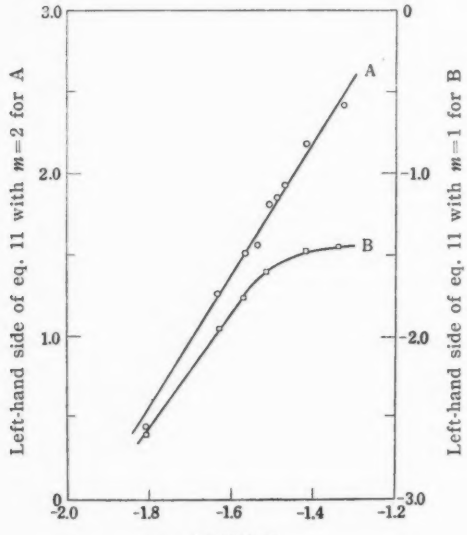


Fig. 3. Plot of the left-hand side of eq. 11 against $\log[CN^-]$ with $m=2$ (curve A) and $m=1$ (curve B).

Substituting $n=4$, eq. 10 may be written as

$$\log\left(-\frac{d[CuY^{2-}]}{dt}\right) + \log[Y^{4-}] - 4\log[CN^-] = \log\frac{k_1k_3}{k_2} + m\log[CuY^{2-}] \quad (12)$$

Although $m$ was decided to be 2 from the treatment mentioned above, the left-hand side of eq. 12 was plotted against $\log[CuY^{2-}]$ using the values of $-\frac{d[CuY^{2-}]}{dt}$, $[Y^{4-}]$, $[CN^-]$ and $[CuY^{2-}]$ which were obtained at various $t$'s on one concentration-time curve and also at $t=120$ (sec.) on several concentration-time curves recorded with varied initial concentrations of $CuY^{2-}$ but at the constant initial concentrations of cyanide and EDTA. As shown in Fig. 4, the plot gave a straight line with a slope of 2.1, which definitely showed that the reaction is second order on the $CuY^{2-}$ concentration.

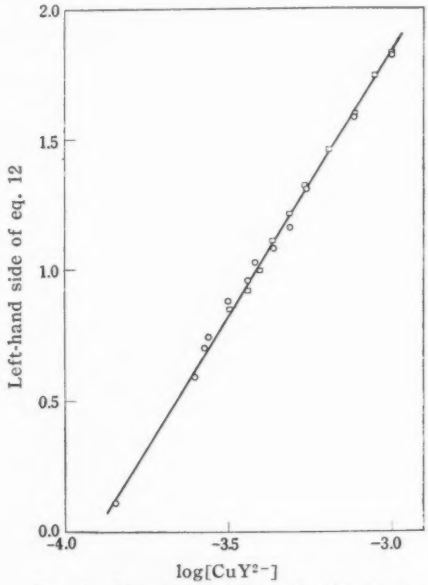


Fig. 4. Plot of the left-hand side of eq. 12 against $\log[CuY^{2-}]$: □, values obtained at various $t$'s on one concentration-time curve; ○, values obtained at $t=120$(sec.) on various concentration-time curves.

The diffusion current-time curves were also recorded at various initial concentrations of EDTA but at the constant initial concentrations of $CuY^{2-}$ and cyanide. Eq. 10 is rearraged as

$$\log\left(-\frac{d[CuY^{2-}]}{dt}\right)-2\log[CuY^{2-}]-4\log[CN^-]=\log\frac{k_1k_3}{k_2}-\log[Y^{4-}] \quad (13)$$

where 2 is substituted for $m$ and 4, for $n$. The left-hand side of eq. 13 was plotted against $\log[Y^{4-}]$ with the values obtained at $t=120$ (sec.). The plot gave a straight line with a slope of $-0.95$ (Fig. 5), and confirmed the first-order dependence on the reciprocal of the $Y^{4-}$ concentration.

The rate constant for the overall reaction, $k_1k_3/k_2$, was calcuated from the concentration-time curves obtained under various conditions (Table I), and determined to be $6.8\times10^7$ l.$^4$ mole$^{-4}$ sec.$^{-1}$

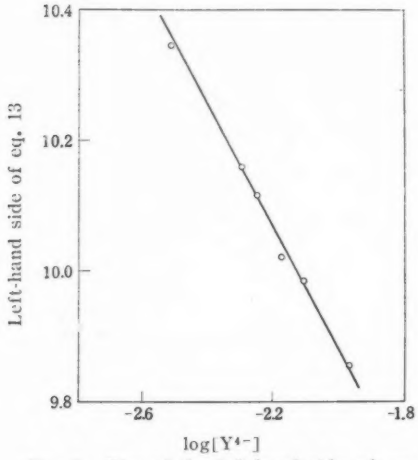


Fig. 5. Plot of the left-hand side of eq. 13 against $\log[Y^{4-}]$.

TABLE I

DETERMINATION OF THE OVERALL RATE CONSTANT, $k_1k_3/k_2$

| $[CuY^{2-}]\times10^4$, M | $[Y^{4-}]\times10^3$, M | $[CN^-]\times10^2$, M | $(k_1k_3/k_2)\times10^{-7}$, l.$^4$ mole$^{-4}$ sec.$^{-1}$ |
|---|---|---|---|
| $3.18_7$ | 6.63 | 2.89 | 6.85 |
| $3.25_4$ | 6.71 | 3.20 | 6.55 |
| $4.81_4$ | 6.50 | 2.94 | 7.13 |
| $4.91_6$ | 6.93 | 3.11 | 6.70 |
| $5.25_5$ | 6.55 | 3.27 | 6.65 |
| $5.45_8$ | 6.45 | 2.96 | 6.91 |
| $7.69_5$ | 6.28 | 3.05 | 6.63 |
| 10.00 | 6.11 | 3.13 | 6.60 |
| $4.33_9$ | 6.54 | 2.93 | 6.94 |
| $4.33_9$ | 6.97 | 3.09 | 6.72 |
| $5.18_7$ | 8.22 | 3.09 | 6.15 |
| $2.20_4$ | 5.46 | 3.82 | 7.11 |
| $5.83_1$ | 6.51 | 3.29 | 6.84 |
| $3.96_6$ | 6.57 | 2.92 | 6.31 |
| $6.37_3$ | 6.05 | 2.31 | 6.16 |

Mean $6.8\times10^7$ l.$^4$ mole$^{-4}$ sec.$^{-1}$

In similar experiments carried out at pH 9.2 the rate of the reaction showed a second-order depence on the $CuY^{2-}$ concentration, a fourth-order depence on the cyanide ion concentration and a first-order dependence on the reciprocal of the $Y^{4-}$ concentration. The value of $k_1k_3/k_2$ obtained at pH 9.2 was in fair agreement with that obtained at pH 10.0.

It has been reported that some metal-EDTA complex ions, such as $PbY^{2-}$, $CoY^-$ and $HgY^{2-}$, react with excessive metal ions to form salt-like compounds of the formula of MYM-type[15-17]. On the other hand, there has been no report in which the compounds of MYM(or MYM')-type are confirmed to be present in the solution at an appreciable concentration. Bennett and Wise[18] concluded from their polarographic investigation that there is no measurable quantity of CuYCd in the solution containing Cu(II), Cd(II) and EDTA. Some experiments carried out in this study were not successful in showing the existence of CuYCu in the solution. Nevertheless, it would not be unreasonable to consider that CuYCu exists, more or less, in the solution containing $CuY^{2-}$, CuYCu being in equilibrium with $CuY^{2-}$ according to the reaction 1.

It might be interesing to note that the reaction of Cu(II)-ammine complexes and cyanide ion is first order on the concention of the complexes[1], while the reaction of Cu(II)-EDTA complex and cyanide ion is second order on the concentration of the complex. The reason is not quite understood at present and it is also difficult to speculate upon the form of the activated complex. However, the greater stability of the ethylenediaminetetra-acetate complex owing to the chelate formation may be unfavorable for the reaction which takes place through the dissociation process, and the reaction between CuYCu and cyanide may favor the formation of an activated complex which leads to the spontaneous reduction of cupric to cuprous copper.

15) N. Tanaka, K. Kato and R. Tamamushi, This Bulletin, **31**, 283 (1958).
16) G. Schwarzenbach, *Helv. Chim. Acta*, **32**, 839 (1949).
17) R. W. Schmid and C. N. Reilley, *J. Am. Chem. Soc.*, **78**, 5513 (1956).
18) M. C. Bennett and W. S. Wise, *Trans. Faraday Soc.*, **52**, 696 (1956).

## Summary

The reaction between copper(II)-ethylenediaminetetra-acetate complex and cyanide ion has been investigated by measuring the change of the polarographic diffusion current of the complex as a function of time after the initiation of reaction.

The rates of the reaction obtained with various concentrations of Cu(II)-EDTA complex, cyanide and unchelated EDTA showed that the reaction is of second order on the concentration of the Cu(II)-EDTA complex, fourth order on that of the cyanide and first order on the reciprocal of that of the unchelated EDTA. The reaction mechanism proposed is

$$2\,CuY^{2-} \underset{k_2}{\overset{k_1}{\rightleftharpoons}} CuYCu + Y^{4-}$$

$$CuYCu + 4\,CN^- \xrightarrow[\text{(rate-determining)}]{k_3} Cu(CN)_4^{2-} + CuY^{2-}$$

$$Cu(CN)_4^{2-} \longrightarrow Cu(I)\text{-cyano complex} + 1/2(CN)_2$$

and the rate of the reaction is expressed as

$$-\frac{d[CuY^{2-}]}{dt} = \frac{k_1 k_3}{k_2}\frac{[CuY^{2-}]^2[CN^-]^4}{[Y^{4-}]}$$

The value of $k_1k_3/k_2$ was determined to be $6.8\times10^7$ l.$^4$ mole$^{-4}$ sec.$^{-1}$ in a carbonate-bicarbonate buffer of pH 10.0, at ionic strength 0.5 and at 25°C.


The authors thank the Ministry of Education for the financial support to this research.

*Department of Chemistry*
*Faculty of Science*
*Tohoku University*
*Katahira-cho, Sendai*

---

# *Estimation of Specific Surface Area of Particles in Colloidal Silica Sols From the Rate of Dissolution*

By Katsumi GOTO

(Received May 12, 1958)

The performance of colloidal silica in many of its applications largely depends on particle size or specific surface area. However, the application of currently available methods[1-7] for the determination of this property encounters difficulty in many cases, and a more rapid and simple method is urgently needed. An attempt has been made in the present investigation to determine the specific surface area of colloidal silica from the rate of dissolution of particles in a solution containing sodium fluoride and hydrochloric acid.

1) G. B. Alexander, *J. Am. Chem. Soc.*, **75**, 2887 (1953).
2) G. B. Alexander, ibid., **76**, 2094 (1954).
3) G. B. Alexander and R. K. Iler, *J. Phys. Chem.*, **57**, 932 (1953).
4) P. V. Nauman and P. Debye, *J. Phys. & Colloid Chem.*, **55**, 1 (1951).
5) M. F. Bechtold, *J. Phys. Chem.*, **59**, 532 (1955).
6) R. K. Iler, "The Colloid Chemistry of Silica and Silicates." Cornell Univ. Press, New York (1955), p. 100.
7) G. W. Sears, Jr., *Anal. Chem.*, **28**, 1981 (1956).

## Experimental

**Materials.**—*Colloidal silica.*—Sols of colloidal silica were prepared by allowing to stand the mixture of the solution of sodium metasilicate and the solution of silicic acid prepared from sodium metasilicate by ion exchange. Colloidal silica having a small specific surface area was prepared by aging at higher temperatures.

*Aluminum chloride solution.*—Two hundred and seventy g. of aluminum chloride hexahydrate was dissolved in distilled water and made up to 1 l. One mililitre of this solution contains about 30 mg. of aluminum ions.

*Ammonium molybdate solution.*—Ten % (w/v) aqueous solution.

*Concentrated hydrochloric acid solution*

All reagents were of purest grade commercial products and used without further purification.

**Apparatus.**—A photoelectric colorimeter equipped with a glass prism and a barrier layer cell was employed for the colorimetric determination of molecularly-dispersed form of silica. The dissolution reaction was conducted in polyethylene

bottles to avoid contamination from glass vessels.

**Measurements of dissolution rate.**—Colloidal silica is dissolved in a medium prepared fulfilling the conditions given in Table I. Ten millilitre portions of the solution in which the colloidal silica sample is being dissolved are taken at definite intervals in beakers containing 0.5 ml. of aluminum chloride solution, the dissolution reaction being stopped by this procedure. To each beaker 0.5 ml. of ammonium molybdate solution is then added and the absorbancy is measured after 6 or 8 min. at wave-length of 430 mμ. The amount of conecntration of a molecularly-dispersed form of silica is calculated from the color intensity and is plotted against the time of sampling. Since, as is discussed later, the plot was a straight line over a wide range of time, the dissolution rate, which is expressed by the ratio of the initial rate of increase in the concentration of molecularly-dispersed silica (mg./l./min.) to the initial concentration of colloidal silica (mg./l.), could be easily obtained from the slope.

TABLE I
CONDITIONS EMPLOYED FOR THE DISSOLUTION REACTION

| | |
|---|---|
| Concentration of sodium fluoride | 300 mg./l. with respect to $F^-$ |
| Concentration of hydrochloric acid | 0.12 N |
| Temperature | 25.0±0.1°C |
| Concentration of colloidal silica sample | around 20 mg./l. with respect to $SiO_2$ |

## Results

Fig. 1 shows the dissolution rate as a function of the specific surface area as determined by the titration procedure developed by Sears[7]. Correction was made, in the titration, for molecularly-dispersed silica which exists in equilibrium with colloidal silica and also reacts with the titrant. For sols of higher degrees of secondary aggregation, the dissolution rate is generally higher than is expected from the titration. This may be due to the gelation taking place during the titration of such sols, giving rise to difficulty in reaching equilibrium between the silica particles and the titrant.

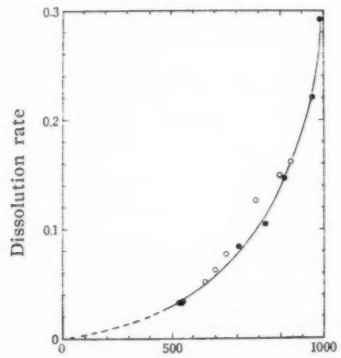


Fig. 1. Correlation of dissolution rate with specific surface area. ● indicates that gelation did not take place during titration.

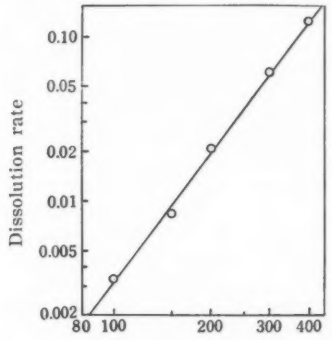


Fig. 2. Fffect of fluoride ion concentration on the dissolution rate.

The effect of fluoride ion concentration on the dissolution rate is shown on logarithmic scale in Fig. 2, from which it is apparent that the dissolution rate is roughly proportional to the 2.6th power of fluoride concentration.

The concentration of hydrochloric acid in the range 0.09 to 0.14 N has little effect on the dissolution rate, as is shown in Table II.

TABLE II
EFFECT OF THE CONCENTRATION OF HYDROCHLORIC ACID ON THE DISSOLUTION RATE

| Normality of HCl | Dissolution rate |
|---|---|
| 0.03 | 0.050 |
| 0.06 | 0.039 |
| 0.09 | 0.0314 |
| 0.12 | 0.0320 |
| 0.14 | 0.0315 |

The fact that, as is shown in Table III, the aluminum ion greatly reduces the dissolution rate at high concentrations permits the use of aluminum salt to stop the dissolution reaction. Although 600 mg./l. of the aluminum ion is sufficient for this purpose, an aluminum-ion concentration of about 1500 mg./l. was used in the present investigation. It is shown in Table

TABLE III
EFFECT OF ALUMINUM ION (a)

| Concentration of Al (mg./l.) | Dissolution rate |
|---|---|
| 0 | 0.0675 |
| 150 | 0.0025 |
| 300 | ca. $8\times10^{-5}$ |
| 600 | ca. $2\times10^{-5}$ |
| 0, in the absence of fluoride | ca. $1\times10^{-5}$ |

TABLE IV
EFFECT OF ALUMINUM ION (b)

| Concentration of Al (mg./l.) | Dissolution rate |
|---|---|
| 0 | 0.0300 |
| 0.2 | 0.0315 |
| 0.4 | 0.0280 |
| 0.6 | 0.0278 |
| 0.8 | 0.0264 |

TABLE V
EFFECT OF THE CONCENTRATION OF COLLOIDAL SILICA SAMPLE

| Concentration (mg. $SiO_2$/l.) | Dissolution rate |
|---|---|
| 10.8 | 0.068 |
| 20.0 | 0.065 |
| 32.0 | 0.062 |
| 40.5 | 0.053 |

IV, however, that small amounts of aluminum, which is the most common among the impurities in colloidal silica, have little effect on the dissolution rate.

The concentration of a colloidal silica sample in a dissolution medium also affects the dissolution rate as shown in Table V. It is essential, therefore, to measure the dissolution rate at about a constant concentration of colloidal silica.

## Discussion

The foregoing results indicate a possibility of estimating the specific surface area of colloidal silica particles from the measurement of dissolution rate in an acid solution of sodium fluoride under carefully controlled conditions.

It is very interesting to note in Fig. 1 that the surface of a smaller particle is more reactive than that of a larger one: the dissolution rate per unit surface area increases with decreasing particle size. Since, therefore, the decrease in surface area during dissolution is compensated by the increasing rate of dissolution per unit surface area, the concentration of molecularly-dispersed silica increases linearly with time over an unexpectedly wide range, permitting an easy graphical determination of the initial rate of dissolution.

The dissolution reaction may be of first order with respect to colloidal silica, since the dissolution rate given in Table V is about the same for varying silica concentrations. It is interesting to note that the dissolution reaction is of the order between 2 and 3 with respect to the fluoride concentration and that it is more rapid at lower acidities. Further discussion of the reaction mechanism, however, is not described here since it is beyond the scope of this paper.

The variation of the rate of dissolution per unit surface area with particle size, however, prevents the accurate determination of a specific surface area of colloidal silica in polydisperse systems. It is also a serious question associated with this method whether the dissolution rate is the same or not for sols prepared under different conditions. However, since the sols used in the present investigation were prepared under alkaline conditions, where silica particles of uniform size can be formed[8], the method may be applicable at least to alkaline sols, including the active silica used in water purification.[9]

Sears' titration procedure[7] is applicable only to sols containing more than 10 g./l. of silica since it deals with 150 ml. of sols containing 1.5 g of silica. On the other hand, only a few mg. of silica is sufficient for the present method, which may therefore be applicable also to extremely dilute sols. This may well offset the disadvantage discussed above.

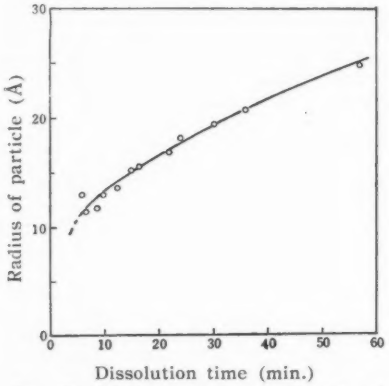


Fig. 3. Relation between particle size and dissolution time.

8) R. K. Iler and R. L. Dalton, *J. Phys. Chem.*, **60**, 955 (1956).
9) Ref. 6 p. 119

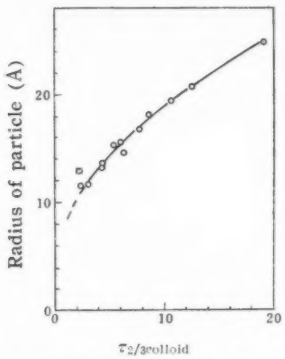


Fig. 4. Relation between the particle size and the time required for the dissolution of two thirds of colloidal silica.

It is essential, in determining a specific surface area from Fig. 1, to observe as strictly as possible the conditions given in Table I, since the reduction in the concentration of available fluoride during the dissolution reaction was not taken into account in the present investigation.

Molecularly-dispersed silica, when present in large amounts, may interfere with the method by reducing the concentration of available fluoride. This, however, may be removed by passing through a column containing a mixture of cation- and anion-exchange (strongly basic type) resins.

In our earlier report[10], dissolution time was used as a measure of particle size. It is the time required for the complete dissolution of particles and was determined by plotting the cube root of the concentration of colloidal silica versus time and extrapolating the plot to the abscissa, based on the assumption that the rate of dissolution per unit surface area remains constant during the process of dissolution. Though such an assumption has been proved to be incorrect, the dissolution time may still be a rough measure of the particle size, and is shown in Fig. 3 as a function of the particle size calculated from the result of titration on the assumption that the particles are spheres with a specific gravity of 2.2[11].

The reactivity toward alkaline solutions was also used in earlier works[12,13] as a measure of particle size. The reaction with alkali, however, is greatly retarded by traces of aluminum[14] and thus may be applicable only to sols prepared with special precautions.

It is also desirable to use the time, $\tau_{2/3colloid}$, required for particles to lose two thirds of their initial masses under conditions given in Table I. As the concentration of remaining colloidal silica decreases linearly with time at least up to this point, the $\tau_{2/3colloid}$ can be easily determined graphically. In Fig. 4 is shown the relation between $\tau_{2/3colloid}$ and particle size.

The author wishes to express his thanks to Professors G. Okamoto and T. Okura for their valuable advice and suggestion. The author is also indebted to the Asahi Glass Foundation for the Promotion of Researches in Chemical Industries for the financial support of this work.

*Faculty of Engineering, Hokkaido University, Sapporo*

10) T. Okura, K. Goto and T. Komatsu, This Bulletin, **31**, 139 (1958).

11) Ref. 6 p. 135.
12) K. Goto, *J. Phys. Chem.*, **60**, 1007 (1956).
13) K. Goto, *J. Chem. Soc. Japan, Pure Chem. Sec., (Nippon Kagaku Zassi)*, **77**, 957 (1956).
14) G. Okamoto, T. Okura, and K. Goto, *Geochim. et Cosmochim. Acta*, **12**, 123 (1957).

# *Ultraviolet Absorption Spectra of Nitro-, Dinitro- and Trinitro-substituted Benzenes*

By Takehiro ABE

(Received May 28, 1958)

The near ultraviolet absorption spectrum of nitrobenzene shows an intense band at 260 mμ and two shoulders at about 290 and 340 mμ[1-3]. The maximum absorption band at 260 mμ, which has been measured in various solvents[4,5], has been interpreted by Doub and Vandenbelt[6] and later by Wenzel[7] to correspond to the 200 mμ band of benzene but has been interpreted by Nagakura and Tanaka[8] in terms of the strong electron-attracting nature of the nitro group. The hidden transition near 290 mμ and the weak band at 340 mμ have been shown by Wenzel to be related to the 256 mμ transition of benzene and to be due to the nitro group, respectively.

In the present paper, an attempt is made to investigate the influence of the number of nitro groups on the spectra of polynitrobenzenes in various solvents, together with the solvent effects upon their spectra. The ultraviolet absorption spectra of nitrobenzene (NB), *m*-dinitrobenzene (DNB), 1,3,5-trinitrobenzene (TNB) and 2,4,6-trinitrotoluene (TNT) have been measured in solvents like water, water-hydrochloric acid, water-sodium hydroxide, ethanol, benzene and acetone.

## Experimental

**Materials.** — Nitro compounds of commercial extra pure grade were purified by distillation or by recrystallization several times. NB: b. p. 210°C, DNB: m. p. 90.4°C, TNB: m. p. 123.1°C, TNT: m. p. 81.3°C. Commercial guaranteed solvents were fractionally distilled after usual treatments.

**Spectra.** — The spectra of the solutions were measured with a Hitachi quartz spectrophotometer, Model EPU-2 at room temperature. The path length of absorption cells was 1 cm.

## Results

**The Spectra of Nitro Compounds in Some Solvents.**—*In ethanol* (Fig. 1).—In Table I progressive blue shifts of the 260 mμ band of nitrobenzene for the nitro compounds are seen in the following order: NB, DNB, TNT and TNB. Their molar extinction coefficients also increase in the same order. It is obvious that these blue shifts are attributed to the numbers of nitro groups attached to a benzene nucleus.

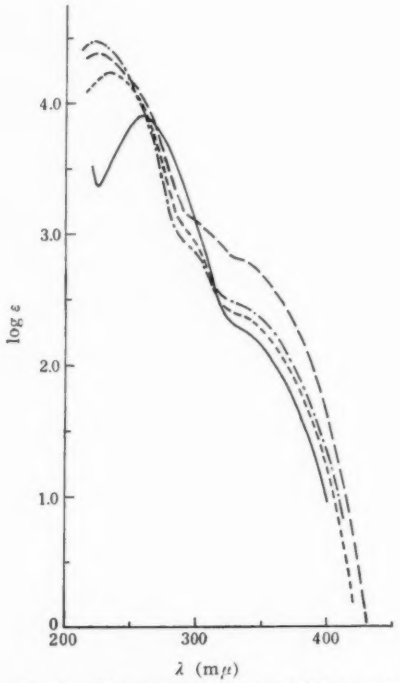


Fig. 1. Absorption spectra of NB (——), DNB (- - -), TNB (—·—) and TNT (— —), all in ethanol.

1) Landolt-Börnstein, "Physikalish-chemishe Tabellen", Springer, Berlin, 1951, 6th ed., Part 3 (II), p. 267.
2) G. S. Hammond and F. Modie, *J. Am. Chem. Soc.*, **75**, 1385 (1953).
3) H. Ungnade, ibid., **75**, 432 (1953).
4) N. S. Bayliss and E. G. McRae, *J. Phys. Chem.*, **58**, 1006 (1954).
5) W. M. Schubert, J. Robins and J. L. Haun, *J. Am. Chem. Soc.*, **79**, 910 (1957).
6) L. Doub and J. M. Vandenbelt, ibid., **69**, 2714 (1947).
7) A. Wenzel, *J. Chem. Phys.*, **22**, 1623 (1954).
8) S. Nagakura and J. Tanaka, ibid **22**, 236 (1954).

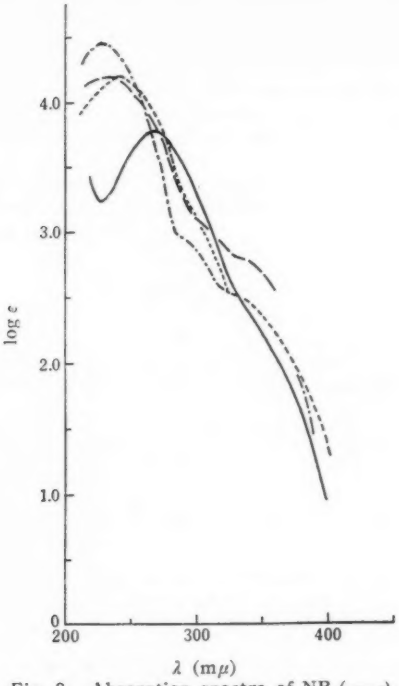


Fig. 2. Absorption spectra of NB (——), DNB (- - -), TNB (—·—) and TNT (— —), all in water.

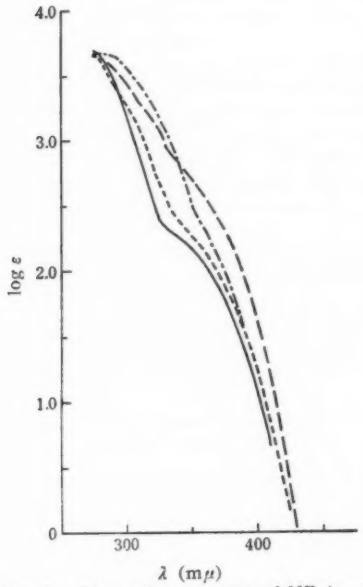


Fig. 3. Absorption spectra of NB (——), DNB (- - -), TNB (—·—) and TNT (— —), all in benzene.

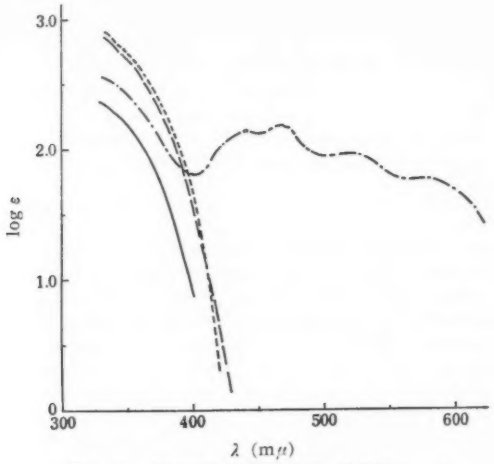


Fig. 4. Absorption spectra of NB (——), DNB (- - -), TNB (—·—) and TNT (— —), all in acetone.

TABLE I
VALUES OF THE ABSORPTION MAXIMA OF NITRO COMPOUNDS IN ETHANOL AND IN WATER

| Compound | Solvent: Ethanol a) $\lambda_{max}$ (mμ) | Ethanol ε | Water b) $\lambda_{max}$ (mμ) | Water ε | b)-a) (mμ) |
|---|---|---|---|---|---|
| NB | 260 | 8,140 | 267 | 6,910 | 7 |
| DNB | 233 | 17,200 | 244 | 15,400 | 11 |
| TNB | 223 | 29,700 | 229 | 28,100 | 6 |
| TNT | 225 | 22,900 | 233 | 15,800 | 8 |

λ: Wavelength.
ε: Molar extinction coefficient.

Let us consider an electron migration between the benzene nucleus and the nitro groups in each nitro compound. By substituting nitro groups for hydrogen atoms in the nucleus, the π-electron density at the nucleus decreases owing to their strong electron-attracting nature as illustrated in Fig. 5. The positive charges of the nuclei of the nitro compounds increase in the order of the increasing numbers of nitro groups:

$$NB < DNB < TNT < TNB \qquad (1)$$

Here the charge of TNB is more positive than that of TNT, because the σ-electron of the methyl group can migrate to some extent, through hyperconjugation, toward the nucleus of TNT. The order in Eq. 1 is in good agreement with that of the blue shifts in Table I. Consequently, it is

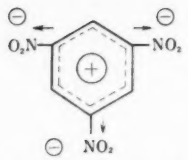


Fig. 5. Charge distribution of TNB.

noticed that the absorption maxima of the nitro compounds shift to the blue, as the electron densities of their nuclei decrease by the action of the nitro groups.

The shoulders near 290 mμ are more distinct with increasing number of nitro groups. Owing to the influence of methyl group in TNT, the molar extinction coefficient of the absorption maximum of TNT is smaller than that of TNB, but the coefficient of the 340 mμ shoulder of the former is greater than that of the latter.

*In water* (Fig. 2).—There are similar blue shifts as in ethanol. In Table I it is also found that the maximum absorption bands of the respective nitro compounds are to a great extent shifted to the blue in ethanol as compared with those in water and that their molar extinction coefficients are greater in ethanol than in water.

*In benzene* (Fig. 3). — The shoulder at about 340 mμ becomes indistinct with the increasing number of nitro group. In all the spectra, a small shoulder can be observed at about 280 mμ.

*In acetone* (Fig. 4).—All the nitro compounds show absorption shoulders at about 340 mμ. There is no correlation between their intensities and the numbers of nitro groups. Only TNB shows weak absorption bands in the visible range as given in Table II.

TABLE II
THE VISIBLE ABSORPTION BANDS OF TNB IN ACETONE

| λ(mμ) | 441 | 469 | 524 | 575 |
|---|---|---|---|---|
| ε | 135 | 148 | 93 | 58 |

**Effects of Acid and Alkali in Water** (Fig. 6).—The positions of the absorption maxima of nitro compounds have not been found to be influenced by hydrochloric acid in water. In Fig. 6 it is seen that in an aqueous solution of sodium hydroxide the nitro compounds show intense absorption bands at longer wavelengths in the order of increasing number of nitro groups. In these regions no absorption bands are observed in ethanol. The trinitro compounds give red colors with alkali. These colors are reversively decolorized by addition of acids. DNB and NB give yellow colors on treatment with a concentrated solution of sodium hydroxide. These yellow colorations are very slow, but become faster by warming.

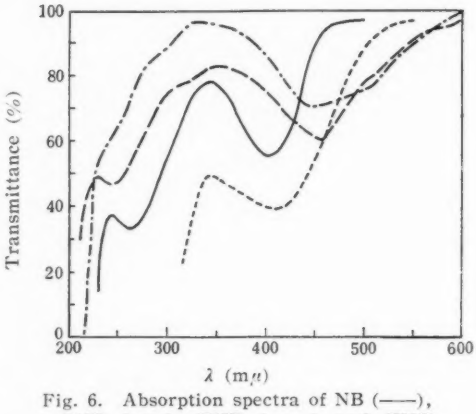


Fig. 6. Absorption spectra of NB (——), DNB (– – –), TNB (—·—) and TNT (— —), all in $H_2O$+NaOH.

Analogous color reactions of sodium ethoxide with TNT and TNB in ethanol have been, by Caldin and his coworkers[9,10], interpreted in terms of a proton-transfer reaction for TNT and in terms of an addition reaction for TNB. The color of the nitro compounds with sodium hydroxide seems to be also produced by the formation of complexes between the compounds and the hydroxide ion, because the compounds give the same color with other alkalies and the position of the absorption maxima of nitro compounds in water is not influenced by hydrochloric acid.

**Solvent Effects on the Spectra of the Respective Nitro Compounds** (Figs. 1–4). —The intensity of the 340 mμ band of DNB is very strong only in acetone. At wavelengths longer than 260 mμ the spectra of the trinitro compounds in ethanol are close to those in water.

The trinitro compounds show absorption bands near 280 mμ in benzene, probably owing to the formation of molecular complexes between the compounds and benzene. In this region Briegleb and Czekalla[11]

9) E. F. Caldin and G. Long, *Proc. Roy. Soc.*, **A228**, 263 (1955).
10) J. B. Ainscough and E. F. Caldin, *J. Chem. Soc.*, **1956**, 2528, 2540, 2546.
11) G. Briegleb and J. Czekalla, *Z. Elektrochem.*, **59**, 184 (1955).

have already found an absorption band of a molecular complex between TNB and benzene. The corresponding bands in the spectra of DNB and NB can not be determined owing to the presence of other absorption bands near 280 mμ, although DNB seems to show the band at 280 mμ. The formation of a complex between NB and benzene has been reported by Cheshko and Tavadze[12].

### Summary

1) In ethanol and in water the progressive blue shifts of the 260 mμ band of nitrobenzene for the nitro compounds are observed in the order of increasing number of nitro groups.

2) Only TNB shows visible weak absorption bands in acetone.

3) In an aqueous solution of sodium hydroxide these nitro compounds show intense absorption bands at longer wavelengths as the number of nitro group increases.

The author is particularly indebted to Professor Y. Nomura for his suggestion and encouragement through this work. Thanks are also due to Assistant Professor S. Maeda for the use of the spectrophotometer.

*Department of Chemistry*
*Defense Academy*
*Yokosuka, Kanagawa*

12) F. F. Cheshko and N. Sh. Tavadze, *Doklady Akad. Nauk S. S. S. R.*, **95**, 833 (1954).

---

# *Studies on Polymerization and Depolymerization of ε-Caprolactam Polymer. V*. On the Reaction Mechanism of the Catalytic Polymerization of ε-Caprolactam by Alkali Metal***

By Hirosuke YUMOTO and Naoya OGATA

(Received may 9, 1958)

The rapid polymerization of ε-caprolactam catalyzed by alkali metal behaves in a manner quite different from the polymerization by water, acids or amino acids. W. Griehl[1,2] found that the molecular weight distribution of poly-ε-capramide obtained in the presence of alkali metal or its salt is very sharp just after reaching the ring-chain equilibrium and then gradually changes into Flory's distribution. O. Wichterle[3] and D. Heikens[4] proposed the mechanism of ε-caprolactam polymerization catalyzed by alkali metal salt.

### Experimental

**(1) The Initial Reaction between ε-Caprolactam and Alkali Metal.**—The Mixture of equal moles of ε-caprolactam and alkali metal was heated together at 100°C. The generated gas was brought to copper oxide heated at 400°C with a stream of nitrogen. It was found as shown in Table I that 1/2 mole of hydrogen molecule to 1 mole of alkali metal is produced.

TABLE I
THE REACTION DEGREE OF SODIUM TO ε-CAPROLACTAM AT 100°C

| Sodium (mole) | Produced water (mole) | Molar ratio of hydrogen to sodium |
|---|---|---|
| $1.34\times10^{-2}$ | $6.1\times10^{-3}$ | 2.2 |
| 1.58 〃 | 7.2 〃 | 2.2 |
| 1.49 〃 | 9.7 〃 | 1.6 |

The infrared spectrum of the reaction product is shown in Fig. 1. The absorption bands of =NH group at 3.16 μ and 3.28 μ is very weak. After the product was exposed in the atmosphere for only 5 minutes, the spectrum came to be similar to that of ε-caprolactam (Fig. 2). Therefore the reaction product is thought to react easily with water moisture in the atmosphere and to change into ε-caprolactam. By dissolving the reaction product in the heavy water, the solution

* IV. *Makromolekulare Chem.*, **25**, 91 (1958).
** Presented at the 3rd Autumn Meeting of the Chemical Society of Japan in Tokyo, Nov. 24, 1957.
1) W. Griehl, *Faserforsch. u. Textiltech.*, **6**, 260 (1955).
2) W. Griehl, ibid., **7**, 207 (1956).
3) O. Wichterle, ibid., **6**, 237 (1955).
4) D. Heikens, *Makromolekulare Chem.*, **18**, 62 (1956).

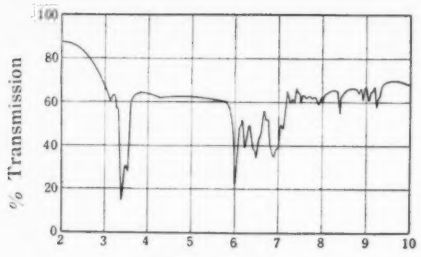


Fig. 1. The infrared spectrum of the reaction product of ε-caprolactam and sodium.

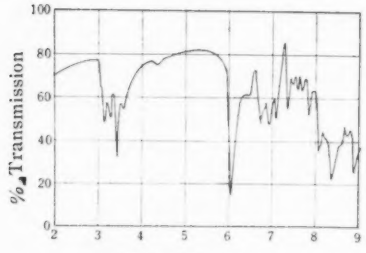


Fig. 2. The infrared spectrum of ε-caprolactam.

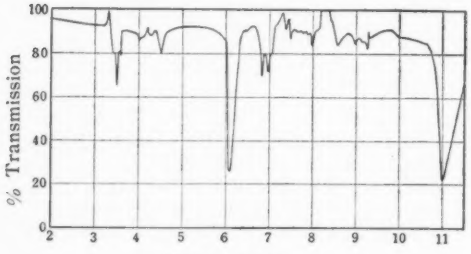


Fig. 3. The infrared spectrum of the product in the lower layer of the heavy water solution.

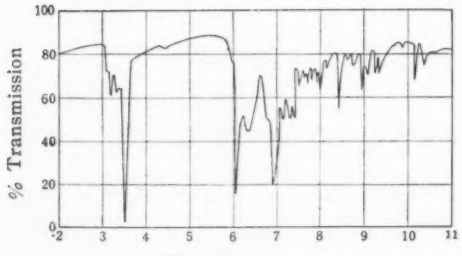


Fig. 4. The infrared spectrum of the reaction product of ε-caprolactam and lithium.

was separated into two layers. The substance extracted in chloroform from the lower layer has the absorption band of =N—D group at 4.46 μ as shown in Fig. 3 and that from the upper layer has both absorption bands of =N—H and =N—D. It was ascertained in an experiment that the hydrogen of the amide group in ε-caprolactam cannot be substituted by deutrium, when it was only dissolved in the heavy water. It is concluded that the following reactions take place:

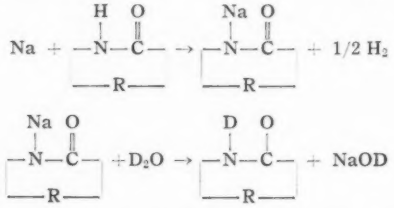


The reaction product of equal moles of ε-caprolactam and lithium has absorption bands at 8.75 μ and 9.05 μ (Fig. 4), which are expected to be assigned to =N—Li.

**(2) The Rate of Polymerization.** — The mixture of sodium and dried ε-caprolactam (water content of 0.01% or less) at the molar ratio of 1/25, 1/50, 1/100 or 1/200, was heated in a sealed glass tube at 232°C and the quantity of ε-caprolactam in product was determined from the soluble fraction in chloroform. The result is shown in Table II and Fig. 5. Similar experiments using lithium were carried on and the

TABLE II

THE RATES OF POLYMERIZATION OF ε-CAPROLACTAM WITH SODIUM

| Sodium (mole/mole) | Time (min.) | Quantity of ε-caprolactam (%) | $[\eta]^{25°C}_{cresol}$ of polymer |
|---|---|---|---|
| 1/25 | 2.5 | 40.0 | |
| | 5 | 14.6 | |
| | 10 | 8.9 | |
| | 15 | 9.1 | |
| | 20 | 7.5 | |
| | 30 | 6.4 | 0.602 |
| 1/50 | 5 | 61.3 | |
| | 10 | 9.0 | |
| | 15 | 7.8 | |
| | 20 | 5.0 | |
| | 30 | 4.9 | 0.809 |
| 1/100 | 5 | 84.4 | |
| | 10 | 13.6 | |
| | 15 | 10.5 | |
| | 20 | 5.0 | |
| | 30 | 4.7 | 1.085 |
| 1/200 | 5 | 91.4 | |
| | 10 | 81.0 | |
| | 15 | 55.9 | |
| | 20 | 30.8 | |
| | 30 | 5.3 | 1.435 |

TABLE III
THE RATE OF POLYMERIZATION OF ε-CAPROLACTAM WITH LITHIUM

| Lithium (mole/mole) | Time (min.) | Quantity of ε-caprolactam (%) | $[\eta]^{25°C}_{cresol}$ of polymer |
|---|---|---|---|
| 1/50 | 1 | 94.5 | |
| | 2 | 89.3 | |
| | 3 | 68.4 | |
| | 6 | 4.3 | |
| | 9 | 4.8 | 0.824 |
| 1/100 | 2 | 90.7 | |
| | 3 | 83.1 | |
| | 4 | 48.5 | |
| | 5 | 32.2 | |
| | 6 | 6.1 | 2.110 |
| 1/200 | 2 | 98.4 | |
| | 4 | 86.0 | |
| | 5 | 72.3 | |
| | 6 | 49.6 | |
| | 10 | 5.6 | 2.210 |

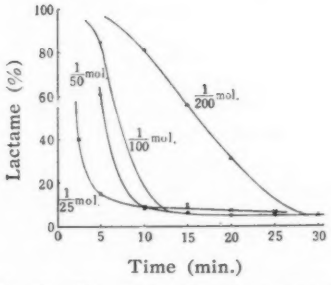


Fig. 5. The rate of polymerization of ε-caprolactam with sodium at 232°C.

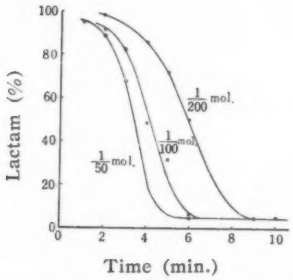


Fig. 6. The rate of polymerization of ε-caprolactam with lithium at 232°C

result is shown in Table III and Fig. 6. The catalytic effect is greater in case of lithium than sodium. Induction periods for the polymerization appear in both cases. The rate of polymerization increases with the quantity of catalyser as shown in Fig. 7.

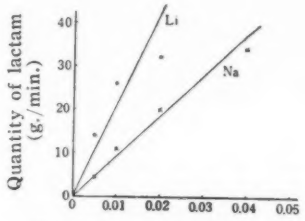


Fig. 7. The rates of polymerization at various quantities of catalyst.

A mixture of 0.041 g. of sodium and 5 g. of ε-caprolactam was heated at 280°, 255°, 238° or 230°C for 10 minutes and then 95 g. of dry ε-caprolactam heated previously at the same temperature was mixed to polymerize. The rate of polymerization is given in Table IV. The induction period disappears in such a case.

TABLE IV
THE RATE OF POLYMERIZATION OF ε-CAPROLACTAM WITH 1/200 MOLES OF SODIUM AT VARIOUS TEMPERATURES

| Temp. (°C) | Time (min.) | Quantity of ε-caprolactam (%) |
|---|---|---|
| 280 | 1 | 6.8 |
| | 5 | 7.6 |
| 255 | 0.3 | 86.2 |
| | 1.5 | 54.9 |
| | 1.75 | 51.9 |
| | 3.5 | 6.4 |
| 238 | 1 | 78.7 |
| | 2 | 65.0 |
| | 2.5 | 59.2 |
| | 2.75 | 54.7 |
| | 3.5 | 45.2 |
| | 4.5 | 31.0 |
| | 10.0 | 5.7 |
| 230 | 0.5 | 91.0 |
| | 1.5 | 85.3 |
| | 2.5 | 81.2 |
| | 3.5 | 73.1 |
| | 4.0 | 67.5 |
| | 4.5 | 63.6 |
| | 5.0 | 55.8 |
| | 5.5 | 54.5 |
| | 7.0 | 44.7 |
| | 8.0 | 34.4 |
| | 9.0 | 22.8 |
| | 11.0 | 21.0 |
| | 15.0 | 15.0 |
| | 30.0 | 5.4 |

The rate of polymerization decreases with the increase in the water content as shown in Fig. 8. When the water content is less than 0.01%,

its influence on polymerization can be assumed to be negligible. The acidic substance in trace makes the polymerization retard. The ε-caprolactam used in experiments, therefore, was once distilled in the presence of 0.1% of sodium hydroxide to remove volatile acidic substances.

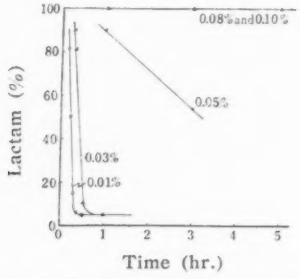


Fig. 8. The rate of polymerization at various water contents.

**(3) Electric Conductivities.** — The change of electric conductivity during polymerization was measured. The results are shown in Figs. 9 and 10. It increases to maximum and then

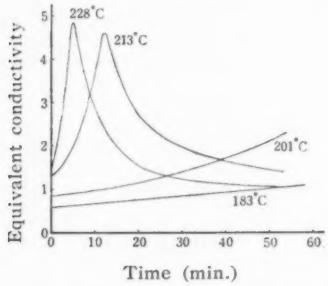


Fig. 9. The electric conductivities of ε-caprolactam during the polymerization in the presence of 0.5 mole % of sodium.

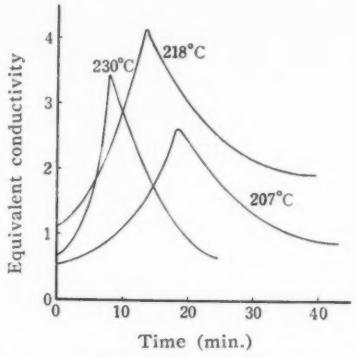


Fig. 10. The electric conductivities of ε-caprolactam during the polymerization in the presence of 0.5 mole % of lithium.

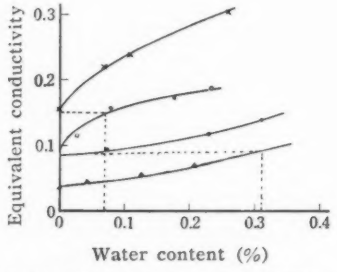


Fig. 11. The electric conductivity of ε-caprolactam at 100°C.
× 0.2 mole % of sodium hydroxide
○ 0.2 mole % of sodium
● 2 mole % of sodium hydroxide
△ 2 mole % sodium

decreases to the equilibrium. It is seen in Fig. 11 that the electric conductivity of ε-caprolactam containing 0.5 or 2 mole percents of sodium and water together is almost the same as that of

TABLE V
ANALYTICAL VALUES OF POLYMER OBTAINED BY HEATING ε-CAPROLACTAM WITH 1/4 MOLES OF SODIUM

| Time of polymerization (min.) | Mole of added sodium (mole/mole) | Condition of extraction | Quantity of alkali in water (mole/mole) | Number of acidic groups (mole/113 g.) | Number of basic groups (mole/113 g.) | Quantities of water-soluble chain oligomers (%) | Quantities of ring monomer (%) | Quantities of ring oligomers (%) |
|---|---|---|---|---|---|---|---|---|
| 5 | 0.252 | 25°C, 2 hrs. | 0.268 | $4.0\times10^{-2}$ | $9.90\times10^{-2}$ | — | — | |
| | | 100°C, 2 hrs. | 0.262 | 2.99 〃 | 8.65 〃 | — | — | |
| 10 | 0.218 | 25°C, 2 hrs. | 0.210 | $3.90\times10^{-2}$ | $9.92\times10^{-2}$ | 12.7 | 28.8 | 0 |
| | | 100°C, 2 hrs. | 0.191 | 2.20 〃 | 8.65 〃 | — | — | — |
| 20 | 0.247 | 25°C, 2 hrs. | 0.273 | $3.24\times10^{-2}$ | $11.2\times10^{-2}$ | 9.7 | 13.7 | 1.2 |
| | | 100°C, 2 hrs. | 0.246 | 3.28 〃 | 9.1 〃 | — | — | — |
| | | 25°C, 5 hrs. | 0.244 | 3.40 〃 | 11.3 〃 | — | — | — |
| | | 100°C, 5 hrs. | 0.245 | 3.11 〃 | 10.5 〃 | — | — | — |

ε-caprolactam containing 0.5 or 2 mole percent of sodium hydroxide. It is expected in the presence of water, therefore, that sodium transforms into its hydroxide before it reacts with ε-caprolactam and loses the catalytic effect. Sodium hydroxide has only a catalytic effect on the ε-caprolactam polymerization in a boiling[3,5] state.

**(4) Quantitative and Qualitative Determination of End Groups of polymer.**—The polymer was steeped in water and then the number of acidic and basic groups were measured[6]. The quantities of alkali, water-soluble chain-oligomers, ring-monomer and oligomers were determined from the analyses of water extracts. The results are shown in Table V. Sodium bonded to polymer is dissolved easily in water. The number of acidic groups of polymer is hardly changed by the polymerization time and the condition of water steeping. It is always about one-third of the number of basic groups.

As concerns the polymer heated in 0.2 N sodium hydroxide solution at 70°C, the number of acidic groups did not change at all as shown in Table VI. The polmer was steeped in absolute methanol, aqueous ammonia solution or isopropyl amine, for 5 hours at room temperature and then washed repeatedly with methanol and water until the washing did not show alkaline. The results

TABLE VI

THE NUMBER OF ACIDIC GROUPS IN POLYMER BEFORE AND AFTER HYDROLYSIS BY 0.2 N SODIUM HYDROXIDE

| Time of polymerization (min.) | Number of acidic groups before hydrolysis (mole/113 g.) | Number of acidic groups after hydrolysis (mole/113 g.) |
|---|---|---|
| 5 | $4.00\times10^{-2}$ | $3.87\times10^{-2}$ |
| 10 | 3.00 〃 | 3.32 〃 |
| 20 | 3.24 〃 | 3.12 〃 |

TABLE VII

THE NUMBER OF ACIDIC AND BASIC GROUPS IN POLYMERS STEEPED IN VARIOUS SOLUTIONS

| Time of polymerization (min.) | Kind of solution | Number of acidic groups (mole/113 g.) | Number of basic groups (mole/113 g.) |
|---|---|---|---|
| 10 | Water | $2.28\times10^{-2}$ | $10.1\times10^{-2}$ |
| | Methanol | — | — |
| | Ammonia | $1.70\times10^{-2}$ | $10.4\times10^{-2}$ |
| | Isopropyl amine | 0.40 〃 | 10.5 〃 |
| 20 | Water | 1.96 〃 | 12.4 〃 |
| | Methanol | 0.10 〃 | 12.7 〃 |
| | Ammonia | 0.25 〃 | 10.8 〃 |
| | Isopropyl amine | 0.36 〃 | 11.1 〃 |

5) H. Yumoto and N. Ogata, to This Bulletin, **31**, 913 (1958).

6) J. E. Walz and G. B. Taylor. *Anal. Chem.*, **91**, 448 (1947).

7) H. Zahn and H. Wolf, *Melliand Textilber.*, **32**, 317 (1951).

are given in Table VII. The number of acidic groups in case of isopropyl amine was very small and isopropyl amine was found on the hydrolysis.

The polymer and its water extract were colorized reddish yellow by the diazo reaction and grey by the Nessler's reagent, while ε-aminocaproic acid was not. On the paperchromatogram of the water extract, a spot having the same Rf value as that of 6-aminohexanol appear as shown in Table VIII, besides those corresponding to ε-aminocaproic acid, di- and tri-ε-aminocaproic acids. In the infrared spectrum of the water extract, the absorption bands of hydroxyl and free =N—H group appear at 2.8 μ and 2.98 μ.

TABLE VIII

$R_f$ VALUES OF PRODUCTS OBTAINED BY EXTRACTION OF POLYMER WITH WATER

| Sample | $R_f$ values of spots | | | | |
|---|---|---|---|---|---|
| Product | 0.19 | 0.37 | 0.46 | 0.54 | 0.94 |
| ε-Aminocaproic acid | 0.19 | | | | |
| Di-ε-aminocaproic acid | | 0.37 | | | |
| Tri-ε-aminocaproic acid | | | 0.46 | | |
| 6-Aminohexanol | | | | | 0.94 |

The polymer, of which basic groups had previously been acetylated, was steeped in 1% alkaline solution of potassium permanganate for 2 hours at room temperature. The number of acidic groups increases to the number of basic groups as shown in Table IX.

TABLE IX

THE NUMBER OF END GROUPS OF POLYMER OXIDIZED BY 1% ALKALINE POTASSIUM PERMANGANATE SOLUTION

| Sample | Number of carboxyl groups (mole/113 g.) | Number of amino groups (mole/113 g.) |
|---|---|---|
| Polymer at first | $2.50\times10^{-2}$ | $10.2\times10^{-2}$ |
| Acetylated polymer | 3.50 〃 | 0 |
| Oxidized polymer | 7.50 〃 | 0 |

From these experimental results, it is expected that the end groups of polymer steeped in water are carboxyl, amino and hydroxyl groups. The third is probably produced by the reduction. No decarboxylation occures because neither carbon monoxide nore dioxide was found during the polymerization.

## Discussion

It is expected that the catalytic polymerization of ε-caprolactam by alkali metal is an ionic reaction and the reaction proceeds through the following mechanism:

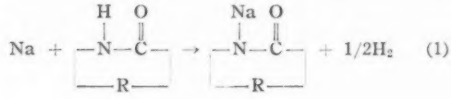


(1)

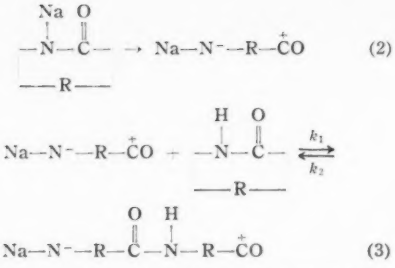

(2)



(3)

As the number of amino groups is about 40 percent of the mole number of added sodium, the reactions between chain molecules may also occur as shown below;

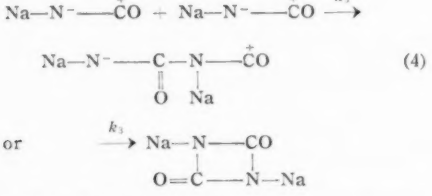

(4)



If the following termination reaction occured, the number of carboxyl groups should be increased by boiling the polymer in the aqueous solution of acid or base, because the bond such as $-C(=O)-N-C(=O)-$ is easily hydrolyzed. The number of carboxyl groups was scarely changed. It is expected therefore that the termination reaction such as shown in equation 5 does not occur.

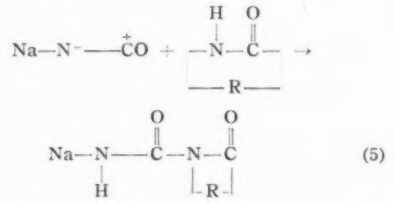

(5)

Sodium combined to polymer dissolves in water because the bond >N—Na is affected by water and amino groups are formed. On the other hand carbonyl cations react with water to form carboxyl groups. When polymer is steeped in an amine, carbonyl cations are changed into acid amides.

When dry ε-caprolactam is added to the molten polymer catalyzed by sodium, reactions 3 and 4 may occur and the following equations can be derived, where $[\sum M_i]$ and $[L]$ are chain molecule and lactam monomer and $k_1$, $k_2$ and $k_3$ are rate constants of reactions shown by arrows and $A$ is the mole number of the Brownian motion unit in whole reaction phase[8].

$$d[L/A]/dt = k_2([\sum M_{i+1}]/A) - k_1([\sum M_i][L]/A^2) \quad (6)$$

$$-d[\sum M_i/A]/dt = k_3([\sum M_i]^2/A^2) \quad (7)$$

Suppose $d[L/A]/dt=0$ at equilibrium and $[\sum M_i] \fallingdotseq [\sum M_{i+1}]$ in high polymeric system, then

$$k_2 = k_1([L_\infty]/A) \quad (8)$$

where $[L_\infty]$ represents $[L]$ at equilibrium. Substituting Eq. 8 into Eq. 6, the following equation is obtained;

$$d[L/A]/dt = k_1([\sum M_i]/A^2)([L_\infty]-[L]) \quad (9)$$

Integreating Eq. 7 under the conditions that $[\sum M_i]$ is $[\sum M_i^0]$ at $t=0$ and $A$ is invariable.

$$[\sum M_i]/A = [\sum M_i^0]/(k_3[\sum M_i^0]t + A) \quad (10)$$

Substituting Eq. 10 into Eq. 9 and integrating it under the condition that $[L]$ is $[L^0]$ at $t=0$:

$$\begin{aligned}\ln\{([L_\infty]-[L^0])/([L_\infty]-[L])\} &= (k_1/k_3)\ln\{(k_3[\sum M_i^0]t/A)+1\} \\ &= (k_1/k_3)\{k_3[\sum M_i^0]t/A \\ &\quad -(1/2)(k_3/A[\sum M_i^0])^2t^2+\cdots\} \\ &= k_1[\sum M_i^0]t/A \\ &\quad -(k_1/k_3/2)([\sum M_i^0]/A)^2t^2+\cdots \end{aligned} \quad (11)$$

When $\ln\{([L_\infty]-[L^0])/([L_\infty]-[L])\}$ are plotted against $t$ a linear relation is obtained from the data of Table IV (Fig. 12). Therefore, the rest below the second term can be assumed to be negligible. Then

$$\ln([L_\infty]-[L^0])/([L_\infty]-[L]) \fallingdotseq k_1[\sum M_i^0]t/A \quad (12)$$

The value of $k_1[\sum M_i^0]/A$ can be determined from Fig. 12, as shown in Table X.

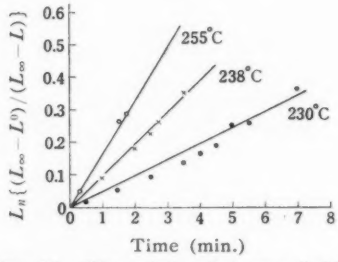


Fig. 12. The relation between $L_n\{(L_\infty - L^0)/(L_\infty - L)$ and time.

8) H. Yumoto, This Bulletin, **28**, 101 (1955).

TABLE X

| Temp. (°C) | $k_1\sum M_i^0/A$ (mole/mol, min.) | $L_\infty$ (%) | $K/A$ |
|---|---|---|---|
| 230 | 0.14 | 5.4 | 18.4 |
| 238 | 0.27 | — | — |
| 255 | 0.38 | 6.4 | 15.6 |
| 280 | — | 7.2 | 13.9 |

The logarithm of $k_1[\sum M_i^0]A$ is plotted against the reciprocal of the absolute temperature in which $\Delta E_{act.}$ of about 22 kcal./mole is estimated. This value is greater than the activation energy of 8.7 kcal./mole for the polymerization of ε-caprolactam in the presence[7] of water.

## Summary

When alkali metal reacts with ε-caprolactam, it was found experimentally that hydrogen and *N*-alkali metal ε-caprolactam are produced at first. The rate of polymerization of ε-caprolactam in the presence of *N*-alkali metal derivative was studied. The change in the electric conductivity during polymerization was also measured. In this case the polymerization is expected to proceed by an ionized molecule.

The authors wish to thank to Dr. K. Hoshino and Dr. H. Kobayashi who instructed them in these studies and permitted this publication and Mr. M. Ishikawa et al. who collaborated with them on experiments.

*Research Department of Toyo Rayon Co. Ltd. Minato-ku, Nagoya,*

---

# *Studies on Polymerization and Depolymerization of ε-Caprolactam Polymer VI*. On the Reaction Mechanism of the ε-Caprolactam Polymerization by Alkali Metal Compound.***

By Hirosuke YUMOTO and Naoya OGATA

(Received on June 2, 1958)

It is well known that[1,2,3] alkali metal compounds cause the polymerization of ε-caprolactam and the high polymer can be obtained in several minutes. The mechanism of the reaction has been also studied[2]. It is the main object of this paper to elucidate the reaction mechanism and to find the method for giving reproducible results.

## Experimental

**1. The Reaction Product of ε-Caprolactam and Alkali Metal Compound.**—The mixtures of dry ε-caprolactam and sodium hydroxide or sodium carbonate were heated at 270°C for 30 minutes in a nitrogen stream. In this case a stream of nitrogen was passed through a calcium chloride tube or aqueous barium hydroxide solution in order to detect the generated volatile compound. Water in case of sodium hydroxide or water and carbon dioxide in case of sodium carbonate were detected. Since the mixed components were not dissolved completely, the molar ratio of the product to the added sodium hydroxide or carbonate was smaller than 1 as shown in Tables I and II.

TABLE I

MOLAR RATIO OF WATER TO SODIUM HYDROXIDE (270°C)

| Molar ratio of NaOH to lactam | reaction time (min.) | Molar ratio of water to NaOH |
|---|---|---|
| 1 | 25 | 0.191 |
| 1 | 45 | 0.251 |
| 1/2 | 60 | 0.664 |
| 1/2 | 50 | 0.588 |
| 1/2 | 20 | 0.368 |

TABLE II

MOLAR RATIO OF CARBON DIOXIDE TO SODIUM CARBONATE (270°C)

| Molar ratio of $Na_2CO_3$ to lactam | Reaction time (min.) | Molar ratio of $CO_2$ to $Na_2CO_3$ |
|---|---|---|
| 1 | 60 | 0.102 |
| 1 | 60 | 0.250 |

* V, This Bulltin, **31**, 907 (1958).

** Presented at the 11 th Annual Meeting of the Chemical Society of Japan in Tokyo on April 5, 1958.

1) BIOS Final Reports, No. 1472, p. 14.
2) O. Wichterle, *Faserforsch. und Textiltech.*, **6**, 237 (1955).
3) W. Griehl, ibid., **7**, 207, (1956).

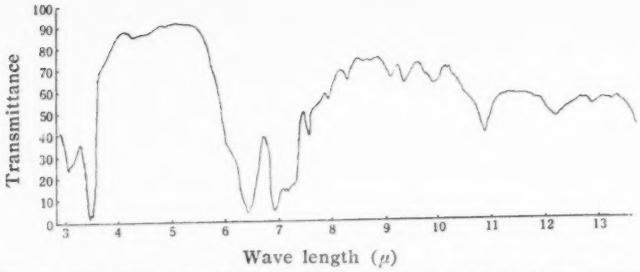


Fig. 1. The infrared spectrum of the reaction product of equal mole of sodium hydroxide and ε-caprolactam (270°C, 30 min.)

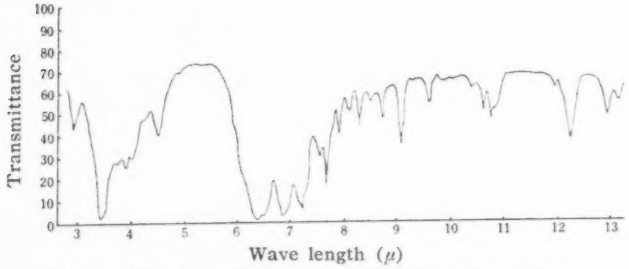


Fig. 2. The infrared spectrum of sodium ε-aminocaproate.

The reaction product of equal moles of sodium hydroxide and ε-caprolactam resembles sodium ε-aminocaproate in the infrared spectrum as shown in Figs. 1 and 2. The quantities of sodium ε-aminocaproate, ε-caprolactam-monomer and -oligomers in the product were analyzed[4,5]. The results are given in Table III.

TABLE III
ANALYSIS OF REACTION PRODUCT OF EQUAL MOLES OF ε-CAPROLACTAM AND SODIUM HYDROXIDE

| Product | Yield (%) |
|---|---|
| Sodium ε-aminocaproate | 85 |
| Lactam monomer | 15 |
| Lactam oligomers | 0 |

**2. Polymerization of ε-Caprolactam by Alkali Metal Compounds.**—The alkali metal compound must be added to the boiling ε-caprolactam for the polymerization. ε-Caprolactam was kept boiling at 290°C previously and 0.5 mole percent of sodium -hydroxide, -carbonate, -cyanate, -acetate, -formate, -ε-aminocaproate, potassium -hydroxide or -carbonate, was added subsequently. The rate of polymerization is given in Fig. 3.

When alkali metal compound is mixed previously in ε-caprolactam and then the mixture is boiled, it is difficult to polymerize and the rate of the reaction is not reproducible. When an alcoholic solution of alkali metal hydroxide is added to the boiling ε-caprolactam, the polymerization hardly ever occurs either. It may be said, therefore, that the solid surface must be considered for the catalytic effect.

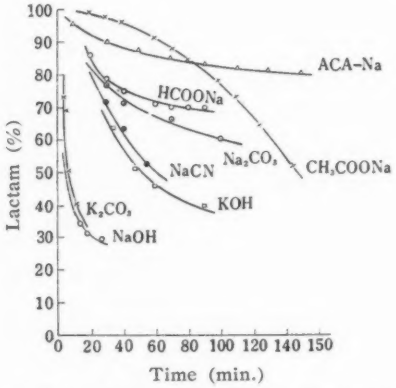


Fig. 3. The rate of polymerization in the presence of various alkali compounds.

In case of the polymerization of pyrolidone (γ-butyrolactam), *N*-acetyl pyrolidone is the promotor in the presence of potassium hydroxide[6]. ε-Caprolactam was heated at 290°C in the presence of 0.5 mole percent of sodium hydroxide and various mole percents of *N*-acetyl-ε-caprolactam.

4) H. Zahn and H. Wolf, *Melliand Textilber.*, **32**, 317 (1951).
5) P. H. Hermans, *J. Appl. Chem.*, **5**, 493 (1955).
6) W. O. Ney et al., U. S. *Atomic Energy Comm. Nuclear Soc. Abstr.*, 2,739,959 (1956).

TABLE IV

THE RATE OF POLYMERIZATION OF ε-CAPROLACTAM BY COLLOIDAL SODIUM CARBONATE

| $Na_2CO_3$ (mole %) | Time (min.) | Water-soluble component (%) | $\eta_{rel}^{98\%\ H_2SO_4}$ | 25°C $[\eta]_{cresol}$ |
|---|---|---|---|---|
| 0.5 | 30 | 15.0 | 2.10 | 0.754 |
| 0.25 | 2 | 98.2 | — | |
| | 3 | 37.2 | 4.47 | |
| | 4 | 16.5 | 4.68 | 2.017 |
| | 10 | 13.5 | 3.35 | |
| | 30 | 14.0 | 2.85 | |
| 0.10 | 2.5 | 19.8 | 8.69 | 2·850 |
| | 5 | 21.4 | 5.35 | 2.210 |
| | 10 | 17.7 | 4.56 | |
| | 30 | 13.6 | 3.09 | 1.172 |
| 0.05 | 6 | 49.5 | 7.45 | |
| | 10 | 38.5 | 7.77 | |
| | 15 | 22.9 | 3.92 | |
| | 30 | 29.8 | 4.18 | |
| 0.025 | 60 | 68.2 | — | |

TABLE V

ANALYSES OF POLYMERS OBTAINED BY HEATING ε-caprolactam at 250°C UNDER REDUCED PRESSURE OF 250 mmHg WITH COLLOIDAL SODIUM CARBONATE

| $Na_2CO_3$ (mole %) | Time (min.) | Water-soluble component (%) | $\eta_{rel}^{98\%\ H_2SO_4}$ | 25°C $[\eta]_{cresol}$ |
|---|---|---|---|---|
| 0.1 | 30 | 11.0 | 11.2 | 3.27 |
| 0.05 | 30 | 76.9 | — | — |

TABLE VI

ANALYSES OF POLYMERS OBTAINED BY HEATING ε-CAPROLACTAM WITH 0.1 MOLE % OF COLLOIDAL SODIUM CARBONATE AT VARIOUS CONDITIONS

| Polymerization condition | Temp. (°C) | Time (min.) | Water-soluble component (%) | $\eta_{rel}^{98\%\ H_2SO_4}$ |
|---|---|---|---|---|
| with 10% tetralin | 290 | 10 | 17.3 | 6.27 |
| with 10% toluene | 290 | 10 | 14.9 | 5.69 |
| with 20% xylene | 250 | 120 | 64.0 | 2.84 |
| with 30% xylene | 250 | 60 | 43.7 | 6.55 |
| with 20% toluene | 250 | 60 | 100.0 | — |
| with 30% toluene | 250 | 60 | 41.3 | 6.59 |
| with 30% xylene | 230 | 60 | 100.0 | — |
| with 30% toluene | 230 | 60 | 100.0 | — |
| with blowing dry | 250 | 60 | 13.5 | 6.69 |
| nitrogen into | 250 | 60 | 17.6 | 8.80 |
| ε-caprolactam | 250 | 37 | 16.4 | — |
| | 230 | 60 | 100.0 | |

TABLE VII

THE RATE OF POLYMERIZATION OF ε-CAPROLACTAM BY COLLOIDAL POTASSIUM CARBONATE (290°C)

| $K_2CO_3$ (mole %) | Time (min.) | Water-soluble component (%) | 25°C $[\eta]_{cresol}$ |
|---|---|---|---|
| 0.2 | 3 | 13.5 | 4.52 |
| | 5 | 14.3 | 4.18 |
| | 10 | 16.8 | 3.84 |
| | 30 | 14.4 | 2.88 |
| 0.1 | 3 | 25.7 | 7.57 |
| | 5 | 35.4 | 5.93 |
| | 11.5 | 20.4 | 4.78 |
| | 30 | 29.3 | 3.16 |
| 0.05 | 10 | 68.8 | — |
| | 30 | 57.4 | 4.77 |

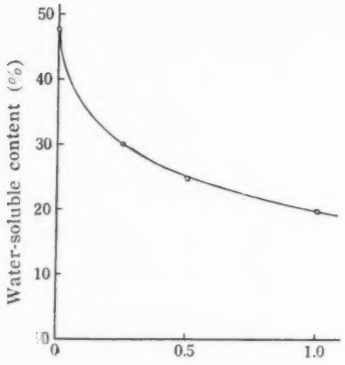


Fig. 4. The quantity of water-soluble content in the polymer in the presence of various mole percents of *N*-acetyl-ε-caprolactam (290°C, 1 hr.)

The quantities of water-soluble contents in the products are shown in Fig. 4.

Since the alkali metal compound is assumed to have great catalytic effect at its surface as stated above, it is expected that the greater effect can be obtained in case of dispersing the alkali metal compound colloidally in ε-caprolactam in order to increase the solid surface. Sodium hydroxide is dissolved previously in ε-caprolactam at 100°C and then carbon dioxide is bubbled for about 30 min. to 1 hour. The stable colloidal dispersion of sodium carbonate is obtained. The diameter of sodium carbonate is less than 0.1 μ. ε-Caprolactam containing 0.5 to 0.025 mole percent of colloidal sodium carbonate was boiled at 290°C. The rate of polymerization is given in Table IV. In case of 0.25 to 0.1 mole percent it took 3 to 4 minutes to polymerize. The reaction is reproducible. The degree of polymerization reaches maximum after 2 to 5 minutes and then decreases gradually. Even if sodium carbonate is pulverized finely in a mortar and added to the boiling ε-caprolactam, such a high rate of reaction can not be obtained. When ε-caprolactam was boiled at 250°C under the reduced pressure of 250 mmHg in the presence of the colloidal sodium carbonate, the decrease in the polymerization degree after the maximum is slower than at 290°C as shown in Table V.

When the solvent of low boiling point is dissolved in ε-caprolactam, the boiling can occur under the boiling temperature of ε-caprolactam (263°C). As shown in Table VI, ε-caprolactam containing 0.1 mole percent of colloidal sodium carbonate, polymerizes in the presence of 30% of xylene or toluene for about 20 minutes at 250°C.

When dry nitrogen was bubbled, polymerization also occurred under the boiling temperature as shown in Table VI. The polymerization by the colloidal potassium carbonate is slower than that by sodium carbonate, as shown in Table VII.

## Discussion

At first sodium hydroxide or carbonate may react with ε-caprolactam into *N*-sodium ε-caprolactam as follows:

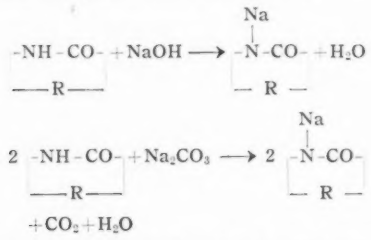


Water or carbon dioxide is analysed as mentioned above. Sodium ε-aminocaproate is also found in the reaction product practically. It can be assumed that sodium ε-caprolactam is hydrolyzed easily into sodium ε-aminocaproate in the presence of water. The reason why boiling is necessary for the polymerization seems to be ascribed to rapid removal of water or carbon dioxide from the reaction phase. Therefore the salt such as sodium stearate or adipate which yields non-volatile acid can not cause the polymerization. It has been reported that –COONa does not cause the reaction[7].

*N*-Acetyl ε-caprolactam functions slighlty as a promotor in the presence of alkali metal hydroxide. After *N*-alkali metal ε-caprolactam is formed, the reaction mechanism can be assumed to be similar to that of polymerization in the presence of alkali metal[8]. The catalytic effect of alkali metal compound is expected to be eminent at its solid surface, because the colloidal dispersion is much more effective than the pulverized solid. The degree of polymerization is very large in case of using colloidal alkali metal compound. The polymer has a rubber-like elasticity in a molten state.

## Summary

The basic compound of alkali metal reacts with ε-caprolactam and gives at first *N*-alkali metal ε-caprolactam. It can cause the polymerization of ε-caprolactam. The boiling of the reaction phase is necessary for making the reaction proceed. The polymerization is especially rapid and reproducible in case of dispersing alkali

7) H.Yumoto and N. Ogata, *Makromolekulare Chem.*, **25**, 91 (1958).
8) H. Yumoto and N. Ogata, This Bulletin, **31**, 907 (1958).

metal compound colloidally in ε-caprolactam. It is supposed, therefore, that the solid surface of the catalyser is a very important factor in the polymerization.

The authors wish to thank to Dr. K. Hoshino and Dr. H. Kobayashi who instructed them and permitted the publication of this study and Mr. S. Yamauchi et al. who collaborated with them on experiments.

*Research Department of Toyo Rayon Co., Ltd., Minato-ku, Nagoya*

# *The Determination of Boron in Glass Using Radium-Beryllium Neutron Source (Neutron Absorption Technique)*

By Yuzuru KUSAKA

(Received February 10, 1958)

When a substance containing an element with a high absorption cross section for neutron is placed in a flux of neutrons, a reduction of the flux is caused. When the neutron absorption of other elements in the sample is negligibly small, the reduction degree of the neutron flux can be used as a measure of the quantity of the neutron-absorbing elements.

Such a neutron absorption method has been utilized as a means of determining the boron content of various substances[1-4], because of the high cross section of boron for thermal neutrons ($\sigma_{abs.}=755$ barn), of which the nuclear reaction is $^{10}B(n.\alpha)^{7}Li$. The author has applied this neutron absorption technique to the determination of boron in borosilicate glass with some interesting results.

## Experimental and Discussion

The activation source consisted of a mixture of 84.2 mg. of radium bromide (49.3 mg. as radium element) with beryllium, which was sealed in a platinum tube (length: 40.0 mm., diameter: 5.0 mm., wall-thickness: 0.5 mm.). The source was surrounded by paraffin to moderate the fast neutrons to thermal velocities and to reflect these neutrons.

**Studies on the Arrangements of Paraffin.**—In order to obtain as much thermal neutron flux as possible, the following experiments were tried. In these experiments, the neutron detector was a silver plate (silver content, 75%; diameter, 23 mm.; weight, 4.6 g.). The time of neutron irradiation was 20 minutes and, after an interval of 30 seconds, the induced radioactivity ($^{110}$Ag [24.2 sec.], $^{108}$Ag[2.3 min.]) was measured for 5 minutes by means of an end-window G. M. counter (thickness of mica window: 1.96 mg./cm$^2$) at a fixed position.

When a cadmium filter (thickness: 0.6 mm.) which absorbs all the neutrons with energies less than 0.4 eV. is used, the radioactivity produced by thermal neutrons only is given by the following equation.

$$I_{thermal}=I_0-I_{Cd}$$

$I_{thermal}$: the radioactivity obtained by thermal neutrons.

$I_0$: the radioactivity obtained without cadmium filter.

$I_{Cd}$: the radioactivity obtained with cadmium filter*.

In the first experiment the relationship between the thermal neutron density at the center of an upper surface of paraffin and its distance from the neutron source was studied. The maximum neutron flux was obtained at 2.5 cm. from the source as is shown Fig. 1.

In the second experiment, a cylindrical hole (diameter: 4.2 cm.) was bored through the paraffin block above the neutron source, as is shown by the dotted line in Fig. 2, and the relationship between the thermal neutron density at the outlet of the hole and the hole length was investigated.

The results obtained are shown in Fig. 3.

1) P. Süe and J. Martelly, *Bull. Soc. Chim. France*, **1946**, 103, 410.
2) J. Govaerts, *Exper.* **6**, 459 (1950).
3) M. Green and G. R. Martin, *Trans. Faraday Soc.* **48**, 416 (1950).
4) R. P. Hamlen and W. S. Koski, *Anal. Chem.* **28**, 1631 (1956).

* As shown on Fig. 2, a cadmium plate is put on the silver detector at every $I_0$ and $I_{Cd}$ measurement to shut out thermal neutrons from the upper side of the detector. In the case of $I_{Cd}$ measurement, two Cadmium plates must be put separately on and beneath the silver detector to shut out thermal neutrons from each side of the detector.

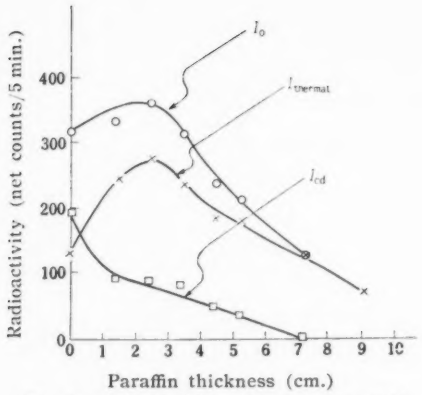


Fig. 1. Relationship between paraffin thickness and radioactivity induced in silver plate.

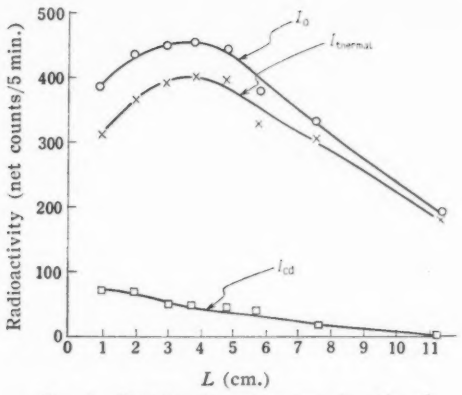


Fig. 3. Relationship between length of hole in paraffin ("L" in Fig. 2) and radioactivity induced in silver plate.

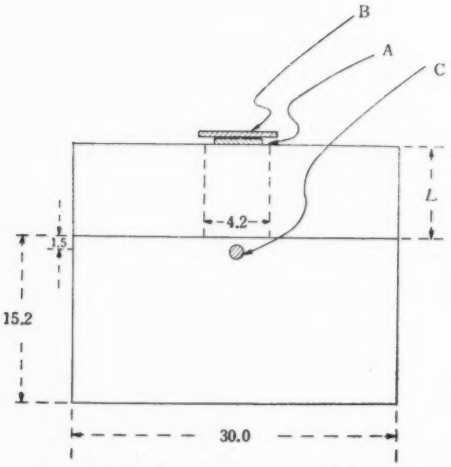


Fig. 2. Irradiation geometry (Dimensions in cm.)
A=silver plate. B=cadmium plate.
C=radium+beryllium neutron source.

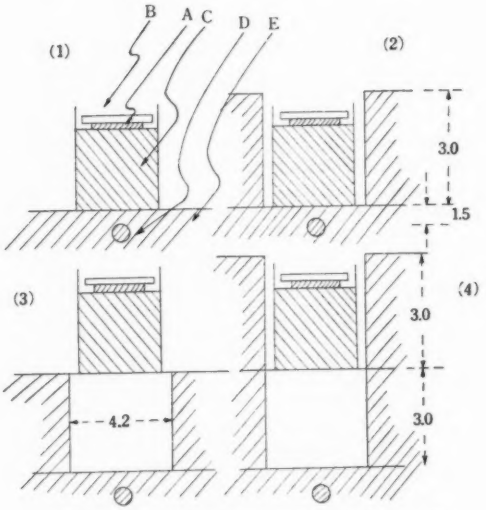


Fig. 4. Experiments for evaluating irradiation geometry. (Dimensions in cm.)
A=silver plate. B=cadmium plate.
C=sample powder. D=radium+beryllium neutron source. E=paraffin.

From these experimental results it is observed that a remarkable increase in neutron flux is caused by the use of a paraffin block with a hole in its centre. For example, the thermal neutron density at 5 cm. from the neutron source is about 2.2 times as great as that obtained by the use of a paraffin block without a hole. This phenomenon must be due to the "howitzer effect"[5,6], by which the collimation of neutrons is caused.

This effect was also observed in the following experiment. Ten grams of silicic oxide power (sieved through a 100 mesh screen) was placed in an aluminum cup (diameter: 3.0 cm., thickness: 0.05 cm.) and was irradiated with neutrons as shown in Fig. 4. The radioactivities of the silver detector in each case are shown in Table I. Then, in order to obtain stronger thermal

TABLE I
TESTS FOR IRRADIATION GEOMETRY

| Geometry No. (in Fig. 4) | $I_{thermal}$ (net counts/5 min.) |
|---|---|
| 1 | 82 |
| 2 | 477 |
| 3 | 90 |
| 4 | 439 |

5) F. L. Hopwood and T. A. Chalmers, *Nature*, **135**, 341 (1935).
6) G. A. Fink, *Phys. Rev.*, **50**, 738 (1936).

neutron flux, such geometrical arrangement as 2 or 4 in Fig. 4 would be more advantageous for neutron absorption analysis.

**Studies on the Determination of Boron Content in Borosilicate Glass.**—Relative cross section values of the various components in three practical examples of borosilicate glass were calculated[7] and summarized in Table II. As is shown in the table, the greater part of the cross section values (about 99% in $\sigma_{abs}$ and about 95% in $\sigma_t$) in borosilicate glass is attributed to boron in the sample. Therefore it would be possible to apply the neutron absorption technique effectively to boron analysis of such samples.

TABLE II
RELATIVE CROSS SECTION VALUES OF VARIOUS COMPONENTS IN GLASS

Example 1
(Mean value of borosilicate glass[8])

| Component | Composition (%) | $\sigma_{abs}$ (%) | $\sigma_t$ (%) |
|---|---|---|---|
| $SiO_2$ | 80 | 0.06 | 4.23 |
| $Na_2O$ | 4 | 0.02 | 0.26 |
| $B_2O_3$ | 14 | 99.92 | 95.41 |
| $Al_2O_3$ | 2 | — | 0.10 |

Example 2

| Component | Composition (%) | $\sigma_{abs}$ (%) | $\sigma_t$ (%) |
|---|---|---|---|
| $SiO_2$ | 68.60 | 0.03 | 2.37 |
| $Na_2O$ | 3.84 | 0.01 | 0.17 |
| $K_2O$ | 5.41 | 0.05 | 0.13 |
| $Al_2O_3$ | 0.34 | — | 0.01 |
| $B_2O_3$ | 21.81 | 99.91 | 97.32 |

Example 3
(BK-7 glass)

| Component | Composition (%) | $\sigma_{abs}$ (%) | $\sigma_t$ (%) |
|---|---|---|---|
| $SiO_2$ | 69.58 | 0.07 | 5.09 |
| $Na_2O$ | 8.44 | 0.06 | 0.77 |
| $K_2O$ | 8.32 | 0.16 | 0.42 |
| MgO | 0.08 | — | 0.01 |
| CaO | 0.10 | — | 0.01 |
| BaO | 2.55 | 0.01 | 0.10 |
| $B_2O_3$ | 9.91 | 99.69 | 93.54 |
| $Al_2O_3$ | 0.44 | — | 0.03 |
| $As_2O_3$ | 0.31 | 0.01 | 0.02 |

The geometrical arrangement of the paraffin, the analyzed sample and the neutron source in the experiments is shown in Fig. 5. In these cases, a round

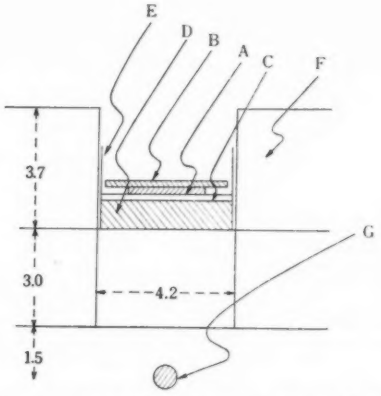


Fig. 5. Irradiation geometry for analysis (Dimensions in cm.)
A=indium plate. B=cadmium plate. C=plastic plate (thickness: 0.1 cm.). D=sample powder. E=plastic sample container. F=paraffin. G=radium+beryllium neutron source.

metallic plate of indium (diameter, 22 mm.; weight, 2.1 g.) was used as neutron detector. The irradiation samples were the mixed powder (100 mesh) of glass and aluminum oxide as the diluent (weight ratio=1:1.5). Ten grams of it were irradiated for 2.0 hours, in which case the saturation factor of $^{116m}In$ is 0.78. After an interval of one minute, the induced radioactivity of the indium detector was measured for 20 minutes. The method of determining the thermal neutron density is similar to that illustrated above.

By using a calibration curve, as shown

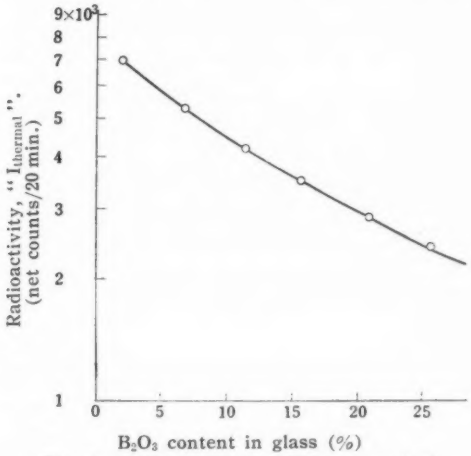


Fig. 6. Calibration curve in boron analysis.

7) The values in Table II were calculated from D. J. Hughes and J. A. Harvey's, "Neutron Cross Section", BNL 325 (1955), (U. S. A. E. C).
8) "Encyclopedia of Chemical Technology" Vol 7, Interscience Encyclopedia Inc., New York, p 181.

TABLE III

BORON ANALYSIS BY THIS METHOD AND COMPARISION WITH CHEMICAL METHOD

| Sample* | Induced radioactivity (net counts/20 min.) | | | | $B_2O_3$ content (%) | |
|---|---|---|---|---|---|---|
| | $I_0$. | $I_{cd}$. | $I_{thermal}$ | Probable error | Neutron method | Chemical method |
| 1 | 8159 | 2081 | 6078 | 68 | 4.3±0.2 | 4.44 |
| 2 | 6457 | 1994 | 4463 | 62 | 10.1±0.3 | 9.91 |
| 3 | 5593 | 1861 | 3732 | 58 | 14.4±0.4 | 13.15 |
| 4 | 5544 | 1930 | 3614 | 58 | 15.2±0.4 | 15.91 |
| 5 | 4390 | 1817 | 2573 | 53 | 23.9±0.6 | 23.28 |

* The samples used for this study were as follows;
No. 1: Optical glass containing BaO (19.7%), ZnO (11.9%) and PbO (3.2%), called as BaK-4.
No. 2: Optical glass containing BaO (2.5%), called as BK-7.
No. 3 and No. 4.: Commercial borosilicate glasses.

in Fig. 6, which is obtained from measurements on the glass of known boron content, it is possible to determine the boron content in any borosilicate glass.

Some experimental results by this method and the comparisons with the chemical method[9] are summarized in Table III.

The results given in Table III indicate the validity of the neutron absorption method. Fig. 7 shows the plots of the probable error in analysis versus the content of boric oxide in glass. This graph represents the degree of accuracy that can be expected from the method.

The most striking error involved in this method is due to the statistical uncertainty during the radioactivity measurement.

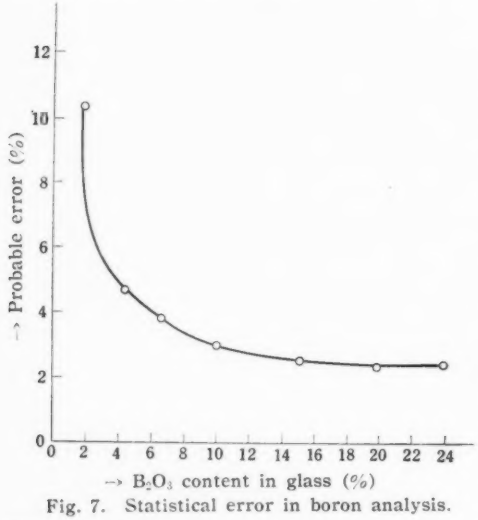


Fig. 7. Statistical error in boron analysis.

9) W. F. Hillebrand and G. E. F. Lundell, "Applied Inorg. Analysis", Wiley, New York, (1929), p 611.

## Summary

The neutron absorption technique using radium-beryllium neutron source has been shown to be useful for rapid assay of boron in the samples containing other low cross-section elements. This method may also be useful for the analyses of other high cross-section elements.

The writer wishes to express his hearty thanks to Professor Masayoshi Ishibashi of Kyoto University and President Bunsaku Arakatsu and other members of the Chemical and Physical Laboratory of Kōnan University for their kind guidance and valuable advice through this study, to Professor Shoji Tsuchihashi of Kōbe University for furnishing glass samples, and to Mr. Haruo Tsuji for considerable help in repeating and checking the procedures in many of the experiments.

*Department of Chemistry, Faculty of Science, Kōnan University, Higashinada-ku, Kōbe*

# *Rotatory Dispersion of Metallic Co-ordination Compounds. I. Rotatory Dispersion in the First and the Second Absorption Bands of Cobaltic Compounds*[1,2]

By Jinsai HIDAKA, Shoichiro YAMADA and Ryutaro TSUCHIDA

(Received June 11, 1958)

In order to understand the nature of absorption bands, analyses of rotatory dispersion curves are considered to be of importance. In fact, there are a number of reports available concerning the rotatory dispersion of cobaltic complexes with ethylenediamine[3-7] but many of these studies are confined within a comparatively narrow wave-length region. Rotatory dispersion measurements over wider wave-length regions have been reported in some of the compounds, but only a very few of them have been precisely analyzed. In these circumstances, it was thought to be desirable to study more systematically the rotatory dispersion of metallic complexes on the basis of measurements in wider wave-length regions.

This paper presents rotatory dispersion measurements of optically active *cis*-dichloro-bis-(ethylenediamine)-cobalt(III) chloride and *cis*-chloronitro-bis-(ethylenediamine)-cobalt(III) chloride in the visible and ultraviolet region, and discusses the results of the measurements in relation to their absorption spectra.

## Experimental

**Measurements.**—A Rudolph photoelectric polarimeter 200S-80 was employed in the rotatory dispersion measurement.

The measurements were made at room temperature in the region from 666 mμ to 312 mμ using mainly the lines of the mercury spectrum: $58\times10^{13}$/sec. (577 mμ), $55\times10^{13}$/sec. (546 mμ), $68.8\times10^{13}$/sec. (436 mμ), $74\times10^{13}$/sec. (405 mμ), $82\times10^{13}$/sec. (365 mμ) and $89.8\times10^{13}$/sec. (334 mμ). A xenon-or a tungsten lamp was used occasionally.

The solvent employed was methyl alcohol for *cis*-dichloro-bis-(ethylenediamine)-cobalt(III) chloride and 50% hydrochloric acid for *cis*-chloronitro-bis-(ethylenediamine)-cobalt(III) chloride.

In the measurements with *cis*-dichloro-bis-(ethylenediamine)-cobalt(III) chloride, its solution was alternated with a new one at times. As *cis*-chloronitro-bis-(ethylenediamine)-cobalt (III) chloride is so unstable in solution that it is liable to undergo aquotization[8]. Therefore, its freshly prepared solution was used in each measurement. The measurements were made as rapidly as possible after preparation of the solution to keep the reactions of the complex with water at a minimum.

The concentrations for the measurements of *cis*-dichloro-bis-(ethylenediamine)-cobalt(III) chloride were $1/3\times10^{3}$ F, $1/6\times10^{3}$ F and $1/8\times10^{3}$ F, and the cell lengths 20, 10 and 2 cm. For *cis*-chloronitro-bis-(ethylenediamine)-cobalt(III) chloride, the concentrations used were $1/3\times10^{3}$ F, $1/6\times10^{3}$ F and $1/8\times10^{3}$ F, and the cell lengths 20, 10 and 2 cm.

**Material.**—Racemic *cis*-dichloro-bis-(ethylenediamine)-cobalt(III) chloride was prepared in violet crystals by the method of Werner[8] and resolved by the method of Bailar et al[9]. The preparation and the resolution of racemic *cis*-chloronitro-bis-(ethylenediamine)-cobalt(III) chloride were made according to the directions of Werner[10].

Both the optically active compounds, which were precipitated as more insoluble salts with *d*-α-bromocamphorsulphonic acid, gave positive values of optical rotation in sodium D line. According to Bailar, *cis*-dichloro-bis-(ethylenediamine)-cobalt(III) chloride was a levo-salt and gave a negative value in sodium D line, but our and Douglas's experiments[11] have given a positive one. Thus the reagents employed in the present study may be regarded as *cis*-dextro-[Co $en_2Cl_2$]Cl and *cis*-dextro-[Co $en_2ClNO_2$]Cl.

1) R. Tsuchida, S. Yamada and J. Hidaka, Presented before the Symposium on Metallic Co-ordination Compounds, Nagoya, October, 1957.

2) Abstracted in part from a thesis submitted by J. Hidaka to the Faculty of Science of Osaka University in partial fulfillment of the requirements for the degree of Master of Science, 1958.

3) R. Tsuchida, *J. Chem. Soc. Japan, (Nippon Kwagaku Kwaisi)*, **58**, 621 (1937); M. Kobayashi, ibid., **64**, 684 (1943).

4) W. Kuhn and K. Bein, *Z. physik. Chem.*, **B24**, 355 (1934).

5) J. P. Mathieu, *Bull. soc. chim. France*, (5) **6**, 873 (1939).

6) J. P. Mathieu, ibid., (5) **3**, 476 (1936).

7) J. P. Mathieu, *J. chim. phys.*, **83**, 78 (1936).

8) A. Werner, *Ann.*, **386**, 48, 107 (1912).

9) J. C. Bailar, Jr. and R. W. Auten, *J. Am. Chem. Soc.*, **56**, 774 (1934).

10) A. Werner, *Ber.*, **44**, 3276 (1911); *Ann.*, **386**, 284 (1912).

11) B. E. Douglas and W. C. Erdman, *J. Am. Chem. Soc.*, **79**, 3012 (1954).

### Analyses

***Cis*-dichloro-bis-(ethylenediamine)-cobalt(III) chloride.**—The rotatory dispersion of D-*cis*-[Co $en_2Cl_2$]Cl in the wave-length region from 450 m$\mu$ to 680 m$\mu$, which has been reported by Mathieu[12], coincides with our result in this wave-length region. The first rotatory inversion in the longer wave-length side involves a positive value of the Cotton effect. Thus the molar rotations change from negative to positive values at about 636 m$\mu$. On the other hand, the second inversion appears at about 520 m$\mu$, and shows a negative Cotton effect.

The dispersion curve in the shorter wave-length side, as determined in the present work, was analyzed as follows. It is assumed that the observed curve is the superposition of partial rotations in the visible region and the tail of a large partial rotation which has its inversion centre in the far ultraviolet region. In the analysis of the curve, the method of trial and error was employed. The result of the analysis is shown in Fig. 1.

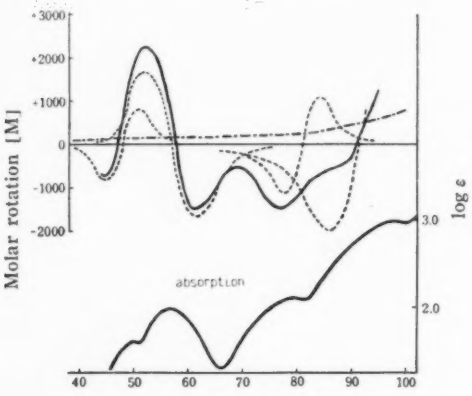


Fig. 1. Rotatory dispersion of D-*cis*-[Co $en_2Cl_2$]Cl in methanol: —— observed curve, ------ partial rotation obtained through analysis.

According to this result, the rotatory inversion with its centre at about 370 m$\mu$ shows a negative value of rotation in the longer wave-length side, its magnitude being almost equal to the rotatory inversion in the wave-length region of the "first absorption band". The rotatory inversion with its center at about 330 m$\mu$ is seen to give a negative value of rotation in the longer wave-length side.

***Cis*-chloronitro-bis-(ethylenediamine)-cobalt(III) chloride.**—In the wave-length region of the "first absorption band", the rotatory inversion with its center at about 544 m$\mu$, which gives a positive value in the longer wave-length side, coincides with Mathieu's results[13] on the whole.

As the observed curve indicates, the maximal value of molar rotation in the region of the "first absorption band" is greater in the shorter wave-length side than in the longer wave-length side and the total dispersion curve is apparently displaced to the negative side. Therefore, it is assumed in the analysis of the curve that the observed curve is the superposition of the partial rotations under consideration in the visible region and the tail of a large partial rotation which has its inversion center in the far ultraviolet region. The curve was analyzed in the same way as in the former. The result of the analysis is shown in Fig. 2.

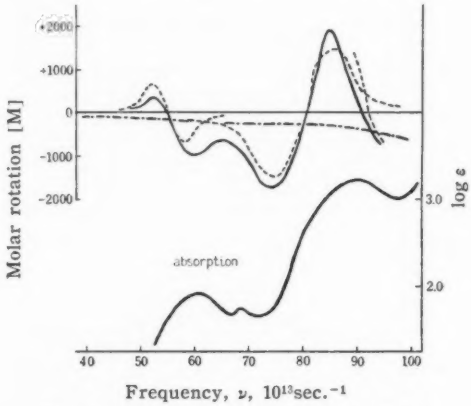


Fig. 2. Rotatory dispersion of D-*cis*-[Co $en_2ClNO_2$]Cl in 50% hydrochloric acid: —— observed curve, ------ partial rotation obtained through analysis.

### Discussion

As described in the preceding part, the dextro-rotatory *cis*-dichloro-bis-(ethylenediamine)-cobalt(III) chloride shows, in the wave-length region of the "first absorption band", two inversive rotatory dispersions. One of them has a positive value for the Cotton effect and the other

12) J. P. Mathieu, *Bull. soc. chim. France*, (5) **3**, 483 (1936).

13) J. P. Mathieu, ibid., (5) **3**, 485 (1936).

a negative value. These may be regarded as corresponding to the two component absorptions resulting from the splitting of an original "first absorption band". In fact, the dichroism as determined in the crystalline state indicates that the violeo-salt shows two absorption bands at $51\times10^{13}$/sec. (588 m$\mu$) and $57\times10^{13}$/sec. (527 m$\mu$) which correspond to the component absorptions of the "first absorption band"[14]. This result is found to be in good agreement with the above described result of the present measurement.

In the wave-length region of the "first absorption band", dextro-rotatory *cis*-chloronitro-bis-(ethylenediamine)-cobalt (III) chloride shows a rotatory inversion with its center at about $55.5\times10^{13}$/sec. (541 m$\mu$), a rotatory dispersion which is quite different from that of the violeo-salt. Judging from the symmetry of the complex ion, however, it is presumed that the chloronitro-salt shows separate absorption maxima corresponding to the components of the "first absorption band". In fact, the dichroism measurement indicates that the *cis*-chloronitro chloride in the crystalline state shows absorption bands at $54\times10^{13}$/sec. (551 m$\mu$) and $58\times10^{13}$/sec. (517 m$\mu$)[14], which may be regarded as corresponding to the first absorption band.

On the basis of the above consideration, the present observation that only one rotatory inversion appears in the wave-length region of the "first absorption band" might be understood in the following way. There would be actually two or more "rotatory inversions" which are superposed upon each other. The component absorptions are so close together that the superposition of the "rotatory inversions" gives the curve that has been experimentally determined.

A rotatory inversion at $81\times10^{13}$/sec. (370 m$\mu$) for the violeo-salt and a similar sort of a rotatory inversion at about $81\times10^{13}$/sec. (370 m$\mu$) for the chloronitro-salt may originate from the transitions closely related with the second absorption band. The magnitudes of both the inversive dispersions are found to be of an equal order. It is to be noted that such a type of rotatory inversion, as had previously been reported for the "first band", was observed for the "second band" as well.

Another inversive dispersion showing a Cotton effect with a negative sign is observed at about $91\times10^{13}$/sec. (330 m$\mu$) for the violeo-salt. A rotatory inversion with a Cotton effect of a positive sign is also observed at an almost identical wave-length in the *cis*-chloronitro-complex. These inversions may be regarded as originating from the "specific absorption band" due to the chloride or nitro group in co-ordination with the metal.

Summarizing the results obtained in the present study, we may be able to derive the following conclusion (Table I and II.)

In the wave-length region of the "first absorption band", there appear two "inversive dispersions" due to the component absorptions, the sign of the Cotton effect for one being reverse to that for the other.

In the wave-length region of the "second absorption band", only one "inversive dispersion" is observed, its magnitude being of an identical order with that for the "first absorption band". An inversive rotatory dispersion is also observed in the wave-length region of the "specific absorption band", its magnitude being greater than that for the "first or the second absorption band".

## General Discussion

As has been described in the preceding part of the present paper, optically active complex-ions such as *cis*-$[Co\ en_2X_2]^+$ and *cis*-$[Co\ en_2XY]^+$ show rotatory inversions corresponding to the component absorptions of the "first absorption band". Reexamining formerly reported data on the basis of the above result, complex ions may be divided into the following two groups from the nature of rotatory dispersion in the wave-length region of the "first absorption band". (1) In the first group, the sign of the Cotton effect for one component differs from that for the other, the examples of this type being *cis*-$[Co\ en_2Cl_2]^+$ and *cis*-$[Co\ en_2ClNCS]^+$. (2) In the second group, the sign of the Cotton effect is the same for the two components, the examples being *cis*-$[Co\ en_2NH_3OH_2]^{3+}$, *cis*-$[Co\ en_2NH_3Br]^{2+}$ and *cis*-$[Co\ en_2NH_3Cl]^{2+}$.

Typical curves for the two types are shown in Fig. 3. The absolute configuration of optically active complexes has not been determined except for the tris-(ethylenediamine)-cobalt(III) ion[15].

14) S. Yamada and R. Tsuchida, to be published later.

15) N. Nakatsu, Y. Saito and H. Kuroya, This Bulletin, **29**, 428 (1956).

TABLE I

ROTATORY DISPERSION AND UV ABSORPTION SPECTRA OF D-*cis*-[Co $en_2Cl_2$]Cl

| | | First band | | Second band | Specific band |
|---|---|---|---|---|---|
| Absorption band $\nu_{max}$ | solution | 49.5 | 57.5 | 79 | 98 |
| | crystal | 51 | 57 | | |
| Inverted dispersion | $\nu$ | 48 | 57 | 81 | 91 |
| | sign of Cotton effect | − | + | − | − |
| | $[M]_{max}$ | 750 | 1650 | 1150 | |

[M]: molar rotation, $\nu$: frequency, $10^{13}$ sec.$^{-1}$

TABLE II

ROTATORY DISPERSION AND UV ABSORPTION SPECTRA OF D-*cis*-[Co $en_2ClNO_2$]Cl

| | | First band | | | Second band | Specific band |
|---|---|---|---|---|---|---|
| Absorption band $\nu_{max}$ | solution | | 60 | 68 | | 89.5 |
| | crystal | 54.5 | 58 | 71 | | |
| Inverted dispersion | $\nu$ | 55 | | | 81 | 91 |
| | sign of Cotton effect | − | | | − | + |
| | $[M]_{max}$ | 600 | | | 1500 | |

[M]: molar rotation, $\nu$: frequency, $10^{13}$ sec.$^{-1}$

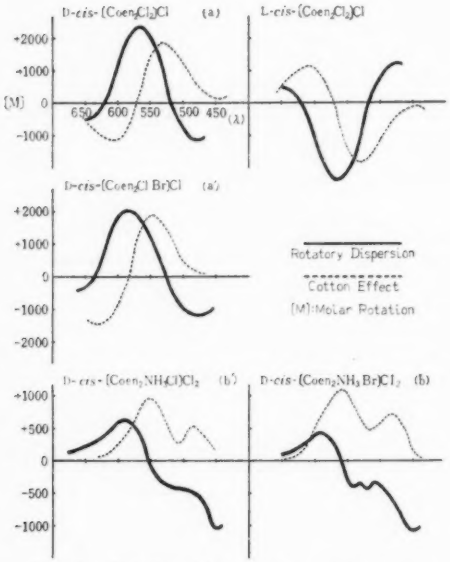


Fig. 3. Relationship between rotatory dispersion and Cotton effect. Data are taken from J. P. Mathieu, *Bull. soc. chim. France*, **3**, 476 (1936).

Making measurements of rotatory dispersion in the longer wave-length range, Mathieu[16] suggested a possibility of determining the absolute configuration from the rotatory dispersion curves in the long wave-length range. This possibility, however, has not been fully examined up to the present. In the following, we will discuss this possibility by using the results obtained in the present study.

It has been shown in the present work that the "first absorption band" of *cis*-disubstituted-bis-(ethylenediamine)-complexes splits itself into components, each of which gives rise to a rotatory inversion of its own. If these components correspond to the same type of electronic transition in the optically active complex under consideration, the sign of the Cotton effect for these components should depend only upon the absolute configuration. Therefore, the Cotton effect may be used as a criterion for determining the absolute configuration of metallic complexes if precautions are taken.

In other words, if a comparison is made among compounds which are closely similar in the linkage involved, and consequently in the stability order of energy states of the metallic complex, we may assume that the compounds with the same type of absolute configuration would show the same sign of the Cotton effect and the same type of the rotatory inversion.

Now, if we choose complexes resembling each other in the linkage from the complexes in the group 1 or in the group 2, their absolute configuration may be determined on the basis of the sign of the Cotton effect. Thus, in the case of *cis*-[Co $en_2Cl_2$]$^+$ and *cis*-[Co $en_2ClBr$]$^+$, in which the above-mentioned requirements are satisfied, it seems possible to determine the absolute configuration.

It is seen in Fig. 3 that the diastereomer of *cis*-[Co $en_2ClBr$]$^+$, which forms a more

16) J. P. Mathieu, *J. chim. phys.*, **33**, 78 (1936).

insoluble compound with *d*-α-bromocamphorsulfonate than does the other diastereomer, shows a rotatory dispersion curve represented by the curve (a′) in Fig. 3. If we tentatively define a D-form of *cis*-[Co $en_2Cl_2$]$^+$ to be the optically active form[17] related with the curve (a) in Fig. 3, it may be reasonable to assume that the former diastereomer of *cis*-[Co $en_2ClBr$]$^+$ belongs to the D-series.

A similar consideration applies to the components classified as the group 2. Thus *cis*-[Co $en_2NH_3Br$]$^{2+}$, *cis*-[Co $en_2NH_3Cl$]$^{2+}$ and *cis*-[Co $en_2NH_3OH_2$]$^{3+}$, all showing the rotatory dispersion of the type 2, closely resemble one another in the respect of the linkage involved.

It is seen in Fig. 3 that the diastereomer of *cis*-[Co $en_2NH_3Br$]$^{2+}$, which forms with *d*-α-bromocamphorsulfonate a more insoluble salt than does the corresponding salt of the other diastereomer, has the same sign for the Cotton effect as the sign possessed by the optically active form related with the curve b in Fig. 3.

If we tentatively assume that the curve b in Fig. 3 refers to the salt of the D-series, then the curve b′ may also be regarded as corresponding to the D-series.

So far, we have taken account of the rotatory behavior in the wave-length region of the "first absorption band" alone. The above discussion may be expected to become more reliable when due account is taken of the Cotton effect in the region covering the "second absorption band" as well. The discussion on this phase of the problem will be made in the succeeding papers of this series.

17) a diastereomer which forms with ammonium *d*-α-bromocamphorsulfonate a less easily soluble compound than does the other diastereomer of the complex salt.

## Summary

Rotatory dispersions in the visible and the ultraviolet region have been determined with *cis*-[Co $en_2Cl_2$]Cl and *cis*-[Co $en_2ClNO_2$]Cl, and dispersion curves have been analyzed by the method of successive approximation.

Both the complexes show two inversive dispersions in the wave-length region of the "first absorption band", and only one dispersion in the region of the "second absorption band".

The magnitude of those dispersions was found to be of the same order.

An inversive dispersion was also observed in the region of the "specific absorption band".

In the wave-length region of the "first absorption band", there appear two inversive dispersions due to the component absorptions, in accordance with the dichroism measurement. As for the inversive dispersions in the region of the "first absorption band", the sign of the Cotton effect for the one is reverse to that for the other in the violeo-salt, but in the *cis*-chloronitro-salt, the Cotton effect is the same for the two components.

A possibility of determining the absolute configuration was suggested from the rotatory dispersion curve in the wave-length region of the "first absorption band".

The present authors wish to thank the Ministry of Education for a grant-in-aid.

*Department of Chemistry, Faculty of Science*
*Osaka University, Kita-ku, Osaka*

# *Synthesis of Histidyl Peptides**

By Fumio SAKIYAMA, Kenji OKAWA, Tsuneo YAMAKAWA and Shiro AKABORI

(Received June 18, 1958)

Peptides containing L-histidine have frequently been obtained from biologically active substances such as ribonuclease[1], insulin[2], bacitracin[3] and strepogenin[4], and it has recently been suggested that the histidyl residue constitutes an essential part of the active sites of $\alpha$-chymotrypsin, cholinesterase, lysozyme[5], and so on. Despite these findings indicating the importance of histidyl peptides in biochemistry, no satisfactory methods have so far been worked out for their convenient synthesis. This appears to be due mainly to the fact that there have been no successful procedures available to protect the imidazole nucleus of histidine.

Even when the $\alpha$-amino group of histidine is masked with an acyl group, the molecule still behaves as a zwitter-ion owing to the presence of the imidazole ring, and this character affords unavoidable difficulties to the subsequent reactions. First of all, the presence of unprotected imidazole residue in the molecule often leads to various undesirable side reactions during the peptide synthesis. Furthermore, restricted solubility in organic solvents of the acylated derivative, e.g., *N*-$\alpha$-carbobenzyloxyhistidine, is not favorable for their coupling with amino acid esters. The use of *N*-$\alpha$-carbobenzyloxyhistidine is also impractical in view of the poor yield obtainable in its synthesis from histidine by the direct carbobenzyloxylation method[6].

Theodropoulos[7] has synthesized histidyl peptides using *N-Im*-benzyl-L-histidine prepared by the procedure of du Vigneaud[8]. Although this method is free from most of the defects mentioned above, it is not suitable for practical purpose because of the fact that the benzyl derivative is not easily accessible. Of late, Amiard et al. reported the preparation of the dityrityl histidine through which some of the histidyl peptides were synthesized[9]. The trityl method was valuable for the limited instance as it was rather tedious.

Holley and Sondheimer[10] have prepared a number of histidyl peptides employing the azide procedure in which the imino group of the imiazole ring was not protected. This method, though widely used as the only practical means for the synthesis of histidyl peptides[11], could not be regarded as a very excellent one because of the difficulty associated with the preparation of the intermediate *N*-$\alpha$-carbobenzyloxyhistidine azide and its instability.

In the present paper the authors wish to report the preparation of dicarbobenzyloxy-L-histidine and its availability for the synthesis of histidyl peptides.

**Preparation and Properties of Dicarbobenzyloxyhistidine.** — Using sodium carbonate in place of sodium hydroxide, the authors succeeded in the percarbobenzyloxylation of L-histidine and obtained the $\alpha$, *Im*-dicarbobenzyloxy derivative in 81% yield. Sodium hydroxide was also effective under limited conditions, but the yield in this case was relatively low.

The dicarbobenzyloxy compound thus obtained was found to be rather unstable

* A part of this investigation has been reported in "*Nature*", **181**, 772 (1958).

1) C. H. W. Hirs, *Fed. Proc.*, **16**, 196 (1957); R. R. Redfield and C. B. Anfinsen, *J. Biol. Chem.*, **221**, 385 (1956).

2) H. Brown, F. Sanger and R. Kitai, *Biochem. J.*, **60**, 556 (1956).

3) J. Porath, *Nature*, **172**, 871 (1953); I. M. Lockhart and E. P. Abraham, *Biochem. J.*, **58**, 633 (1954); L. C. Craig et al., *J. Am. Chem. Soc.*, **77**, 731 (1955).

4) R. B. Merrifield and D. W. Woolley, ibid., **78**, 358 (1956).

5) The late Dr. C. Fromageot suggested in the discussion that the histidyl residue might be the active site of lysozyme. (International Symposium on Enzyme Chemistry. Tokyo, Oct., 1957).

6) M. Bergmann and L. Zervas, *Ber.*, **65**, 1199 (1932).

7) D. Theodropoulos, *J. Org. Chem.*, **21**, 1550 (1956).

8) V. du Vigneaud and O. K. Behlens, *J. Biol. Chem.*, **117**, 27 (1937).

9) G. Amiard, R. Heymes and L. Velluz, *Bull. soc. chim. France*, 191 (1956).

10) R. Holley and E. Sondheimer, *J. Am. Chem. Soc.*, **76**, 1326 (1954).

11) R. F. Fischer et al., ibid., **76**, 5076 (1954); R. A. Boissonas et al., *Experientia*, **12**, 446 (1956); D. W. Woolley, et al., *J. Am. Chem. Soc.*, **78**, 4646 (1956); K. Hofmann et al., ibid., **76**, 1641 (1957); R. Schwyzer, et al., *Helv. chim. Acta*, **40**, 614 (1957).

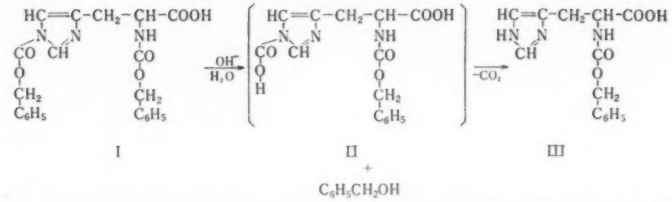

Fig. 1. Decomposition of dicarbobenzyloxy histidine in alkaline media.

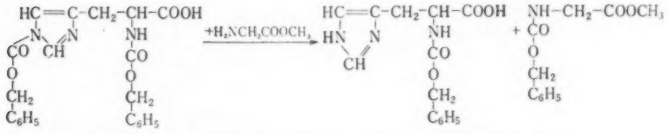

Fig. 2. The transfer of the carbobenzyloxy group.

in alkaline media. The compound was con vertible into *N*-α-carbobenzyloxyhistidine with elimination of the imidazole-linked carbobenzyloxy group (Fig. 1). It was thought that, in alkaline solution, dicarbobenzyloxyhistidine (I) was partly split into an intermediate II and benzyl alcohol by the action of hydroxyl ions. Then, II might spontaneously changed to form the *N*-α-carbobenzyloxy derivative (III) and carbon dioxide. The low yield of the dicarbobenzyloxy compound encountered in the presence of sodium hydroxide may have been due to such instability of the product in alkaline reaction.

In non-aqueous basic media the carbobenzyloxy residue linked to imidazole appeared to act as an active acyl group. When the dicarbobenzyloxy derivative and glycine methyl ester were incubated in dioxane at 50~60°C for one hour, a gelatinous precipitate of silky lustre was formed. Carbobenzyloxy glycine methyl ester and *N*-α-carbobenzyloxy histidine were isolated and identified from the precipitate. These compounds must have been formed by the transcarbobenzyloxylation reaction as illustrated in Fig. 2. This mechanism received some support from the fact that no transfer reaction but the decomposition took place in basic media if an acceptor compound was absent in the reaction mixture. Bergmann[12] and Wieland[13] have already observed that acetyl or amino acyl groups linked to the imidazole nucleus can be transfered to suitable acceptors under mild conditions.

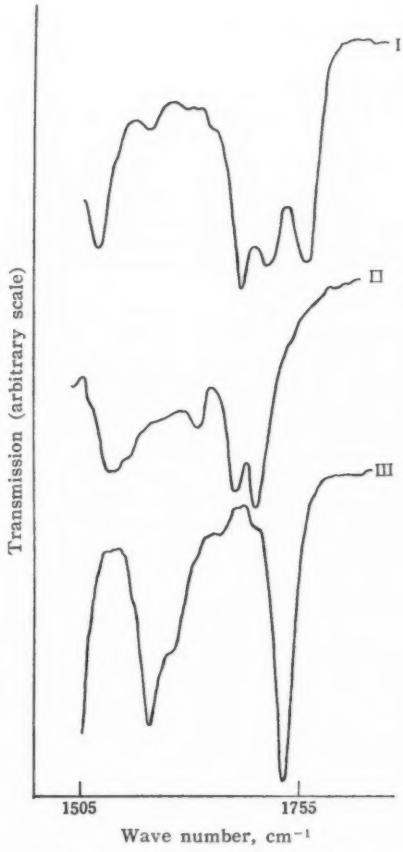


Fig. 3. Infrared absorption spectra of carbobenzyloxy derivatives of L-histidine. I, DCH; II, α-MCH; III, *Im*-MCH. (Rock salt, Hilger H800)

12) M. Bergmann and L. Zervas, *Z. physiol. Chem.*, **175**, 154 (1928).
13) Th. Wieland and G. Schneider, *Ann.*, **580**, 159 (1953).

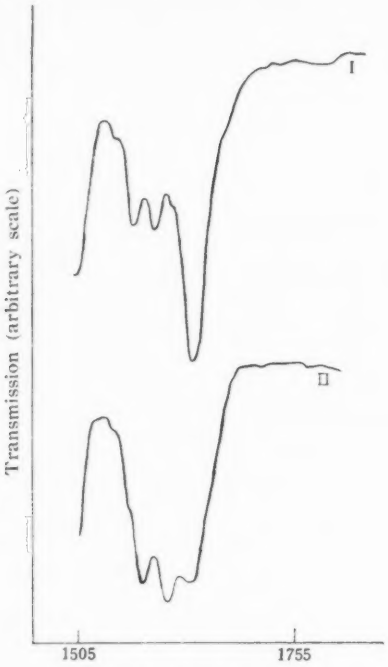


Fig. 4. Infrared absorption spectra of L-histidine (I) and its hydrochloride hydrate (II). (Rock salt, Hilger H800)

As a by-product, a small amount of monocarbobenzyloxy-L-histidine was isolated from the crude dicarbobenzyloxy derivative which was obtained by the reaction between L-histidine and the equivalent mole of carbobenzyloxychloride. It melted at 194~195°C with decomposition and gave a positive ninhydrin and a negative Pauly's reaction. These facts, together with the result of the infrared absorption analysis, were utilized to identify the compound as *N-Im*-carbobenzyloxyhistidine.

Infrared absorption spectra of dicarbobenzyloxy-L-histidine (DCH), $\alpha$-carbobenzyloxy-L-histidine ($\alpha$-MCH) and *Im*-carbobenzyloxy-L-histidine (*Im*-MCH) are shown in Fig. 3. Those of L-histidine and its hydrochloride hydrate are also shown in Fig. 4 for comparison. The band at 1759 $cm^{-1}$ and that at 1733 $cm^{-1}$ were assumed to correspond to the —CO—N= grouping which was formed by the combination of the imidazole nucleus with the carbobenzyloxy group.

These findings might be in good agreement with Otting's observation[14] that those characteristic absorption maxima of several acyl imidazoles appeared in the region of 1744~1748 $cm^{-1}$.

**Synthesis of the Histidyl Peptide.**— Several peptide derivatives of L-histidine, methyl ester of dicarbobenzyloxy-L-histidylglycine, -L-leucine, -L-threonine, -L-methionine, -*O*-benzyl-L-serine and -L-glutamic acid** were synthesized from dicarbobenzyloxy-L-histidine monohydrate and the respective amino acid ester with the aid of *N, N'*-dicyclohexylcarbodiimide[15]. Dicarbobenzyloxy-L-histidine was superior to the monocarbobenzyloxy compound as a starting material in respect to the higher solubility, the easier preparations and less possibility of undergoing some side reactions.

Dicarbobenzyloxy-L-histidyl glycine methyl ester was converted into the $\alpha$-monocarbobenzyloxy dipeptide by alkaline hydrolysis in dimethylformamide[16]. L-Histidyl-L-leucine was prepared from the corresponding dipeptide ester by treatment with concentrated hydrochloric acid at 37°C[17]. The resulting product possessed properties identical with those reported by Holley and Sondheimer[10].

The synthesis of the L-histidyl-L-threonyl-L-valyl-L-glutamic acid derivative, the sequence of which was found in a heme-linked peptide obtained from cytochrome c[18], was explored by the following route. This involved the condensation of dicarbobenzyloxy-L-histidine and the tripeptide ester which was prepared from its carbobenzyloxy derivative by the action of hydrogen bromide in dioxane[19]. The coupling by the Sheehan's reagent proceeded smoothly as in the case of the dipeptide derivative, giving an yield of 50%.

*N*-Carbobenzyloxy-L-threonine was prepared using sodium carbonate in place of sodium bicarbonate[20] or sodium hydroxide, and was isolated as fine crystals, the yield of which was quite satisfactory. The tripeptide derivative, carbobenzyloxy-L-threonyl-L-valyl-L-glutamic acid dimethyl

14) W. Otting, *Ber.*, **89**, 1940 (1956).
15) J. C. Sheehan and G. P. Hess, *J. Am. Chem. Soc.*, **77**, 1067 (1955).
** The diethyl ester was exceptionally used for the peptide synthesis.
16) G. Weitzel, F. Schneider and A-M. Fretzdorff, *Z. physiol. Chem.*, **307**, 23 (1957).
17) R.B. Merrifield and D. W. Woolley, *J. Am Chem. Soc.*, **78**, 4646 (1956).
18) H. Tuppy and S. Paleus, *Acta chim. Scand.*, **9**, 353 (1955).
19) K. Okawa, This Bulletin, **30**, 977 (1957).
20) G. Riley, J. H. Turnbull and W. Wilson, *J. Chem. Soc.*, **1957**, 1373.

ester, was derived from the above compound and L-valyl-L-glutamic acid ester in 78% yield by the carbodiimide method.

In a preliminary experiment, it was observed that both the two carbobenzyloxy groups in dicarbobenzyloxy-L-histidyl-L-threonine methyl ester were quantitatively removed by the action of hydrogen bromide in dioxane as in the case of dicarbobenzyloxy-L-histidine. Then the dipeptide ester produced was coupled with carbobenzyloxy-*S*-benzyl-L-cysteine by carbodiimide and the carbobenzyloxy tripeptide ester was produced (m. p. 114~115°C). Elementary analysis of the product was in good agreement with carbobenzyloxy-*S*-benzyl-L-cysteinyl-L-histidyl-L-threonine methyl ester ($C_{29}H_{35}O_7N_5S$). Furthermore, dicarbobenzyloxy-L-histidyl-L-threonine methyl ester was subjected to the reaction with 80% hydrazine hydrate and the hydrazide of the monocarbobenzyloxy dipeptide, containing one molecule of water, was obtained in a moderate yield (m. p. 186°C). This substance may also be utilized for the synthesis of the L-histidyl-L-threonyl peptide through the azide.

It could be concluded from the results of the present investigation that dicarbobenzyloxy histidine can be utilized for the synthesis of the histidyl peptides by the Sheehan's method though no general procedure for the hydrolysis of dicarbobenzyloxy peptide derivatives has been established.

At the end of this investigation, we had a chance to read the paper by Dr. E. Katchalski[21] on the carbobenzyloxy derivative of histidine, in which he reported the synthesis by a somewhat different method of dicarbobenzyloxy histidine and its chemical properties. It was found that the dicarbobenzyloxy histidine obtained by us showed coincidence with his product in all respects.

## Experimental

***N*-α, *N*-*Im*-Dicarbobenzyloxy-L-histidine.**— L-Histidine monohydrochloride monohydrate (10 g.) was dissolved in 48 ml. of 2 N sodium hydroxide solution and after addition of 2 N sodium carbonate solution (75 ml.), carbobenzyloxychloride (17.2 g.) was portion-wise dropped into the above solution under vigorous stirring*** and cooling for about half an hour. It was about five minutes until the white precipitates began to appear. Stirring was continued for 20 to 30 min. at room temperature and the solution was acidified to Congo red with 6 N hydrochloric acid under cooling. The gelatinous mass produced was separated from the supernatant by decantation. The product was first dissolved and then gradually crystallized out when it was triturated with ethanol. The white crystals were collected and washed with a small amount of ethanol. The yield was about 17g. (81%), m.p. 95~98°C (decomp.). Recrystallization from acetone-cold water gave white needles of dicarbobenzyloxy-L-histidine monohydrate (14g. 66%). m.p. 103~105°C (decomp.). $[\alpha]_D^{14}$ +34.01 (c. 28.99 mg. in 1 ml. of ethyl acetate).

*Anal.* Found: C, 59.86; H, 5.11; N, 9.46. Calcd. for $C_{22}H_{21}O_6N_3 \cdot H_2O$: C, 59.64; H, 5.25; N, 9.52%. Crystallization water: Found: 4.19; Calcd. 4.08%

When the dicarbobenzyloxy derivative was recrystallized from methanol, it was found that the compound, which melted at 105~107°C with decomposition, had one molecule of alcohol in place of water.

*Anal.* Found: C, 60.70; H, 5.50; N, 9.18. Calcd. for $C_{22}H_{21}O_6N_3 \cdot CH_3OH$: C, 60.65; H, 5.53; N, 9.23%.

The product is readily soluble in acetone, dioxane, tetrahydrofuran, chloroform and dimethylformamide, moderately soluble in warm methanol and ethanol, slightly soluble in benzene****, ethyl acetate and ether, and insoluble in petroleum ether and water. The negative Pauly's reaction was given at 0°C, but the solution turned to deep red color at room temperature as it elapsed. It was unstable to moisture and heat, and it decomposed to a material with some oily product, both when it was exposed to the atmosphere and when it was kept in the Abderhalden's apparatus (acetone in jacket) to dry the sample for analysis. This gelatinous substance washed with acetone and ethyl acetate gave hygroscopic powder, from which *N*-α-carbobenzyloxyhistidine was isolated in 70~80% yield by recrystallization from ethanol. Although little decomposition was encountered when it was kept over phosphorous pentoxide, it seemed preferable for the peptide synthesis to use freshly prepared crystals than the stored one. Both the carbobenzyloxy groups were quantitatively removed by the Ben-Ishai's procedure and the paper chromatography in the system of *n*-butanol-acetic acid-water (4 : 1 : 1 by volume) showed no spots except one corresponding to histidine.

**The reaction of dicarbobenzyloxy-L-histidine with glycine methyl ester.**— Dicarbobenzyloxy-L-histidine monohydrate (2.2 g.) and glycine methyl ester (prepared from its hydrochloride (1.3 g.) and ammonia-chloroform solution) were dissolved in 20 ml. of absolute dioxane and the mixture was kept at 50~60°C for 3 hours. The white precipitate produced was separated

21) A. Patchornik, A. Berger and E. Katchalski, *J. Am. Chem. Soc.* **79**, 6416 (1957).

*** Vigorous shaking of the vessel containing the mixture of histidine, alkali and acylchloride also gave the dicarbobenzyloxy derivative in the same yield.

**** Though, in a preliminary paper published in "Nature", it was reported that the dicarbobenzyloxy derivative of histidine was soluble in benzene, ethyl acetate and ether, further invesitigation on the solubility showed that the derivative in pure state had the least solubility in those solvents.

from the supernatant by decantation and was washed with ethyl acetate. The resulting white crystals were recrystallized from ethanol and identified to be *N*-α-carbobenzyloxy-L-histidine, which gave the positive Pauly's reaction. m. p. 165~166°C $[\alpha]_D^{25}$ −24.56 (c. 11.7 mg. in 1 ml. of 6 N hydrochloric acid).

*Anal.* Found: N, 14.50: Calcd. for $C_{14}H_{15}O_4N_3$: N, 14.50%.

On the paper chromatogram it showed an Rf. 0.64 in the system of *n*-butanol-acetic acid-water (4 : 1 : 5 by volume) and an Rf. 0.79 in that of the same solvents (4 : 1 : 1 by volume). Carbobenzyloxy glycine was obtained from the supernatant and washing by concentration and hydrolysis. When dicarbobenzyloxyhistidine was subjected to the reaction with twice equivalent mole of triethylamine under the same condition except the absence of any primary amine, it partly decomposed to give *N*-α-carbobenzyloxy-L-histidine.

***N-Im*-Carbobenzyloxy-L-histidine.**—From L-histidine monohydrochloride monohydrate (5.1 g. 0.025 M), 2 N sodium carbonate and an equivalent mole of carbobenzyloxychloride (5.1 g. 0.03 M), the crude material was obtained by the same procedure as the preparation of the dicarbobenzyloxy derivative. The crystals of this compound happened to separate from the solution when the crude carbobenzyloxy derivative, most of which was composed of the dicarbobenzyloxy derivatives, was recrystallized from the mixture of acetone-water (3 : 1 by volume). The yield was very poor. It was slightly soluble in water and in organic solvents. m. p. 193~194°C (decomp.).

*Anal.* Found: N, 14.44. Calcd. for $C_{14}H_{15}O_4N_3$: N, 14.53%.

**Dicarbobenzyloxy-L-histidyl amino acid esters.**—The same procedure as in the synthesis of dicarbobenzyloxy-L-histidyl-L-threonine methyl ester was applied to other histidyl peptide derivatives.

**Dicarbobenzyloxy-L-histidyl-L-threonine methyl ester.**—Freshly prepared dicarbobenzyloxy-L-histidine monohydrate (4.4 g.) was dissolved in 33 ml. of absolute chloroform and the solution was added to the chloroform solution containing L-threonine methyl ester (prepared from its hydrochloride (2.5 g.) and 1.5 N ammonia-chloroform solution (14 ml.) and *N, N'*-dicyclohexylcarbodiimide (2.1 g.). Dicyclohexylurea was precipitated after a few minutes with evolution of heat. The solution was cooled with water for several minutes and allowed to stand overnight at room temperature. About 1 ml. of glacial acetic acid was added and the precipitate produced was filtered off after an hour. The filtrate was washed with 0.2 N hydrochloric acid, 1% sodium bicarbonate and water successively, dried over anhydrous sodium sulfate and concentrated in vacuo to a paste-like mass. The residue was triturated with ether and the resulting crystals were collected. White needles of dicarbobenzyloxy-L-histidyl-L-threonine methyl ester (4.25 g.) were obtained in 78.8% yield. m. p. 140~144°C. After recrystallization from ethyl acetate-petroleum ether, the melting point was raised to 149~150°C. $[\alpha]_D^{14}$ +12.74 (c. 30.5 mg. in 1 ml. of glacial acetic acid).

*Anal.* Found: C, 59.61; H, 5.77; N, 10.21. Calcd. for $C_{27}H_{30}O_8N_4$: C, 60.21; H, 5.61; N. 10.40%.

**Dicarbobenzyloxy-L-histidyl glycine methyl ester.**—By the same procedure, fine crystals (3.4 g.) were obtained in 68% yield from dicarbobenzyloxy-L-histidine (4.4 g.) and glycine methyl ester. The dicarbobenzyloxy dipeptide ester was recrystallized from ethyl acetate. m. p. 68~70°C. $[\alpha]_D^{10}$ +10.47 (c. 19.4 mg. in 1 ml. of methanol).

*Anal.* Found: C, 59.75; H. 5.68; N, 10.23. Calcd. for $C_{25}H_{26}O_4N_7 \cdot CH_3OH$: C, 59.31; H, 5.74; N, 10.64%.

**Dicarbobenzyloxy-L-histidyl-L-leucine methyl ester.**—L-Leucine methyl ester, prepared from its hydrochloride (2.4 g.), was coupled with dicarbobenzyloxy-L-histidine monohydrate (2.8 g.) by carbodiimide. Dicarbobenzyloxy-L-histidyl-L-leucine methyl ester (2.4 g.) was obtained as a white precipitate in 68% yield. Recrystallization from ethyl acetate-petroleum ether gave fine crystals. m. p. 101~103°C. $[\alpha]_D^{14}$ +21.44° (c. 29.0 mg. in 1 ml. of ethyl acetate).

*Anal.* Found: C, 63.14; H, 6.31; N, 10.44. Calcd. for $C_{29}H_{34}O_7N_4$: C, 63.26; H, 6.22; N, 10.18%.

**Dicarbobenzyloxy-L-histidyl-L-glutamic acid diethyl ester.**—From dicarbobenzyloxy-L-histidine monohydrate (1.4 g.) and L-glutamic acid diethyl ester was prepared dicarbobenzyloxy-L-histidyl-L-glutamic acid diethyl ester (1.25 g. 70%), melting at 78~80°C. $[\alpha]_D^{14}$ +0.21 (c. 28.5 mg. in 1 ml. of ethyl acetate).

*Anal.* Found: C, 60.42; H, 5.92; N, 9.06; Calcd. for $C_{31}H_{36}O_9N_4$: C, 61.17; H, 5.96; N, 9.19%.

**Dicarbobenzyloxy-L-histidyl-*O*-benzyl-L-serine methyl ester.**—The coupling reaction between dicarbobenzyloxy-L-histidine monohydrate (1.4 g.) and *O*-benzyl-L-serine methyl ester by the carbodiimide procedure gave 1.5 g. of dicarbobenzyloxy-L-histidyl-*O*-benzyl-L-serine methyl ester: yield 81%. m. p. 113~115°C. $[\alpha]_D^{14}$ +19.80 (c. 29.6 mg. in 1 ml. of ethyl acetate).

*Anal.* Found: C, 64.75; H, 5.57; N, 9.54. Calcd. for $C_{33}H_{34}O_8N_4$: C, 64.48; H, 5.58; N, 9.12%.

**Dicarbobenzyloxy-L-histidyl-L-methionine methyl ester.**—White crystals (1.5 g.) of dicarbobenzyloxy-L-histidyl-L-methionine methyl ester were prepared from dicarbobenzyloxy-L-histidine monohydrate (1.3 g.) and L-methionine methyl ester. The dipeptide derivative (m. p. 110~113°C) was recrystallized from chloroform-petroleum ether. $[\alpha]_D^{22}$ +9.07 (c. 28.0 mg. in 1 ml. of glacial acetic acid).

*Anal.* Found: C, 59.10; H, 5.55: N, 9.72. Calcd. for $C_{28}H_{32}O_7N_4S$: C, 59.14; H, 5.67; N, 9.85%.

**Carbobenzyloxy-L-histidyl glycine.**—The dimethylformamide solution (2 ml.) containing the dicarbobenzyloxy dipeptide ester (2 g.) was adjusted to pH 9.0~9.2 with 2 N sodium hydroxide solution under cooling. The solution was kept for 30 min. at room temperature and then acidified to pH 5.0 with 1 N hydrochloric acid. By concentration and addition of acetone a swollen

material (1 g.) was obtained. m. p. 140~145°C Recrystallization from methyl alcohol gave the carbobenzyloxy dipeptide (0.5 g.) melting at 237~238°C.

*Anal.* Found: C, 54.40; H, 5.47; N, 15.79. Calcd. for $C_{16}H_{18}O_6N_4$: C, 55.48; H, 5.24; N, 16.17%.

**Carbobenzyloxy-L-threonyl-L-valyl-L-glutamic acid dimethyl ester.**—Carbobenzyloxy-L-threonine (2.5 g.) was dissolved in 5 ml. of chloroform and the solution was added to the chloroform solution containing *N, N'*-dicyclohexylcarbodiimide (2.1 g.) and L-valyl-L-glutamic acid dimethyl ester (prepared from its hydrobromide (4.3 g.) and triethylamine). As the reaction proceeded with evolution of heat, the resulting dicyclohexylurea was precipitated. After 3 hours the precipitate was filtered off, a few drops of glacial acetic acid was added to the filtrate and the solution was kept overnight at 5°C. The filtrate liberated from dicyclohexylurea (0.3 g.) was washed with 0.2 N hydrochloric acid, 0.25 N sodium carbonate and water successively, and dried. By concentration and dilution with petroleum ether, white crystals (3.9 g.) were obtained. From the filtrate an additional 0.1 g. of the product was obtained. The two crops were combined and recrystallized from ethyl acetate-petroleum ether. The yield was 3.6 g. (72%). m. p. 172~174°C. (sintered at 145~150°C). It gave the positive biuret reaction. $[\alpha]_D^{10}$ −56.5 (c. 23 mg. in 1 ml. of methanol).

*Anal.* Found: C, 56.70; H, 7.33; N, 8.47. Calcd. for $C_{24}H_{35}O_9N_3$: C, 56.57; H, 6.92; N, 8.25%.

**Dicarbobenzyloxy-L-histidyl-L-threonyl-L-valyl-L-glutamic acid dimethyl ester.** — Into the dimethylformamide solution containing L-threonyl-L-valyl-L-glutamic acid dimethyl ester (1.4 g.) and *N, N'*-dicyclohexylcarbodiimide (0.7 g.) was added the dimethylformamide solution (3 ml.) of dicarbobenzyloxy-L-histidine monohydrate (1.4 g.) under stirring. The resulting dicyclohexylurea appeared within 5 minutes and was filtered off after 30 minutes. The filtrate was allowed to stand overnight at 5°C. A small amount of dicyclohexylurea precipitated was filtered and the solvent of the filtrate was replaced by chloroform (20 ml.). Then it was washed with 0.2 N hydrochloric acid and water, successively, and dried over anhydrous sodium sulfate. The fluffy precipitate appeared when twice the volume of petroleum ether was added to the above solution. Additional material was obtained from the mother liquor by dilution with petroleum ether for the total of 1.2 g. (50%) of white powders. m. p. 95~98°C. $[\alpha]_D^{10}$ +20.1 (c. 16.4 mg. in 1 ml. of chloroform).

*Anal.* Found: C, 57.53; H, 6.71; N, 10.65. Calcd. for $C_{35}H_{48}N_6O_{12}\cdot H_2O$: C, 57.13; H, 6.31; N, 10.72%.

The dicarbobenzyloxy tetrapeptide ester was positive to the biuret reaction and its acid hydrolysate gave all the constitutional amino acids on the paper chromatogram.

**Carbobenzyloxy-L-valyl-L-glutamic acid dimethyl ester.**—From the syrupy carbobenzyloxy-L-valine (15 g.), glutamic acid dimethyl ester (prepared from its hydrochloride (17 g.)) and *N, N'*-dicyclohexylcarbodiimide (12 g.) was obtained the carbobenzyloxy dipeptide ester in 80% yield using dioxane as a reaction solvent. m. p. 117~120°C (sintered at 102~103°C). A sample for the analysis was twice recrystallized from ethyl acetate-petroleum ether. m. p. 122~123°C (sintered at 115~116°C). $[\alpha]_D^{10}$ −130.7 (c. 16 mg. in 1 ml. of methanol).

*Anal.* Found: C, 59.24; H, 7.08; N, 6.76. Calcd. for $C_{20}H_{28}O_7N_2$: C, 59.10; H, 6.94; N, 6.89%.

L-Threonyl-L-valyl-L-glutamic acid dimethyl ester and L-valyl-L-glutamic acid dimethyl ester were quantitatively obtained by decarbobenzyloxylation with hydrogen bromide in dioxane from the respective carbobenzyloxy derivative.

***N*-Carbobenzyloxy-L-threonine.**—To the cold solution of 2 N sodium hydroxide (25 ml.) containing L-threonine (6 g.) was added 2 N sodium carbonate (38 ml.) and carbobenzyloxychloride (8.5 g.). The mixture was shaken vigorously for 15 minutes at room temperature. Excess of carbobenzyloxychloride precipitated was removed into ether and the aqueous layer was acidified to Congo red with 6 N hydrochloric acid. Then the oily product precipitated was extracted into ethyl acetate (30 ml. three times) and the united extracts were dried over anhydrous sodium sulfate. Concentration, followed by addition of petroleum ether, afforded silky crystals (12 g. 95%). m. p. 95~98°C. Recrystallization from ethyl acetate-petroleum ether gave white needles. m. p. 103~105°C. $[\alpha]_D^{25}$ −2.4 (c. 11.7 mg. in 1 ml. of ethanol).

*Anal.* Found: C, 57.50; H, 6.25; N, 5.67. Calcd. for $C_{12}H_{15}O_5N$: C, 56.91; H, 5.97; N, 5.53%.

**L-Histidyl-L-leucine.** — Dicarbobenzyloxy-L-histidyl-L-leucine methyl ester (2.4 g.) was suspended in 20 ml. of concentrated hydrochloric acid and was kept at 37°C for 50 minutes. The opaque solution was spread on a glass plate and evaporated to dryness over concentrated sulfuric acid under reduced pressure. The residue was dissolved in a small amount of 99% ethanol and triethyl amine was added after the removal of insoluble substance. A fluffy material precipitated was collected. Yield 0.5 g. (42%). The dipeptide was recrystallized from 33% ethanol. m. p. 212~214°C (decomp.) $[\alpha]_D^{14}$ −43.5 (c. 10 mg. in 1 ml. of 0.1 N sodium hydroxide) (lit.[9] $[\alpha]_D^{25}$ −43.5 (c. 1.0, 0.1 N sodium hydroxide)).

*Anal.* Found: N, 20.54. Calcd. for $C_{12}H_{20}O_3N_4$: N, 20.88%.

## Summary

*N*-α,*N*-*Im*-Dicarbobenzyloxyhistidine was prepared in good yield using sodium carbonate, and some histidyl peptide derivatives were synthesized by Sheehan's method using the compound as a starting material.

Grateful acknowledgement is due to Ajinomoto Company for supplying materials of amino acids.

*Department of Chemistry*
*Faculty of Science, and*
*Institute for Protein Research*
*Osaka University*
*Kita-ku, Osaka*

# *The Molecular and Crystal Structure of Allokainic Acid**

By Hideo WATASE

(Received June 4, 1958)

As parts of our studies[1] on the structures of kainic acid and its isomer, we reported in the previous papers the X-ray investigations on zinc kainate[2] and kainic acid[3], which determined the three-dimensional structure of kainic acid $C_{10}H_{15}O_4N$, the most active component of *Digenea simplex* Agardh. *Digenea simplex* Agardh contains also an isomer of kainic acid, allokainic acid[4], in a very small proportion. Allokainic acid $C_{10}H_{15}O_4N$ is an acidic and optically active** compound of m. p. 237° (decomp.), and is said to have a very weak anthelmintic effect if any. It is of interest to elucidate the relationship between the structures of the two isomers of which the physiological nature (anthelmintic effect) of one is very different from that of the other.

According to the reports[5] based on organic chemistry, the chemical behavior of one of the two isomers is similar to that of the other, and the structural formula of allokainic acid is concluded to be the same as that of kainic acid, 2-carboxy-3-carboxymethyl-4-isopropenylpyrrolidine.

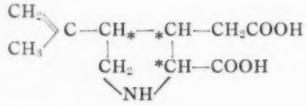

To confirm this conclusion and to determine moreover the stereochemical configuration of the molecule, the structure of allokainic acid has been investigated by means of X-ray crystal analysis. The electron-density projections along the two principal crystal axes were derived by the trial method, and the three-dimensional structure of the molecule was determined quantitatively.

In this paper is described the structure determination of allokainic acid in detail.

## Experimental

Allokainic acid crystallizes with no molecules of water from its aqueous solution. Crystalline allokainic acid is of a colorless prism elongated along a principal crystal axis chosen as the *b* axis, having a plane of cleavage perpendicular to another principal axis (*a* axis).

Oscillation and Weissenberg photographs were taken about two principal crystal axes (*b* and *c* axes), using filtered Cu $K_\alpha$ radiation. The specimens used had the following cross-sections at right angles to the axis of rotation; 0.15×0.2 mm. for the *b* axis rotation and 0.2×0.4 mm. for the *c* axis***.

The intensity data of (*h* 0 *l*) and (*h k* 0) used in the two-dimensional analyses were prepared from the integrated Weissenberg photographs. By comparing them with a calibrated scale, the intensities of the reflections were estimated visually, multiple-film technique being used for accurate measurements of strong reflections. The corrections for polarization and Lorentz factors were made in the usual way, and the effects of absorption were neglected, the linear absorption coefficient for Cu $K_\alpha$ radiation being $\mu = 10.1/\text{cm}$****.

Relative structure factors were then deduced from these intensity data by the ordinary process.

* Part of this paper was presented at the autumnal joint meeting of chemical societies of Japan, Tokyo, 1956.

1) I. Nitta, H. Watase and Y. Tomiie, *Nature*, **181**, 761 (1958).

2) H. Watase and I. Nitta, This Bulletin, **30**, 889 (1957).

3) H. Watase, Y. Tomiie and I. Nitta, This Bulletin, **31**, 714 (1958).

** $[\alpha]_D^{10}$: +8.0° ($H_2O$).

4) S. Murakami, T. Takemoto, Z. Tei, K. Daigo and S. Takagi, *J. Pharm. Soc. Japan* (*Yakugaku Zasshi*), **75**, 766 (1955).

5) H. Morimoto, ibid., **75**, 937 (1955); S. Murakami, K. Daigo, S. Takagi, T. Takemoto and Z. Tei, ibid., **75**, 1252 (1955).

*** The specimen used for the *c* axis rotation was prepared by cutting the crystal at right angle to the elongated *b* axis.

**** This value comes from the unit cell containing four molecules (see next section).

## Results and Discussion

**Unit Cell and Space Group.**—From the X-ray examinations, the crystal is found to belong to the orthorhombic system, and the dimensions of the unit cell are as follows;

$$a = 26.08 \pm 0.07 \text{ Å}$$
$$b = 5.83 \pm 0.02 \text{ Å}$$
$$c = 6.95 \pm 0.03 \text{ Å}$$

Systematic absence of reflections being recognized only in ($h$ 0 0), (0 $k$ 0) and (0 0 $l$) when $h$, $k$ and $l$ are odd respectively, the space group is uniquely determined to be $D_2^4$-$P2_12_12_1$. The unit cell with this crystal symmetry has four-fold general positions[6]. Judging from the cell size, in the present case, four formula units of $C_{10}H_{15}O_4N$ are expected to be contained in the unit cell, an asymmetric unit being unimolecular.

The axial periods of the $b$ and $c$ axes seemed to be short enough to permit a good resolution of many of the atoms, while the $a$ axis is very long, and the projections along the $b$ and $c$ axes were tried to obtain the atomic parameters.

**Determination of the Structure.**—As already given, the space group involved is $D_2^4$-$P2_12_12_1$, and each two-dimensional projection was treated separately with the origin lying on the two-fold screw axis so that the origin is a center of symmetry in the projection, as in the analysis of zinc kainate dihydrate[2] with the same space group. However, the atomic parameters (Table I), the final electron-density projections (Figs. 2 and 3) and the projections of the crystal structure (Figs. 6 and 7) are described returning to the customary space group origin.

The structure-factor maps (see Fig. 1 given below) for all the possible reflections of ($h$ 0 $l$) and ($h$ $k$ 0) were prepared in order to locate all the atoms by the trial method in the projections along the $b$ and $c$ axes. By assuming the structure of allokainic acid to be 2-carboxy-3-carboxymethyl-4-isopropenylpyrrolidine, the $b$ axis projection was investigated in the first place.

The sign of (6 0 1) with a large $F$ value was defined to be negative. Considering

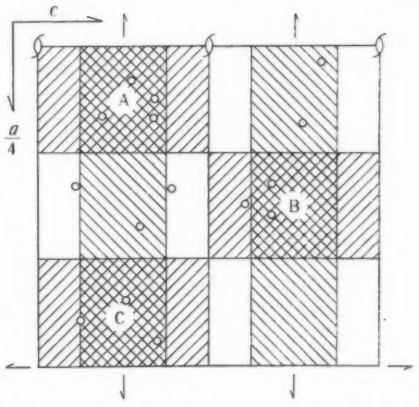


Fig. 1. Superposed structure-factor maps for (6 0 1) with negative sign and (0 0 2) with negative sign, the positive areas being shaded. The $F$ values of these reflections being large, the regions **A**, **B** and **C** are strongly positive. Circles show the final atomic positions. Origin is on the projection of a two-fold screw.

the various structures compatible with the structure factors for the lower order reflections, the absolute values of the structure factors were roughly known, and the sign of (0 0 2) with the largest $F$ value was determined to be negative. Fig. 1 shows the structure-factor map by superposing those for (6 0 1) and (0 0 2), in which the positive areas are shaded. The regions around **A**, **B** and **C** of Fig. 1 being strongly positive, it seems probable that most of the atoms will be found in these regions, and it might be considered at this stage that each of the three side-chains of allokainic acid has its location in each of these regions; the carboxyl group in the region **A** or **C**, the carboxyl group of the carboxymethyl group in the region **B** and the isopropenyl group in the region **A** or **C**.

There was an ambiguous point about the probable positions of the carboxyl and the isopropenyl group. Since packing consideration of the isopropenyl group was found helpful for the further analysis, the trial was carried out, using the structure-factor maps only for the reflections with $h$ even because the $|F|$ values of these reflections are estimated independently of the above ambiguity. All the atoms were then roughly located, leaving the ambiguity about the choice of the origin of the projection out of the

6) "Internationale Tabellen zur Bestimmung von Kristallstrukturen", Bornträger, Berlin (1935); "International Tables for X-ray Crystallography", Kynoch Press, Birmingham (1952).

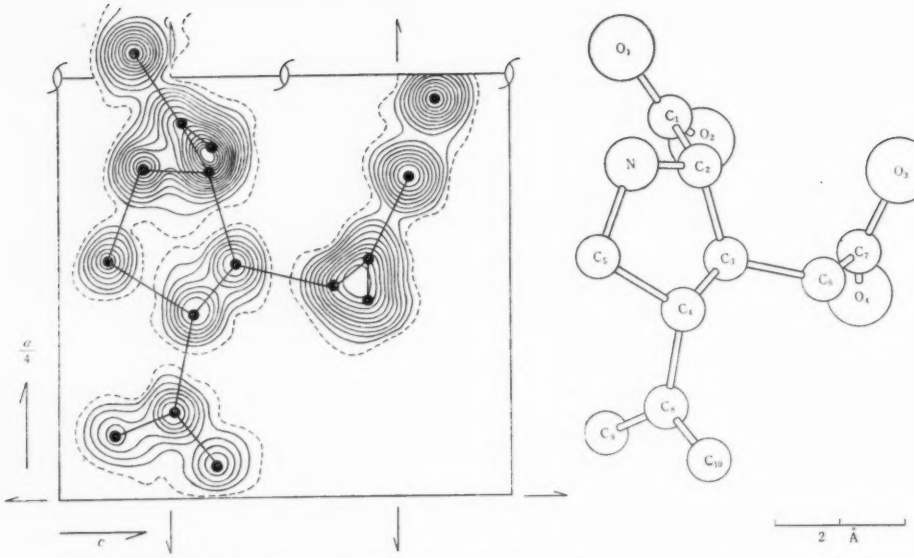


Fig. 2. Electron-density projection along the *b* axis. Contour lines at unit electron intervals, the lowest line, broken line, being 2 electron per Å$^2$. Black circles show the atomic positions. The interpretation of the density map is given on the right side.

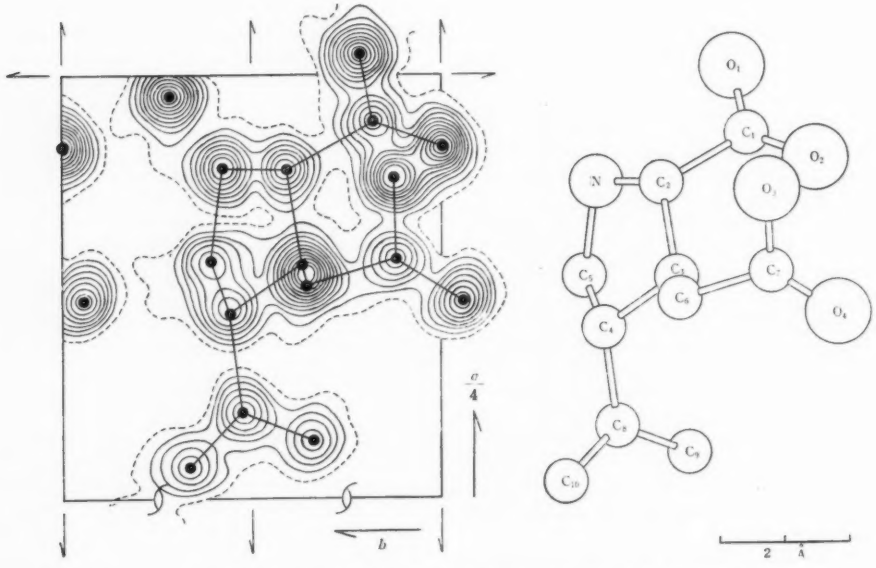


Fig. 3. Electron-density projection along the *c* axis. Contours and symbols are the same as those of Fig. 2. The interpretation of the density map is given on the right side.

question, and in order to be compatible with the $F$ values of (5 0 2) and (7 0 2) it was determined that the carboxyl group is in the region **A** and the isopropenyl group in the region **C**. In this trial (12 0 0) could be used powerfully. The observed structure factors were reduced from the relative values nearly to those in the absolute scale.

Determining the signs of the structure factors, the quantitative trial was carried on step by step from the lower to the higher orders so as to obtain a good agreement between the calculated and the observed $F$ values, until all the atoms were located satisfactorily to permit the Fourier refinements. In this way the electron-density projection along the $b$ axis was derived.

On the basis of the $x$ parameters obtained from the $b$ axis projection, the electron-density projection along the $c$ axis was derived in the same way. Figs. 2 and 3 show the final electron-density projections along the $b$ and $c$ axes respectively. In these maps, each peak has a reasonable height, the peaks of oxygen or nitrogen being higher than those of carbon. The final atomic parameters referred to the customary space group origin are listed in Table I.

TABLE I
ATOMIC PARAMETERS

| Atom | $x/a$ | $y/b$ | $z/c$ |
|---|---|---|---|
| $C_1$ | $0.222_9$ | 0.183 | 0.273 |
| $C_2$ | $0.194_2$ | 0.402 | 0.339 |
| $C_3$ | $0.138_8$ | 0.363 | 0.393 |
| $C_4$ | $0.109_2$ | 0.558 | 0.298 |
| $C_5$ | $0.140_8$ | 0.608 | 0.115 |
| $C_6$ | $0.126_6$ | 0.353 | 0.607 |
| $C_7$ | $0.142_2$ | 0.117 | 0.683 |
| $C_8$ | $0.051_7$ | 0.525 | 0.260 |
| $C_9$ | $0.035_8$ | 0.337 | 0.123 |
| $C_{10}$ | $0.020_0$ | 0.663 | 0.350 |
| N | $0.195_1$ | 0.578 | 0.184 |
| $O_1$ | $0.237_1$ | 0.718 | 0.828 |
| $O_2$ | $0.208_3$ | 0.998 | 0.340 |
| $O_3$ | $0.190_0$ | 0.127 | 0.773 |
| $O_4$ | $0.117_5$ | 0.942 | 0.683 |

At this stage, the discrepancy indices ($R=\sum||F_o|-|F_c||/\sum|F_o|$) are 0.178 for ($h$ 0 $l$) and 0.192 for ($h$ $k$ 0), employing the data up to $\sin\theta/\lambda=0.640$ for ($h$ 0 $l$) and 0.642 for ($h$ $k$ 0), assuming the values of the unobserved structure factors to be precisely zero and neglecting the contributions from hydrogen atoms. In the structure-factor calculations, the value of $B=4.0$ Å$^2$ was used for each zone as the temperature factor common to all the atoms. The atomic scattering factors were taken from McWeeny's paper[7]; for oxygen $f_o=1/3(f_{\parallel}+2f_{\perp})$ and for carbon the values for 'valence states'.

The observed and the calculated structure factors for ($h$ 0 $l$) and ($h$ $k$ 0) are listed in Tables II and III respectively, in which the signs of the calculated structure factors are given as those for the coordinates used in the analysis for each projection.

**Molecular Structure.**—The bond lengths and bond angles, calculated from the atomic parameters of Table I, are shown in Fig. 4. It may be said that the bond lengths will be correct to ±0.03 Å and the bond angles to ±3°. As a result, it is confirmed that allokainic acid is a stereoisomer of kainic acid, its structure being 2-carboxy-3-carboxymethyl-4-isopropenylpyrrolidine. Namely, the five-membered ring (N, $C_2$, $C_3$, $C_4$, $C_5$) is of pyrrolidine, and the side-chains $C_2$–($C_1$–$O_1$, $O_2$), $C_3$–($C_6$–$C_7$–$O_3$, $O_4$) and $C_4$–($C_8$–$C_9$, $C_{10}$) are the carboxyl, the carboxymethyl and the isopropenyl group respectively. In the isopropenyl group, the $C_8$–$C_{10}$ bond of the length 1.31 Å is its double bond.

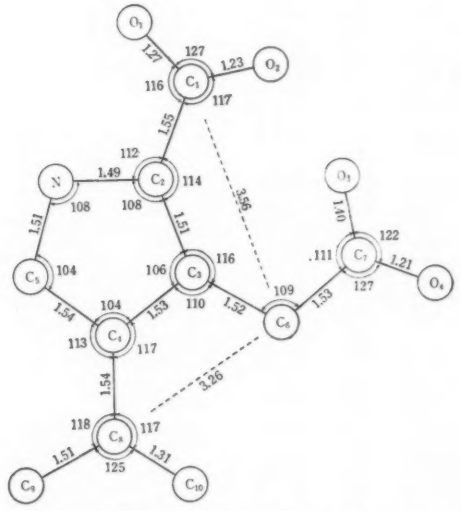


Fig. 4. Bond lengths (Å) and bond angles (°).

The observed bond lengths except for the $C_7$–$O_3$ distance are in agreement within ±0.03 Å with those of the corresponding

7) R. McWeeny, *Acta Cryst.*, **4**, 513 (1951).

TABLE II

OBSERVED AND CALCULATED STRUCTURE FACTORS $F(h\ 0\ l)$

THE VALUES FOR $(h\ 0\ 0)$ ARE LISTED IN TABLE III

| $h\ k\ l$ | $1/4F_o$ | $1/4F_c$ | $h\ k\ l$ | $1/4F_o$ | $1/4F_c$ | $h\ k\ l$ | $1/4F_o$ | $1/4F_c$ | $h\ k\ l$ | $1/4F_o$ | $1/4F_c$ |
|---|---|---|---|---|---|---|---|---|---|---|---|
| 1 0 1 | 6.6 | − 8.1 | 21 0 2 | — | 0.6 | 11 0 4 | — | − 0.2 | 8 0 6 | 0.7 | 0.7 |
| 2 0 1 | 10.2 | − 7.7 | 22 0 2 | — | −0.4 | 12 0 4 | 1.6 | 2.6 | 9 0 6 | — | 0.0 |
| 3 0 1 | 7.6 | 7.0 | 23 0 2 | 2.0 | 2.0 | 13 0 4 | — | − 0.6 | 10 0 6 | 2.2 | −2.4 |
| 4 0 1 | 0.7 | 0.5 | 24 0 2 | 3.1 | 1.9 | 14 0 4 | 1.8 | 2.0 | 11 0 6 | — | 0.8 |
| 5 0 1 | 8.6 | 9.4 | 25 0 2 | 0.7 | −1.0 | 15 0 4 | 1.4 | − 2.0 | 12 0 6 | — | −0.2 |
| 6 0 1 | 21.4 | −21.7 | 26 0 2 | 2.2 | 1.8 | 16 0 4 | 0.7 | 0.8 | 13 0 6 | 0.7 | −0.6 |
| 7 0 1 | 4.4 | − 4.3 | 27 0 2 | 1.4 | 1.4 | 17 0 4 | 2.0 | − 0.6 | 14 0 6 | 1.0 | 0.5 |
| 8 0 1 | 0.8 | 0.0 | 28 0 2 | 1.0 | 1.0 | 18 0 4 | 4.6 | − 3.9 | 15 0 6 | 1.2 | 1.3 |
| 9 0 1 | — | − 0.3 | 29 0 2 | — | 0.1 | 19 0 4 | — | − 0.2 | 16 0 6 | — | 0.0 |
| 10 0 1 | 4.4 | − 2.8 | 30 0 2 | 0.7 | −0.7 | 20 0 4 | 0.7 | 0.7 | 17 0 6 | 1.6 | 0.9 |
| 11 0 1 | 7.9 | 7.5 | 31 0 2 | 1.1 | 0.8 | 21 0 4 | — | − 0.2 | 18 0 6 | 1.4 | 0.8 |
| 12 0 1 | 1.5 | 1.7 | 32 0 2 | 0.7 | 0.3 | 22 0 4 | — | − 0.5 | 19 0 6 | — | 0.1 |
| 13 0 1 | 3.2 | 4.2 | 1 0 3 | 6.4 | 5.6 | 23 0 4 | 0.7 | − 0.6 | 20 0 6 | 1.0 | 0.4 |
| 14 0 1 | 3.6 | 1.6 | 2 0 3 | 4.4 | −3.9 | 24 0 4 | 1.0 | − 0.8 | 21 0 6 | — | 0.2 |
| 15 0 1 | 1.3 | 1.0 | 3 0 3 | 10.5 | −8.8 | 25 0 4 | — | 0.1 | 22 0 6 | 1.6 | 1.7 |
| 16 0 1 | 4.3 | 5.0 | 4 0 3 | 5.3 | −5.0 | 26 0 4 | 1.4 | − 0.8 | 23 0 6 | 0.8 | −0.4 |
| 17 0 1 | 0.8 | − 1.4 | 5 0 3 | 8.7 | −6.9 | 27 0 4 | 0.6 | − 0.6 | 24 0 6 | — | −0.1 |
| 18 0 1 | 6.5 | 7.2 | 6 0 3 | 2.2 | 1.0 | 28 0 4 | 0.6 | − 0.5 | 1 0 7 | 0.7 | −0.4 |
| 19 0 1 | 1.7 | 2.3 | 7 0 3 | 4.1 | 3.3 | 29 0 4 | — | 0.0 | 2 0 7 | 1.0 | 1.0 |
| 20 0 1 | 2.3 | 2.6 | 8 0 3 | 6.4 | 5.5 | 1 0 5 | 0.9 | − 0.2 | 3 0 7 | 1.0 | −1.2 |
| 21 0 1 | 0.7 | − 1.1 | 9 0 3 | 1.3 | 0.9 | 2 0 5 | 1.3 | 1.2 | 4 0 7 | 1.4 | −1.6 |
| 22 0 1 | — | − 0.3 | 10 0 3 | — | 0.2 | 3 0 5 | 2.6 | 4.0 | 5 0 7 | 0.7 | 0.6 |
| 23 0 1 | 0.7 | − 0.5 | 11 0 3 | 7.8 | −8.5 | 4 0 5 | 3.6 | 3.6 | 6 0 7 | 1.7 | −1.6 |
| 24 0 1 | 1.4 | 1.7 | 12 0 3 | 0.8 | 1.5 | 5 0 5 | — | 0.2 | 7 0 7 | 1.9 | 2.0 |
| 25 0 1 | 1.0 | − 1.1 | 13 0 3 | 5.3 | −4.2 | 6 0 5 | 2.4 | 4.3 | 8 0 7 | 1.9 | −1.7 |
| 26 0 1 | 0.8 | 0.9 | 14 0 3 | — | −0.1 | 7 0 5 | 1.5 | − 1.4 | 9 0 7 | 1.8 | 1.8 |
| 27 0 1 | — | − 0.2 | 15 0 3 | 2.0 | −2.0 | 8 0 5 | 1.2 | − 0.9 | 10 0 7 | 1.9 | 1.9 |
| 28 0 1 | 0.7 | − 0.6 | 16 0 3 | 4.1 | 4.0 | 9 0 5 | 1.2 | − 1.9 | 11 0 7 | 1.0 | 1.0 |
| 29 0 1 | — | − 0.1 | 17 0 3 | — | −0.7 | 10 0 5 | 1.5 | − 1.2 | 12 0 7 | 5.6 | 3.2 |
| 30 0 1 | — | − 0.2 | 18 0 3 | — | 0.0 | 11 0 5 | 0.7 | 1.4 | 13 0 7 | — | −0.2 |
| 31 0 1 | 0.7 | − 0.5 | 19 0 3 | 1.7 | −2.8 | 12 0 5 | 5.1 | − 4.8 | 14 0 7 | 1.8 | 1.1 |
| 32 0 1 | 1.3 | 0.7 | 20 0 3 | 3.3 | −3.3 | 13 0 5 | 0.7 | 0.8 | 15 0 7 | — | 0.4 |
| 33 0 1 | — | 0.4 | 21 0 3 | 1.7 | 1.7 | 14 0 5 | 1.7 | − 1.5 | 16 0 7 | 0.6 | 0.8 |
| 0 0 2 | 37.1 | −34.8 | 22 0 3 | 1.0 | −0.9 | 15 0 5 | 0.7 | 0.9 | 17 0 7 | 1.7 | −1.5 |
| 1 0 2 | 2.6 | − 3.0 | 23 0 3 | 0.7 | 0.9 | 16 0 5 | 4.2 | − 4.0 | 18 0 7 | — | 0.0 |
| 2 0 2 | 13.4 | −12.3 | 24 0 3 | 0.7 | −0.6 | 17 0 5 | 3.1 | 2.9 | 19 0 7 | 0.7 | −0.4 |
| 3 0 2 | 1.1 | − 0.2 | 25 0 3 | 1.0 | 0.9 | 18 0 5 | 1.0 | − 1.2 | 20 0 7 | 0.9 | 0.9 |
| 4 0 2 | 2.6 | − 3.7 | 26 0 3 | 1.6 | 1.3 | 19 0 5 | — | 0.7 | 0 0 8 | — | −0.1 |
| 5 0 2 | 14.4 | 14.4 | 27 0 3 | 1.0 | 0.8 | 20 0 5 | — | 0.4 | 1 0 8 | — | 0.1 |
| 6 0 2 | — | − 1.4 | 28 0 3 | — | −0.5 | 21 0 5 | 1.6 | − 0.5 | 2 0 8 | 1.0 | −1.3 |
| 7 0 2 | 12.4 | 12.6 | 29 0 3 | 0.9 | 0.8 | 22 0 5 | — | 0.2 | 3 0 8 | — | −0.3 |
| 8 0 2 | 4.6 | 4.4 | 30 0 3 | 1.2 | −1.0 | 23 0 5 | — | − 0.3 | 4 0 8 | — | 0.4 |
| 9 0 2 | 5.7 | 5.2 | 31 0 3 | 0.7 | 0.6 | 24 0 5 | 1.1 | 0.8 | 5 0 8 | 0.8 | 0.9 |
| 10 0 2 | 7.7 | 6.9 | 0 0 4 | 6.7 | −6.7 | 25 0 5 | 0.6 | 0.4 | 6 0 8 | — | −0.5 |
| 11 0 2 | 2.2 | − 3.1 | 1 0 4 | 1.2 | −1.3 | 26 0 5 | 0.5 | − 0.3 | 7 0 8 | — | 0.0 |
| 12 0 2 | 6.5 | 6.9 | 2 0 4 | — | 0.5 | 27 0 5 | 0.7 | − 0.7 | 8 0 8 | — | −0.3 |
| 13 0 2 | 2.6 | 4.2 | 3 0 4 | 1.1 | −0.2 | 0 0 6 | 2.4 | 3.0 | 9 0 8 | — | 0.4 |
| 14 0 2 | 2.5 | − 2.7 | 4 0 4 | 2.0 | 1.7 | 1 0 6 | 0.7 | 1.1 | 10 0 8 | 1.8 | 1.2 |
| 15 0 2 | 2.3 | 1.7 | 5 0 4 | 4.3 | −6.2 | 2 0 6 | 2.2 | 2.2 | 11 0 8 | — | 0.1 |
| 16 0 2 | 2.7 | − 3.2 | 6 0 4 | 2.7 | 2.6 | 3 0 6 | — | 0.0 | 12 0 8 | 0.7 | −0.4 |
| 17 0 2 | 0.9 | − 0.1 | 7 0 4 | 5.7 | −6.0 | 4 0 6 | 1.6 | 1.5 | 13 0 8 | — | 0.0 |
| 18 0 2 | — | 0.5 | 8 0 4 | 6.5 | −5.8 | 5 0 6 | — | − 0.1 | 14 0 8 | 0.9 | −0.3 |
| 19 0 2 | 0.7 | − 0.7 | 9 0 4 | 3.4 | −2.9 | 6 0 6 | — | 0.2 | | | |
| 20 0 2 | 1.9 | − 1.6 | 10 0 4 | 2.0 | −2.0 | 7 0 6 | 1.4 | 0.9 | | | |

TABLE III

OBSERVED AND CALCULATED STRUCTURE FACTORS $F(h\ k\ 0)$

| $h\ k\ l$ | $1/4F_o$ | $1/4F_c$ | $h\ k\ l$ | $1/4F_o$ | $1/4F_c$ | $h\ k\ l$ | $1/4F_o$ | $1/4F_c$ | $h\ k\ l$ | $1/4F_o$ | $1/4F_c$ |
|---|---|---|---|---|---|---|---|---|---|---|---|
| 0 0 0 | | 114 | 0 2 0 | 7.3 | −8.5 | 18 3 0 | 0.4 | − 0.8 | 9 5 0 | 1.7 | 1.7 |
| 2 0 0 | 20.1 | −21.0 | 1 2 0 | 9.2 | −9.8 | 19 3 0 | 3.2 | − 3.1 | 10 5 0 | 0.6 | 0.3 |
| 4 0 0 | 5.5 | − 5.7 | 2 2 0 | 1.3 | 0.1 | 20 3 0 | — | 0.1 | 11 5 0 | 2.0 | −2.2 |
| 6 0 0 | 7.6 | 7.1 | 3 2 0 | 7.8 | 8.6 | 21 3 0 | 2.4 | 2.3 | 12 5 0 | 0.9 | 0.3 |
| 8 0 0 | 8.4 | 6.9 | 4 2 0 | 9.7 | 10.4 | 22 3 0 | 1.2 | 1.7 | 13 5 0 | 2.2 | −2.4 |
| 10 0 0 | 5.2 | 5.4 | 5 2 0 | 1.1 | −2.3 | 23 3 0 | — | − 0.1 | 14 5 0 | 1.2 | −1.1 |
| 12 0 0 | 22.2 | −21.3 | 6 2 0 | 2.4 | −2.3 | 24 3 0 | 1.1 | 1.1 | 15 5 0 | 0.6 | 0.5 |
| 14 0 0 | 0.3 | − 0.3 | 7 2 0 | 3.5 | −5.3 | 25 3 0 | 0.3 | 0.1 | 16 5 0 | 2.2 | 2.1 |
| 16 0 0 | 6.3 | 5.7 | 8 2 0 | 8.3 | 6.6 | 26 3 0 | 1.3 | − 1.1 | 17 5 0 | 0.9 | 1.3 |
| 18 0 0 | 5.8 | − 5.6 | 9 2 0 | 3.5 | 3.6 | 27 3 0 | 0.5 | − 0.5 | 18 5 0 | 1.1 | −1.2 |
| 20 0 0 | 1.5 | 1.7 | 10 2 0 | 8.7 | −8.3 | 28 3 0 | 2.1 | 1.6 | 19 5 0 | 0.7 | −0.4 |
| 22 0 0 | 1.3 | 0.4 | 11 2 0 | 0.8 | 0.9 | 29 3 0 | 0.6 | 0.4 | 20 5 0 | 0.6 | 0.7 |
| 24 0 0 | 3.3 | − 2.5 | 12 2 0 | 7.4 | 8.0 | 30 3 0 | 1.1 | − 0.8 | 21 5 0 | 1.1 | 0.9 |
| 26 0 0 | 1.5 | 1.6 | 13 2 0 | 2.0 | −1.8 | 0 4 0 | 4.3 | − 5.5 | 22 5 0 | 0.3 | −0.3 |
| 28 0 0 | 1.2 | − 0.7 | 14 2 0 | 0.5 | −1.0 | 1 4 0 | 0.7 | − 1.3 | 23 5 0 | 0.5 | −0.1 |
| 30 0 0 | — | 0.0 | 15 2 0 | 1.1 | −2.8 | 2 4 0 | — | − 0.2 | 24 5 0 | — | 0.1 |
| 32 0 0 | 1.6 | − 1.0 | 16 2 0 | 1·8 | −2.3 | 3 4 0 | 4.0 | 3.9 | 0 6 0 | 0.4 | −0.7 |
| 1 1 0 | 3.6 | − 4.1 | 17 2 0 | 0.6 | −1.4 | 4 4 0 | 5.7 | 5.0 | 1 6 0 | 1.0 | −0.6 |
| 2 1 0 | 10.6 | − 8.2 | 18 2 0 | 1.1 | −1.6 | 5 4 0 | 2.3 | − 2.0 | 2 6 0 | 0.5 | −1.2 |
| 3 1 0 | 9.5 | 10.4 | 19 2 0 | 0.4 | 1.4 | 6 4 0 | 7.3 | − 6.2 | 3 6 0 | 0.6 | 0.4 |
| 4 1 0 | 9.5 | −10.1 | 20 2 0 | 3.8 | −3.3 | 7 4 0 | 2.3 | 2.6 | 4 6 0 | 1.2 | −1.8 |
| 5 1 0 | 1.8 | − 3.9 | 21 2 0 | 1.7 | −1.9 | 8 4 0 | 0.4 | − 0.8 | 5 6 0 | 1.8 | −1.7 |
| 6 1 0 | 0.2 | − 1.3 | 22 2 0 | 2.3 | 2.1 | 9 4 0 | 0.6 | − 0.5 | 6 6 0 | 0.5 | 0.0 |
| 7 1 0 | 0.5 | − 0.6 | 23 2 0 | 3.8 | −3.7 | 10 4 0 | 0.4 | 0.2 | 7 6 0 | 0.8 | 0.8 |
| 8 1 0 | 9.3 | −10.3 | 24 2 0 | 0.5 | −0.9 | 11 4 0 | 0.4 | − 0.2 | 8 6 0 | 0.5 | 0.0 |
| 9 1 0 | 5.4 | 5.1 | 25 2 0 | 2.2 | 1.7 | 12 4 0 | 0.7 | 1.5 | 9 6 0 | 0.6 | −0.3 |
| 10 1 0 | 1.4 | − 0.2 | 26 2 0 | 0.3 | 0.2 | 13 4 0 | 1.0 | − 1.5 | 10 6 0 | 0.8 | 0.8 |
| 11 1 0 | 1.8 | 1.8 | 27 2 0 | 0.4 | 0.4 | 14 4 0 | 0.6 | − 0.7 | 11 6 0 | 0.3 | 0.3 |
| 12 1 0 | 0.6 | − 0.4 | 28 2 0 | 0.4 | −0.2 | 15 4 0 | 0.8 | − 0.9 | 12 6 0 | 0.7 | 0.9 |
| 13 1 0 | 2.5 | 4.1 | 29 2 0 | 0.9 | −0.4 | 16 4 0 | 2.0 | − 1.6 | 13 6 0 | 0.3 | 0.1 |
| 14 1 0 | 1.9 | 0.6 | 30 2 0 | 0.9 | 0.8 | 17 4 0 | 0.5 | − 0.1 | 14 6 0 | 1.4 | −0.7 |
| 15 1 0 | 4.9 | − 4.7 | 31 2 0 | — | 0.0 | 18 4 0 | 5.1 | 4.2 | 15 6 0 | 0.3 | 0.5 |
| 16 1 0 | — | 0.4 | 32 2 0 | 0.4 | 0.5 | 19 4 0 | 1.9 | − 2.5 | 16 6 0 | 1.8 | 1.2 |
| 17 1 0 | 2.5 | 3.3 | 1 3 0 | 2.2 | −2.9 | 20 4 0 | 0.4 | 0.4 | 17 6 0 | 0.4 | 0.7 |
| 18 1 0 | 0.4 | − 0.4 | 2 3 0 | 4.4 | −4.4 | 21 4 0 | 0.5 | 0.2 | 18 6 0 | 1.0 | −0.4 |
| 19 1 0 | 0.6 | 0.8 | 3 3 0 | 1.4 | −1.3 | 22 4 0 | 1.9 | − 1.6 | 19 6 0 | 0.3 | −0.3 |
| 20 1 0 | 2.8 | 3.1 | 4 3 0 | 0.5 | −0.2 | 23 4 0 | — | 0.2 | 20 6 0 | 1.2 | 0.8 |
| 21 1 0 | 0.6 | − 0.7 | 5 3 0 | 5.6 | 5.3 | 24 4 0 | 1.8 | 1.7 | 1 7 0 | 0.8 | −0.7 |
| 22 1 0 | 2.6 | − 2.9 | 6 3 0 | 1.6 | 1.1 | 25 4 0 | 0.4 | 0.2 | 2 7 0 | 0.5 | 0.1 |
| 23 1 0 | 3.4 | − 3.0 | 7 3 0 | 0.5 | −0.9 | 26 4 0 | 0.3 | − 0.5 | 3 7 0 | 0.4 | 0.3 |
| 24 1 0 | 0.5 | − 0.1 | 8 3 0 | — | −1.3 | 27 4 0 | 0.7 | − 0.6 | 4 7 0 | 2.2 | 1.7 |
| 25 1 0 | 0.8 | 0.8 | 9 3 0 | 2.2 | −2.5 | 28 4 0 | 0.2 | − 0.2 | 5 7 0 | — | 0.1 |
| 26 1 0 | 0.6 | − 0.4 | 10 3 0 | 7.1 | −7.5 | 1 5 0 | 4.5 | 4.2 | 6 7 0 | 2.6 | −1.4 |
| 27 1 0 | 1.7 | − 1.7 | 11 3 0 | — | −0.3 | 2 5 0 | 1.9 | 0.8 | 7 7 0 | — | −0.2 |
| 28 1 0 | 0.7 | 0.6 | 12 3 0 | 1.3 | −0.6 | 3 5 0 | 4.9 | − 4.3 | 8 7 0 | 2.0 | 1.4 |
| 29 1 0 | 0.3 | 0.4 | 13 3 0 | 2.5 | 3.1 | 4 5 0 | 3.0 | − 3.0 | 9 7 0 | 0.6 | 0.2 |
| 30 1 0 | 0.3 | 0.3 | 14 3 0 | 0.5 | −0.4 | 5 5 0 | 0.6 | − 0.9 | 10 7 0 | 0.6 | 0.8 |
| 31 1 0 | 2.0 | − 1.5 | 15 3 0 | 0.4 | 0.2 | 6 5 0 | 1.2 | 0.7 | 11 7 0 | 1.1 | −0.7 |
| 32 1 0 | 1.2 | − 0.9 | 16 3 0 | 2.5 | −2.7 | 7 5 0 | — | − 0.4 | | | |
| 33 1 0 | 0.4 | 0.1 | 17 3 0 | 1.1 | −0.6 | 8 5 0 | 2.5 | − 2.0 | | | |

bonds in kainic acid[3], the differences being not definitely significant, while some of the bond angles are fairly different from the corresponding ones of kainic acid.

The C–O distances of the carboxymethyl group of $C_3$ are found to be 1.40 Å for $C_7$–$O_3$ and 1.21 Å for $C_7$–$O_4$, the oxygen $O_3$ being of the hydroxyl group (OH) and forming a hydrogen bond as will be described in the next section (Figs. 6 and 7). The corresponding distances of kainic acid are found to be 1.34 and 1.23 Å, both the oxygens being linked to others by hydrogen bonds.

The C–O distances of the carboxyl group of $C_2$ are 1.27 Å for $C_1$–$O_1$ and 1.23 Å for $C_1$–$O_2$, both forming hydrogen bonds. These values are in good agreement with those of the carboxyl group in kainic acid (1.24 and 1.27 Å), similarly hydrogen bonded.

Judging from the dimensions of the carboxyl group of $C_2$ and the consideration about the observed hydrogen bonds, as in the case of kainic acid, the allokainic acid molecule is considered to be of the 'zwitter ion' structure in which the carboxyl group of $C_2$ is of $(COO)^-$ and the nitrogen is of $N^+H_2$, although the positions of no hydrogen atoms are located in the present work.

As for the stereochemical relations of the atoms in allokainic acid molecule, the carboxyl group of $C_2$ and the carboxymethyl group of $C_3$ take the *trans*-configuration relative to the ring. This relation is the same as that in kainic acid. The carboxymethyl group of $C_3$ and the isopropenyl group of $C_4$ are in the *trans*-configuration, while in kainic acid it was the *cis*-configuration. This fact supports the reasoning based on chemical evidences[8]. The relationship between the structure of kainic acid and allokainic acid is shown in Fig. 5. It is of interest that the anthelmintic effects of the two isomers are very different from each other due only to the configurations of their isopropenyl groups.

The five-membered pyrrolidine ring being fairly flexible, as found in the case of kainic acid, this ring is in the present case also considerably distorted from the planar form owing presumably to the influences of its side-chains and of the interactions between molecules. Deviations from the ordinary values of the

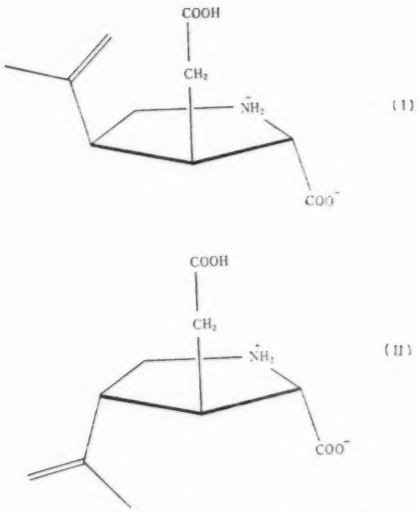


Fig. 5. Stereochemical configuration, (I) kainic acid, (II) allokainic acid.

bond angles of the pyrrolidine ring (108°, 108°, 106°, 104°, 104°) are found to be of the same order as those of hydroxyproline[9] (109°, 105°, 108°, 104°, 105°), the deviations being, however, smaller than those of kainic acid (108°, 104°, 103°, 102°, 105°) or zinc kainate[2] (105°, 110°, 102°, 105°, 102°).

**Crystal Structure.**—The projections of the crystal structure along the *b* and *c* axes are illustrated in Figs. 6 and 7 respectively, giving the intermolecular distances. The unit cell contains four zwitter ion molecules of allokainic acid. As a whole, the crystal structure resembles that of kainic acid[3].

From the short intermolecular N...O or O...O distances, three kinds of hydrogen bond are considered to be formed among the molecules. The two hydrogens of $N^+H_2$ form the intermolecular hydrogen bonds between the nitrogen of one molecule and the carboxyl groups $(COO)^-$ of other two molecules. These hydrogen bond distances are 2.82 Å for N—H...$O_1$ and 2.70 Å for N—H...$O_2$. The hydrogen of the oxygen $O_3$ of the carboxymethyl group also forms an intermolecular hydrogen bond between this group and the carboxyl group, its $O_3$—H...$O_1$ distance being 2.71 Å. The hydrogen bond angles are as follows:

8) H. Morimoto and R. Nakamori, *J. Pharm. Soc. Japan* (*Yakugaku Zasshi*), **76**, 294 (1956); *Proc. Japan Acad.*, **32**, 41 (1956); T. Takemoto, Z. Tei and K. Daigo, *J. Pharm. Soc. Japan* (*Yakugaku Zasshi*), **76**, 298 (1956).

9) J. Zussman, *Acta Cryst.*, **4**, 493 (1951); J. Donohue and K. N. Trueblood, ibid., **5**, 419 (1952).

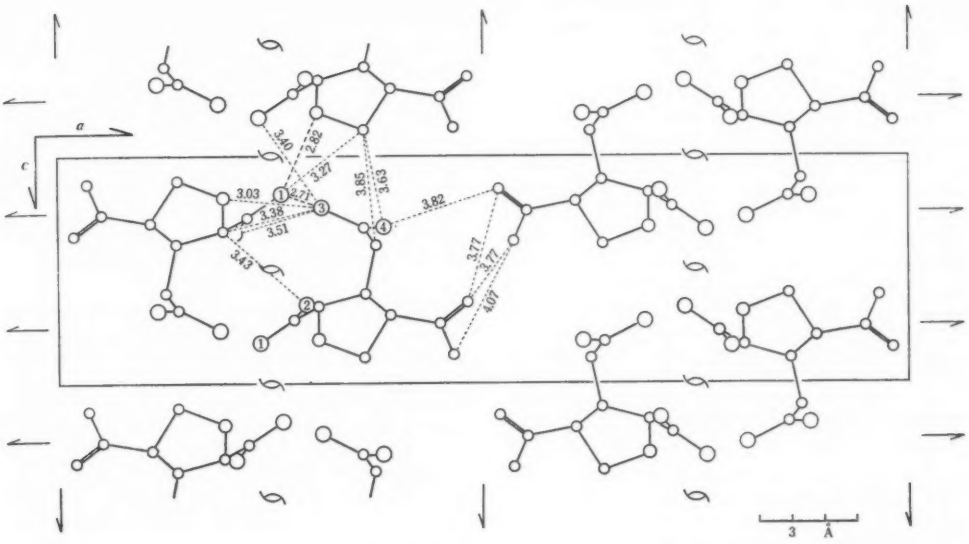


Fig. 6. View of the crystal structure along the *b* axis. The intermolecular distances are shown in Å. Large circles represent oxygens, intermediate nitrogens and small carbons.

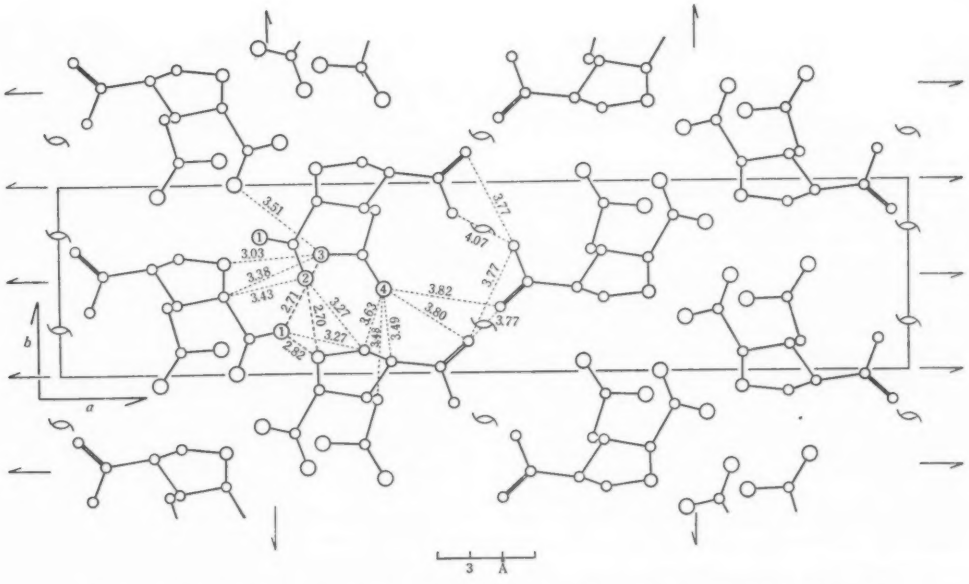


Fig. 7. View of the crystal structure along the *c* axis. The intermolecular distances are shown in Å. Symbols are the same as those of Fig. 6.

$C_2$—N...$O_1$ = 144° $C_2$—N...$O_2$ = 110°
$C_3$—N...$O_1$ = 93° $C_3$—N...$O_2$ = 98°
$O_1$...N...$O_2$ = 93° $C_1$—$O_1$...$O_3$ = 116°
$C_1$—$O_1$...N = 139° $O_3$...$O_1$...N = 102°
$C_1$—$O_2$...N = 132° $C_1$—$O_3$...$O_1$ = 114°

By these hydrogen bonds, the molecules are linked to each other infinitely, forming a layered structure perpendicular to the *a* axis. Between the layers, the isopropenyl groups are in contact with each other, the distances of the closest approach being 3.77 Å for $C_9$...$C'_{10}$, 3.77 Å for $C_9$...$C''_{10}$, 3.77 Å for $C_{10}$...$C'_{10}$ and 4.07 Å for $C_9$...$C'_9$. It is compatible with the existence of the cleavage along the (1 0 0) plane.

The configuration of the isopropenyl group in allokainic acid being different from that of kainic acid as shown in Fig. 5, crystalline allokainic acid has no sufficient space to contain water of crystallization among molecules, while kainic acid crystallizes with one water molecule which is packed in the space and links the kainic acid molecules by forming the hydrogen bonds in addition to the other hydrogen-bridges such as described above. Corresponding to this difference between the crystal structures, allokainic acid is found to be much more soluble in water than kainic acid. In connection with this fact, it is of interest to note that, although zinc kainate easily crystallizes with two waters, the zinc salt of allokainic acid is too soluble in water to obtain crystals. The crystal structure of zinc kainate[2] being, in a sense, similar to that of kainic acid[3], it seems that in the case of zinc allokainate, water molecules may not be packed so as to link the molecules to form the crystal because of the configuration of the molecule.

The author wishes to express his hearty thanks to Professor I. Nitta for his kind guidance and encouragement throughout this work. He is indebted to Professor-Emeritus S. Murakami, Dr. T. Takemoto and their collaborators of this University for supplying the specimen and kind discussion. Thanks are also due to Dr. Y. Tomiie and Mr. Y. Sasada of this University for helpful advice and continued interest.

*Department of Chemistry, Faculty of Science, Osaka University*
*Kita-ku, Osaka*

# *Studies on the Synthesis of Metal Complexes. IV*[1]. *The Cobalt(III) Complexes of Ammoniatriacetic Acid*

By Motoshichi MORI, Muraji SHIBATA, Eishin KYUNO and Yoshito OKUBO

(Received June 26, 1958)

It is commonly known that ammoniatriacetic acid (ATA) acts as a tetradentate donor in combining with metal ions, and this has been proved by Schwarzenbach and his co-workers[2] by the titration of the acid with a base in the presence of a number of metal ions. In the event that one molecule of ATA co-ordinates to a cobalt(III) ion having a co-ordination number six, it is to be expected that two positions around the cobalt ion, not occupied by the chelating agent, are filled by solvent molecules or other donors in the solution. On the other hand, if two molecules of ATA combined with the ion, it would be expected that the two nitrogen atoms and four of the carboxyl groups participate in the bonding, and the remaining two carboxyl groups are uncomplexed. It was the purpose of this investigation to ascertain whether ATA could behave in this way. A few complexes containing only one ammoniatriacetate ion per cobalt(III) as a quadrivalent ligand have been isolated and identified by chemical analysis, thermal decomposition, absorption spectroscopy etc. The attempt to prepare a complex containing

1) Presented at the 10th Annual Meeting of the Chemical Society of Japan, Tokyo, April 6, 1957. For a previous paper in this series see M. Mori, M. Shibata, E. Kyuno and K. Hoshiyama, This Bulletin, **31**, 291 (1958).
2) G. Schwarzenbach et al., *Helv. Chim. Acta*, **28**, 828 (1945); G. Schwarzenbach and W. Biedermann, ibid., **31**, 331 (1948).

TABLE I
ANALYTICAL RESULTS (amounts in %)

| | Co | | N | | K | | $H_2O$ | |
|---|---|---|---|---|---|---|---|---|
| | calcd. | obsd. | calcd. | obsd. | calcd. | obsd. | calcd. | obsd. |
| $\alpha$-K[Co ata(OH)$(OH_2)$]·$2H_2O$ | 16.5 | 16.1 | 3.86 | 3.75 | 10.9 | 10.4 | 10.1 | 10.3 |
| $\beta$-K[Co ata(OH)$(OH_2)$]·$3H_2O$ | 15.7 | 16.0 | 3.75 | 3.66 | 10.4 | 9.8 | 14.4 | 14.0 |
| $K_2$[ataCo$(OH)_2$Co ata]·$6H_2O$ | 16.5 | 16.0 | 3.97 | 3.89 | 10.9 | 10.9 | 15.2 | 15.5 |
| $K_2$[Co ata$(CO_3)$]·$H_2O$ | 14.6 | 14.2 | 3.47 | 3.19 | 19.3 | 19.0 | 4.5 | 4.7 |
| $K_2$[Co ata$(C_2O_4)$]·$H_2O$ | 13.6 | 13.4 | 3.24 | — | 18.1 | 17.9 | 4.2 | 4.2 |

two ammoniatriacetate ions was unsuccessful.

## Experimental

**Synthesis.** — 1) *α-Form of potassium hydroxoammoniatriacetatoaquocobaltate(III)*, α-K[Co ata(OH)$(OH_2)$]·$2H_2O$*. — To a solution of 4 g. of ATA in 25 ml. of 2.5 N potassium bicarbonate were added 5 g. of cobalt chloride hexahydrate and 1 ml. of 30% hydrogen peroxide, and the mixture was placed in an ice-bath until blue crystals separated out (about 5 hr.). The crystals were filtered, washed several times with a little cold water, dissolved in a little hot water containing potassium acetate and then recrystallized by the usual procedure. The product was washed with ethanol and ether in turn. Yield, about 1 g. This complex will hereafter be referred to as α-form. It is slightly soluble in water and is converted into another variety (β-form) by heating the solution or acidifying it with acetic acid.

2) *β-Form of potassium hydroxoammoniatriacetatoaquocobaltate(III)*, β-K[Co ata(OH)$(OH_2)$]·$3H_2O$.—This was prepared from a filtrate in 1); after the filtrate was acidified with 6N-acetic acid (about 10 ml.), a large amount of ethanol was added to it, and the solution was kept overnight in a refrigerator. The reddish violet crystals deposited were collected and recrystallized from the cooled solution by the addition of ethanol. The final product was washed with ethanol and ether. Yield, about 2.5 g.

3) *Potassium bis-(ammoniatriacetato)-μ-diol-dicobaltate(III)*, $K_2$[ata Co$(OH)_2$Co ata]·$6H_2O$. — This also was prepared from a separate filtrate in 1); after the filtrate was acidified with 1 N-hydrochloric acid (about 5 ml.), the solution was heated on a boiling water-bath until a pink solution appeared. On cooling, pink precipitates began to appear, which were collected and dissolved in hot water and reprecipitated by cooling and washed with ethanol and ether in turn. Yield, about 2 g.

4) *Potassium carbonatoammoniatriacetatocobaltate(III)*, $K_2$[Co ata$(CO_3)$]·$H_2O$. — Approximately 4 g. of ATA was added to a cold green solution of potassium tricarbonatocobaltate(III) prepared from 20 g. of $KHCO_3$ and 10 g. of $CoCl_2 \cdot 6H_2O$ — 5 ml. of 30% $H_2O_2$ by the previous method[3]. The mixture was warmed on a water-bath until the green color of the solution changed into violet (about 10 min.). After the solution was cooled, about an equal volume of ethanol was added to it and the whole was kept overnight in a refrigerator. The crystals were recrystallized from water in the hot. They were brilliant violet in color. Yield, about 2.5 g.

5) *Potassium oxalatoammoniatriacetatocobaltate (III)*, $K_2$[Co ata$(C_2O_4)$]·$H_2O$.—About 3.5 g. of the α-form obtained in 1) was dissolved in 25 ml. of 2 N-potassium acetate solution containing 1.3 g. of oxalic acid. The solution was warmed on a water-bath until the color changed to reddish violet, and then cooled and about 12 ml. of ethanol was added, whereupon crystallization of the substance took place. It was recrystallized in the form of bright, reddish-violet needles. This was also obtained by using the β-form or the carbonato-complex obtained in 4).

**Determination of the Chemical Formulae.** —For this purpose, chemical analysis, thermal decomposition, coagulation of ferric oxide sol and spectroscopic measurement were used in the same manner as described in the previous papers[3,4].

## Results and Discussion

**Chemical Analysis.** — The numerical values are given in Table I. The water of crystallization was estimated from the weight loss in the thermal decomposition. For the determination of cobalt and potassium, the residues from the thermal decompositions of the complexes were used as samples. The nitrogen content was determined by Kjeldahl's method.

**Thermal Decomposition.** — When a sample was heated with gradual elevation of temperature up to nearly 300°C, decomposition took place in several steps, and finally a residue containing an oxide of cobalt (perhaps, $Co_2O_3$) and potassium carbonate was left behind. Decomposition curves showing the weight loss per millimole vs. temperature are shown in Fig. 1.

It may be noted that the weight loss of the β-form at 150~190°C corresponds closely to one molecule of water (curve

* "ata" stands for ammoniatriacetate ion.

3) M. Mori et al., This Bulletin, **29**, 883 (1956).

4) M. Mori et al., This Bulletin, **31**, 291 (1958).

2). In fact the product had exactly the same pink color as the diol-complex reported in the previous syntheses. However, the weight loss of the $\alpha$-form in the same temperature range is too great for one to assume the formation of the diol-complex and it is at present unknown what happens in that stage (curve 1). In the case of the carbonato- and the oxalato-complexes, the weight loss corresponding to removal of a carbonate or an oxalate ion from each of the complexes was observed prior to the final decomposition (curves 4 and 5).

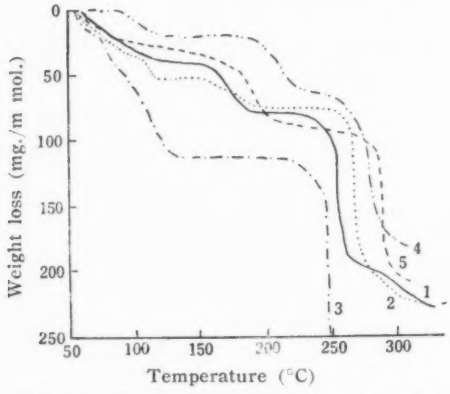


Fig. 1. Thermal decomposition curves of:
1. $\alpha$-K[Co ata(OH)(OH$_2$)]·2H$_2$O
2. $\beta$-K[Co ata(OH)(OH$_2$)]·3H$_2$O
3. K$_2$[ataCo(OH)$_2$Co ata]·6H$_2$O
4. K$_2$[Co ata(CO$_3$)]·H$_2$O
5. K$_2$[Co ata(C$_2$O$_4$)]·H$_2$O

**Coagulation Value.**—Nakahara and coworkers[5] have given 6.6 mF and 0.48 mF as the average values for uni- and bivalent complex anions respectively, but the values obtained in the present experiment deviated from the average to a considerable extent. Namely, (i) $\alpha$-K[Co ata(OH)(OH$_2$)]...2 mF, (ii) $\beta$-K[Co ata(OH)(OH$_2$)]...0.6 mF, (iii) K$_2$[Co$_2$(ata)$_2$(OH)$_2$]...0.2 mF, (iv) K$_2$[Co ata(CO$_3$)]...0.3 mF, (v) K$_2$[Co ata(C$_2$O$_4$)]...0.3 mF.

Among these, the values for the species of the $\beta$-form and the diol-salt are too low for a uni- or a bivalent anion respectively, but they may be explained by assuming the following reactions;

$$[\text{Co ata(OH)(OH}_2)]^- \rightleftarrows [\text{Co ata(OH)}_2]^{2-} + \text{H}^+$$

$$[\text{ataCo}\langle^{\text{OH}}_{\text{OH}}\rangle\text{Co ata}]^{2-} \rightleftarrows$$

$$[\text{ataCo}\langle^{\text{OH}}_{\text{O}}\rangle\text{Co ata}]^{3-} + \text{H}^+$$

As an evidence for these equilibria, it was found that the pH values of the $\beta$-form and the diol-salt were 5.8 and 3.6 in the M/500 solutions. The coagulation value for the $\alpha$-form is also lower than the average, but this deviation may be attributed to partial conversion into the $\beta$-form, because the sample solution was prepared by heating.

**Visible and Ultraviolet Absorption Spectra.**—All the absorption curves are shown in Figs. 2 and 3, and the numerical data are given in Table II. As is seen in Fig. 2, the curves 1 and 2 have shoulders at about $100\times10^{13}$/sec. probably owing to the ligand $OH^-$ in the complex radicals. This is supported by the fact that the shoulder disappears in an acidified solution but remains in an alkaline solution, as are illustrated by the curves 3 and 4.

The curve 1 in Fig. 3 also has a shoulder at nearly the same frequency as the above and this may be considered as a specific band of diol-bond, because a similar band has been found in octammine-$\mu$-diol-dicobalt(III) salt[6].

For the carbonato- and the oxalato-complex, the absorption curves are similar to each other in appearance (Figs. 3-2 and 3). It may be noted that both complexes are perhaps the first examples represented by the general type [CoNO$_5$].

TABLE II
ABSORPTION MAXIMA AND log $\varepsilon$ ($10^{13}$/sec.)

| | $\nu_1$ | log $\varepsilon_1$ | $\nu_2$ | log $\varepsilon_2$ | $\nu_s$ | log $\varepsilon_s$ | $\nu_3$ | log $\varepsilon_3$ |
|---|---|---|---|---|---|---|---|---|
| $\alpha$-K[Co ata(OH)(OH$_2$)]·2H$_2$O | 54.25 | 2.28 | 74.62 | 2.48 | ca 100 | 3.54 | 132.74 | 4.21 |
| $\beta$-K[Co ata(OH)(OH$_2$)]·3H$_2$O | 55.56 | 1.72 | 73.89 | 1.73 | ca 100 | 2.94 | 134.53 | 3.69 |
| K$_2$[ataCo(OH)$_2$Co ata]·6H$_2$O | 58.36 | 1.65 | — | — | ca 100 | 2.54 | — | — |
| K$_2$[Co ata(CO$_3$)]·H$_2$O | 53.19 | 2.22 | 77.32 | 2.18 | — | — | 123.97 | 4.09 |
| K$_2$[Co ata(C$_2$O$_4$)]·H$_2$O | 54.55 | 2.30 | 77.32 | 2.29 | — | — | 127.12 | 4.33 |

5) S. Nakahara et al., *J. Chem. Soc. Japan, Pure Chem. Sec.* (*Nippon Kagaku Zassi*), **74**, 488 (1953).

6) Y. Inamura and Y. Kondo, ibid., **74**, 627 (1953).

Fig. 4 is a diagram in which the frequency values for the first band of the complexes belonging to the types $[CoN_5O]$, $[CoN_3O_3]$ and $[CoNO_5]$ are plotted against the number of nitrogen atoms co-ordinated.

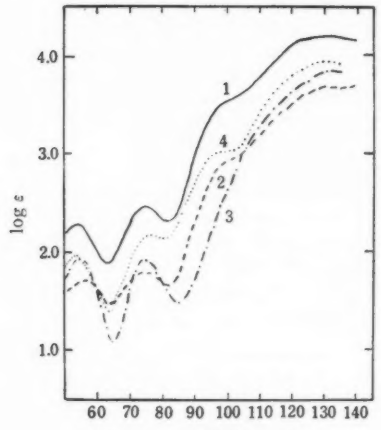


Fig. 2. Absorption spectra of:
1. α-K[Co ata(OH)(OH$_2$)] (aqueous sol.)
2. β-K[Co ata(OH)(OH$_2$)] (aqueous sol.)
3. β-K[Co ata(OH)(OH$_2$)] (at pH 2.6)
4. α-K[Co ata(OH)(OH$_2$)] (at pH 13.3)

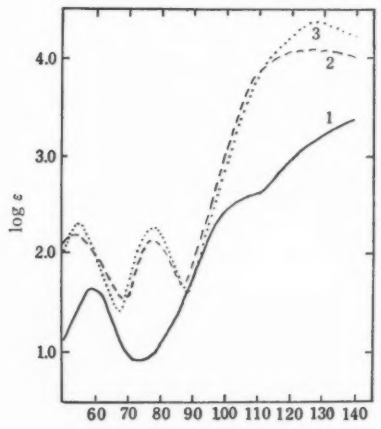


Fig. 3. Absorption spectra of:
1. K$_2$[ataCo(OH)$_2$Co ata]
2. K$_2$[Co ata(CO$_3$)]
3. K$_2$[Co ata(C$_2$O$_4$)]

**Infrared Spectra.**—These were measured in order to confirm the fact that the three carboxyl groups in the chelate agent were complexed. Strong split bands were observed at 1718 and 1735 cm$^{-1}$ for the free acid. On the other hand, the

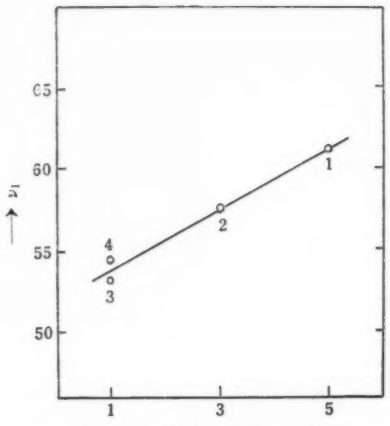


Fig. 4. Frequency position of:
1. [Coen$_2$(gly)]ClO$_4$[7]
2. β-[Co(gly)$_3$][7]
3. K$_2$[Co ata(CO$_3$)]
4. K$_2$[Co ata(C$_2$O$_4$)]

α-form shows bands at 1672 and 1618 cm$^{-1}$, the β-form at 1667 cm$^{-1}$ and the diol-salt at 1600 cm$^{-1}$. It is obvious that these bands are due to the co-ordinated carboxyl groups since such an assignment has been best established for the EDTA-complexes[8].

**Structure.** — The structures of the complexes must be considered on the basis of the above discussion. In the case of the α- and the β-form, a type of isomerism illustrated by formula I and II in Fig. 5 is possible and to the other complexes the structures illustrated by formula III, IV and V may be assigned. It is hard to say conclusively, which of the formulae, I or II, is the α-form and which the β-form, but an assumption is possible based upon the following discussion.

In the previous paper[3], the authors reported that the absorption maximum of the first band for the blue variety of potassium dicarbonatodiamminecobaltate K[Co(NH$_3$)$_2$(CO$_3$)$_2$], shifted to a somewhat longer wave length than that for the corresponding violet variety, and the former variety may be *cis*- and the latter *trans*-form. The same relationship exists in the present case, too; the α-form has a maximum at longer wave length than the β-form (Table II). In addition to this, when the fact that ligands H$_2$O and NH$_3$ stand in a near position and ligands OH$^-$ and CO$_3^{2-}$

7) Y. Shimura and R. Tsuchida, This Bulletin, **28**, 573 (1955).
8) D. H. Bush and J. C. Bailar *J. Am. Chem. Soc.*, **75**, 4574 (1953); **78**, 716 (1956).

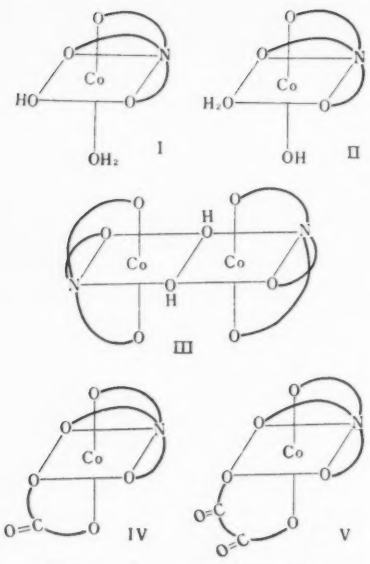


Fig. 5. Structural formulae.

in almost the same position of the spectrochemical series is taken into consideration*, formula I in which ligand $H_2O$ is cis to the co-ordinated nitrogen atom will be assigned to the $\alpha$-form.

## Summary

The cobalt(III) complexes containing ammoniatriacetato group (ata) as a quadridentate ligand are newly prepared:

i) $\alpha$-K[Co ata(OH)$(OH_2)$]$\cdot 2H_2O$
ii) $\beta$-K[Co ata(OH)$(OH_2)$]$\cdot 3H_2O$
iii) $K_2$[ataCo$(OH)_2$Co ata]$\cdot 6H_2O$
iv) $K_2$[Co ata$(CO_3)$]$\cdot H_2O$
v) $K_2$[Co ata$(C_2O_4)$]$\cdot H_2O$

In order to determine the structural formulae of these complexes, their visible, ultraviolet and infrared spectra were measured, as well as their thermal decomposition and their potency to coagulate ferric oxide sol.

*Department of Chemistry, Faculty of Science, Kanazawa University*
*Kanazawa*

* $NO_2^-$ $SO_3^{2-}$ en $NH_3$ $ONO^-$ $NCS^-$ $OH_2$ $C_2O_4^{2-}$ $ONO_2^-$ $OSO_3^{2-}$ $OCHO^-$ $OH^-$ $CO_3^{2-}$ $OCOR^-$ .....

# *Formation and Aging of Precipitates. VIII.* Formation of Monodisperse Particles (1) Gold Sol Particles by Sodium Citrate Method*

By Kazuyoshi TAKIYAMA

(Received May 23, 1958)

Recently many investigations on the precipitation from homogeneous solution have been made to prepare pure and filterable precipitates. The author prepared a few kinds of monodisperse particle by the homogeneous solution method to study the reaction of precipitation. In this paper the formation of gold sol, containing monodisperse particles, is reported. A great many methods for preparing the gold sol have been investigated, but only the sodium citrate method, reported by Turkevich, Stevenson and Hillier[1], seems to be suitable to produce monodisperse gold particles. The author took advantage of the sodium citrate method to prepare the gold sol, and studied the relationship between the condition of formation and the properties of particles produced, and the growth process of gold particles by electron microscopy.

## Experimental

**Formation of Gold Sol.**—Varying amounts (1, 2, 5, 7.5, 10, 15, 20 and 25 ml.) of chlorauric acid solution (0.10% Au) were taken into Erlenmeyer flasks with two openings and diluted with

* The seventh paper of this series, This Bulletin, **31**, 555 (1958).

1) J. Turkevich, R. C. Stevenson and J. Hillier, *Discuss. Faraday Soc.*, **11**, 55 (1951).

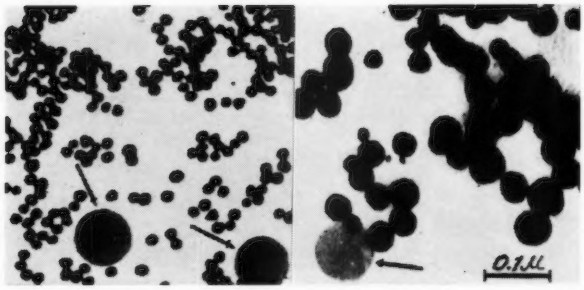


(a) (b) (×100,000)

Fig. 1. Electron micrographs of gold sol particles.
a: Sodium citrate sol b: Zsigmondy sol
(Larger particles in micrographs (arrow) are polystyrene latex particles (880 Å in diameter) using as calibration standard)

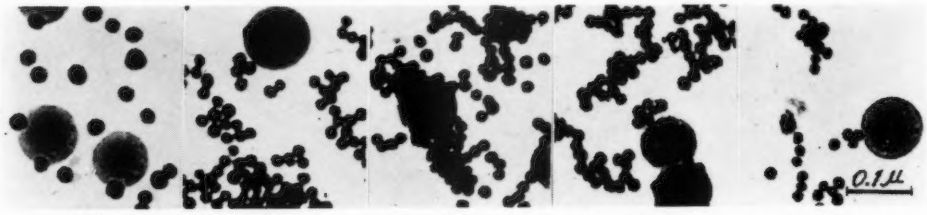


(a) (b) (c) (d) (e)
(×100,000)

Fig. 4. Electron micrographs of gold particles prepared from the various initial concentrations of auric ion at 80°C.
a : $10.15\times10^{-5}$ moleAu/l. (2 mg.Au/100 ml.)
b : $25.37\times10^{-5}$ moleAu/l. (5 mg.Au/100 ml.)
c : $50.75\times10^{-5}$ moleAu/l. (10 mg.Au/100 ml.)
d : $76.13\times10^{-5}$ moleAu/l. (15 mg.Au/100 ml.)
e : $101.50\times10^{-5}$ moleAu/l. (20 mg.Au/100 ml.)

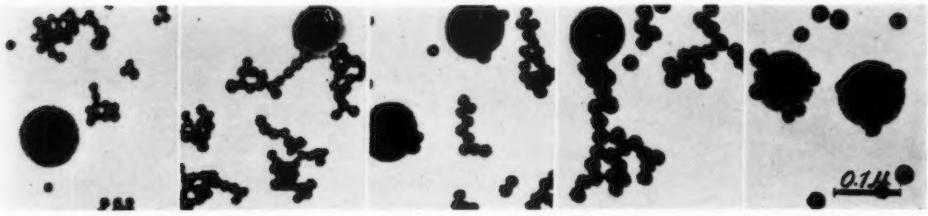


(a) (b) (c) (d) (e)
(×100,000)

Fig. 6. Electron micrographs of gold particles prepared at various temperatures.
($25.37\times10^{-5}$ moleAu/l.)
a: 50°C b: 60°C c: 70°C d: 80°C e: 100°C

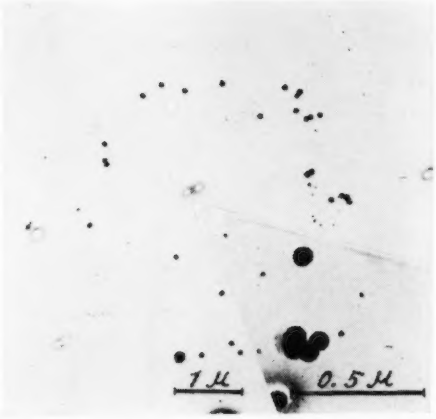


Fig. 8. Electron micrograph of spray mounted drop pattern of gold sol. (Small particles are gold and large particles are polystyrene latex.) (×10,000)
One segment further enlarged. (×40,000)

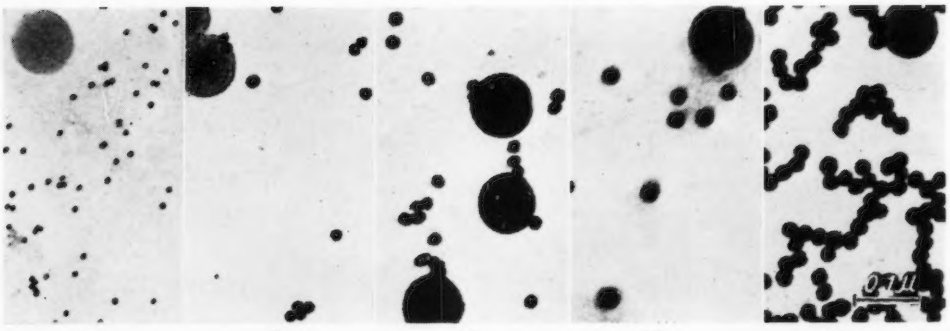


(a) (b) (c) (d) (e)
(×100,000)

Fig. 9. Electron micrographs of gold particles during the growth process.
($25.37 \times 10^{-5}$ moleAu/1., 80°C)
a: 5 min. b: 10 min. c: 20 min. d: 30 min. e: 60 min.

water to 90 ml. After the solutions were warmed to a desired temperature (50, 60, 70, 80 and 100°C), 10 ml. of sodium citrate solution (1.0%) was added to them, the reaction flask connected with a reflux condenser and a thermometer was held in a thermostatted bath.

**Measurement of Size of Gold Particles with Electron Microscope.**—The diameter of gold sol particles has been determined by electron microscopy. Particle-diameter measurement was made from micrographs enlarged at ten-fold magnification. The particle-diameter distribution, the mean particle-diameter** and the standard deviation*** were obtained. The monodisperse polystyrene latex, run No. LS-040-A (880 Å in mean diameter)[2], of the Dow Chemical Co., has been used as calibration standard to measure the particle-diameter****. At different intervals during the course of a reaction, a drop of the reaction mixture was taken onto a small Formvar film, and the film with the drop was floated on the surface of cold water. About ten minutes, the drop on the film was allowed for diffusion of mother liquid ions from the drop into the water below. The film was scooped up with a grid for electron microscopy and was mounted with polystyrene latex. The specimen was observed with electron microscope to determine the growth rate of gold particles.

**Determination of the Number of Gold Particles by Spray Method**[3].—At fixed intervals during the reaction of sol formation, about 10 ml. of the reaction mixture was taken and was poured into a test tube, dipped in an ice bath, to stop the reduction of the auric ion. 5.0 ml. of this sample was mixed thoroughly with 1.0 ml. of polystyrene latex to a definite concentration, and then the mixture was sprayed with a Vaponefrin Nebulizer onto a film made on grid for electron microscopy, which was placed about 20 cm. away from the nozzle of the nebulizer. The specimen was observed with an electron microscope. The number of gold particles during the course of sol formation was estimated by counting the number of gold and polystyrene latex particles in droplet patterns.

**Determination of Gold Sol Concentration by Absorption Spectroscopy.**—An absorption spectrum of gold sol was measured with Hitachi spectrophotometer, using 1-cm. cell, at intervals of 5 mμ over a range of 350 to 700 mμ and a relation between concentration and absorbance was obtained at the wave length of absorption maximum. Absorption spectra of the reaction mixture during the course of sol formation were also obtained.

## Experimental Results

**Size of Gold Sol Particles.**—*Uniformity of gold sol particles.*—The gold sol particles prepared by sodium citrate method were almost spherical. An electron micrograph of particles in one of the gold sol, which was formed from chlorauric acid solution at the initial concentration of $25.37\times10^{-5}$ mole per liter (5 mg. Au/100 ml.) at 80°C, is shown in Fig. 1 a and the particle-diameter distribution of gold particles is shown in Fig. 2 a. The mean particle-diameter was 172 Å and the standard deviation was 13 Å. To compare the property of the gold sol, an electron micrograph of particles in the Zsigmondy's sol ($25.37\times10^{-5}$ mole Au/l.) prepared by the reduction with an alkaline formaldehyde solution is shown in Fig. 1 b, and the particle-diameter distribution is shown in Fig. 2 b. The shape of particles in Zsigmondy's sol was also spherical, but the mean diameter was 417 Å and the standard deviation was 145 Å. Then the particles in Zsigmondy's sol were polydisperse. Larger spherical particles contained in the electron micrographs (arrows) are polystyrene latex particles. The polystyrene latex particles are also contained in every micrograph indicated below. The size of gold sol particles was affected by the condition of formation as described in the next section. An example of the change of standard deviation by the variation of the condition of formation

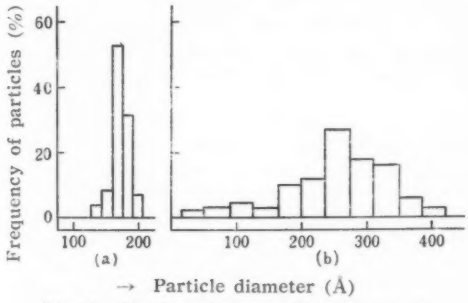


Fig. 2. Particle-diameter distribution of gold sol particles.
a: Sodium citrate sol
b: Zsigmondy sol

2) E. B. Bradford and J. W. Vanderhoff, *J. Appl. Phys.*, **26**, 864 (1955).

** The mean particle-diameter used here is the arithmetic mean obtained by

$$d_0=\frac{\sum n_i d_i}{N}$$

where $d_0$ is the arithmetic mean particle-diameter, $n_i$ is the frequency of particles having diameter $d_i$, and $N$ is the total number of particles.

*** The standard deviation, $\sigma$, is obtained by

$$\sigma=\sqrt{\frac{\sum(d_i-d_0)^2 n_i}{N}}$$

**** Polystyrene latex used here was sent from Dr. E. B. Bradford of Dow Chemical Co. to whom the author's thanks are due.

3) R. C. Backus and R. C. Williams, *J. Appl. Phys.* **21**, 11 (1950).

TABLE I
THE SIZE OF GOLD PARTICLES PREPARED FROM VARIOUS INITIAL CONCENTRATION OF AURIC ION AT 80°C

| | | | | | | | | |
|---|---|---|---|---|---|---|---|---|
| Concn. $C_0$ (moleAu/l.$\times 10^5$) | 5.07 | 10.15 | 25.37 | 38.06 | 50.75 | 76.13 | 101.50 | 126.87 |
| Mean particle dia. $d_0$ (Å) | 149 | 191 | 172 | 173 | 168 | 155 | 140 | 146 |
| Standard deviation $\sigma$ (Å) | 31.5 | 9.4 | 7.5 | 8.1 | 8.3 | 7.1 | 21.5 | 28.1 |
| Particle weight $M\times 10^{-5}$ | 203 | 430 | 312 | 317 | 290 | 233 | 168 | 191 |
| Particle number* $N\times 10^{-10}$ | 29 | 28 | 97 | 144 | 209 | 390 | 720 | 793 |

* Particle number per ml. of sol. $N=(C_0/\text{mole number of one particle})\times 10^{-3}$

is listed in Table I, and the summarized results are indicated in Fig. 3. For the gold particles in sodium citrate sols prepared over a range of the initial concentration from $20\times 10^{-5}$ to $80\times 10^{-5}$ mole auric ion per liter and at the reaction temperature above 70°C, the values of standard deviation ranged below 10% of the particle-diameter. Thus the particles are recognized to be monodisperse. The

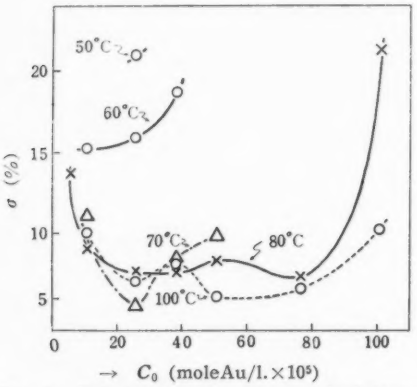


Fig. 3. Relation between the standard deviation of particle-diameter ($\sigma$%) and the initial concentration of auric ion ($C_0$ mole Au/l.$\times 10^5$) of sodium citrate sol.

size distribution of the gold sol particles prepared outside the range of concentration and reaction temperature described above became wide, and the particles were not monodisperse.

*Relation between initial concentration of the auric ion and size of gold sol particles.*— The size of particles in the gold sols was only affected by the initial concentration of auric ions and was not affected by the concentration of sodium citrate over the range from five-fold to ten-fold mole of the auric ion. As the initial concentration of auric ion was increased, the particles became smaller as indicated in Fig. 4 and in Table I. The size of particles is expressed by the particle weight in molecular weight unit, $M$, calculated according to the following equation:

$$M=(4/3)\pi(d_0/2)^3\rho A$$

where $d_0$ is the mean particle diameter (cm.), $\rho$ is the density of gold, and $A$ is Avogadro's number. The logarithm of particle weight of the gold sol particles prepared at 70, 80 and 100°C, log $M$, was linear with the initial concentration of auric ion, $C_0$ (mole Au/l.), as shown in Fig. 5. Then the particle weight, $M$, is represented by

$$M=\alpha e^{-\beta C_0} \qquad (1)$$

where $\alpha$ and $\beta$ are constants. $\alpha$ is dependent upon the reaction temperature showing the values of 3.63, 4.79 and $6.31\times 10^{-7}$ at 70, 80 and 100°C respectively. $\beta$ is always constant and is 1000.

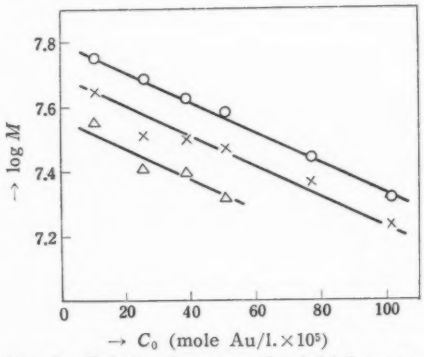


Fig. 5. Relation between the initial concentration of the auric ion and the size of gold particles.
○ 100°C × 80°C △ 70°C

The number of particles per ml. gold sol was related to the size of particles and increased with increasing initial concentration of the auric ion.

*Relation between reaction temperature and size of particle.*— The size of gold sol particles increased with temperature as shown in Fig. 6. The logarithm of particle weight of gold particles prepared at various concentrations, log $M$, is linear with the reaction temperature, $T$ (°C),

as shown in Fig. 7. Then the particle weight, $M$, is represented by

$$M=\gamma e^{\delta T} \qquad (2)$$

where $\gamma$ and $\delta$ are constants. $\gamma$ is a function of initial concentration of the auric ion. They are 9.55, 7.08, 6.76, 6.17, 5.01 and $3.55\times10^{5}$ at 10.15, 25.37, 38.06, 50.75, 76.13 and $101.50\times10^{-5}$ mole Au/l. respectively. $\delta$ is always constant and is 0.0184.

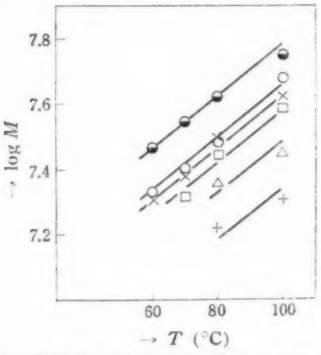


Fig. 7. Relation between the reaction temperature of sol formation and the size of gold particles.

- ◒ $10.15\times10^{-5}$ mole Au/l.
- ○ 25.37 〃
- × 38.06 〃
- □ 50.75 〃
- △ 76.13 〃
- + 101.50 〃

The number of particles per ml. sol prepared at a fixed concentration decreased with the rise of the reaction temperature.

**Formation Process of Gold Sol Particle.**—*Number of gold particles determined by spray method.*—A spray mounted drop pattern of the reaction mixture during the sol formation is shown in an electron micrograph of Fig. 8. Every droplet sprayed is deposited individually in a circular form and it is possible to determine the number of gold and polystyrene latex particles in each droplet pattern. The relationship between the number of particles of gold and polystyrene latex in the droplet patterns prepared at different times after the commencement of the reaction of the sol formation, is shown in Table II. The polystyrene latex sol used here was the same, so its concentration was unchanged throughout the experiment. The ratio of the number of particles of gold and polystyrene latex in the same run was kept almost constant, and it was recognized that the number of gold particles during the reaction of sol formation was constant over the range of time spent in measuring the number of particles.

*Observation of growth process of gold particles with electron microscope.*—The growth process of gold particles during the course of sol formation is shown in a series of electron micrographs of Fig. 9. The particles were monodisperse from the initial stage of the reaction. The size of a particle measured at the time $t$ (min.) is expressed by the mole number of one particle, $x$ (mole), calculated from the mean particle-diameter, $d$ (cm.), according to the following equation:

$$x=(4/3)\pi(d/2)^3\rho/W$$

TABLE II

THE NUMBER OF PARTICLES OF GOLD AND POLYSTYRENE LATEX IN DROPLET PATTERNS PREPARED BY THE SPRAY METHOD DURING THE FORMATION OF GOLD SOL

| No. | Initial concn. of auric ions $C_0$ (mole Au/l.$\times10^5$) | Reaction time $t$ (min.) | Number of gold particles $A_n$ | Number of polystyrene latex particles $P_n$ | $(A_n/P_n)\times100$ |
|---|---|---|---|---|---|
| 1 | 25.37 | 5 | 329 | 386 | 85.2 |
| | | 10 | 502 | 579 | 86.7 |
| | | 30 | 1142 | 1319 | 86.6 |
| | | 60 | 358 | 417 | 85.8 |
| 2 | 25.37 | 5 | 142 | 169 | 84.1 |
| | | 10 | 64 | 73 | 88.0 |
| | | 20 | 231 | 271 | 85.0 |
| | | 30 | 304 | 352 | 86.5 |
| 3 | 50.75 | 5 | 193 | 103 | 187 |
| | | 10 | 130 | 72 | 180 |
| | | 20 | 429 | 229 | 186 |
| | | 30 | 152 | 82 | 185 |

where $W$ is the molecular weight of gold. The plot of $x$ vs. $t$ in two runs exhibits S-shaped curve as shown in Fig. 10.

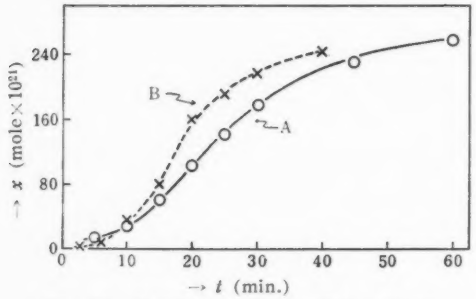


Fig. 10. Growth curve of gold particle measured by electron microscopy.
A: $25.37\times10^{-5}$ mole Au/l.
B: $50.75\times10^{-5}$ mole Au/l.

The rate of growth of a single gold particle is supposed to be expressed by the following equation:

$$dx/dt = kx^{2/3}(x_\infty - x) \qquad (3)$$

where $x$ and $x_\infty$ are the size of particles at time $t$ and after the completion of the sol, respectively; $k$ is the rate constant. The value of $x^{2/3}(x_\infty - x)$ was calculated and $dx/dt$ was obtained from the tangent of the growth curve at time $t$, and the value of $k$ was calculated from equation 3 and was shown in Fig. 11. The value

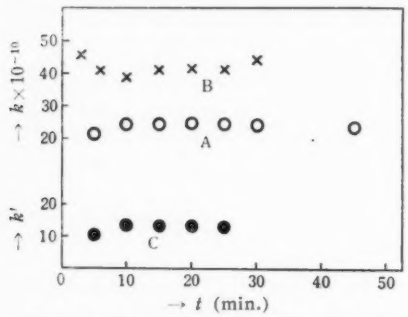


Fig. 11. Constancy of the rate constant.
A: $25.37\times10^{-5}$ mole Au/l. } obtained
B: $50.75\times10^{-5}$ mole Au/l. } from Fig. 10
C: $25.37\times10^{-5}$ mole Au/l. obtained from Fig. 12

of $k$ was constant except the very initial stage of the reaction. Then the rate of growth of a gold particle was proved to obey equation 3.

A study was made of the rate of disappearance of the auric ion during the formation of gold sol in the reaction mixture by withdrawing at definite times aliquot portions and analysing by means of iodometry*. The results of the experiment are given in Fig. 12.

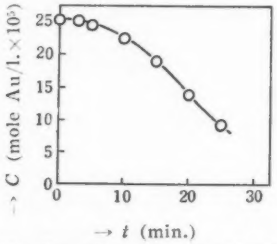


Fig. 12. Reaction rate of gold sol formation measured by the titration.
$25.37\times10^{-5}$ mole Au/l.

The rate of disappearance of the auric ion is supposed to be shown by the following equation:

$$-dC/dt = k'(C_0 - C)^{2/3}C \qquad (4)$$

where $k'$ is the rate constant, and $C_0$ and $C$ are concentrations of auric ion at initial and at time $t$ during the sol formation. $k'$ calculated from the experimental data is constant as shown in Fig. 11, and it is confirmed that equation 4 was proper.

**Absorption Spectra of Gold Sol.**—The absorption spectra of the reaction mixture

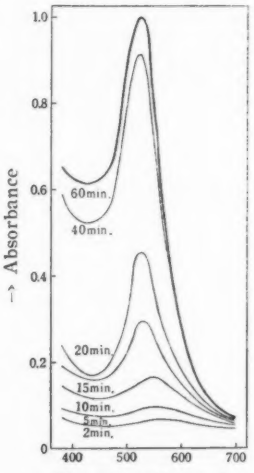


Fig. 13. Absorption spectra of gold sol.
($25.37\times10^{-5}$ mole Au/l., 80°C)

* Iodine liberated by the reduction of $Au^{3+}$ to $Au^{+}$ oxidize gold particles to $Au^{+}$ and the experimental data were obtained from the corrected volume of standard thiosulfate solution.

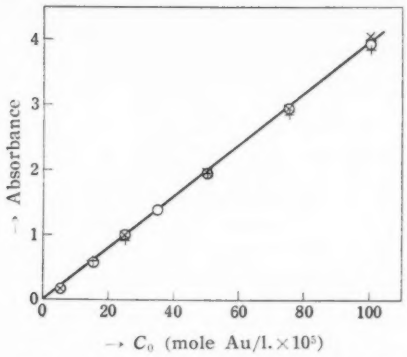


Fig. 14. Calibration curve of gold sol at 525 mμ.

measured at various times after the commencement of the reaction of sol formation are shown in Fig. 13. The maximum absorption shifted slightly toward the shorter wave length as the reaction proceeded. But after the lapse of about one fourth of the total reaction time, the wave length of maximum absorbance was fixed at 525 mμ. The maximum absorbance of gold sol formed under various conditions lay also at 525 mμ. The absorbance of gold sol at 525 mμ was linear with the initial concentration of auric ion as shown in Fig. 14, and the plots of absorbance vs. initial concentration of auric ion of the gold sols prepared above 70°C gave the same straight line.

## Discussion

Gold particles in sodium citrate sol were the monodisperse and highly reproducible. Then particles can be used as a calibration standard in the measurement of particle sizes.

The size of particles decreased exponentially with increasing initial concentration of the auric ion. It has been reported that the gold sol particles prepared with various reducing agents in a basic medium increased in size with increasing initial concentration of the auric ion[4] and these phenomena were caused by the auric hydroxide produced as an intermediate. The sodium citrate sol is slightly acidic and the pH value is about 5.5. It is supposed that the auric ion exists as a chloride complex[5] before the reduction, and that free auric ion produced slowly from the complex reacts with citrate. Turkevich, Stevenson and Hillier[1] asserted that acetone dicarboxylate, generated from sodium citrate, reduced chlorauric acid. But as a pure sodium citrate solution was not known to be changed by heating, a certain kind of complex ion may be formed at first between gold and citrate ions, and the complex may be changed to acetone dicarboxylate. It seems that the formation of acetone dicarboxylate is the reaction from homogeneous solution and that the formation of gold sol proceeds homogeneously.

In order to prepare monodisperse particles it is necessary that the nucleation in the formation of gold sol should occur rapidly at the initial stage of the reaction, and that the new particle should not be produced during the growth period of gold particles. It was proved that new particles were not created during the growth process of gold sol particles by the spray method. Turkevich, Stevenson and Hillier[1] studied the rate of nucleation in gold sol. But it seems that at high temperature when a certain quantity of substance (acetone dicarboxylate) is generated homogeneously as described above, nuclei of gold are formed rapidly[6], and after the nucleation the growth of the particles seems to balance the deposition of gold, and the new particles are not formed.

The growth of gold particles after the nucleation is slow in the initial stage, then rapid and finally the size of particles approaches a definite value. The rate of growth is represented by equation 3. The general nature of the growth process is of an autocatalytic type with respect to the surface of gold particles. This process is also proved by equation 4 obtained from the rate of the disappearance of the auric ion.

The absorption maximum of gold sol shifts toward the shorter wave length as the reaction proceeds; that is, as the size of particle is increased and finally to 525 mμ. The relation between the absorbance at 525 mμ of gold sol produced and the initial concentration of auric ions gives the same straight line for every gold sol containing monodisperse particles ranging from 100 to 200 Å in diameter and the relation is not affected by the reaction temperature. This phenomenon is proved by Mie's theory that the absorbance of

4) H. B. Weiser and W. O. Milligan, *J. Phys. Chem.*, **36**, 1950 (1930).
5) H. M. Irving and D. Phil, *Quart. Rev.*, **5**, 200 (1951).
6) V. K. LaMer and R. H. Dinegar, *J. Am. Chem. Soc.*, **73**, 380 (1951).

gold sol containing very fine particles is proportional to the product of the volume of one particle with the number of particles in unit volume. Then the small quantity of gold can be determined by the sodium citrate method using the calibration curve described above.

**Summary**

Gold sol particles prepared by sodium citrate method were monodisperse. The size of gold particles decreased exponentially with increasing initial concentration of the auric ion, and increased exponentially with the reaction temperature. At the initial stage of the reaction of the gold sol formation, the gold nuclei were formed rapidly. After the nucleation the number of particles was kept constant over the whole period of reaction and the particles grew with the autocatalysis-like reaction at the surface of the particle.

The author acknowledges with thanks the guidance and discussion of Professor Eiji Suito of Kyoto University. He also wishes to express his hearty thanks particularly to Professor Masayoshi Ishibashi of Kyoto University for his discussion and encouragement throughout this investigation. The expense of this study was defrayed in part by a grant from the Ministry of Education.

*Institute for Chemical Research*
*Kyoto University, Takatsuki*
*Osaka*

# *Formation and Aging of Precipitates. IX*. Formation of Monodisperse Particles (2) Barium Sulfate Precipitate by EDTA Method*

By Kazuyoshi TAKIYAMA

(Received June 13, 1958)

Sparingly soluble salts were suitable in the study of the physicochemical properties of precipitates and the precipitation reaction in analytical chemistry. Barium sulfate has been widely used for these purposes. The author previously reported the size and shape of barium sulfate particles precipitated by the direct mixing of ions[1]. In this paper the monodisperse particles of barium sulfate precipitated from a homogeneous solution, are reported. A few methods, e.g. the dimethyl sulfate method[2], and the sulfamic acid method[3] have been investigated to precipitate barium sulfate from a homogeneous solution, but the particles produced by these procedures were almost all polydisperse. The author has produced the monodisperse particles by means of the decomposition of the complex of barium and ethylenediaminetetra-acetate (EDTA) with hydrogen peroxide in the presence of sulfate. The EDTA method was used to precipitate ferric hydroxide by McNevin and Dunton[4] and the present author improved the method of precipitating barium sulfate.

## Experimental

**Formation of the Precipitate.**—Equivalent quantities of barium chloride and EDTA solutions were mixed and an ammonium chloride-ammonia buffer was added to bring the pH of the solution to 10. After addition of ammonium sulfate which was equivalent to barium chloride, the mixed solution was warmed at 80°C and hydrogen peroxide was added to decompose EDTA. The reaction mixture was kept at 80°C during the course of reaction.

**Measurement of the Particle Size.**—Barium sulfate precipitates produced were observed with

* The eighth paper of this series, This Bulletin, **31**, 944 (1958).

1) E. Suito and K. Takiyama, This Bulletin, **27**, 121, 123 (1954); **28**, 305 (1955).

2) P. J. Elving and R. E. van Atta, *Anal. Chem.*, **22**, 1375 (1950).

3) W. F. Wagner and J. A. Wuellner, ibid., **24**, 1031 (1952).

4) W. M. McNevin and M. L. Dunton, ibid., **26**, 1246 (1954).

TABLE I

PARTICLE SIZES OF BARIUM SULFATE PRECIPITATES

| Concn. $C$ (M) | Size of particle: Length of long axis $a$ (mμ) | Standard deviation $\sigma_a$ (mμ)* | Length of short axis $b$ (mμ) | Standard deviation $\sigma_b$ (mμ)* | Mole number of particle $M$ (mole) | Number of particle $N$ (per ml.) |
|---|---|---|---|---|---|---|
| 0.0022 | 993 | 34 | 298 | 21 | $8.89\times10^{-16}$ | $2.47\times10^{9}$ |
| 0.0033 | 1022 | 63 | 346 | 37 | $1.23\times10^{-15}$ | $2.68\times10^{9}$ |
| 0.0044 | 1066 | 68 | 420 | 44 | $1.87\times10^{-15}$ | $2.35\times10^{9}$ |
| 0.0066 | 1237 | 67 | 473 | 32 | $2.79\times10^{-15}$ | $2.37\times10^{9}$ |
| 0.0088 | 1400 | 58 | 535 | 41 | $4.04\times10^{-15}$ | $2.20\times10^{9}$ |

| Reaction mixture | | | |
|---|---|---|---|
| | $BaCl_2$ | original solution (0.022, 0.22 M) | same volume (3~10 ml.) |
| | EDTA | original solution (0.022, 0.22 M) | |
| | $(NH_4)_2SO_4$ | original solution (0.022, 0.22 M) | |
| | Buffer solution | 5 ml. | |
| | $H_2O_2$ (30%) | 20 ml. | |
| | Total volume | 100 ml. | |

* $\sigma_a$ and $\sigma_b$ are the standard deviation of $a$ and $b$ respectively.

an electron microscope. All particles were spindle-shaped, and the mean lengths of long and short axes and their standard deviation were determined. Then, the mole number of one particle, $M$ (mole), was calculated according to the following equation:

$$M=(4/3)\pi(a/2)(b/2)^2\rho/W \qquad (1)$$

where $a$ and $b$ are the mean length of long and short axes, $\rho$ and $W$ are the density and the molecular weight of barium sulfate.

**Measurement of the Reaction Rate.**—The quantity of EDTA present at any given time was determined by titration. At various times during the course of the reaction, 10 ml. samples of the reaction mixture were poured into beakers, which were kept in ice water, and were titrated with 0.010 M zinc sulfate using Eriochrome Black T as indicator in the presence of a large excess of ammonium sulfate.

The growth of the particles was determined by electron microscopy as follows. At various intervals one drop of the reaction mixture was taken onto a tiny Formvar film floating on the surface of cold water. About ten minutes, the product was allowed for the diffusion of mother liquid ions from the drop into the water below. The film was then scooped up with a sample grid for electron microscopy.

## Exprimental Results

**Relation between the Particle Size and the Concentration of Reagents.**—Barium sulfate particles precipitated at various concentrations of the reagents* are shown in Fig. 1 and the sizes of particles determined are listed in Table I. Particles are spindle-shaped and monodisperse over a range of 0.0022 to 0.0088 M

* The concentraton of reagents means the initial concentration of barium ion which is equivalent to that of EDTA or sulfate, and is expressed by mole per liter.

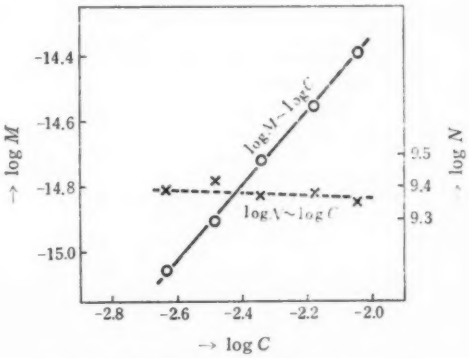


Fig. 2. Relation of the particle size to the concentration of reagents.

of the reagents. The size of particles increased with the increase of concentration of reagents. The logarithm of the mole number of particle, $\log M$, is linear with the logarithm of the concentration, $\log C$, as shown in Fig. 2. Then the relation between $M$ and $C$ is expressed by the following equation:

$$MC^{\alpha}=K \qquad (2)$$

where $\alpha$ and $K$ are constants, being $-1.2$ and $1.15\times10^{-12}$ respectively. As the number of particles per ml., $N$, is given as $C/M\times10^{-3}$, $\log N$ is also linear with $\log C$ as shown in Fig. 2. The number of particles per ml. remained almost constant over the range of cocentration listed in Table I.

**Growth Process of Particle.**—*Reaction rate determined by titration.*—The rate of decomposition of EDTA in two series of experiments, in which the concentrations

of reagents were 0.0022 and 0.0044 M, was expressed by curve (EDTA) in Fig. 3. The decomposition of EDTA was of the first order with respect to EDTA concentration. Barium ion liberated with decomposition of EDTA was expressed by curve ($Ba^{2+}$) in Fig. 3.

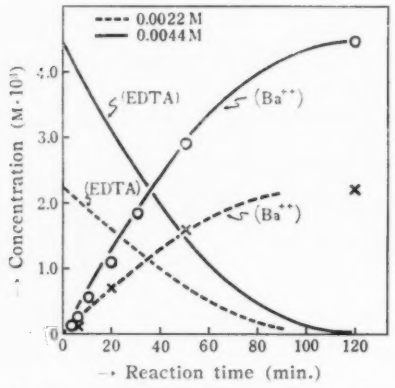


Fig. 3. Rate of formation of barium sulfate precipitate.
(EDTA): Concentration of EDTA in the reaction mixture
($Ba^{2+}$): Rate of liberation of barium ion calculated from (EDTA)
○, ×: Quantity of barium sulfate precipitate determined by electron microscopy

*Growth rate of particle observed by electron microscopy.*—The particles during the course of reaction are shown in Fig. 4. The particles were monodisperse from the initial stage of the reaction. The value obtained by multiplication of the mole number of one particle, $x$(mole), obtained by electron microscopy at the time listed by the number of particles per liter of suspension, $N\times10^3$, calculated after completion of the reaction is equal to the quantity of barium sulfate precipitated. The values obtained as described above are shown by ○ and × in Fig. 3. It was proved from Fig. 3 that the rate of formation of barium sulfate determined by electron microscopy was almost the same as that of liberation of the barium ion obtained by titration.

## Discussion

Barium sulfate precipitates formed at the concentration of reagents over a range from 0.0022 to 0.0088 M by EDTA method contained monodisperse particles. According as the concentration of the barium ion generated by the decomposition of EDTA increased, the ion product ($Ba^{2+}$) × ($SO_4^{2-}$) increased. It seemed that, when the ion product exceeded a certain critical value, corresponding to the limiting degree of supersaturation reported by LaMer and Dinegar[5], crystal nuclei were formed rapidly and after the nucleation the particles grew according to the liberation of barium ion as discussed later. If the concentration of reagents was too high, the rate of the generation of barium ion was rapid and the new particles were formed even after the nucleation. If the concentration of reagents was too low, the rate of formation of nuclei was slow and the growth of the nuclei previously formed proceeded faster than those formed later. Then in these cases the particles produced were polydisperse.

The relation of the particle size to the concentration of reagents was expressed by equation 2. The value of $\alpha$ in the equation was negative and the size of particles increased with the increase of concentration. The number of particles per unit volume of the suspension formed at various concentrations was almost constant as shown in Fig. 2. Thus a definite number of nuclei was formed over the range of concentration described above. O'Rourke and Johnson[6,7] reported that the number of particles per unit volume of barium sulfate suspension formed by direct mixing of ions over a range of initial concentration of $10^{-3}$ to $10^{-1}$ M was almost independent of concentration and the size of particles increased with the increase of initial concentration. These relations were also confirmed by the EDTA method over the range of concentration slightly above that proved by the direct mixing method.

The author previously reported the shape and size of particles of barium sulfate precipitated by direct mixing of ions[1]. Taking the data from that report, the logarithm of the mole number of one particle, $\log M$, and the logarithm of the initial concentration of barium sulfate, $\log C$, were calculated. The relation of $\log M$ to $\log C$ was shown in Fig. 5, and $M$ and $C$ were expressed by equation 2. The value of $\alpha$ was 2.7 and −1.4 at the concentration above and below about

5) V. K. LaMer and R. H. Dinegar, *J. Am. Chem. Soc.*, **73**, 380 (1951).
6) R. A. Johnson and J. D. O'Rourke, ibid., **76**, 2124 (1954).
7) J. D. O'Rourke and R. A. Johnson, *Anal. Chem.*, **27**, 1699 (1955).

a b c d

(×15,000)

Fig. 1. Electron micrographs of barium sulfate particles produced at various concentrations.
a: 0.0022 M, b: 0.0044 M, c: 0.0066 M, d: 0.0088 M

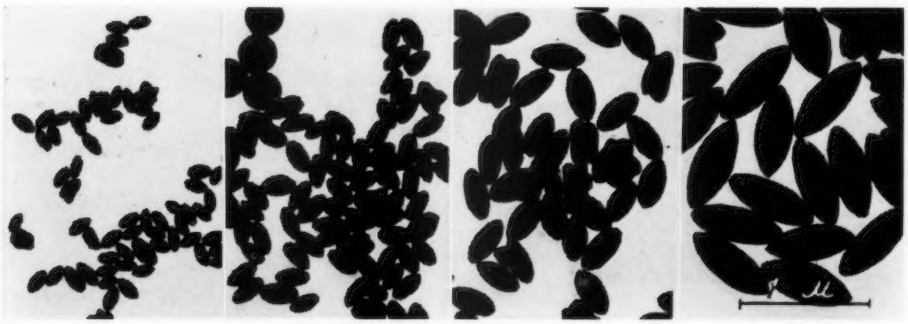


a b c d

(×20,000)

Fig. 4. Electron micrographs of barium sulfate particles during the growth process.
($C$=0.0044 M) a: 3 min., b: 5 min., c: 10 min. d: 40 min.
(Spherical particles shown in b are polystyrene latex used as the calibration standard to measure the particle size.)

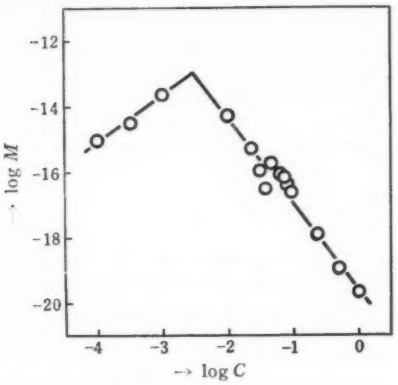


Fig. 5. Relation of the particle size to the initial concentration of barium sulfate formed by direct mixing of ions.

0.002 M respectively. The value of $K$ was always constant and was $2.2\times10^{-20}$. The number of particles per ml. suspension, which was calculated from the initial concentration and the mean size of particles, increased rapidly with the increase of concentration above about 0.002 M, but was nearly constant at the concentration below about 0.002 M. The induction period of the precipitation appeared over the range of the initial concentration below about 0.002 M, that is, over the range of $\alpha$ being negative. The precipitation by EDTA method was made above 0.0022 M and the concentration was such that the induction period in the direct mixing did not appear. As EDTA method was one of the homogeneous solution methods, the induction period was, of course, found before the precipitation. It seems that when the induction period appears in the case of the precipitation, the size of particles increases with the increase of concentration of reagents.

Generally speaking, it would be plausible that when the nucleation plays a predominant role in the precipitation, the particle size decreases with the increase of initial concentration (Weimarn theory), and that when the growth of particles plays a predominant role, the particle size increases with the increase of initial concentration.

The rate of liberation of the barium ion calculated from the titration of EDTA agreed with that of the formation of barium sulfate precipitate obtained by electron microscopy. Thus the number of particles per unit volume of suspension was kept constant and no new particles were formed during the growth period of particles. Furthermore, the barium sulfate were deposited on each particle immediately after the liberation of barium ion, and the growth of particles was balanced with the liberation of barium ion.

## Summary

Monodisperse spindle-shaped particles of barium sulfate were formed by means of the decomposion of barium-EDTA complex with hydrogen peroxide in the presence of sulfate. The logarithm of the size of the particle produced was linear with the logarithm of the concentration of reagents. The particles grew at the same rate of liberation of barium ion from the complex. The number of particles per unit volume of the reaction mixture was kept constant during the growth process of particles.

The author desires to thank Professor Eiji Suito of Kyoto University for his guidance and discussion. He also wishes to express his hearty thanks particularly to Professor Masayoshi Ishibashi of Kyoto University for his continuous advice and encouragement. The expense of this study was defrayed in part by a grant from the Ministry of Education.

*Institute for Chemical Research*
*Kyoto University, Takatsuki*
*Osaka*

# *Surface Films of Physically and Chemically Treated Ovalbumin (Dynamic Studies on Monolayer. II)*

By Maresuke KASHIWAGI

(Received May 2, 1958)

Studies have previously been made of monolayer properties of crystalline ovalbumin in which it has been shown that the monolayer structure can be examined conveniently in its spreading process and this spreading of monolayer at the air-water interface was found to be directly linked with the denaturation[1]. The structural status of the spread monolayer can now be investigated to a certain extent from the measurements of surface pressure or potential changes with time at a constant area of a given substrate.

It appears that relatively few studies have been made on the measurement of surface pressure changes with time. Although important roles of experimental conditions, that of substrate in particular, have been fully emphasized, it must also be pertinent to investigate the effect of physical or chemical treatments on protein prior to spreading. Proteins are known to be denatured both by chemical and physical treatments. The surface denaturation of proteins was studied by Bull and Neurath[2-4]. Kaplan also has extensively studied the effect of physical and chemical treatments on ovalbumin monolayers[5-8].

Since denaturation is essentially an intramolecular phenomenon, involving changes in an unknown structure, it can be investigated and described in terms of these changes, whether physical, chemical or biological. Among others, the effect of heat with infrared irradiation, acid and alkali treatments on the ovalbumin molecule before spreading are investigated and discussed here.

## Experimental

**Apparatus.**—The surface balance used is the same as the one previously described[1]. Wilhelmy's vertical plate type is found to be more convenient than Langmuir and Adam's apparatus for the measurement of pressure changes with time.

**Materials.**—Ovalbumin was obtained by the usual method as described before[1]. This ovalbumin is treated with heat, acid and alkali, respectively. Except for the treatment with heat, acid and alkali treatments are based partially on MacPherson and Heidelberger's studies[9]. The temperature condition of heat treatment in this case is made somewhat mild. The protein under those conditions is expected to be slightly denatured as indicated by the nitroprusside test[10]. This test was also applied to the untreated native protein with negative result. Conditions adopted hereby are summarized in Table I.

**Experimental procedure.**—Protein is spread from its aqueous solution by means of a micropipet over a large area (2.5 $m^2$/mg.) and the film is kept there for exactly 5 minutes before the start of compression for *F-t* curve measurement. To determine pressure-area diagrams, the time allowed for after spreading is 20 minutes instead of 5 minutes. The most commonly used substrate is aqueous 20% ammonium sulfate solution at pH 4.8 since this is one of the best substrates[1].

TABLE I

CONDITIONS OF OVALBUMIN TREATMENTS

| Modification | Concn. | Reagent used | Temp. | Time | pH | Nitroprusside test |
|---|---|---|---|---|---|---|
| Acid | 0.224 mg./cc. | 0.1 N HCl | 2~4°C | 17 hrs. | 2.2 | + |
| Alkali | 〃 | 0.04 N NaOH | 2~4°C | 17 hrs. | 9.6 | + |
| Heat | 〃 | infrared light 100 V. 250 W | 42°C | 1/3 hrs. | — | + |

1) M. Kashiwagi, This Bulletin, **31**, 176 (1958).
2) H. B. Bull and H. Neurath, *J. Biol. Chem.*, **118**, 163 (1937).
3) H. B. Bull, ibid., **125**, 585 (1938).
4) H. Neurath, *J. Phys. Chem.*, **40**, 361 (1936).
5) J. G. Kaplan, *J. Colloid Sci.*, **7**, 382 (1952).
6) J. G. Kaplan and M. J. Fraser, *Biochim et Biophys. Acta*, **9**, 585 (1952).
7) J. G Kaplan, D. H. Andrews and M. J. Fraser, *J. Colloid Sci.*, **9**, 203 (1954).
8) J. G. Kaplan and M. J. Fraser, *J. Biol. Chem.*, **210**, 57 (1954).
9) C. F. C. MacPherson and M. Heiderberger, *J. Am. Chem. Soc.*, **67**, 574 (1945).
10) D. Glick, "Methods of Biochemical Analysis", Vol. 1, p. 20 (1954).

## Results

Fig. 1 represents measured surface pressure changes $\Delta F$ with time of heat-treated ovalbumin monolayers at various surface areas and on the substrate of 0.1 N hydrochloric acid. Pressure-time curves of the same sample on the substrate of 20% ammonium sulfate solution are also shown in Fig. 2. It can be seen from Fig. 1 that $F$ increases with time, but the rate of increase is markedly dependent on surface area, being only slightly noticeable at 1.18 $m^2$/mg., while it is very pronounced at 0.914 $m^2$/mg. On the other hand, as shown in Fig. 2, $F$ decreases in the initial stage on ammonium sulfate substrate and then becomes constant at 0.92 $m^2$/mg., while at larger areas, $F$ seems to increase very slowly but linearly with time. Surface pressures of acid-treated ovalbumin remain practically constant for the whole period of the experiment, or very slightly increase on the substrate of 20% ammonium sulfate (Fig. 3). $F$-$t$

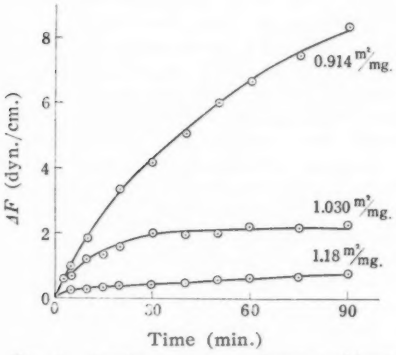


Fig. 1. Surface pressure changes of heat-denatured ovalbumin (Substrate 0.1 N HCl, 14°C).

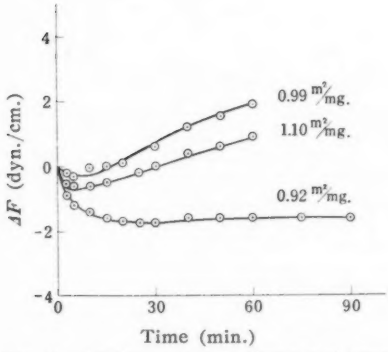


Fig. 2. Surface pressure changes of heat-denatured ovalbumin (Substrate 20% $(NH_4)_2SO_4$, 15°C) pH 4.8.

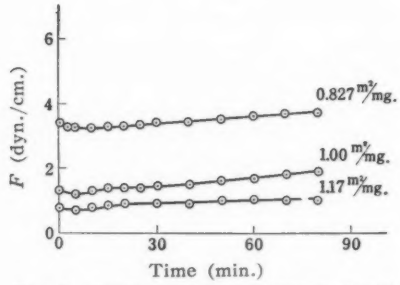


Fig. 3. Surface pressure changes of acid-treated ovalbumin (Substrate 20% $(NH_4)_2SO_4$, pH adjusted 7.1, 19°C).

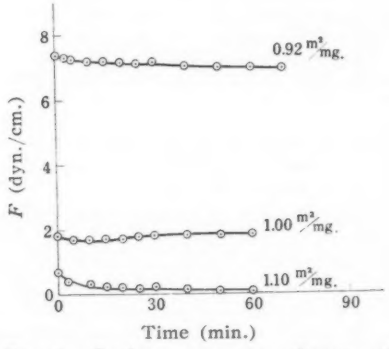


Fig. 4. Surface pressure change of alkali-treated ovalbumin (Substrate 20% $(NH_4)_2SO_4$, 16°C) pH 4.8.

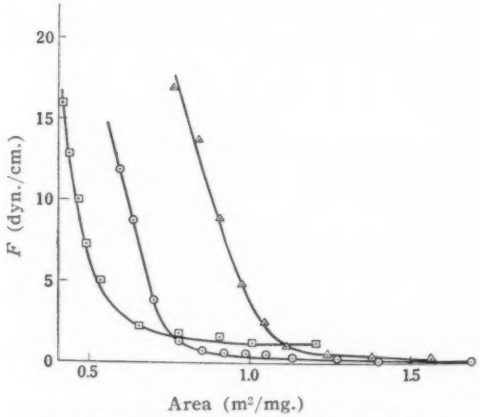


Fig. 5. Pressure-area diagram of heat-treated ovalbumin.
△ 20% $(NH_4)_2SO_4$ Substrate pH 4.8
⊙ 0.1 N HCl Substrate
⊡ untreated ovalbumin on 0.1 N HCl

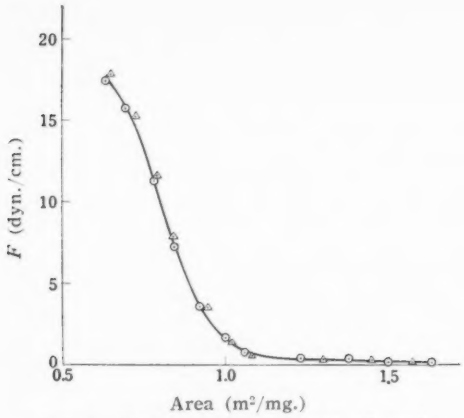


Fig. 6. Pressure-area diagrams of ovalbumin (Substrate 20% $(NH_4)_2SO_4$).
△ alkali-treated
• acid-treated
PH of Substrate
△ 4.8
• 7.1

curves of alkali-treated ovalbumin soon reach a final equlibrium pressure and remain constant (Fig. 4).

All the actual measurements of pressure changes with time are carried out every three minutes at least, but the recording of all points on *F-t* curves are not attempted for convenience' sake. Pressure-area diagrams of these treated ovalbumin monolayers are shown in Figs. 5 and 6, respectively, together with that of untreated native ovalbumin for comparison. *F-A* curves of both acid- and alkali-treated protein are identical within the limit of the present experimental condition, as indicated in Fig. 6.

## Discussion

It may be expected that all these treatments applied here would not cause substantial structural change in the protein[9,11]. The present condition of heat treatment was rather milder than in the case of ordinary conditions for denaturation, but it is interesting to note that surface pressure of heat treated ovalbumin increases with time on 0.1 N hydrochloric acid as indicated in Fig. 1, while with the untreated native protein surface pressure decreased with time on the same substrate[1], indicating partial desorption. Pressure-area diagrams of the former also shift obviously from that of the untreated. By heat treatment the intramolecular cohesion forces are lessened to such an extent that the protein spreads to a larger area than they normally occupy[2,8] and the ease of molecular unfolding increased by heat must have retarded the factor to cause desorption from the surface.

The protein denaturation is often followed inevitably by intermolecular aggregation, which makes the interpretation of the denaturation effect very difficult, but ovalbumin molecules under the present condition would not proceed progressively to marked aggregation or dissociation[9,11].

We have seen in Figs. 3 and 4, that under a constant film area, the surface pressure is independent of time, that is

$$\left(\frac{\partial F}{\partial t}\right)_{A_0} = 0$$

where $A_0$ refers to co-area.

But since we have a general relation

$$\left(\frac{\partial A_0}{\partial t}\right)_F = -\left(\frac{\partial F}{\partial t_0}\right)_{A_0} \Big/ \left(\frac{\partial F}{\partial A_0}\right)_t$$

where $\left(\frac{\partial F}{\partial A_0}\right)_t$ shows a finite value, $\left(\frac{\partial A_0}{\partial t}\right)_F$ vanishes, which means, that $A_0$ is independent of time. Therefore we can expect that under such a condition, molecules in the film would be fully denatured in accordance with our former report[1].

## Summary

Monolayer properties of acid, alkali and heat-treated ovalbumin are investigated from the measurements of surface pressure changes with time and surface pressure-area diagrams.

These treated specimens are found to be characteristically different from the untreated native protein in their surface behavior. The process of surface denaturation is also discussed.

The author wishes to express thanks to Professor Ryohei Matsuura of Kyushu University and Professor Taro Tachibana of Ochanomizu Women's University for their kind discussion of the subject.

*Mitsuwa Chemical Laboratory*
*Marumiya Co., Ltd.*
*Terashima, Sumida-ku, Tokyo*

11) V. A. Belister and T. V. Saenko, *Biokhimiya*, **22**, 274 (1957).

# *Kinetics of Hydrolytic Reaction Catalyzed by Crystalline Bacterial α-Amylase. I. The Influence of pH*

By Sôzaburo ONO, Keitaro HIROMI and Yoshiko YOSHIKAWA

(Received February 24, 1958)

It is well known that enzyme reactions consist of two elementary processes, namely formation of an intermediate enzyme-substrate complex and the subsequent breakdown of the complex into reaction products and free enzyme. These processes are represented kinetically by two parameters, i. e., the Michaelis constant and the rate constant for the breakdown of the complex, respectively. Systematic investigation of the influence of various extrinsic factors such as temperature, pH, ionic strength, dielectric constant of the medium, pressure, inhibitors, etc., upon these parameters, provides a means for elucidating the mechanisms of the enzyme reactions. Recently certain enzyme reactions have been studied along these lines and important information on the mechanisms has been obtained[1-4].

Bacterial amyloclastic α-amylase of *Bac. amyloliquefaciens* Fukumoto has long been studied by Fukumoto and his co-workers, and was crystallized by Hagihara[5]. Although various investigations have been made about this crystalline enzyme[6,7], few kinetic studies have been reported on it[8,9]. In our laboratory the influence of various factors on the rate of reactions catalyzed by this crystalline enzyme has been studied from the kinetic point of view, using substrates as simple and pure as possible. In the present report, the influence of pH on the reaction rate was investigated with the hope of obtaining a certain clue for elucidating the mechanism of the enzyme reaction involved.

1) R. Lumry, E. L. Smith and R. R. Glantz, *J. Am. Chem. Soc.*, **73**, 4330 (1951).
2) R. Lumry and E. L. Smith, *Discussions Faraday Soc.*, No. **20**, 105 (1955).
3) K. J. Laidler, ibid., No. **20**, 83 (1955).
4) A. Stockell and E. L. Smith, *J. Biol. Chem.*, **227**, 1 (1957).
5) B. Hagihara, *Proc. Japan Acad.*, **27**, 346 (1951).
6) T. Yamamoto, *Bull. Agr. Chem. Soc. Japan*, **19**, 121 (1955).
7) T. Yamamoto, ibid., **20**, 188 (1956).
8) J. Osugi, *Rev. Phys. Chem. Japan*, **22**, 66, 71 (1952).
9) J. Osugi and K. Hiromi, ibid., **22**, 76 (1952).

## Experimental

**Materials.** — 1) *Substrate.* — Potato amylose (degree of polymerization ca. 900) manufactured by Nagase Sangyô Co. Ltd. was used. 2) *Enzyme.* —Bacterial amyloclastic α-amylase (six-times recrystallized; molecular weight 45,000) was kindly provided by Professor J. Fukumoto of Osaka City University. The enzyme was dissolved in four-times redistilled water, and the solution was stored in a refrigerator as the stock solution. The enzyme concentration in this solution was determined from the optical density at 280 mμ to be $3.88\times10^{-6}$ M. The enzyme activity in this solution was constant throughout the whole experiment. 3) *Buffer solution.*—A solution of 0.15 M veronal sodium and sodium acetate was mixed with 0.1 N hydrochloric acid in various ratios. This buffer solution was confirmed to have no specific effect on the reaction rate and on the determination of products.

**Methods.** — A mixture of 10 ml. of amylose solution in 0.5 N sodium hydroxide and 13 ml. of the buffer was neutralized with 5 ml. of 1 N hydrochloric acid in a reaction vessel immersed in a thermostat adjusted to 25°±0.05°C, unless otherwise stated. After equilibrium temperature was reached, 2 ml. of the enzyme solution (containing an appropriate amount of the stock solution in 1/300 M calcium acetate) was added quickly to make the total volume 30 ml. The reaction mixture was stirred mechanically. Two ml. of the reaction mixture was pipetted into 1 ml. of 0.5 N sodium hydroxide to stop the reaction at intervals of one minute during the first four minutes of the reaction.

The reducing end-groups produced as the result of the reaction were determined photometrically with 3,5-dinitrosalicylate[10]. In lower concentrations of the products (below $1.4\times10^{-4}$ mole of reducing end group per liter), the atomspheric oxygen made the determination impossible because of its oxidizing action. Therefore, the nitrogen was bubbled through the reaction mixture and the reagents used in the analytical procedure before and during the experiment.

The pH of the reaction mixture was measured by means of a quinhydrone electrode at the same temperature as that of the reaction. The error of the measurements was within ±0.01 pH. The concentrations of substrate and products were

10) G. N. Smith and C. Stocker, *Arch. Biochem.*, **21**, 95 (1949).

expressed in mole per liter of the bond hydrolyzable and hydrolyzed, respectively. The initial reaction rate was estimated from the tangent of the reaction-time curve at zero time. The error in this procedure was minimized by choosing appropriate concentrations of enzyme so that the curves would not show any marked curvature.

## Results

The initial rate $v$ was in good proportionality with the enzyme concentration [E], as shown in Fig. 1. The plots of the reciprocals of the initial rate $v$ versus substrate concentration [S] were found to fulfil the linear relationship required by the Lineweaver-Burk equation[11],

$$\frac{1}{v} = \frac{K_m}{k_2[\mathrm{E}]} \cdot \frac{1}{[\mathrm{S}]} + \frac{1}{k_2[\mathrm{E}]} \qquad (1)$$

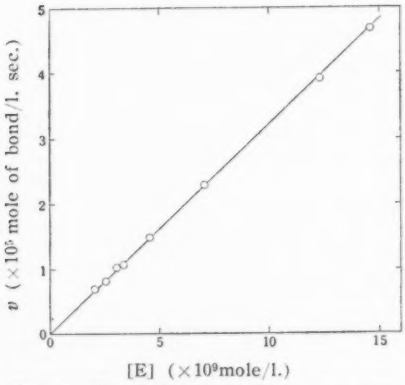


Fig. 1. Plot of initial rate versus enzyme concentration (substrate concentration, 0.0154 mole of bond/l.; 25°C; pH 5.41).

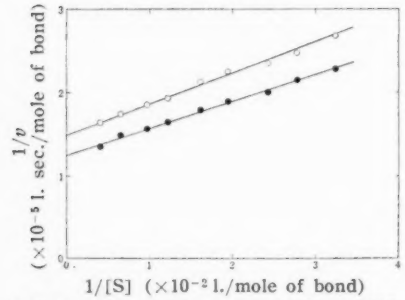


Fig. 2. Plot of $1/v$ versus $1/[S]$ at 25°C. ○ pH 7.51, ● pH 4.84

This relationship holds for any pH studied (see Fig. 2). The concentration of the enzyme [E] being known, the apparent Michaelis constant $\bar{K}_m$, and the apparent rate constant $k_2$ for the breakdown of the enzyme-substrate complex, were obtained from the formula. The values of $K_m$ and $k_2$ at various pH's are summarized in Table I. In Fig. 3, $\log 1/\bar{K}_m$ and $\log k_2$ are plotted versus pH. $K_m$ is constant over the pH range examined (pH 3.6~8.4), while $k_2$ decreases on both the acid and the alkaline side.

TABLE I

VALUES OF $K_m$ AND $k_2$ AT VARIOUS pH'S AT 25°C

| pH | [E]×10⁹ mole/l. | $K_m$×10³ mole of bond/l. | $k_2$×10⁻³ sec.⁻¹ |
|---|---|---|---|
| 3.59 | 7.05 | 2.3±0.4 | 0.37±0.03 |
| 3.73 | 9.94 | 2.3±0.3 | 0.61±0.02 |
| 4.16 | 3.38 | 2.3±0.2 | 1.91±0.05 |
| 4.84 | 2.56 | 2.6±0.2 | 3.20±0.04 |
| 5.60 | 2.56 | 2.6±0.2 | 3.94±0.15 |
| 5.95 | 2.06 | 1.8±0.2 | 3.91±0.11 |
| 6.25 | 1.54 | 2.1±0.2 | 3.80±0.10 |
| 6.92 | 2.06 | 2.6±0.1 | 3.90±0.05 |
| 7.51 | 3.08 | 2.4±0.2 | 2.18±0.04 |
| 8.23 | 4.58 | 2.1±0.3 | 0.75±0.02 |
| 8.40 | 14.6 | 2.6±0.2 | 0.47±0.02 |

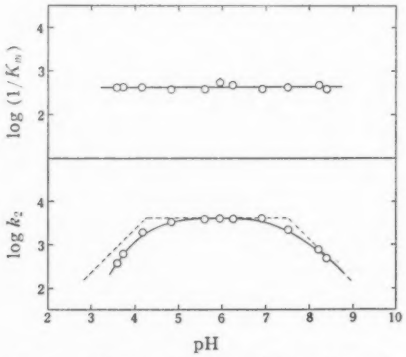


Fig. 3. Plots of $\log (1/K_m)$ and $\log k_2$ versus pH at 25°C.

The results of another series of experiments are shown in Fig. 4, in which the ratio of the initial rate $v$ at a given pH, to that $v_{max}$ at the optimum pH, measured at constant substrate and enzyme concentration, was plotted against pH. A nearly symmetrical bell-shaped curve was obtained. Neither the shape nor the position of the curve was affected by varying the substrate concentration. The solid line in Fig. 4 represents the theoretical curve which will be described below. The experimental points satis-

11) H. Lineweaver and D. Burk, *J. Am. Chem. Soc.*, **56**, 658 (1934).

factorily fit the theoretical curve except in the narrow region below pH 4, where the occurrence of a rapid irreversible inactivation of the enzyme was observed. The influence of temperature on the $v/v_{max}$—pH curve was also investigated, and the results are presented in Table III, which will be discussed below.

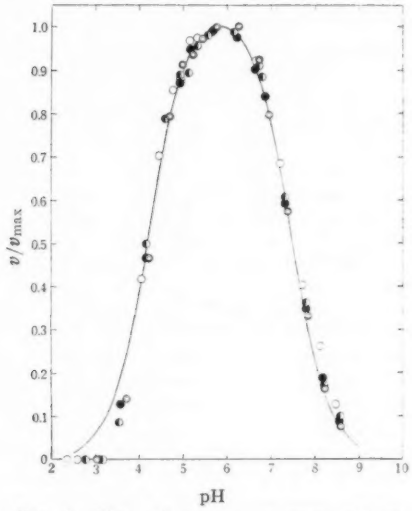


Fig. 4. Plot of $v/v_{max}$ versus pH at various substrate concentrations at 25°C.
○ 0.0247, ◐ 0.0123, ● 0.00617,
◎ 0.00308 mole of bond/l.

## Discussion

The results will be analyzed according to the following scheme which has been employed by various authors[12-15]:

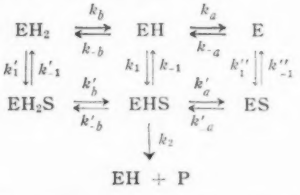


where E represents the enzyme in a particular state of ionization, H a proton, S the substrate and P the products. Of the three forms of enzyme-substrate complexes, only the complex EHS is assumed to break down into the reaction products. The various rate constants $k$'s are indicated above.

The initial rate $v$ can be expressed as follows:

$$v=\frac{k_2[E][S]}{K_m\left(1+\frac{K_a}{[H]}+\frac{[H]}{K_b}\right)+[S]\left(1+\frac{K_a'}{[H]}+\frac{[H]}{K_b'}\right)} \quad (2)^*$$

where

$$K_m=(k_{-1}+k_2)/k_1$$

and

$$K_a=k_a/k_{-a}, \quad K_b=k_b/k_{-b}$$
$$K_a'=k_a'/k'_{-a}, \quad K_b'=k_b'/k'_{-b}$$

Thus $K_a$, $K_b$, $K_a'$ and $K_b'$ are the ionization constants of the two ionizable groups taken into account in the scheme, in the substrate-free enzyme and enzyme-substrate complex, respectively.

Comparing Eqs. 1 and 2, $\overline{K_m}$ and $\overline{k_2}$ are represented in the following formula;

$$K_m=\overline{K_m}\cdot\frac{1+\frac{K_a}{[H]}+\frac{[H]}{K_b}}{1+\frac{K_a'}{[H]}+\frac{[H]}{K_b'}} \quad (3)$$

$$\overline{k_2}=\frac{k_2}{1+\frac{K_a'}{[H]}+\frac{[H]}{K_b'}} \quad (4)$$

From our results which show that $\overline{K_m}$ is constant over a wide range of pH in which $\overline{k_2}$ varies (see Fig. 3), it is concluded that $K_a$ equals to $K_a'$ and $K_b$ equals to $K_b'$ in Eq. 3; that is to say, the ionization of the two groups considered is not affected by the substrate binding. If these ionizable groups were directly involved in the complex formation, their ionization constants would be changed considerably by the combination of the substrate with the enzyme[16]. Thus it may be most reasonable to conclude that these groups in the enzyme molecule are not directly responsible for the complex formation. The variation of $\overline{k_2}$ with pH is in accordance with the prediction of the theory (see Fig. 3 and Eq. 4) and it is evident that the breakdown of the complex occurs only when group A (whose ionization constant is $K_a$) is undissociated and group

12) S. G. Waley, *Biochim. et Biophys. Acta*, **10**, 27 (1953).
13) R. A. Alberty and V. Massey, ibid., **13**, 347 (1954).
14) K. J. Laidler, *Trans. Faraday Soc.*, **51**, 528 (1955).
15) A. Takamiya, "Kôso-kenkyûhô", edited by S. Akabori, Asakura Shoten, Tokyo (1955), p. 198.

* The exact steady-state treatment[14] leads to the expression which includes the perturbation term in the denominator of Eq. 2. But this term is reasonably neglected in the present case (see the foot-note** below).
16) K. J. Laidler, *Trans. Faraday Soc.*, **51**, 540 (1955).

B (whose ionization constant is $K_b$) is dissociated.

When $K_a$ equals to $K_a'$ and $K_b$ equals to $K_b'$, Eq. 2 reduces to a simpler form;

$$v = \frac{k_2[E][S]}{\left(1+\frac{K_a}{[H]}+\frac{[H]}{K_b}\right)(K_m+[S])} \tag{5}$$

Let $v_{max}$ denote the initial rate at the optimum hydrogen ion concentration $[H]_{opt}$ with a given substrate concentration [S]. Then differentiation of Eq. 5 with respect to [H] leads to the following relationships;

$$[H]_{opt} = \sqrt{K\ K_b} \tag{6}$$

$$v_{max} = \frac{k_2[E][S]}{(1+2\sqrt{K_a/K_b})(K_m+[S])} \tag{7}$$

Consequently,

$$\frac{v}{v_{max}} = \frac{1+2\sqrt{K_a/K_b}}{1+\frac{K_a}{[H]}+\frac{[H]}{K_b}} \tag{8}$$

Thus $v/v_{max}$ should be a function independent of the substrate concentration over the whole range of pH. The results shown in Fig. 4 obviously fulfil this requirement, again confirming the validity of the theory.

Moreover, several conclusions of considerable importance can be drawn from the foregoing results. (i) The apparent Michaelis constant $\bar{K}_m$ at any pH is equal to the true Michaelis constant $K_m$ (see Eq. 3). (ii) The constancy of $\bar{K}_m$, as pointed out by Morales[17] and Laidler[16], leads to a reasonable conclusion that $k_2 \ll k_{-1}$**, i.e., there is equilibrium between enzyme, substrate and complex. The Michaelis constant may be regarded as the dissociation constant of the enzyme-substrate complex, i.e., $K_m = k_{-1}/k_1$. (iii) The apparent rate constant $\bar{k}_2$ at the optimum pH is equal to $k_2/(1+2\sqrt{K_a/K_b})$ (compare Eqs. 1 and 7), about 5 per cent less than the true rate constant $k_2$ at 25°C.

The ionization constants of the groups, $K_a$ and $K_b$, were evaluated[13,15] according to Eq. 8, using the experimental values shown in Fig. 4. These values expressed in p$K$ at various substrate concentrations at 25°C are presented in Table II. The mean values of these are 7.45 for p$K_a$ and 4.22 for p$K_b$, from which the optimum pH is found from Eq. 6 to be 5.84, which is in good agreement with the experimental value 5.85. The solid line in Fig. 4 represents the theoretical curve drawn according to Eq. 8 using the mean p$K$ values thus obtained. Except for the narrow region below pH 4, where the irreversible inactivation of the enzyme was detected, the coincidence between the theory and the experiment is remarkable.

TABLE II
THE p$K$ VALUES AT VARIOUS SUBSTRATE CONCENTRATIONS AT 25°C

| $[S] \times 10^2$ mole of bond/l. | p$K_b$ | p$K_a$ |
|---|---|---|
| 2.47 | 4.18 | 7.49 |
| 1.23 | 4.20 | 7.45 |
| 0.617 | 4.24 | 7.45 |
| 0.308 | 4.27 | 7.41 |
| Mean | 4.22 | 7.45 |

TABLE III
TEMPERATURE DEPENDENCE OF pK'S

| Temp. °C | p$K_b$ | p$K_a$ |
|---|---|---|
| 6.0 | 4.44 | 7.60 |
| 12.0 | 4.29 | 7.56 |
| 18.0 | 4.38 | 7.46 |
| 25.0 | 4.24 | 7.45 |
| 32.0 | 4.28 | 7.37 |

Substrate concentration: 0.00617 mole of bond/l.

The p$K$ values of the groups at various temperatures are summarized in Table III. The heats of ionization of these groups are calculated to be $\Delta H_a = 4$ kcal. for group A, and $\Delta H_b = 2$ kcal. for group B. From these values of p$K$ and $\Delta H$, one can infer the nature of the ionizing groups under consideration by comparing them with the reported values of various ionizing groups found in proteins[18]. Considering some deviations from these values which might be expected in the actual enzyme molecule, it may be reasonable to conclude that group B, having a p$K$ of 4.22 and a $\Delta H$ of 2 kcal. is a carboxyl group, and that group A, having a p$K$ of 7.45 and a $\Delta H$ of 4 kcal., may be either an imidazolium or an ammonium group (the $\Delta H$ value is in favor of the former possibility). As already stated, these groups are not considered to be involved in the complex formation, but to be essential in the breakdown of the complex into reaction products in the forms, respectively, of $COO^-$ and $>NH^+$ (or $-NH_3^+$).

17) M. F. Morales, *J. Am. Chem. Soc.*, **77**, 4169 (1955).

** This is the condition under which the perturbation term which would appear in the denominator of Eq. 2, can be neglected (see ref. 14).

18) J. T. Edsall, "Proteins, Amino Acids and Peptides", Reinhold Pub. Corp., New York (1943), p. 444.

Yamamoto[6] examined the activity of this enzyme treated with several specific reagents, and concluded that the phenoxyl group of the tyrosine residue is essential. Since the p$K$ value of this group lies outside the pH range in which kinetic studies are feasible (see Fig. 4), it is impossible to determine whether this group is involved in the formation or the breakdown of the complex. The above-stated constancy of $\bar{K}_m$ over the pH range examined (3.6~8.4) implies that no ionizable group having its p$K$ in this range is involved in the complex formation. However, it does not exclude the possibility that some group having its p$K$ outside this region may also participate in the formation and/or breakdown of the complex. His conclusion, therefore, is not incompatible with our findings.

Recently mechanisms of certain hydrolytic enzyme reactions have been considered in terms of bifunctional catalysis, or concerted mechanism[19-21]. It seems likely that the acidic (proton-donating) and basic (proton-accepting) groups of the enzyme function as an acid and a base simultaneously in the enzyme-catalyzed hydrolysis. From this point of view, a tentative scheme on the mechanism of this enzyme reaction is presented in Fig. 5.

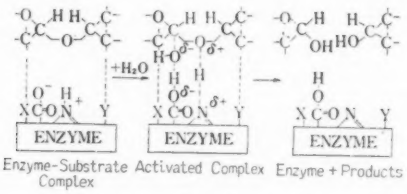


Fig. 5.

In this scheme it is supposed that the imidazolium cation, acting as an acid, attacks the etheric oxygen atom of the glucosidic bond, and simultaneously the carboxylate anion, acting as a base, pulls the proton from the water molecule which is situated between $C_1$ atom of the glucoside residue at the left and the carboxylate anion. X and Y represent the unknown groups of the enzyme which are responsible for binding the substrate in a geometrically favorable position so that the carboxylate and imidazolium groups will be able to form an activated complex with the substrate. The nature of groups X and Y cannot be determined from the present study. If they are ionizable groups, their p$K$'s must lie either below 3.6 or above 8.4. Another possible mechanism is presented in the scheme[22] shown in Fig. 6.

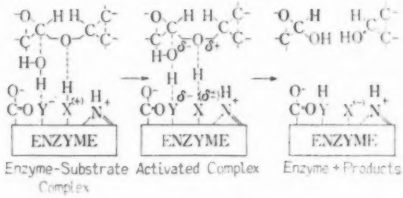


Fig. 6.

The possible charge separation in the activated complex, as depicted in each scheme, can be inferred from the study of the solvent effect upon this enzyme reaction, which will be reported in a later paper.

## Summary

The influence of pH on the rate of the hydrolytic reactions of amylose catalyzed by the crystalline bacterial α-amylase of *Bac. amyloliquefaciens* Fukumoto has been examined at various substrate concentrations and temperatures.

The apparent Michaelis constant $K_m$ is constant over the pH range examined (3.6~8.4), whereas the apparent rate constant $k_2$ for the breakdown of the enzyme-substrate complex into the reaction products and free enzyme decreases on both the acid and the alkaline side of the optimum pH 5.85. The relative rate - pH curves are not affected by the substrate concentration. From these facts, it is concluded that at least two ionizable groups in the enzyme are involved in the breakdown of the complex, although these groups are not directly responsible for the formation of the enzyme-substrate complex.

The ionization constants and the heats of ionization of the two groups involved in the reaction have been determined. From these values, the ionizing groups are inferred to be the carboxyl and imidazole (or amino) groups. The ionized

19) C. G. Swain and J. F. Brown, *J. Am. Chem. Soc.*, **74**, 2534, 2538 (1952).
20) H. Lindley, *Advances in Enzymol.*, **15**, 271 (1954).
21) K. J. Laidler, "Introduction to the Chemistry of Enzymes", McGraw-Hill Book Co., New York (1954), p. 155.
22) S. Ono, K. Hiromi and Y. Yoshikawa, *Symposia on Enzyme Chem. Japan*, **12**, 1, 291 (1957).

form of the former and the positively charged form of the latter are considered to be essential for the breakdown process.

Tentative mechanisms of the reaction are proposed.

The kindness of Professor J. Fukumoto and Dr. T. Yamamoto of Osaka City University in providing the crystalline enzyme is gratefully acknowledged.

*Laboratory of Biophysical Chemistry*
*College of Agriculture*
*University of Osaka Prefecture*
*Sakai, Osaka*

# *Irreversible Photobleaching of the Solutions of Fluorescent Dyes. VI. Photobleaching of Uranin in Alkaline Solutions**

By Masashi IMAMURA

(Received on June 20, 1958)

Previous papers[1-6] in this series have described the photobleaching of two halogenated xanthene dyes, eosin and erythrosin, in aerated and deaerated solutions. Photochemical primary processes of these dyes both in aqueous and in alcoholic solutions have been concluded. Reactivities of the triplet-excited states toward oxygen and alcohol molecules have also been discussed.

The present paper concerns with the photobleaching reactions of uranin, an unhalogenated xanthene dye, in water and in aqueous alcohols in the presence of alkali. Comparative studies on the photoreduction of uranin and its halogenated derivatives have been done by Adelman and Oster[7]. The present study has been performed under aerated and deaerated conditions, and some new facts have been revealed.

## Experimental

**Uranin (sodium fluoresceinate).** — Ishizu Chemicals guaranteed uranin was employed without further purification. Its purity was stated to be greater than 98.5%. (*Anal.* Found: C, 63.02; H, 2.70. Calcd. for $C_{20}H_{10}O_5Na_2$: C, 63.83; H, 2.67.) Maximum molar extinction coefficient (at $\lambda$ 490 m$\mu$) was reported by several authors to be $7.85\times10^4$ [8], $7.82\times10^4$ [9], $7.62\times10^4$ [10] and $5.46\times10^4$(at pH 7)[7]. Under the consideration of a fluorescence error accompanying absorption measurements with Beckman Model DU Spectrophotometer[11-13], real molar extinction coefficient in an alkaline (pH more than 9) aqueous solution was measured to be $7.80\times10^4$ at $\lambda_{max}$ 490 m$\mu$.

**Other Materials.**—Commercial alcohols were purified by the usual methods[14] and were distilled with a fractionating column of a high efficiency. Takeda Chemicals sodium hydroxide (extra pure) and doubly distilled water were used in all mixtures.

**Procedures.**—Apparatus and technique were essentially identical with those described previously[2]. Matsuda V-B2-photographic Y1 combination, which transmits $\lambda$ 450~570 m$\mu$ with maximum transmission 52% at $\lambda$ 490 m$\mu$, was used as a filter. Concentration was determined from the optical density at $\lambda_{max}$ of the solution. Aqueous or aqueous alcoholic solution of uranin exhibits stronger fluorescence than that of eosin or erythrosin. Accordingly, measured optical densities would more or less include the fluorescence error mentioned above. This error was, however, evaluated experimentally to be less than 1.6%, which was within experimental error.

* Presented in part before the 11th Annual Meeting of the Chemical Society of Japan, Tokyo, April 5, 1958.

1) M. Imamura and M. Koizumi, This Bulletin, **28**, 117 (1955).
2) M. Imamura, *J. Inst. Polytech. Osaka City Univ.*, **5C**, 85 (1956).
3) M. Imamura and M. Koizumi, This Bulletin, **29**, 899 (1956).
4) M. Imamura and M. Koizumi, ibid., **29**, 913 (1956).
5) M. Imamura, ibid., **30**, 249 (1957).
6) M. Imamura, ibid., **31**, 62 (1958).
7) A. H. Adelman and G. Oster, *J. Am. Chem. Soc.*, **78**, 3977 (1956).
8) J. Q. Umberger and V. V. LaMer, ibid., **67**, 1107 (1945).
9) V. L. Levschin, *Z. Phys.*, **72**, 368 (1931).
10) W. R. Orndorff, R. C. Gibbs and C. V. Shapiro, *J. Am. Chem. Soc.*, **50**, 819 (1928).
11) K. S. Gibson and H. J. Keegan, *J. Opt. Soc. Am.*, **28**, 180 (1938); E. A. Braude, J. S. Fawcett and C. J. Timmons, *J. Chem. Soc.*, **1950**, 1019.
12) T. C. J. Ovenston, *P. S. G. Bull.*, No. 6, 132 (1953).
13) J. J. Moran and H. I. Stonehill, *J. Chem. Soc.* **1957**, 779.
14) A. Weissberger and E. S. Proskauer, "Organic Solvents", Interscience, New York (1955).

Observed values of optical density were therefore not calibrated except in the cases where higher precise values were needed. Deviation from Beer's law resulting from re-absorption of fluorescence by the solution[13] was not observed at $\lambda$'s 450, 470, 490 and 500 m$\mu$ in the concentration range $0 \sim 10 \times 10^{-6}$ mole/l.

pH of the solution was determined with Horiba Glass Electrode pH-Meter Model P.

## Results

**Photobleaching of Aerobic Aqueous Solutions.**—*Effect of pH.*—Data on the photobleaching of aerated aqueous solutions to which no alkali was added have been reported[1,2]. Absorption spectrum of aqueous uranin solution below pH 7.5 depends sensitively on pH of the solution, while above pH 7.5 it is independent[15] of it. Over the whole pH-range investigated the simple rate formula, which has been applied to the cases of eosin and erythrosin[3], is applicable:

$$-\frac{dc}{dt} = \frac{k}{d} I_0 (1 - e^{-\alpha c d}) \times 10^3 \qquad (1)$$

Integrated form:

$$\alpha c d + \ln(1 - e^{-\alpha c d}) = -k\alpha I_0 t \cdot 10^3 + [\alpha c_0 d + \ln(1 - e^{-\alpha c_0 d})] \qquad (2)$$

The mean molar absorption coefficient, $\alpha$, was determined experimentally with a thermopile or by calculation[4].

Quantum yields, $k$'s, which were obtained with the solutions of various alkali concentrations or pH's are listed in Table I. It shows that the quantum yield is constant at least down to pH 7.17, where the absorption spectrum is affected to a certain extent; at pH 5.9, however, $k$ is reduced considerably.

TABLE I.
QUANTUM YIELDS FOR AEROBIC AQUEOUS URANIN SOLUTION. EFFECT OF pH. 30°C

| Mean molar absorption coeff. $\alpha \times 10^{-4}$ | NaOH concn. N | pH | Quantum yield $k \times 10^4$ |
|---|---|---|---|
| 2.7 | 0.0242 | | 1.6 |
| 2.7 | 〃 | | 2.0 |
| 2.7 | 〃 | | 1.7 |
| 2.7 | 0.0121 | | 1.7 |
| 2.7 | 〃 | | 1.7 |
| 2.7 | 0.0024 | | 1.7 |
| 2.7 | 〃 | | 1.7 |
| 2.3 | — | 7.17* | 1.7 |
| 1.6 | — | 5.9* | 0.8 |
| 1.6 | — | 5.9* | 1.1 |

* Phosphate (1/15 N) buffer solutions.

15) In contrast to uranin, absorption spectra of eosin and erythrosin are quite independent of pH at pH above 5.5 and 6.5, respectively.

**Effect of Concentration of Oxygen Dissolved in the Aqueous Solution upon the Quantum Yield.**—As already reported[1,2], pure aqueous uranin solution does not photobleach in vacuo and its quantum yield gradually increases with increasing concentration of oxygen dissolved in the solution; with eosin and erythrosin, at a considerably low oxygen concentration, their quantum yields reach the constant values which are equal to those obtained with the aerated solutions. An analogous phenomenon to that in the pure aqueous uranin solution is observed also in the presence of alkali (sodium hydroxide 0.0121 N).

**Retarding Effect of Ethanol on the Aerobic Photobleaching.**—On addition of ethanol to the aqueous alkaline (sodium hydroxide 0.0121N) solution, photobleaching of uranin is strongly retarded as in the cases of eosin and erythrosin. Rates of reaction for all solutions investigated can be reproduced by Eq. 1 or 2. Since absorption spectra show the shift of $\lambda_{max.}$ for longer wavelengths with increase in ethanol concentration, $\alpha$ was calculated for each solution.

Quantum yield decreases with increasing concentration of ethanol as shown in Fig. 1. Irradiated solutions do not show any shift of $\lambda_{max.}$ compared with the initial ones. In the low concentration range of ethanol, $0 \sim 20$ vol. %, the experimental formula[1,2]

$$\frac{1}{k} = \frac{1}{k^0} + K\frac{[EtOH]}{[H_2O]} \qquad (3)$$

holds well also for the present case (see Fig. 2). Here, $k^0$ and $k$ are the quantum yields for aqueous and aqueous ethanolic solutions (ethanol concentration: [EtOH]), respectively. From the slope of the straight line of Fig. 2. one obtains

$$K = 1.0_9 \times 10^6 \quad (30°C) \qquad (4)$$

then

$$k^0 K = 185 \qquad (5)$$

**Photobleaching of Alkaline Solutions in Aqueous Alcohol in Vacuo.**—On the contrary to the aerobic system described above, alkaline (sodium hydroxide 0.0121 N) aqueous solution of uranin, in the absence of air, does not photobleach. With increase in ethanol concentration, however,

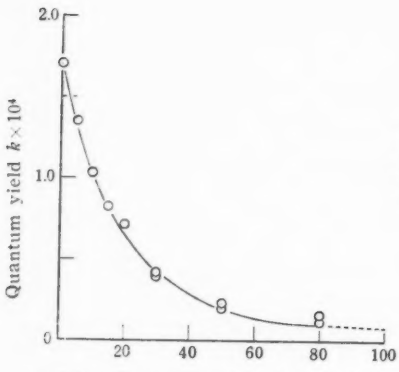


Fig. 1. Variation of $k$ with ethanol concentration. Aerobic, 30°C.

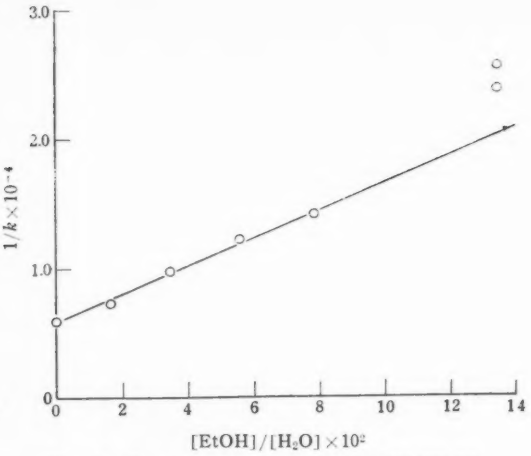


Fig. 2. Dependence of $1/k$ on $[EtOH]/[H_2O]$. (Eq. 3).

the rate of photobleaching becomes appreciable and reaches a constant value after passing through a maximum point, as shown in Fig. 3. An essentially analogous phenomenon is observed in the isopropanol system. In both cases the rates of photobleaching for the solutions of every alcohol concentration are expressed by Eq. 1 or 2.

Similar photobleaching in vacuo to that of alkaline uranin solutions is also observed in the case of eosin or erythrosin. A characteristic feature for the present case is that, at pH above a certain value, photobleaching of uranin is almost reversible. Photobleaching of eosin or erythrosin solution in the absence of alkali and of

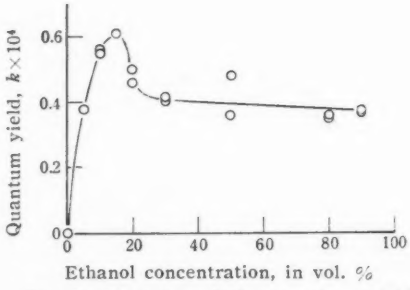


Fig. 3. Variation of the quantum yield with ethanol concentration in vacuo. NaOH, 0.0121 N, 30°C.

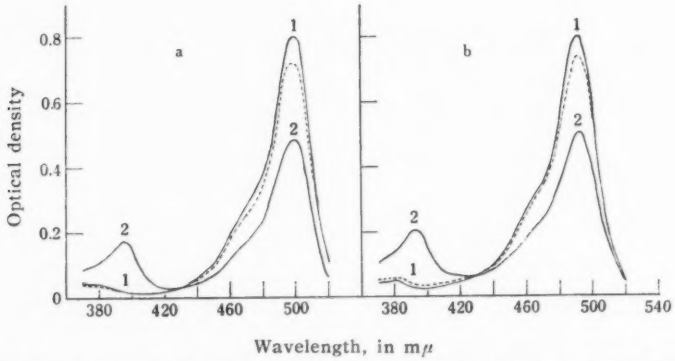


Fig. 4. Spectrum changes on irradiation in vacuo. NaOH, 0.0121 N, 30°C.
a: 80 vol. % aqueous ethanol: 1, initial; 2, 180 min.-irradiation.
b: 10 vol. % aqueous ethanol: 1, initial; 2, 123 min.-irradiation.

uranin solution of a lower alkali-concentration, are, on the other hand, irreversible. A few examples of the spectrum change of uranin resulting from irradiation are illustrated in Figs. 4 and 5. Fig. 4 shows the results obtained with alkaline solutions in aqueous ethanol, and Fig. 5 with an alkaline solution in aqueous isopropanol.

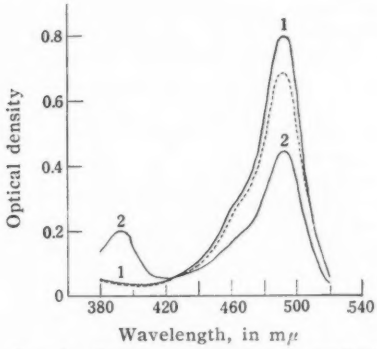


Fig. 5. Spectrum changes on irradiation in vacuo. NaOH, 0.0121 N, 30°C. 20 vol. % aqueous isopropanol: 1, initial; 2, 110 min.-irradiation.

In Figs. 4 and 5 full curves represent absorptions of the solutions unirradiated (1) and those irradiated for a while (2). On introduction of air into the irradiated solutions, their absorption curves 2 are immediately restored to a great extent, which are shown in Figs. 4 and 5 by dotted curves.

A striking feature is that, as shown in Figs. 4 and 5, a new absorption band appears at $\lambda$ 390~400 mμ by irradiation, which is enhanced with decrease in the optical density at $\lambda_{max.}$ near 490 mμ, and which disappears immediately by introducing air. A distinct isosbestic point is seen in each figure. A quite analogous but very slow restoration of the absorption curve is realized even in vacuo, when an irradiated solution is kept in the dark for a long time. Since it usually takes 20~40 hours to attain the same degree as air-restoration, the slight restoration during absorption measurement which should result in an error on determining concentration could be neglected.

Degree of air-restoration, which is almost 80~90% of the initial height, is almost independent of the alcohol concentration of the solution, no definite relationship between them being able to be found. Two or more cycles of photobleaching with new band formation and restoration in the dark and in vacuo, are possible without appreciable variation of the individual rates.

As mentioned above, such a reversible photobleaching is predominant in the higher pH range, while, in the lower alkali-concentration range, it is almost irreversible. In the case where irreversible photobleaching predominates, the new band formation is hardly observed at all. In Table II are given the results on the pH-dependency of the photobleaching of the alkaline uranin solutions in 20 vol. % aqueous isopropanol performed at 20°C.

In Table II, $D^0$ and $D_b^V$ are the optical densities determined at $\lambda_{max.}$ for the initial and the irradiated (in vacuo 80 min.) solutions, respectively. $D_r^V$ and $D_r^A$ are for the solutions which are, after irradiation, kept in vacuo and in the dark for 60 min., and for the solutions into which air is introduced (determined immediately after air-introduction), respectively. $\Delta D^V_{b395}$ is an increase in optical density at $\lambda$ 395 mμ by irradiation. All the values of optical density correspond to the 10 mm-path length.

TABLE II

pH-DEPENDENCY OF THE PHOTOBLEACHING OF THE SOLUTIONS IN 20 VOL. % ISOPROPANOL IN VACUO, AT 20°C

$\alpha = 2.7 \times 10^4$ $\lambda_{max.} = 492$ mμ

| pH | $D^0$ | $D_b^V$ (80 min.) | $D_r^V$ (60 min.) | $D_r^A$ | $\frac{D_r^A - D_b^V}{D^0 - D_b^V}$ | $\frac{D_r^V - D_b^V}{D_r^A - D_b^V}$ | $\frac{\Delta D^V_{b395}}{D_r^A - D_b^V}$ | $k \times 10^4$ |
|---|---|---|---|---|---|---|---|---|
| 9.24 | 0.812 | 0.500 | 0.538 | 0.721 | 0.708 | 0.172 | 0.629 | 0.57 |
| 8.70 | .822 | .536 | .565 | .768 | .812 | .125 | .647 | .57 |
| 8.34 | .822 | .532 | .560 | .770 | .821 | .118 | .643 | .51 |
| 8.00 | .826 | .545 | .607 | .785 | .854 | .258 | .613 | .54 |
| 7.92 | .822 | .542 | .610 | .753 | .755 | .322 | .597 | .52 |
| 7.42 | .830 | .615 | .680 | .692 | .358 | .845 | .695 | .31 |
| 7.30 | .820 | .645 | .700 | .702 | .326 | .965 | .175 | .27 |
| 7.04 | .815 | .600 | .655 | .660 | .279 | .834 | .083 | .31 |

Thus, $(D_r^A - D_b^V)/(D^0 - D_b^V)$ represents a fraction of the amount of an intermediate which can be restored by air to that of photobleached dye. It is seen that this fraction increases with increase in pH, having its highest value 0.8~0.9. On the other hand, $(D_r^V - D_b^V)/(D_r^A - D_b^V)$ may give a measure for the stability of the reversible intermediate in vacuo. This value increases with decrease in pH-value, indicating that the reversible intermediate, in vacuo, is relatively unstable at low pH.

In the last column of Table II are given the quantum yields, which may include slight errors resulting from a back reaction. Since the time required for determining optical densities of the irradiated solution is as short as possible, the errors from the dark back reaction may, even in a low pH solution, be considerably small or negligible. Essentially analogous results have been obtained with the solutions in 50 vol. % ethanol in vacuo at 20°C. It is presumable, from these data, that the completely reversible photobleaching would give a quantum yield which is twice that of the completely irreversible one. The molar extinction coefficient of the newly formed intermediate can be estimated from the limiting value of $\Delta D^V_{b395}/(D_r^A - D_b^V)$ to be $6.5 \times 10^4$ at $\lambda$ 395 m$\mu$ in alkaline aqueous ethanol and isopropanol.

## Discussion

**Photobleaching of the Alkaline Solutions in Aqueous Alcohol in Vacuo.**—As in the case of uranin at a lower pH, alcoholic eosin and erythrosin solutions into which no alkali is added show an irreversible photobleaching in vacuo[3-6]. It has been concluded experimentally that the primary process in these systems is the dehydrogenation from alcohol molecules by the excited (in the triplet state) dyes. No distinct absorption in the near ultraviolet region as the one observed for the irradiated uranin solutions at higher pH is detected. It has been assumed therefore that the succeeding process is the formation of leuco dye $DH_2$[16], which have no distinct absorption in near ultraviolet and may decompose into irreversible products under the experimental conditions.

Quite a different result obtained with alcoholic uranin solutions at higher pH in vacuo may be interpreted as assuming the formation of a carbinol base. It is known that triphenylmethane dyes, such as crystalviolet, form their carbinol bases in the presence of alkali[17]. Though it is not the case for xanthene dyes, it may probably be assumed that the presence of sufficient alkali in the reductive condition is preferable to form a carbinol base.

Carbinol bases should reverse to the original dyes not only by oxidation with oxygen (or air) but also by spontaneous separation of water from them. Their stabilities in vacuo and in the dark may probably be more or less higher at higher pH than at lower pH. These expectations are all realized in the present experimental results summarized in Table II, at least qualitatively.

Next, it is noted that the quantum yield at a higher pH is nearly twice those at lower pH. At lower pH, uranin photobleaches preferentially in an irreversible fashion. The situation will be the same as those for eosin and erythrosin, i.e.,

$$D^t + RH \rightarrow DH\cdot + R\cdot \qquad \text{(i)}$$

$$DH\cdot + DH\cdot \rightarrow DH_2 + D \qquad \text{(ii)}$$

$$DH_2 \rightarrow \text{Products.} \qquad \text{(iii)}$$

On the other hand, in the case of higher pH solutions, where the formation of carbinol base is assumed to occur as mentioned above, the succeeding process followed i should be quite a different one:

$$DH\cdot \xrightarrow{OH^-} DH(OH) \qquad \text{(iv)}$$

Here DH(OH) represents a carbinol base. From the above schemes it is shown that, in the former case, of one mole of DH· formed by i, one-half should return to the original dye by the disproportionation reaction ii, whereas, in the latter where the reaction ii is almost negligible, such a regeneration of a dye, on neglect of a slow dark back reaction, does not occur. Thus, for limiting conditions of these two cases, it is apparent that the quantum yield of the latter case may reach a value close to twice the value found in the former. Experimental data are, therefore, considered as good evidence for the formation of carbinol base of uranin at higher pH, and it follows therefrom that the appearence of a new absorption at $\lambda$ 390~395 m$\mu$ may be due to this formation.

16) Leuco forms of these dyes are obtained by reduction of their alkaline solutions with zinc powder, which exhibit no absorption in ultraviolet region.

17) a) L. Gattermann, "Die Praxis des organischen Chemikers", Walter de Gruyter, Berlin (1940), p. 328. b) K. Venkataraman, "The Chemistry of Synthetic Dyes", Vol. II, (1952), pp. 705–754.

**Primary Process in Alcoholic Solutions and the Reactivity of the Excited Uranin toward Alcohol.** — It is clear from the above discussion that the primary process conducted in the deaerated alcoholic solutions should, independently of pH, be given by mechanism i. Excited uranin is assumed to be in the triplet state, in analogy with the cases of eosin and erythrosin. So far as semileuco-dye DH· is assumed to be colorless, the specific rate (quantum yield) of the photobleaching of the deaerated alcoholic solutions is given as

$$k = \varphi_{S\to T}\frac{k_2[\mathrm{RH}]}{k_1{}^S[\mathrm{H_2O}]+k_2{}^S[\mathrm{RH}]} \tag{6}$$

Here, transition probability $\varphi_{S\to T}$ for uranin without substituted halogen atoms may be considered to be lower than those for eosin and erythrosin with substituted halogen atoms[18]. From Eq. 6 one obtains

$$\frac{1}{k}\frac{[\mathrm{RH}]}{[\mathrm{H_2O}]} = \frac{1}{\varphi_{S\to T}}\frac{k_1{}^S}{k_2} + \frac{1}{\varphi_{S\to T}}\frac{k_2{}^S[\mathrm{RH}]}{k_2[\mathrm{H_2O}]} \tag{7}$$

Plotting $[\mathrm{RH}]/k[\mathrm{H_2O}]$ against $[\mathrm{RH}]/[\mathrm{H_2O}]$ using the results obtained with the alkaline (sodium hydroxide 0.0121 N) solutions in aqueous ethanol at 30°C, one obtains a straight line in the relatively low alcohol concentration region, as shown in Fig. 6.

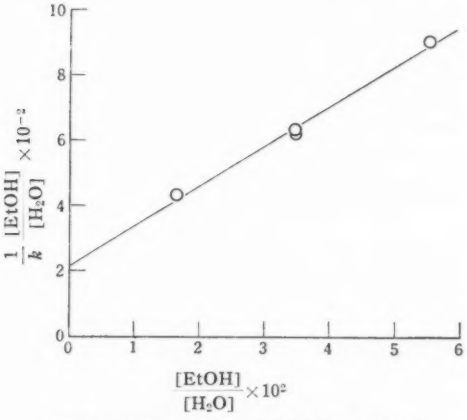


Fig. 6. Dependence of $[\mathrm{EtOH}]/k[\mathrm{H_2O}]$ on $[\mathrm{EtOH}]/[\mathrm{H_2O}]$ in vacuo, 30°C. (Eq. 7).

From the slope and the intercept of this straight line, respectively,

$$\varphi_{S\to T}\frac{k_2}{k_2{}^S} = 0.81\times 10^{-4} \tag{8}$$

and

$$\varphi_{S\to T}\frac{k_2}{k_1{}^S} = 4.7\times 10^{-3} \tag{9}$$

and from these two values

$$\frac{k_2{}^S}{k_1{}^S} = 57 \tag{10}$$

The last value gives a ratio of the interaction probability of $D^t$ with alcohol to that with water molecules.

**Primary Process in Aerobic Aqueous Solution and the Reactivity of the Excited Uranin toward Oxygen.**—As to the primary process in the aerobic aqueous solutions, the following two possible mechanisms have been suggested[1,2]:

$$D^t + O_2 \rightarrow D\cdots O_2 \xrightarrow{H_2O} \cdots \mathrm{Prod.}$$

$$D^t + H_2O \rightarrow D\cdots HOH \xrightarrow{O_2} \cdots \mathrm{Prod.}$$

On the kinetic ground, it has been concluded[5] that, if the former mechanism is a correct one,

$$\frac{k_2{}^{tS}}{k_1{}^{tS}} = k^0K \tag{11}$$

on the other hand, if the latter is a correct one,

$$\frac{k_2{}^S}{k_1{}^S} = k^0K \tag{12}$$

Though it is difficult to obtain the value of $k_2{}^{tS}/k_1{}^{tS}$ experimentally in the present investigation, comparison of the value of $k^0K$ (5) obtained in the aerobic systems with that of $k_2{}^S/k_1{}^S$ (10) in the deaerated systems leads to the conclusion that the primary process of the excited uranin in the aerobic aqueous solutions is expressed by the former mechanism, as in the cases of eosin and erythrosin[5,6].

According to the conclusion obtained above, the specific rate (quantum yield) for the photobleaching of the aqueous solutions should be given as

$$k = \varphi_{S\to T}\frac{k_{O_2}[\mathrm{O_2}]}{k^S{}_{O_2}[\mathrm{O_2}]+k_1{}^S[\mathrm{H_2O}]}\frac{k_1{}'[\mathrm{H_2O}]}{k_1{}^{tS}[\mathrm{H_2O}]} \tag{13}$$

The fact that the quantum yields of photobleaching of eosin and erythrosin solutions reach, already at the relatively low oxygen concentrations, the corresponding limiting values which are equal to those for the aerobic solutions, indicates that, in Eq. 13 $k_1{}^S[\mathrm{H_2O}]$ can be neglected against $k_{O_2}{}^S[\mathrm{O_2}]$, above a relatively low oxygen concentration, i.e.,

$$k_{O_2}{}^S[\mathrm{O_2}] \gg k_1{}^S[\mathrm{H_2O}] \tag{14}$$

18) D. S. McClure, N. W. Blake and P. L. Hanst, *J. Chem. Phys.*, **22**, 255 (1954).

In the case of uranin, however, such a limiting value is not attained, indicating that, even under the atmospheric air, neglect of $k_1^S[H_2O]$ is unreasonable for the present case. Then, from Eq. 13, one obtains

$$\frac{1}{k}\frac{[O_2]}{[H_2O]} = \frac{k_1'^S}{\varphi_{S\to T}k_1'}\frac{k_1^S}{k_{O_2}} + \frac{k_1'^S}{\varphi_{S\to T}k_1'}\frac{k_{O_2}^S}{k_{O_2}}\frac{[O_2]}{[H_2O]} \tag{15}$$

Application of Eq. 15 to the results previously obtained with the aqueous uranin solutions at 30°C is illustrated in Fig. 7.

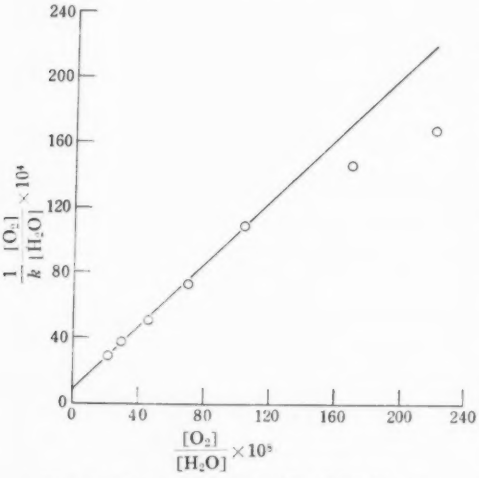


Fig. 7. Dependence of $[O_2]/k[H_2O]$ on $[O_2]/[H_2O]$, 30°C (Eq. 15).

It is shown in Fig. 7 that a linear relation is realized at the oxygen concentration up to $58\times10^{-6}$ mole/l. The intercept and the slope of the line yield, respectively,

$$\frac{k_1'^S k_1^S}{\varphi_{S\to T}k_1'k_{O_2}} = 9\times10^{-4} \tag{16}$$

and

$$\frac{k_1'^S k_{O_2}^S}{\varphi_{S\to T}k_1'k_{O_2}} = 0.96\times10^4 \tag{17}$$

From these values, it follows that

$$\frac{k_{O_2}^S}{k_1^S} = 1\times10^7 \tag{18}$$

which gives the reactivity of $D^t$ toward oxygen relative to that toward water molecules.

If a sufficient amount of oxygen is dissolved in the solution to justify the relation 14, the quantum yield should be given as the reciprocal of the relation 17:

$$\varphi_{S\to T}\frac{k_1'k_{O_2}}{k_1'^S k_{O_2}^S} = 1.0\times10^{-4} \tag{19}$$

Under the atmospheric air, aqueous uranin solution gives a rather higher value ($1.3\times10^{-4}$, at 30°C) than that from Eq. 19. As to the nature of this enhancing effect of oxygen at higher concentrations, it is noteworthy to mind the recent Evans' work[19] on the perturbation of $S\to T$ transitions of organic molecules by oxygen. For eosin and erythrosin such an enhancing effect of oxyen is, at least under the atmospheric air, not observed, and, moreover, the quantum yields at the sufficient oxygen concentrations are quite consistent with those obtained from the slopes of the corresponding plots of Eq. 15. According to the Evans' results, these halogenated dyes may be affected by oxygen far less than the unhalogenated one is. In the case of uranin, the transition probability, $\varphi_{S\to T}$, should depend on oxygen pressure, resulting in an increase in quantum yield with increasing oxygen concentration. This is still in speculation; more quantitative studies must be performed to throw light on this problem.

**Comparison between the Reactivities of Excited Xanthene Dyes toward Oxygen and Alcohol.**—Reactive species of three xanthene dyes so far investigated are in the excited triplet states, and their primary processes are concluded to be the formation of labile complexes with oxygen molecules in the aerobic aqueous solutions, and to be the dehydrogenation from alcohol molecules in the alcoholic solutions. Relative reactivities of excited eosin and erythrosin have been reported previously[5,6]. In Table III are summarized the relative reactivities of these dyes.

TABLE III
RELATIVE REACTIVITIES OF EOSIN, ERYTHROSIN AND URANIN

| | Eosin | Erythrosin | Uranin |
|---|---|---|---|
| $\frac{k_2^S}{k_1^S}$ (ethanol) | 19(27°C) | 3(27°C) | 57(30°C) |
| $\frac{k_{O_2}^S}{k_1^S}\times10^7$ | 7.7(30°C) | 1.3(30°C) | 1.0(30°C) |

The values in Table III are reactivities toward ethanol and oxygen (dissolved) relative to those toward water molecules. Though it is difficult to compare exactly their reactivities in absence of the numerical values of $k_1^S$, it appears possible

19) D. F. Evans, *J. Chem. Soc.*, **1957**, 1351; *Nature*, **178**, 534 (1956).

to say that, in general, halogenated dyes are more reactive toward oxygen than the unhalogenated ones, while toward alcohol vice versa. There seems to be a close relation between such facts and the characteristic pH-dependency of the absorption spectra mentioned before[15].

**Summary**

Investigation of the photobleaching of uranin solutions has led to the same conclusions as for eosin and erythrosin, concerning the primary processes both in aqueous and in alcoholic media. Strongly alkaline solutions of uranin in aqueous alcohol show an irreversible photobleaching in vacuo. On the reactivities of the excited uranin, and on the comparison of them with those of two other xanthene dyes previously investigated, some discussions have been given.

The author thanks Professor M. Koizumi for his valuable advice throughout this investigation, and Professor R. Fujishir for his interest in this work.

*Institute of Polytechnics*
*Osaka City University*
*Kitaku, Osaka*

# *Kinetics of the Caro's Acid Oxidation of Dimethylanilines*

By Yoshiro OGATA and Iwao TABUSHI

(Received June 21, 1958)

It has been reported that Caro's acid (peroxymonosulfuric acid), presumably contained in a mixture of aqueous sulfuric acid and sodium persulfate, converts aniline (or *N*-monomethylaniline) into phenylhydroxyamine, nitrosobenzene, nitrobenzene and azobenzene[1], while *N*-dimethylaniline (abbreviated as DMA) produces a stable amine oxide on oxidation with Caro's acid[2].

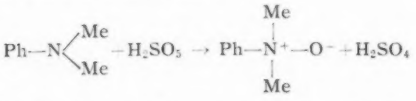

The amine oxide can also be obtained from other tertiary amines, e. g. pyridine, and other oxidizing agents such as hydrogen peroxide[3].

The rate of hydrogen-peroxide oxidation of trimethylamine was measured by Ross[4] only in neutral aqueous solutions. It was found that the rate was proportional to the concentration of the reactants. However, the effects of amine structure and pH of the solution on the rate have not yet been investigated in detail. The present paper describes the data and the probable mechanism of the oxidation of unsubstituted and ring-substituted DMA with Caro's acid in aqueous media.

## Experimental

**Materials.** — DMA was purified by duplicate fractional distillations, b. p. 193°. *p*-Methyl-(b. p. 133°/55 mm.) and *p*-methoxy-dimethylaniline (m. p. 49°) were prepared by the dimethyl-sulfate methylation of *p*-toluidine and *p*-anisidine, respectively[5]. *p*-Chlorodimethylaniline was synthesized by the chlorination of DMA[6], m. p.[7] 35.5°. Caro's acid was prepared by the reaction of potassium persulfate (10 g.) and concentrated sulfuric acid (11 g.) and stored in the form of a dilute solution.

**Rate Measurements.** — A known amount of acidic aqueous solution of DMA with sulfuric acid or a mixture of potassium hydroxide and borate was mixed in a brown flask and kept at a constant temperature. The solution was mixed with a known amount of aqueous Caro's acid solution maintained at a constant temperature and the reaction was caused to start. Aliquots were taken out at appropriate intervals of time and their peroxide contents were determined iodimetrically. The data of the iodometry were corrected for hydrogen peroxide and peroxydisulfate by another iodometry with cuprous iodide

1) E. Bamberger and F. Tschirner, *Ber.*, **31**, 1675 (1899); E. Bamberger and M. Vuk, ibid., **35**, 703 (1902).
2) E. Bamberger and P. Leyden, ibid., **34**, 12 (1901); E. Bamberger and F. Tschirner, ibid., **32**, 342 (1899).
3) E. Ochiai, *J. Org. Chem.*, **18**, 534 (1953).
4) S. D. Ross, *J. Am. Chem. Soc.*, **68**, 1484 (1946).
5) H. Wieland, *Ber.*, **43**, 712 (1910).
6) D. V. Tischtschenko, *J. Russ. Phys Chem. Soc.*, **60**, 153 (1928).
7) T. Heidelberg, *Ber.*, **20**, 149 (1887).

as a catalyst[8]. The rate constants were calculated by means of the usual second-order rate equation or pseudo-first-order equation.

**The Equilibrium Constants for the Protonation of Substituted DMA.**—The equilibrium constant in aqueous solution, $K' = [BH^+]/([B][H^+])$ was determined spectrophotometrically in buffer solutions at various pH's. The spectral data for free and protonated amines were obtained from those in 0.1 N potassium hydroxide and 0.1 N hydrochloric acid, respectively. The used absorption maxima of free and protonated *p*-substituted dimethylanilines were as follows, respectively: MeO, 237 and 223 mμ; Me 237 and below 210 mμ; H, 240 and below 210 mμ; Cl, 250 and 215 mμ.

Since ordinary organic acids showed interference in UV spectra, 0.5 N ammonium chloride solution containing various amounts of ammonium hydroxide, hydrochloric acid or sodium borate was used as a buffer agent. The measurements were carried out at spectral regions of longer wave lengths to avoid the interference of inorganic materials. The results obtained from experiments carried out at more than one kind of wave length agreed well.

The $K'$ values for substituted DMA are listed in Table I. These values are in accord with the Hammett equation. The values are somewhat different from those obtained by Davies[9] probably because of the difference of his solvent, 50% ethanol.

**Supplementary Notes.** — (1) A method of volumetric analysis of tertiary amine is suggested, in which an excess of Caro's acid is titrated by iodometry after oxidation of the amine sample at an appropriate pH (pH 4~5 for DMA). The method may be suitable for the analysis where acidimetry is difficult, e. g. in a buffer solution.

(2) Hall's p$K$ values[10] for anilines are of most systematic ones, but his datum on dimethylaniline somewhat differs from the present datum and seems to be too small on the basis of the following considerations. The increase of p$K$ by the introduction of a second methyl group into monomethylaniline is unusually small, if compared with that of an ethyl group into monomethylaniline or that of a methyl group into monoethylaniline.

| | | |
|---|---|---|
| $PhNH_2$ | 4.62 | |
| PhNHMe | 4.85, | $\Delta^0_{Me}=0.23$ |
| $PhNMe_2$ | 5.06, | $\Delta^{Me}_{Me}=0.21$ |
| PhNHEt | 5.11, | $\Delta^0_{Et}=0.49$ |
| $PHNEt_2$ | 6.26, | $\Delta^{Et}_{Et}=1.15$ |
| PhNMeEt | 5.98, | $\Delta^{Et}_{Me}=0.87$ |
| | | $\Delta^{Me}_{Et}=1.13$ |

On the other hand, our datum on dimethylaniline leads to a reasonable increment ($\Delta^{Me}_{Me}=0.52$).

TABLE I

EQUILIBRIUM CONSTANTS FOR THE PROTONATION OF DIMETHYLANILINE

| Substituent | pH | $K'$ a) | p$K'$ | p$K$ b) |
|---|---|---|---|---|
| *p*-MeO | 5.21 | $0.920\times10^6$ | −5.964 | |
| | 5.73 | $1.03\times10^6$ | −6.013 | |
| | 6.00 | $1.01\times10^6$ | −6.004 | |
| | (av.) | $0.967\times10^6$ | −5.96 | 8.04 |
| *p*-Me | 5.50 | $4.93\times10^5$ | −5.693 | |
| | 5.70 | $5.02\times10^5$ | −5.701 | |
| | 5.90 | $5.06\times10^5$ | −5.705 | |
| | (av.) | $5.00\times10^5$ | −5.70 | 8.30 |
| None | 5.41 | $2.52\times10^5$ | −5.402 | |
| | 5.67 | $2.66\times10^5$ | −5.425 | |
| | 5.80 | $2.39\times10^5$ | −5.378 | |
| | (av.) | $2.52\times10^5$ | −5.40 | 8.60 |
| *p*-Cl | 3.99 | $4.71\times10^4$ | −4.673 | |
| | 4.50 | $4.82\times10^4$ | −4.683 | |
| | (av.) | $4.76\times10^4$ | −4.68 | 9.32 |

a) $K' = \dfrac{[BH^+]}{[B][H^+]}$ b) $K = \dfrac{[BH^+][OH^-]}{[B][H_2O]}$

## Results

The rate data show that the second-order kinetics are satisfied.

$$dx/dt = k(d-x)(p-x) \qquad (1)$$

Here $(d-x)$ and $(p-x)$ represent the concentrations of dimethylaniline and Caro's acid, respectively. Tables II and III list the effect of initial concentration and acidity on the rate with various substituted DMA's, respectively.

It was reported that some deviation of the apparent rate constant $k$ was observed in the persulfate oxidation in alkaline solution[11] probably owing to the radical reaction, but no indication of the deviation was observed in this case, even if a relatively large excess of DMA was used.

TABLE II

SECOND-ORDER RATE CONSTANT $k$ AT VARIOUS INITIAL CONCENTRATIONS FOR THE CARO'S ACID OXIDATION OF DMA

Temp. 20°C, pH 1.35, Solvent, water

| Initial concn. of Caro's acid (M) | Initial concn. of DMA (M) | $k$(l. mole$^{-1}$ sec.$^{-1}$) |
|---|---|---|
| $3.93\times10^{-3}$ | 0.0167 | $3.84\times10^{-3}$ |
| $3.67\times10^{-3}$ | 0.0308 | $4.02\times10^{-3}$ |
| $3.76\times10^{-3}$ | 0.0600 | $3.64\times10^{-3}$ |
| $3.96\times10^{-3}$ | 0.0800 | $3.85\times10^{-3}$ |

8) M. A. Bodin, *Zavodskaya Lab.*, **7**, 1248 (1938).
9) W. C. Davies and H. W. Bdcis, *J. Chem. Soc.*, **1937**, 1622.
10) N. F. Hall and M. R. Spinkle, *J. Am. Chem. Soc.*, **54**, 3469 (1932).
11) L. S. Levitt and E. R. Malinowski, ibid., **77**, 4517 (1955).

TABLE III

SECOND-ORDER RATE CONSTANTS FOR THE CARO'S ACID OXIDATION OF DIMETHYLANILINES

Unsubstituted DMA

| pH | Temp. °C | $k\times10^2$ (l. mole$^{-1}$ sec.$^{-1}$) | $k_4=k\cdot[H^+]\cdot K_2$ |
|---|---|---|---|
| 1.00 | 25.0 | 0.241 | 60.6 |
| 1.22 | 25.0 | 0.384 | 58.5 |
| 1.40 | 25.0 | 0.600 | 60.0 |
| 1.80 | 25.0 | 1.73 | 69.0 |
| 1.85 | 25.0 | 1.80 | 64.2 |
| 1.98 | 25.0 | 2.36[a)] | 62.4 |
| 2.04 | 25.0 | 3.10 | 71.1 |
| 2.29 | 25.0 | 4.70 | 60.5 |
| 2.40 | 25.0 | 6.05 | 60.5 |
| 2.99 | 25.0 | 41.4 | |
| 3.70 | 25.0 | 346 | |
| 4.81 | 25.0 | 3200 | |
| 6.00 | 25.0 | 4250 | |
| 7.30 | 25.0 | 4360 | |
| 8.10 | 25.0 | 3780 | |
| 9.10 | 25.0 | 2700 | |
| 9.44 | 25.0 | 2220 | |
| 10.00 | 25.0 | 680 | |
| 10.50 | 25.0 | 348 | |
| 1.70 | 30.0 | 2.91 | |
| 1.70 | 20.0 | 0.980 | |
| 1.80 | 15.0 | 0.580 | |
| 1.80 | 25.0 | 1.65[b)] | |
| 1.82 | 25.0 | 1.80[c)] | |

*p*-MeO-DMA

| | | | |
|---|---|---|---|
| 1.50 | 25.0 | 0.443 | 135 |
| 1.70 | 25.0 | 0.590 | 114 |
| 1.70 | 15.0 | 0.255 | |
| 2.04 | 25.0 | 1.20 | 101 |
| 2.28 | 25.0 | 2.64 | 134 |
| 3.11 | 25.0 | 18.5 | 139 |
| 4.17 | 25.0 | 185 | 121 |
| 7.90 | 25.0 | 7090 | |
| 9.30 | 25.0 | 4470 | |
| 10.28 | 25.0 | 3080 | |
| 11.52 | 25.0 | 142 | |
| 12.20 | 25.0 | 22.9 | |
| 12.64 | 25.0 | 8.79 | |

*p*-Me-DMA

| pH | Temp. °C | $k\times10^2$ (l. mole$^{-1}$ sec.$^{-1}$) | $k_4=k\cdot[H^+]\cdot K_2$ |
|---|---|---|---|
| 1.26 | 25.0 | 0.403 | 111 |
| 1.36 | 25.0 | 0.490 | 107 |
| 1.75 | 25.0 | 1.12 | 105 |
| 2.30 | 25.0 | 4.16 | 104 |
| 2.42 | 25.0 | 5.99 | 114 |
| 3.00 | 25.0 | 32.4 | 162 |
| 3.50 | 25.0 | 99.6 | 157 |
| 4.00 | 25.0 | 368 | |
| 4.70 | 25.0 | 3260 | |
| 7.30 | 25.0 | 5280 | |
| 8.00 | 25.0 | 5040 | |
| 8.95 | 25.0 | 5720 | |
| 9.93 | 25.0 | 1980 | |
| 10.30 | 25.0 | 944 | |
| 10.63 | 25.0 | 413 | |
| 11.60 | 25.0 | 59.4 | |
| 12.03 | 25.0 | 30.3 | |
| 12.59 | 25.0 | 10.6 | |
| 1.90 | 15.0 | 0.782 | |
| 1.90 | 25.0 | 2.15 | |

*p*-Cl-DMA

| | | | |
|---|---|---|---|
| 1.38 | 25.0 | 2.40 | 47.6 |
| 1.60 | 25.0 | 3.22 | 38.5 |
| 2.03 | 25.0 | 11.8 | 52.5 |
| 2.50 | 25.0 | 36.2 | 54.3 |
| 2.81 | 25.0 | 73.6 | 55.9 |
| 3.21 | 25.0 | 223 | |
| 3.53 | 25.0 | 965 | |
| 4.32 | 25.0 | 3340 | |
| 7.13 | 25.0 | 4110 | |
| 7.80 | 25.0 | 4160 | |
| 8.81 | 25.0 | 3360 | |
| 9.40 | 25.0 | 2360 | |
| 9.95 | 25.0 | 969 | |
| 11.02 | 25.0 | 101 | |
| 11.52 | 25.0 | 38.7 | |
| 11.92 | 25.0 | 20.1 | |
| 1.89 | 15.0 | 1.76 | |
| 1.89 | 25.8 | 9.25 | |

a) $Na_2SO_4$ (100 mg.) was added in 50 ml. of the solution.
b) Benzoyl peroxide (5 mg.) was added in 50 ml. of the solution.
c) Hydroquinone (3 mg.) was added in 50 ml. of the solution.

In strong acid media, the rate constant $k$ increases with increasing pH, the plot of $\log k$ against pH giving a satisfactory straight line with a slope of ca. +1. In the strong acidity the rate constants for substituted DMA at a given pH decrease, in the order: *p*-Cl, *p*-H, *p*-Me and *p*-MeO.

The increase of the $k$ value with decreasing acidity diminishes gradually, and then $k$ reaches a constant value in the neighborhood of the neutrality, where the accurate rate can not be obtained because of its large value together with the spontaneous decomposition of the oxidizing agent.

In weakly alkaline media, $k$ tends to decrease with increasing pH and after reaching a bending point at pH 9.5~10.5 an approximate linear relation is observed between $\log k$ and pH with the slope of

−1. The $k$ values in neutral and an alkaline region decrease with substituents of DMA in the order $p$-MeO, $p$-Me, $p$-H and $p$-Cl.

The energies of activation for substituted DMA are shown in Table IV.

TABLE IV
TEMPERATURE COEFFICIENT AND ENERGY OF ACTIVATION FOR THE CARO'S ACID OXIDATION OF DIMETHYLANILINES

| Substituent | MeO | Me | H | Cl |
|---|---|---|---|---|
| $k_{25}/k_{15}$ | 2.32 | 2.75 | 2.98 | 4.97[a] |
| $E_a$(kcal./mole) | 14.5 | 17.4 | 18.7 | 25.6 |

a) $k_{25.5}/k_{15}$

## Discussion

The observed second-order kinetics and the effects of acidity and substituents suggest the following mechanism which involves a rate-determining electrophilic attack of neutral molecules of Caro's acid on the free dimethylaniline.

$$ArNMe_2 + H^+ \rightleftarrows Ar\overset{+}{N}Me_2H \text{ (rapid)} \quad (2)$$

$$H_2SO_5 \leftrightarrows HSO_5^- + H^+ \text{ (rapid)} \quad (3)$$

$$ArNMe_2 + H_2SO_5 \rightarrow Ar\overset{+}{N}Me_2OH + HSO_4^- \text{ (slow)} \quad (4)$$

$$Ar\overset{+}{N}Me_2{-}OH \rightleftarrows Ar\overset{+}{N}Me_2{-}O^- + H^+ \text{ (rapid)} \quad (5)$$

From this mechanism, the following relation between the apparent rate constant $k$ and the rate constant of rate-determining step 4 should be expected.

$$k = \frac{1}{K_2[H^+]+1} \cdot \frac{[H^+]}{[H^+]+K_3} k_4 \quad (6)$$

where $k$ and $K$ are rate- and equilibrium constant of the steps.

At relatively high acidity, equation 6 will be to

$$k = \frac{1}{K_2[H^+]} k_4 \quad (7)$$

and in alkaline media where $[H^+]$ is very small, equation 6 is reduced to

$$k = K_3[H^+]k_4 \quad (8)$$

These two equations 7 and 8 satisfy the observed effect of acidity. In alkaline and neutral solutions, almost none the amine molecules are protonated, hence an electron-releasing group in the amine will facilitate the reaction (the substituent affects $k_4$ alone in eqation 8). But the protonation equilibria 2 become important at high acidity as is obvious from the substituent effect on $K_2$ in equation 7, and the reverse substituent effect may appear, if the effect on $K_2$ is larger than that for $k_4$. These expectations were actually recognized as described previously.

In the acid media the linearity between $\log k$ and pH breaks when $K_2[H^+]$ becomes comparable with unity as seen in equation 6. This break (Fig. 1) was actually observed at pH 4∼5 and it depended on the $p$-substituent of dimethylaniline, i. e.,

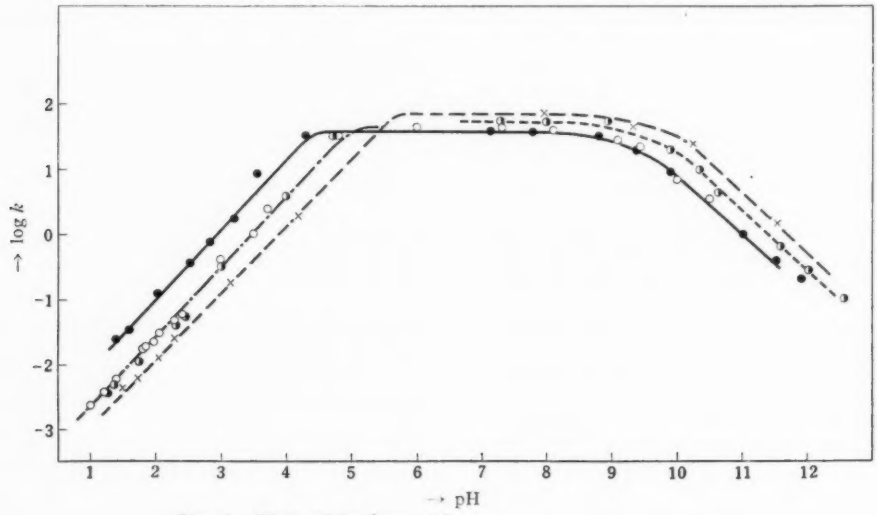


Fig. 1. Plots of $\log k$ vs. pH.
—×— $p$-MeO, ---◑--- $p$-Me, —○— $p$-H, —●— $p$-Cl

the pH value of this break increased in the order: *p*-Cl, *p*-H, *p*-Me and *p*-MeO. This is natural, since the electron-releasing groups increase the $K_2$ value in equation 6. On the other hand, the break in alkaline media was observed at pH 9.5~10.5 and was independent of *p*-substituent of DMA. This phenomenon seems to be attributable to a decrease of the concentration of $H_2SO_5$ because of its dissociation.

On the basis of the prevailing electronic theory, the other mechanisms described below are less probable, but they are discussed briefly. Instead of eq. 4, the rate-determining reaction between

(*a*) $\overset{+}{\text{Ar}}\text{NMe}_2\text{H}$ and $HSO_5^-$

(*b*) $\text{ArNMe}_2$ and $HSO_5^-$

(*c*) $\overset{+}{\text{Ar}}\text{NMe}_2\text{H}$ and $H_2SO_5$

leads to the following relation, respectively.

$$(a)\quad k = \frac{K_2[H^+]}{K_2[H]^+ + 1} \cdot \frac{K_3}{[H^+]+K_3} k_4'$$

$$(b)\quad k = \frac{1}{K_2[H^+]+1} \cdot \frac{K_3}{[H^+]+K_3} k_4''$$

$$(c)\quad k = \frac{K_2[H^+]}{K_2[H^+]+1} \cdot \frac{[H^+]}{[H^+]+K_3} k_4'''$$

The observed linearity of $\log k$ vs. pH at high acidity is at least unexplicable by the mechanism *c*, and that of $-\log k$ vs. pH in alkaline media is unexplicable by the mechanism *b*. The concentrations of the reactants in *b*, $\text{ArNMe}_2$ and $HSO_5^-$, should be much lower in an alkaline solution, hence the possibility of mechanism *b* is inconceivable over the whole pH range. Similarly, the concentrations of reactants, $\overset{+}{\text{Ar}}\text{NMe}_2\text{H}$ and $H_2SO_5$, should be much lower in an alkaline solution, hence the mechanism *c* is unlikely.

The mechanism *a* leads to the observed effects of acidity and substituents, and is indistinguishable from eq. 4 with kinetics alone; but the mechanism is less probable, since it involves a reaction between a very weak acid (aminium ion) and a very weak base (peroxysulfate ion) and the possible reaction should be the transfer of a proton from the cation to the anion. Furthermore, the fact that added salt (sodium sulfate) has little effect on the rate, favors the reaction between neutral molecules than that between ions.

It has been reported that the neutralizing equivalent of Caro's acid is a half of its oxidizing equivalent[12], thus the dissociation of its second hydrogen atom is inappreciable. Therefore, the mechanism, in which equilibrium 3 is replaced by

$$HSO_5^- \rightleftarrows SO_5^{2-} + H^+$$

and the attacking agent is $HSO_5^-$ instead of $H_2SO_5$, is unlikely.

Attempts to isolate pure Caro's acid by way of elimination of sulfuric acid with barium hydroxide or ion-exchange resin failed because of its instability.

No appreciable effect on the rate was recognized on addition of a small amount of hydroquinone or benzoyl peroxide, thus showing the absence of radical intermediates in the main reaction course.

## Summary

The rates of the Caro's acid oxidation of dimethylaniline and *p*-substituted dimethylanilines were measured in aqueous solutions of various pH's and temperatures. The rates were found to be proportional to the product of the concentrations of both reactants. The effects of pH and *p*-substituents on the rate constant were estimated. The rate constant in acid media increased with increasing electron-withdrawing power of the *p*-substituent of dimethylaniline, while the constant in alkaline media increased with decreasing pH or increasing electron-releasing power of the substituent. A probable mechanism involving a rate-determining attack of neutral Caro's acid molecule on free amine was proposed and discussed.

*Department of Industrial Chemistry*
*Faculty of Engineering*
*Kyoto University*
*Sakyo-ku, Kyoto*

# *Studies on Organic Reagents for Inorganic Analysis. IV. Syntheses of New Phenylfluorone Derivatives and their Reactions with Metal Ions*

By Hirotoshi SANO

(Received May 13, 1958)

Although numerous investigations have been published on the colorimetric determination of germanium[1-3], tin[4], titanium[5], and zirconium[6] with phenylfluorone (abbreviation for 2,3,7-trihydroxy-9-phenylfluorone), the research for the phenylfluorone derivatives is far from satisfactory. As is well known, phenylfluorone has some excellent properites as a colorimetric reagent. For instance, phenylfluorone has high sensitivity toward germanium, titanium, and zirconium, and germanium phenylfluoronate shows a high stability. However, it has some weak points such as small solubility of its chelates, somewhat low stability of the chelate of zirconium and undesirably high absorbance of the reagent solution at the wavelength used in the determination of germanium. Therefore, it is desirable to find out a new derivative which keeps the advantages and has no such difficulty. For this purpose, only 2,3,7-trihydroxy-9-(4′dimethylaminophenyl)fluorone was synthesized by the author and his coworkers,[7] and it was applied successfully to the colorimetric determination of germanium by Kimura and Asada[8]. Subsequently, some other derivatives, i. e., 2,3,7-trihydroxy-9-(3′-nitrophenyl) fluorone, 2,3,7-trihydroxy-9-(4′-nitrophenyl) fluorone and 2,3,7-trihydroxy-9-(2′-sulfophenyl) fluorone have been synthesized by a similar procedure. These compounds except 3′-nitrophenyl-fluorone[9] have never been described in the literature.

## Experimental and Results

**Syntheses of Derivatives.**—*Reagents Used.*—*m*-Nitrobenzaldehyde, *p*-nitrobenzaldehyde, and benzaldehyde-*p*-sodium sulfonate were first grade reagents prepared by Tokyo Kasei Ind., Co., Japan, and used without further purification. Hydroxyhydroquinone triacetate was synthesized[10] from commercial *p*-benzoquinone, acetic anhydride and concentrated sulfuric acid, and recrystallized twice or thrice from 95% ethanol. Commercial 95% ethanol was used.

*Procedures for Syntheses.*—For the synthesis of 3′- or 4′-nitro derivative, 20 g. of *m*- or *p*-nitrobenzaldehyde was dissolved in 300 ml. of 20% ethanol in a 500 ml. Erlenmeyer's flask. To the solution were added 100 ml. of ethanolic solution, containing 70 g. of hydroxyhydroquinone triacetate and 10 ml. of concentrated sulfuric acid. A deep red color appeared in the solution by heating it on a steam bath for two or three hours. The solution was allowed to stand for about three weeks. The resulting red crystalline precipitate was filtered, washed with warm 20% ethanol, and suspended in 400 ml. of water at controlled pH of 4. The hydrolyzed precipitate, whose color was deep red, was filtered, washed and dried in a vacuum desiccator.

For 2′-sulfo derivative, the procedure was somewhat different from that described above because of a considerable solubility of the sulfo derivative. Twenty grams of *o*-sulfobenzaldehyde was dissolved in 300 ml. of 20% ethanol in a 500 ml. round-bottom flask. To the solution were added 100 ml. of ethanol containing 70 g. of hydroxyhydroquinone triacetate and 30 ml. of concentrated hydrochloric acid. The solution was heated on a steam bath for two or three hours. Red color appeared in the solution. Even after being allowed to stand for several weeks, no precipitate was formed. The solution was then concentrated on a steam bath by vacuum evaporation. A red precipitate with greenish fluorescence was formed when the volume of the solution was reduced to nearly a half. The crystalline precipitate was filtered, washed with warm 20% ethanol roughly, and suspended in 400 ml. of water at pH 4. The hydrolyzed precipitate, of orange-yellow color which was considered to be sodium-sulfophenylfluorone was filtered, washed and dried. The orange yellow crystalline precipitate was dissolved or suspended in 1 l. of 95% ethanol containing 10 ml. of distilled hydrochloric acid on a steam

1) H. J. Cluley, *Analyst*, **76**, 523 (1951).
2) Y. Oka, T. Kanno and K. Shiba, *Japan Analyst* (*Bunseki Kagaku*), **3**, 389 (1954).
3) C. L. Luke and M. E. Campbell, *Anal. Chem.*, **28**, 1273 (1956).
4) C. L. Luke, ibid., **28**, 1276 (1956).
5) H. Sano, *Japan Analyst* (*Bunseki Kagaku*), **7**, 235 (1958).
6) K. Kimura and H. Sano, This Bulletin **30**, 80 (1957).
7) K. Kimura, H. Sano and M. Asada, ibid., **29**, 640 (1956).
8) K. Kimura and M. Asada, ibid., **29**, 812 (1956).
9) E. Heintschel, *Ber.*, **38**, 2878 (1905).
10) "Organic Syntheses, Collective Vol. I", John Wiley & Sons Inc., New York (1948), p. 317.

bath. The solution was allowed to stand for one or two days, and an orange red precipitate was obtained. The precipitate was filtered, washed, and dried in a vacuum desiccator.

The author is of the opinion that the following reactions occurred in this procedure.

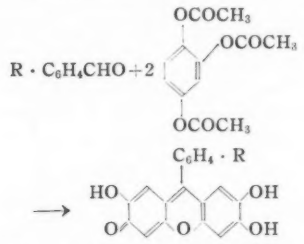

R: *m*-$NO_2$, *p*-$NO_2$ or *o*-$SO_3H$.

in $\begin{cases} H_2O \\ C_2H_5OH \\ H_2SO_4 \text{ or } HCl \end{cases}$

The yields of 3'-nitro, 4'-nitro and 2'-sulfo derivative are 30, 21 and 25% of the theoretical, respectively.

*Anal.* of the 3'-nitro derivative. Found: C, 60.76; H, 3.70. Calcd. for $C_{19}H_{11}O_7N$: C, 62.47; H, 3.04%.

*Anal.* of the 4'-nitro derivative. Found: C, 60.25; H, 3.27. Calcd. for $C_{19}H_{11}O_7N$: C, 62.47; H, 3.04%.

*Anal.* of the 2'-sulfo derivative. Found: C, 56.03; H, 3.35. Calcd. for $C_{19}H_{12}O_9S$: C, 57.01; H, 3.02%.

*Properties of the Products.*—3'-Nitro derivative: m.p.>310°C, orange-red powder, insoluble in water, sparingly soluble in ethanol. Addition of mineral acid to an ethanolic solution of the compound increases its solubility giving a yellow color. This compound is easily soluble in alkaline solution, giving a faded red-violet color. 4'-Nitro derivative: m.p.>310°C, brownish red powder, insoluble in water, soluble in ethanol with difficulty. The general trend of the effect of acid or alkali on the solubility is similar to the case of 3'-nitro derivative. 2'-Sulfo derivative: m.p.>295°C, orange powder, (its addition compound with hydrochloric acid is composed of brownish needles having green fluorescence.) slightly soluble in water or in ethanol, giving yellow color and weak green fluorescence. The addition of a small amount of mineral acid to the solution increases its solubility slightly. The addition of sodium hydroxide greatly increses the solubility, giving red color and strong green fluorescence. In a strong alkaline solution, the color turns red-violet and the fluorescence disappears.

*Absorption Spectra of the Solutions of the Derivatives.*—The absorption spectra of the derivatives in an acidic and an alkaline solution are shown in Figs. 1a, b, c, d and e, together with those of phenylfluorone and dimethylamino-phenylfluorone for comparison. The absorption measurements were made with a Uvispek spectrophotometer and Beckman model DU spectrophotometer

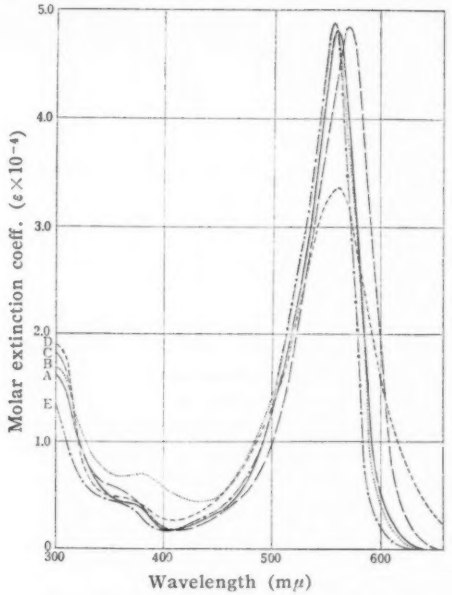


Fig. 1a. Absorption spectra of products in alkaline media.

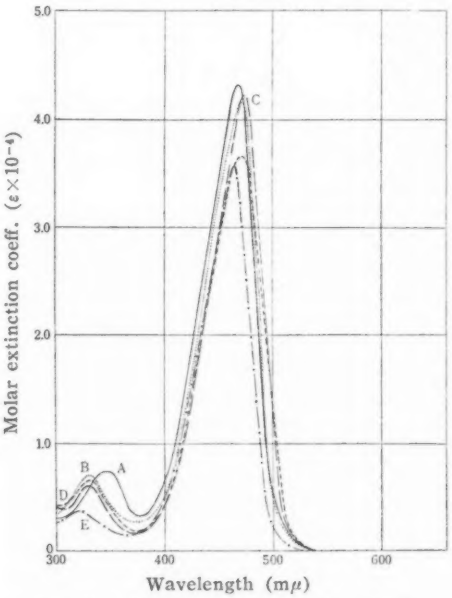


Fig. 1b. Absorption spectra of products in acidic media.

Curve A: Phenylfluorone ———
Curve B: 4'-Dimethylamino- 〃 ·····
Curve C: 3'-Nitro- 〃 — — —
Curve D: 4'-Nitro- 〃 ·····
Curve E: 2'-Sulfo- 〃 — · —

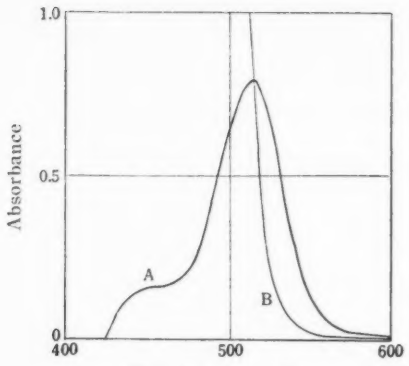


Fig. 2a.

Curve A. Germanium-4′-nitrophenylfluoronate
〃 B. Reagent only (1.0 N HCl solution)

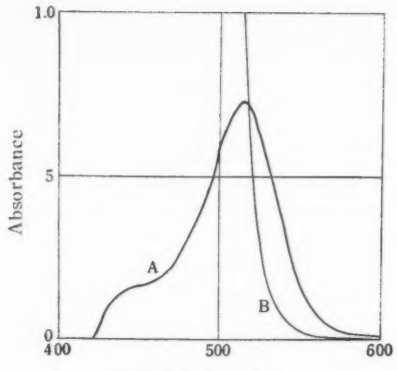


Fig. 2b.

Curve A. Germanium-3′-nitrophenylfluoronate
〃 B. Reagent only (1.0 N HCl solution)

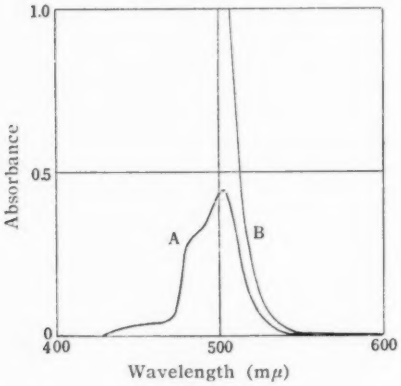


Fig. 2c.

Curve A. Germanium-4′-dimethylaminophenyl-fluoronate
〃 B. Reagent only (2.0 N HCl solution)

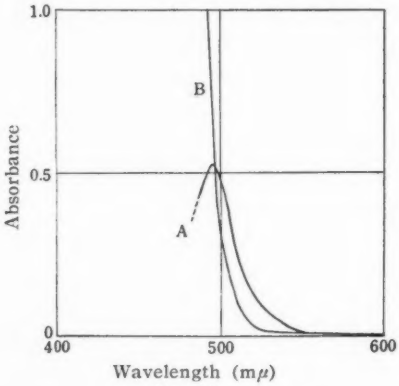


Fig. 2d.

Curve A. Germanium-2′-sulfophenylfluoronate
〃 B. Reagent only (0.1 N HCl solution)

Fig. 2a, b, c and d. Absorption spectra of germanium-fluoronates.

equipped with 1 cm. glass cells. All measurements were made with the blank solution as the reference.

**Reaction of the Derivatives with Metal Ions.**—*Reagents used.*—Germanium solution was prepared by dissolving water-soluble germanium dioxide (99.9% $GeO_2$) in hot water, and standardized gravimetrically. Zirconyl chloride solution and titanium chloride solution were prepared by dissolving zirconyl chloride octahydrate (containing 0.5% hafnium) and titanium tetrachloride in 1 N hydrochloric acid. Ethanolic solutions of phenylfluorone and its derivatives were prepared by dissolving 0.120 g. of the dyes* in 150 ml. of warm ethanol containing 1 ml. of 5.0 N hydrochloric acid, and diluting it to 200 ml. with ethanol. Gum arabic solution was prepared by dissolving 0.5 g. of gum arabic in 200 ml. of warm water. The solution was filtered when necessary. Analytical grade cyclohexanol was used without further purification.

*Procedure.*—Because the metal chelates of 3′- or 4′-nitro derivative are difficultly soluble in many solvents, all the absorbance measurements of the metal chelates were taken in the presence of a suitable stabilizer such as gum arabic or cyclohexanol. The light-scattering effect of the colloidal particle on the absorption spectra is negligible for several hours after the preparation of the solution. The effect of the stabilizer on the absorption maximum of the chelate was also negligibly small. Germanium (15.0 μg.), titanium (60.8 μg.), or zirconium (20.7 μg.) was taken in a 25 ml. volumetric flask. An

* Because the solubility of the sulfo derivative is less than 0.06%, the supersaturated solution of the dye was prepared by dissolving corresponding sodium salt of sulfo derivative similarly. The precipitation of sulfo derivative appeared about two weeks after the preparation.

appropriate volume of hydrochloric acid was added to adjust the acidity of the final solution to desirable strength. Five ml. of ethanol, and 2.5 ml. of gum arabic solution (for germanium) or cyclohexanol (for zirconium) was added. To the solution was added 5 ml. of the phenylfluorone or its derivatives and the final volume of the solution was adjusted to 25 ml. with distilled water. The blank solution was prepared in the same way as that for the sample solution.

*Reaction with germanium.*—The germanium complexes of 4'- and 3'-nitrophenylfluorone are

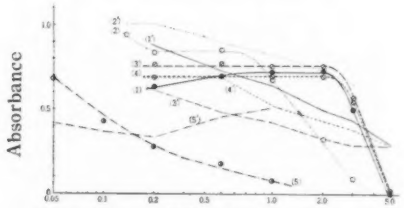


Normality of HCl solution (log. scale)

Fig. 3. Effect of acidity on germanium-fluoronates with germanium concentration fixed**.

Curve (1) Phenylfluorone (510 mμ)
〃 (2) 4'-Dimethylaminophenylfluorone (510 mμ)
〃 (3) 3'-Nitrophenylfluorone (520 mμ)
〃 (4) 4'-Nitrophenylfluorone (520 mμ)
〃 (5) 2'-Sulfophenylfluorone (500 mμ)
〃 (1'), (2'), (3'), (4') and (5') Blank solution, respectively.

almost insoluble in ethanolic solution, whereas that of 2'-sulfophenylfluorone is soluble to the same extent as the 4'- and 3'-nitrophenylfluorone. The last two are almost insoluble in ethanolic solution, whereas germanium complex of 2'-sulfophenylfluorone is soluble to the same extent as that of 4'-dimethylaminophenylfluorone. The absorption spectra of the germanium chelates are shown in Figs. 2a, b, c and d. The absorbance of the solutions of germanium chelates at various acidities is illustrated in Fig. 3, including that of the phenylfluorone and 4'-dimethylaminophenylfluorone, together with that of the blank solutions at the same wavelengths for comparison.

*Reaction with zirconium.*—The zirconium complexes of 4'- and 3'-nitrophenylfluorone are slightly soluble in cyclohexanol-ethanol solution. Figs. 4a and b show the absorption spectra of the zirconium chelates. The reactivities of the dyes with zirconium at various acidities are illustrated in Fig. 5, together with the absorbance of the blank solutions at the same wavelengths. The colored chelates of 2'-sulfo- and 4'-dimethylaminophenylfluorone are found only in a lower acidity region, so they are excluded from the comparison.

*Reaction with titanium.*—The titanium complexes of 4'- and 3'-nitrophenylfluorone are fairly

** The absorbances were measured thirty minutes after the preparation of the solution. They slightly increase with increasing digestion time.

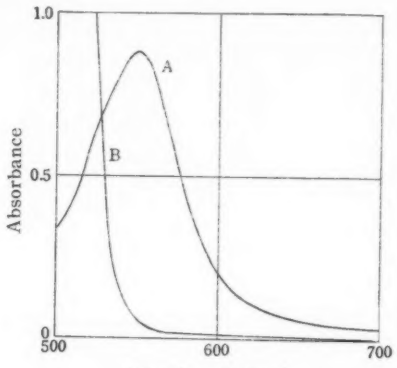


Wavelength (mμ)

Fig. 4a.

Curve A. Zirconium-3'-nitrophenylfluoronate
〃 B. Reagent only (0.15 N HCl solution)

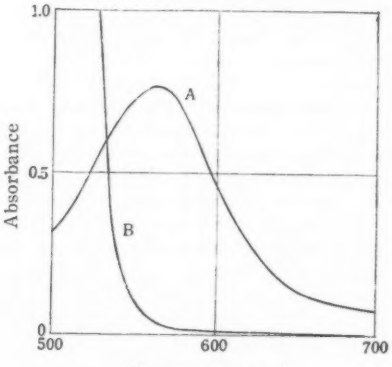


Wavelength (mμ)

Fig. 4b.

Curve A. Zirconium-4'-nitrophenylfluoronate
〃 B. Reagent only (0.15 N HCl solution)

Fig. 4a and b. Absorption spectra of zirconium-fluoronates.

soluble in cyclohexanol-ethanol. The absorption spectra of the titanium chelates are shown in Figs. 6a and b. The reactivities of the dyes with titanium at various acidities are illustrated in Fig. 7, together with the absorbance of the blank solutions at the same wavelength. The stability of titanium chelates is lower than that of zirconium chelates at the same acidity. Colored chelates of 2'-sulfo- or 4'-dimethylaminophenylfluorone is not formed in the acidity above 0.05 N hydrochloric acid concentration.

## Discussion

The process in the syntheses of 3'-nitro, 4'-nitro, and 2'-sulfo derivatives is performed without such a difficulty as was

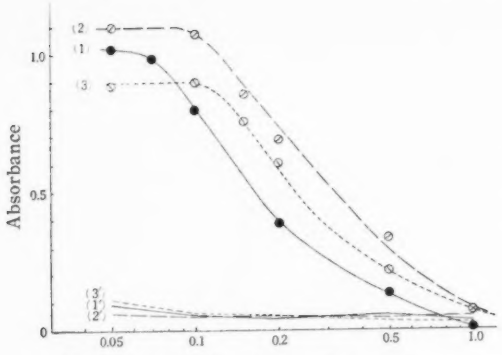


Normality of HCl solution (log. scale)

Fig. 5. Effect of acidity on zirconium-fluoronates with zirconium concentration fixed**.

Curve (1) Phenylfluorone (540 mμ)
〃 (2) 3'-Nitrophenylfluorone (550 mμ)
〃 (3) 4'-Nitrophenylfluorone (560 mμ)
〃 (1'), (2') and (3') Blank solution respectively.

experienced in the formation of oily polymeried products in the synthesis of phenylfluorone. The absorption spectra of the products resemble closely that of phenylfluorone and 4'-dimethlylaminophenylfluorone. The value of shifts of their absorption maxima with variation of the medium from acidic to alkaline agrees with one another and lies at the range from 90 to 95 mμ. In 3'-nitro and 4'-nitro derivative, the absorption maximum shifts toward a longer wavelength than that of phenylfluorone, as is expected because of the increasing electronegativity of the carbon atom at position 9 caused by the "inductive" or the "mesomeric" effect of the nitro group. On the other hand, the absorption maximum shifts toward the shorter side in 2'-sulfo derivative, suggesting that the effect of the phenyl group is reduced by the steric hindrance of the sulfo group at position 2'. These facts convince the author that the products correspond to the compounds named. The wavelength of absorption maximum in the metal chelate of phenylfluorone derivative can be estimated from the maximum wavelength of the phenylfluorone derivative anion and of the metal phenylfluoronate. As a first approximaton, the estimation was performed as follows:

$$\frac{hc}{\lambda_{max}} = \Delta E = \Delta E_0 + \Delta\varepsilon + \Delta'\varepsilon$$

** See the foot note in Fig. 3.

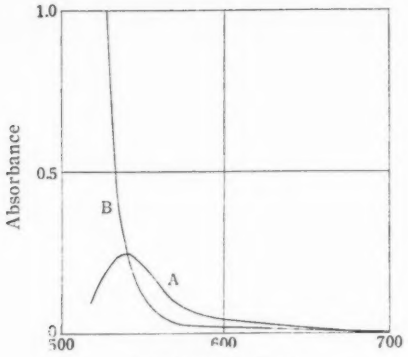


Wavelength (mμ)

Fig. 6a.

Curve A. Titanium-4'-nitrophenylfluoronate
〃 B. Reagent only (0.1 N HCl solution)

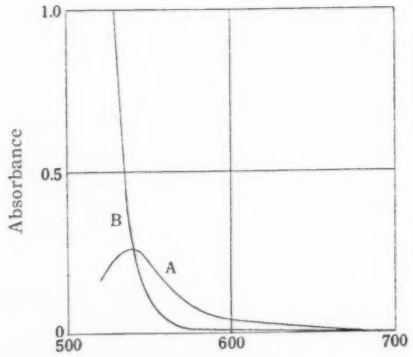


Wavelength (mμ)

Fig. 6b.

Curve A. Titanium-3'-nitrophenylfluoronate
〃 B. Reagent only (0.1 N HCl solution)

Fig. 6a and b. Absorption spectra of titanium-fluoronates.

where $\Delta E_0$ is, the energy difference between the highest ground state and the lowest excited state in phenylfluorone anion,* $\Delta\varepsilon$ the effect of perturbation caused by chelate formation and is calculated from the absorption maximum of the metal phenylfluoronate,* and $\Delta\varepsilon'$ the

* The value, $\Delta E_0$, $\Delta\varepsilon$, or $\Delta\varepsilon'$, is expressed as follows, respectively:
$\Delta E_0 = \boldsymbol{h}^2(N+1)/8\boldsymbol{m}\boldsymbol{c}L^2 = \boldsymbol{hc}/\lambda_{max.\ phenylfluorone\ anion}$,
$\Delta\varepsilon = (1-1/N)V_0 = \boldsymbol{hc}(1/\lambda_{max.\ metal\ phenylfluoronate} - 1/\lambda_{max.\ phenylfluorone\ anion})$,
$\Delta\varepsilon' = 4V_1\boldsymbol{a}/L = \boldsymbol{hc}(1/\lambda_{max.\ phenylfluorone\ anion} - 1/\lambda_{max.\ derivative\ anion})$.
For the information on the physical meaning of $V_0$, $V_1$ $a$, etc., see references; H. Kuhn, *J. Chem. Phys.*, **17**, 1198 (1949), *Helv. Chim. Acta*, **34**, 2371 (1951); H. Sano, This Bulletin, **30**, 790 (1957).

TABLE I

ABSORPTION MAXIMUM OF METAL CHELATES (Å)

| | | (H) | Ti | Ge | Zr | Dye anion |
|---|---|---|---|---|---|---|
| Phenylfluoronate | (obsd.) | 4680 | 5250 | 5080 | 5400 | 5600 |
| 3′-Nitro 〃 | (obsd.) | 4750 | 5390 | 5150 | 5500 | 5700 |
| | (calcd.) | 4750 | 5338 | 5162 | 5487 | — |
| 4′-Nitro 〃 | (obsd.) | 4720 | 5390 | 5150 | 5620 | 5620 |
| | (calcd.) | 4694 | 5268 | 5096 | 5419 | — |
| 2′-Sulfo 〃 | (obsd.) | 4660 | — | 4950 | — | 5570 |
| | (calcd.) | 4659 | — | 5056 | — | — |
| 4′-Dimethylamino 〃 | (obsd.) | 4720 | — | 5030 | 5200 | 5570 |
| | (calcd.) | 4659 | — | 5056 | 5372 | — |
| 4′-Hydroxy 〃 | (obsd.)* | 4590 | — | 5050 | — | — |

* This value was given by Dr. Takuji Kanno.

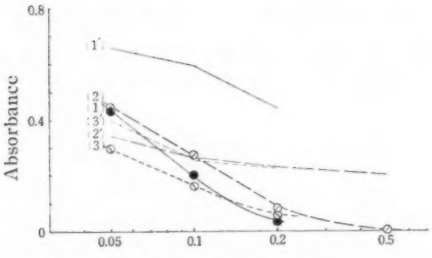


Fig. 7. Effect of acidity on titaniumfluoronates with titanium concentration fixed**.

Curve (1) Phenylfluorone (525 mμ)
〃 (2) 3′-Nitrophenylfluorone (540 mμ)
〃 (3) 4′-Nitrophenylfluorone (540 mμ)
〃 (1′), (2′) and (3′) Blank solution respectively.

effect of perturbation caused by the substituent introduced into the phenyl group and is calculated from the absorption maximum of derivative anion.* The wavelengths calculated and observed for the chelates are shown in Table I.

Only the 4′-nitro derivative shows a certain anomaly in the absorption maximum of the dye anion, which is expected to be a longer wavelength than the observed from its strong electron-attracting effect, and in the absorption maximum of the metal chelate, which lies at a longer side than that expected. The low value of molar extinction of 4′-nitro derivative and these anomalies may be due to the fact that a mesomeric group is substituted at the 4′-position, and that the interaction between $\Delta\varepsilon$ and $\Delta\varepsilon'$ was neglected in the calculation of the absorption maximum of the chelate.

From the reactivities of the derivatives with metal ions shown in Figs. 3, 5, and 7, it will be seen that the stability of the chelate increases with an increasing "inductive" or "mesomeric" effect of the substituent. The low stability of 2′-sulfophenylfluoronate may be due to the steric hindrance of the 2′-sulfo group. This shows that the stability of the chelate increases with the increasing ionizability of the donor oxygen atom of the dye. The absorbance of the 3′-nitrophenylfluoronate is higher than that of the others, except that of 4′-dimethylaminophenylfluoronate, whereas the absorbance of the blank solution is the lowest and the stability is greater than in the case of the others. This suggests the compound may be excellent as the colorimetric reagent for the determination of metal ions such as germanium or zirconium. It will be expected that the other derivatives, e. g., 3′-sulfo, 4′-sulfo, 3′, 4′-disulfo, 3′, 3″-dinitro, and 3′-amino derivative will be useful from the results above mentioned. They are under investigation.

## Summary

2, 3, 7-Trihydroxy-9-(3′-nitrophenyl) fluorone, 2, 3, 7-trihydroxy-9-(4′-nitrophenyl) fluorone, and 2, 3, 7-trihydroxy-(2′-sulfophenyl)fluorone were synthesized by a comparatively simple procedure, for the purpose of studying the reaction between the colorimetric reagent and metal ions and to search for a useful colorimetric reagent. The effects of the substituents introduced on the absorption maxima of the dyes and the metal chelates formed, and on the reactivities of the dyes with metal ions such as germanium(IV), zirconium(IV), and titanium(IV). 2′-Sulfophenylfluorone metal chelates are soluble in an ethanolic or cyclohexanol-ethanolic solution. 3′-Nitrophenylfluorone is most excellent as the colorimetric reagent for the determination of metal

** See the foot note in Fig. 3.

ions because of the high stability, high sensitivity and low absorbance of the blank solution.

The author is indebted to Mr. Shozo Masuda of this Department for elementary analyses of the products, and to Dr. Kenjiro Kimura, Professor Emeritus, and to Professor Nobufusa Saito, in this laboratory, for their encouragement in carrying out this study. Part of the cost of this study was defrayed from a Grant of the Ministry of Education.

*Department of Chemistry*
*Faculty of Science*
*The University of Tokyo*
*Hongo, Tokyo*

---

# *Optical Properties of Colored Colloidal Systems. I. Theoretical Studies on the Extinction of Light by the System of Small Spherical Particles*

By Masayuki NAKAGAKI

(Received May 19, 1958)

Recently the light scattering of colorless systems has been studied quite extensively by many investigators. However, the light scattering of the colloidal systems of colored particles has had little systematic study, although the papers by G. Mie[1] and R. Gans[2] concerned with the optical properties of metal colloids.

In the present paper, theoretical expressions for the extinction, scattering and absorption by a system of colored spherical particles are derived and the numerical values are calculated for systematically varied values of the particle size, refractive index and absorption coefficient of the dispersed phase.

## Theoretical Derivations

**Definitions.**—Consider a system of colored spherical particles dispersed in a colorless medium whose refractive index is $\mu_1$. The refractive index, $\mu_2$, of the colored particle is complex and may be written as follows:

$$\mu_2 = \mu_0(1 - ik) \tag{1}$$

Then, the relative refractive index, $m$, is

$$m = \mu_2/\mu_1 = m_0 - ik_0 \tag{2}$$

where

$$m_0 = \mu_0/\mu_1 \quad \text{and} \quad k_0 = m_0 k \tag{3}$$

Here the physical meaning of the quantities, $\mu_0$, $k$ and $k_0$ are as follows. If the homogeneous phase of the material which composes the colloidal particles is considered, the refractive index of the phase is $\mu_0$, and

$$-\ln(I'/I_0')/l' = 4\pi\mu_0 k/\lambda_0 = 4\pi k_0/\lambda \tag{4}$$

where $l'$ is the thickness of the phase, $I_0'$ and $I'$ are the intensity of the incident and transmitted light, respectively, and $\lambda$ and $\lambda_0$ are the wave lengths, in the medium and in vacuum, respectively. Therefore, $k$ and $k_0$ are both zero if the phase is colorless.

Now consider a colloidal system of thickness $l$, the unit volume of which contains $N$ particles of radius $a$. A parameter $\alpha$ defined by

$$\alpha = 2\pi a/\lambda \tag{5}$$

is used in the studies of light scattering. If the density of the particle is $\rho_2$, the concentration $c$ in g./cc. is

$$c = \alpha^3\lambda^3\rho_2 N/6\pi^2 \tag{6}$$

If the intensities of the incident and transmitted light are $I_0$ and $I$, respectively, the quantity $E$ defined by

$$E = -\ln(I/I_0)/l \tag{7}$$

will be called extinction. It is equal to the turbidity, $\tau$, if the particles are colorless, while it is equal to the product of the specific extinction coefficient, $\varepsilon$, and

1) G. Mie, *Ann. Phys.*, (4), **25**, 377 (1908).
2) R. Gans, *Ann. Phys.*, (4), **37**, 881 (1912); **62**, 331 (1920).

the concentration, $c$, if the particles are colored and the turbidity of the system is small and negligible. In general cases,

$$E/N = R + A \tag{8}$$

where $R$ and $A$ are the energy of light scattered and absorbed, respectively, by one particle par unit time.

**Scattering $R$.**—The total of the energy of light scattered in all directions by one particle par unit time, $R$, is

$$R = 2\pi \int_0^{\pi} J(\gamma) \sin\gamma \, d\gamma = (\lambda^2/2\pi)\Sigma \tag{9}$$

where $J(\gamma)$ is the intensity of light per unit solid angle[3] scattered in the direction designated by the scattering angle, $\gamma$, when the intensity of the incident light is unity, and $\Sigma$ is a dimensionless quantity defined by[4]

$$\Sigma = \sum_{n=1}^{\infty} (|A_n|^2 + |B_n|^2) n^2 (n+1)^2/(2n+1) \tag{10}$$

where $A_n$ and $B_n$ are complex functions expressed by combinations of Bessel's functions, as shown by the Mie theory[1]. If $\alpha$ is small compared to unity, $A_n$ and $B_n$ can be expanded as a power series in $\alpha$ and the results are[5]

$$\begin{aligned} A_1 &= \frac{m^2-1}{m^2+2}\alpha^3 + \frac{3}{5}\frac{(m^2-1)(m^2-2)}{(m^2+2)^2}\alpha^5 \\ &\quad - i\frac{2}{3}\left(\frac{m^2-1}{m^2+2}\right)^2\alpha^6 + \cdots \\ B_1 &= -\frac{1}{30}(m^2-1)\alpha^5 + \cdots \\ A_2 &= -\frac{1}{18}\frac{m^2-1}{2m^2+3}\alpha^5 \cdots \end{aligned} \tag{11}$$

Neglecting the term higher than the eighth power of $\alpha$,

$$\Sigma = \frac{4}{3}\left|\frac{m^2-1}{m^2+2}\right|^2 \alpha^6 \tag{12}$$

This is the well known equation by Rayleigh[6].

In the case of $k \ll 1$ (that is $k_0 \ll m_0$), $\Sigma$ can be expanded as a power series in $k_0$ as follows:

$$\Sigma = \frac{4}{3}\left(\frac{m_0^2-1}{m_0^2+2}\right)^2 \alpha^6 + 8\frac{(3m_0^4+m_0^2+2)}{(m_0^2+2)^4}\alpha^6 k_0^2 + \cdots \tag{13}$$

The quantity $R$ obtained from Eqs. 9 and 13 is the total scattering by one particle, and $RN$ is the scattering by the unit volume of the colloidal system. It is, however, not adequate to call $RN$ turbidity, because the turbidity is extinction in case of colorless systems. The extinction by a colored system should include the contribution of absorption as well as that of scattering. In order to take the absorption into account, it is not sufficient to use complex refractive index in the Rayleigh equation, because the term of $k_0^2$ in Eq. 13 is not the term of absorption but is the term which expresses the effect of absorption on the scattering.

Now $RN/c$ is set as $\kappa$. Then,

$$\kappa = RN/c = (3\pi/\lambda\rho_2)(\Sigma/\alpha^3) \tag{14}$$

In the case of a colorless system, $\kappa$ is the specific turbidity $(\tau/c)$, which can be determined experimentally by the measurement of transmittancy. In the case of a colored system, however, what is obtained by the measurement of transmittancy is not the turbidity but it containes the effect of absorption as well. Therefore, there exists no handy experimental method to determine the value of $\kappa$. It may, however, be worth-while to mention that there should exist, at least principally, an experimental method to determine the value of $\kappa$, although the method is very tedious and almost impossible to practice. It will be done by measuring the intensity of scattered light as a function of the angle of observation in all ranges and integrating the results in all possible directions.

According to Eq. 13, $R$ and $\Sigma$ are zero if $k_0$ is zero and $m_0$ is unity. That is, the scattering does not occur in a colorless system if the refractive index of particles and the medium are equal. In the case of a colored system, however, the scattering occurs even when $m_0$ is equal to unity. Generally, there exists no value of $m_0$ which makes $R$ equal to zero when $k_0$ is not equal to zero.

**Extinction $E$.** — The extinction by one particle, $E/N$, can be calculated theoretically by the equation

$$E/N = -(\lambda^2/\pi) I[j_{\perp}(180)] \tag{15}$$

where $I[j_{\perp}(180)]$ indicates the imaginary

3) In order to avoid the use of photometric distance, the intensity is defined here per unit solid angle, instead of per unit area in the usual definiton of the intensity.

4) See, e. g., W. J. Pangonis, W. Heller and A. Jacobson. "Tables of Light Scattering Functions for Spherical Particles", Wayne State Univ. Press, Detroit, U. S. A. (1957).

5) See, e. g., H. C. van de Hulst, "Optics of Spherical Particles", Chapter 4(a), Holland (1946). His notation is different from that used here. $A_n$ and $B_n$ are $(-1)^n i a_n (2n+1)/n(n+1)$ and $(-1)^{n+1} i b_n (2n+1)/n(n+1)$, respectively, in van de Hulst's notation.

6) Lord Rayleigh, *Phil. Mag.*, (5), **47**, 375 (1899).

part of $j_\perp(180)$, and the latter is the quantity which appeared in the expression[7]:

$$J_\perp(\gamma)=(\lambda^2/4\pi^2)|j_\perp(\gamma)|^2 \tag{16}$$

Therefore, $j_\perp(\gamma)$ is proportional to the amplitude of the light scattered at the direction $\gamma$ and vibrating perpendicularly to the observation plane, the proportionality constant being $(\lambda/2\pi)$. According to the Mie theory,

$$j_\perp(\gamma)=\sum_{n=1}^{\infty}[A_nP_n^1(\cos\gamma)/\sin\gamma + B_n\mathrm{d}P_n^1(\cos\gamma)/\mathrm{d}\gamma] \tag{17}$$

where $P_n^1(\cos\gamma)$ is Legendre's function of the first kind. In the forward direction, or in the case of $\gamma=180$,

$$j_\perp(180)=A_1-B_1-3A_2+\cdots = \frac{m^2-1}{m^2+2}\alpha^3+\left(\frac{m^2-1}{m^2+2}\right)^2\frac{(m^4+27m^2+38)}{15(2m^2+3)}\alpha^5 - i\frac{2}{3}\left(\frac{m^2-1}{m^2+2}\right)^2\alpha^6+\cdots \tag{18}$$

can be obtained using Eq. 11 if $\alpha \ll 1$.

In order to be analogous to the relation between $R$ and $\Sigma$ in Eq. 9, $\Sigma_f$ is introduced by

$$E/N=(\lambda^2/2\pi)\Sigma_f \tag{19}$$

Then,

$$\Sigma_f=-2I[j_\perp(180)] \tag{20}$$

Using Eq. 18 for $j_\perp(180)$ and expanding it as a power series in $k_0$,

$$\Sigma_f=\frac{4}{3}\left(\frac{m_0^2-1}{m_0^2+2}\right)^2\alpha^6+2\left(\frac{6m_0}{(m_0^2+2)^2}\alpha^3+F\alpha^5\right)k_0 + 8\frac{(3m_0^4-11m_0^2+2)}{(m_0^2+2)^4}\alpha^6k_0^2+\cdots \tag{21}$$

where,

$$F=\frac{2m_0}{15}\times\frac{(m_0^2-1)(2m_0^8+20m_0^6+349m_0^4+935m_0^2+674)}{(m_0^2+2)^3(2m_0^2+3)^2} \tag{22}$$

If the particles are colorless and $k_0$ equals to zero, $E/N$ is equal to $R$, and $E$ is equal to $\tau$, indicating that the attenuation of the light is due to the scattering only.

By analogy with the colored system of no scattering, the specific extinction coefficient in a wider sense, $\varepsilon$, is defined here by $E/c$ and it is to be understood that this quantity containes the contribution of both scattering and absorption. Then,

$$\varepsilon=E/c=(3\pi/\lambda\rho_2)(\Sigma_f/\alpha^3) \tag{23}$$

This is the quantity obtained by the measurement of the intensity of transmitted light.

**Absorption *A*.**—The absorption by the colored colloidal system can be obtained directly neither by theoretical calculation nor by experimental determination. It is, however, theoretically obvious that the absorption is the difference of extinction and scattering, as already shown by Eq. 8. Thus, the absorption per one particle, $A$, is given by

$$A=(\lambda^2/2\pi)(\Sigma_f-\Sigma) \tag{24}$$

Using Eqs. 13 and 21,

$$\Sigma_f-\Sigma=2\left[\frac{6m_0}{(m_0^2+2)^2}\alpha^3+F\alpha^5\right]k_0 - \frac{96m_0}{(m_0^2+2)^4}\alpha^6k_0^2 \tag{25}$$

Then, using the symbol $\varepsilon_a$ for the specific extinction coefficient due to the absorption,

$$\varepsilon_a=AN/c=(3\pi/\lambda\rho_2)(\Sigma_f-\Sigma)/\alpha^3 \tag{26}$$

or

$$\varepsilon_a=\varepsilon-\kappa \tag{27}$$

For the homogeneous phase of the material which composes the colloidal particles, the value of $\varepsilon$ and $\varepsilon_a$ obtained from Eq. 4 is

$$\varepsilon(\mathrm{bulk})=\varepsilon_a(\mathrm{bulk})=4\pi k_0/\lambda\rho_2 \tag{28}$$

since no scattering occurs and the concentration in g./cc. is equal to the density, $\rho_2$, for the bulk phase.

## Numerical Computations

The numerical values of $\varepsilon$, $\kappa$ and $\varepsilon_a$ could be calculated if the values of density, $\rho_2$, and the wave length of light to be used, $\lambda$, are assigned. In order to make, however, the results of the computation applicable more widely, the quantities $x$, $y$ and $z$ are defined by

$$x=(\lambda\rho_2/3\pi)\varepsilon=\Sigma_f/\alpha^3 \tag{29}$$

$$y=(\lambda\rho_2/3\pi)\kappa=\Sigma/\alpha^3 \tag{30}$$

and

$$z=(\lambda\rho_2/3\pi)\varepsilon_a=x-y \tag{31}$$

The values of $x$, $y$ and $z$ for systematically varied values of $\alpha$, $m_0$ and $k_0$ are calculated by using these equations together with Eqs. 13 and 21. For the bulk phase,

7) The derivation of Eq. 15 was shown, e. g., by H. C. van de Hulst (loc. cit.) although his notation is different from that used here. In the case of colorless particles, B. H. Zimm and W. B. Dandliker (*J. Phys. Chem.*, **58**, 644 (1954) have also shown the derivation of a similar equation in which the turbidity was used instead of the extinction $E$. However, the negative sign was dropped in their equation by a typographical mistake.

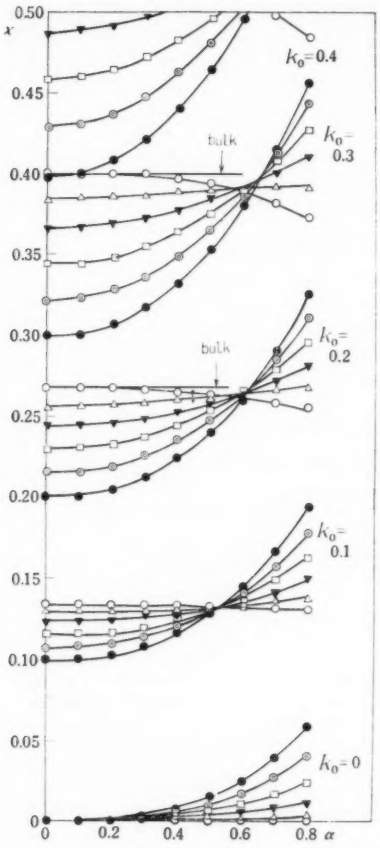


Fig. 1. $x-\alpha$ Relation for $m_0$=1.0 (○); 1.1 (△); 1.2 (▼); 1.3 (□); 1.4 (◎); 1.5 (●).

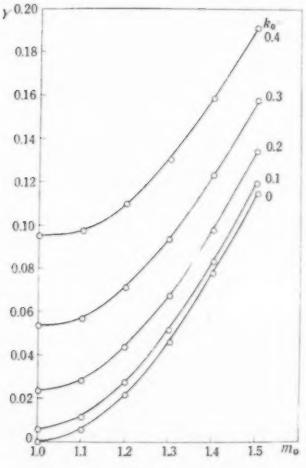


Fig. 2. $Y-m_0$ Relation.

$$\left.\begin{aligned} x(\text{bulk}) &= z(\text{bulk}) = (4/3)k_0 \\ y(\text{bulk}) &= 0 \end{aligned}\right\} \qquad (32)$$

The value of $x$ thus computed as a function of $\alpha$ is shown in Fig. 1, the complex relative refractive index $(m_0-ik_0)$ being the parameter. The rather complicated nature of the curves will be explained as the sum of $y$ and $z$ in the succeeding figures.

As readily understood from Eqs. 30 and 13, the quantity $y$, a quantity proportional to the specific turbidity in the case of colorless particles, is proportional to $\alpha^3$. As the consequence, the value of $y$ increases with $\alpha$ so rapidly that it is not convenient to show it in a figure. Therefore, the proportionality constant, $Y$, in

$$y = Y\alpha^3 \qquad (33)$$

is shown in Fig. 2. The figure shows that

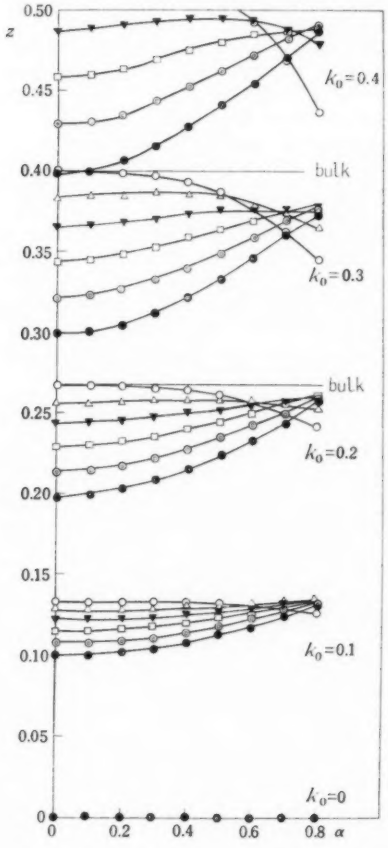


Fig. 3. $z-\alpha$ Relation for $m_0$=1.0 (○); 1.1 (△); 1.2 (▼); 1.3 (□); 1.4 (◎); 1.5 (●).

the value of $Y$ increases with $k_0$ as well as with $m_0$. The value of $Y$ is not equal to zero even when $m_0$ is equal to 1, if the value of $k_0$ is not zero. This means that the scattering occurs not only by the difference of refractive index, but also by the absorption.

The value of absorption, $z$, against $\alpha$ is shown in Fig. 3. The values corresponding to the bulk phase are shown by horizontal lines. It may be worth-while to mention that the value of $z$ is equal to the value of the bulk phase only when $m_0$ is equal to unity and the particles are very small. If the relative refractive index is not equal to unity, the value of the absorption is, even for very small particles, not equal to the value of the bulk phase but is smaller than the latter. The absorption by colloidal particles is the smaller, the larger the value of $m_0$. With the increase of the particle size, $\alpha$, the value of $z$ at first increases and then decreases after passing a maximum. The value of $\alpha$ corresponding to the maximum is zero for $m_0$ is equals 1 and increases with the value of $m_0$.

Considering again the value of $x$, its $\alpha$-dependence can be understood on the basis of the $\alpha$-dependence of $y$ and $z$ since $x$ is the sum of them. The value of $x$ decreases with the increase of $\alpha$ if $m_0$ is small, because the absorption decreases while the scattering is not significant. On the other hand, the value of $x$ increases rapidly if $m_0$ is large, because both the scattering and the absorption increase.

## Check of the Results of Computation

The scattering coefficient of colored particles is considered here. Both the extinction per one particle, $(E/N)$, and the total scattering, $R$, have the dimension of the area. Therefore, the quantity $R$ is called the scattering cross section, and its ratio to the geometrical cross section is called the scattering coefficient, $K$. The extinction and the scattering are the same for colorless particles, but they are different for colored particles. The quantity usually measured is the extinction. Therefore, using the word "scattering coefficient" in its wider sense, $K$ may be defined by[8]

$$K = (E/N)/\pi a^2 = 2\sum_f/\alpha^2 \qquad (34)$$

8) National Bureau of Standards (U. S. A.), "Tables of Scattering Functions for Spherical Particles", Washington, U. S. A. (1948).

for colored particles.

Now, the people in the National Bureau of Standards of the U. S. A.[8] expanded $K$ as a power series in $k_0$,

$$K = C_0 + C_1 k_0 + C_2 k_0^2 + \cdots \qquad (35)$$

and calculated the values of the coefficients, $C_0$, $C_1$ and $C_2$ on the basis of the Mie theory for the $m_0$-values between 1.44

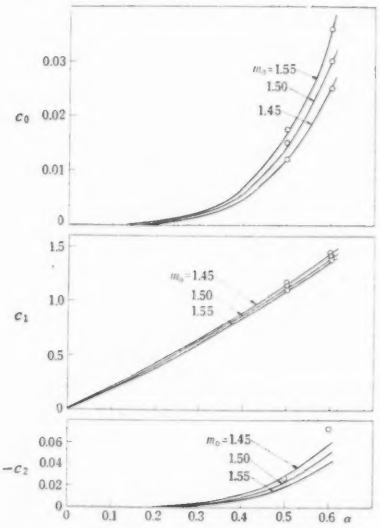


Fig. 4. Comparison with Mie theory.

and 1.55 and for the $\alpha$-values of 0.5, 0.6, 1.0 and so forth. The values of $C_0$, $C_1$ and $-C_2$ by the Mie theory are plotted in Fig. 4 with open circles, while the results by the approximate equations derived in the present paper are shown with solid lines for $m_0$=1.45, 1.50 and 1.55. The agreements are excellent for $C_0$ and $C_1$ in the range of $\alpha$ up to 0.6. As for $-C_2$, the computation by the National Bureau of Standards neglected its dependence on $m_0$, so that the accuracy of their computation is probably rather poor. Taking this into consideration, the agreement between their values and the values by the present paper is sufficient.

## Summary

The extinction, scattering and absorption of light by the colored colloidal systems of small spherical particles have been discussed. Approximate equations for these quantities have been derived for a case where the size of particles and the absorption coefficient of the dispersed

phase are relatively small. Using these equations, the numerical values of the quantities have been computed for the systematically varied values of the relative refractive index, $(m_0-ik_0)$, and of $\alpha$.

It is shown by the results of the computation that the values of the extinction and the absorption by the colloidal systems of small colored spheres (whose $\alpha$-value is smaller than about 0.5) are the smaller, the greater the value of $m_0$. On the other hand, the scattering increases with $m_0$, $k_0$ and $\alpha$.

The values of the scattering coefficient calculated by the approximate equations showed sufficient agreement with the values by the Mie theory as far as $\alpha$ is smaller than 0.6.

*Faculty of the Science of Living*
*Osaka City University*
*Nishi-ku, Osaka*

# *Über die Addition des Bromwasserstoffs auf die Phenylpropiolsäure*[1]. *Eine Betrachtung der Reaktion mit Rücksicht auf den Einfluss des in Lösungsmitteln hinzugefügten Brenzkatechins*

von Hazime KASIWAGI

(Eingegangen am 23. Mai, 1958)

Im Vergleich mit den Untersuchungen über die anomale Additionsreaktion, die bei der Anlagerung von Bromwasserstoff an die Äthylenverbindungen auftritt, sind dieselben über die Reaktion bezüglich der ungesättigten Verbindungen mit einer Dreifachbindung nicht so viel angekündigt worden. Die vorliegende Abhandlung bezieht sich auf die Addition des Bromwasserstoffs auf einen Acetylenanalog der Zimtsäure, die Phenylpropiolsäure, worüber einige Untersuchungen früher von Michael und seinem Mitarbeiter und anderen Forschern berichterstattet worden sind[2]. Angenommen, dass die Anlagerung von Bromwasserstoff an die Phenylpropiolsäure vor sich der elektrophilen Reaktion gemäss gehen sollte, so entstände die $\beta$-Bromderivate als Reaktionsprodukte wie bei der Zimtsäure[3]. So aber gibt sie bei der in den für nicht polaren angesehenen Lösungsmitteln ausgeführten Reaktion das $\alpha$-Bromderivat, zwar die *trans*-Verbindung, die $\alpha$-Bromzimtsäure vornehmlich. Als Lösungsmittel werden die folgenden, die den *trans*-Isomer zu geben als festgestellt betrachtet worden sind, aufgezählt: Benzol, Toluol, Brombenzol, Chloroform, Schwefelkohlenstoff, einschliesslich Tetrachlorkohlenstoffs, der von dem Verfasser neu geprüft worden ist.

Die Bildung der $\alpha$-Bromzimtsäure in den genannten Lösungsmitteln wird vermutet als erklärt durch den Mechanismus von der durch Wirken des Sauerstoffeffekts hervorgebrachten Radikalkettenreaktion. Ausserdem kann man diejenige Säure aus der *cis*-Verbindung durch ihre Stereomerisierung erhalten[4], und zwar ist diese Isomerisierung als veranlassen durch den Sauerstoffeffekt anerkannt worden[5]. Deshalb, wenn die Anlagerung von der elektrophilen Addition liefe, so mag sich ausschliesslich die $\alpha$-Brom*allo*zimtsäure unter den Bedingungen bilden, die das Auftreten von Sauerstoffeffekt streng zurückhalten. Hierauf leitet man den getrockneten Bromwasserstoffstrom in die Benzollösung der Phenylpropiolsäure bei Gegenwart des Brenzkatechins von der nicht mehr als 0.02 Mol. Konzentration

1) Eingebracht in der fünften Jahresversammlung der Japanischen Chemischen Gesellschaft, Tokyo, 1952.

2) A. Michael und G. H. Shadinger, *J. Org. Chem.*, **4**, 128 (1939); M. Sudborough und H. Thompson, *J. Chem. Soc.*, **83**, 1152 (1903).

3) Bei der Reaktion jedoch, in deren Lösung eine beträchtliche Menge von Sauerstoff vorhanden ist, sind einige anomale Reaktionsprodukte isoliert worden. O. Simamura und M. Takahashi, Dieses Bulletin, **22**, 60 (1948). Bezüglich der Reaktion bei der Krotonsäure, siehe O. Simamura, ebenda, **17**, 327 (1942).

4) A. Michael und G. H. Shadinger, loc. cit.; R. Stoermer und P. Heymann, *Ber.*, **46**, 1258 (1913).

5) H. Kasiwagi, Dieses Bulletin, **25**, 81 (1952).

ein, so erhält man nur die β-Bromverbindungen. Unter Niederdrücken desselben Effekts also entsteht keine Verbindung von α-Bromreihe, d.h. weder *trans*-Säure noch *cis*-Säure. Daraus kann man annehmen, dass auch die *cis*-Verbindung der α-Bromsäure das aus der Phenylpropiolsäure durch elektrophile Reaktion entstandene Produkt nicht wäre.

Ferner, wenn man den Bromwasserstoff auf die Phenylpropiolsäure unter jeder Anwendung einer Anzahl Lösungsmittel, wie Acetons, Äthers, Nitromethans, Nitrobenzols usw. addieren lässt, so entstehen die Säuren von α-Bromreihe niemals, sondern nur die β-Bromsäuren. Unter den Lösungsmitteln von gleichem Wirken sind weiter noch das Anisol und das als „Antioxidant" das Brenzkatechin enthaltende Benzol aufgezählt zu werden. Das Nitrobenzol gibt immer nur die β-Bromverbindungen ohne Rücksicht auf das Vorhandensein des „Antioxidants". Genauere Beobachtung der Reaktion aber zeigt den feineren Unterschied bei Gegenwart desselben; jedoch wird näheres darüber noch in anderem Zusammenhang erörtert.

Das durch Addition des Bromwasserstoffs erhaltene Produkt ist ein Gemisch von der *cis*- und *trans*-Säure, und hebt gegen die durch das gleiche Verfahren in der Benzollösung gebildete α-Bromsäure, die ausschliesslich von der *trans*-Säure besteht, scharf ab. Dies weicht auch von dem Ergebnisse Michaels usw. ab, wonach nur die β-Bromzimtsäure(*trans*) bei den in oben genannten Lösungsmitteln ausgeführten Reaktionen erhalten worden sei. Ferner sahen diejenige Ankündiger an, dass die aus den Reaktionsprodukten isolierte β-Bromzimtsäure das sekundär von der *cis*-Säure umlagerte Produkt sein mag, da die letztere durch Einwirkung der Mineralsäure in die *trans*-Säure isomerisieren könnte.

Hierauf hat der Verfasser die Meinung Michaels usw. über die durch Bromwasserstoff hervorzubringende Stereomerisierung der β-Brom*allo*zimtsäure geprüft. Als Lösungsmittel wählte man das Benzol und das Nitrobenzol bei An- und Abwesenheit des Brenzkatechins aus und liess den Bromwasserstoff darauf für zwei Tage reagieren. Die Versuche ergaben, dass die Stereomerisierung in Benzol oberhalb 90 Prozent und in Nitrobenzol ungefähr um die Hälfte verlief, während bei Anwesenheit des Brenzkatechins aber die umlagerte Menge sich auf nur eine Spur beschränkte (Tabelle I). Gerade in Bezug auf die *cis-trans*-Isomerisierung der β-Brom*allo*zimtsäure, wobei mehr als um die Hälfte davon auch in Nitrobenzol sich in die *trans*-Form verändert, muss eine Radikalreaktion in demselben Lösungsmittel stattfinden, weil die Reaktion durch die Wirkung des Brenzkatechins stark verhindert wird. D.h. bezüglich der Additionsreaktion tritt die Ionenreaktion sowohl in Nitrobenzol als auch in Brenzkatechin lösendem Benzol auf, und die damit konkurrierende Radikalreaktion wird verzögert. Im Gegensatz dazu, läuft die Isomerisierung durch Wasserstoffion nicht schnell genug, um die durch Bromatom erregte Reaktion[6] auszugleichen, wobei der Effekt des Bromatoms durch Anwendung Nitrobenzols als Lösungsmittel allein nicht, aber erst bei Anwesenheit „Antioxidants" erfolglos werden kann. Sogar da R. Stoermer und P. Heymann die β-Brom*allo*zimtsäure, die Wirkung des in Chloroform gelösten Broms unter Sonnenlicht erleidend, sich isomerisieren bemerkt haben[4], mag ein durch Bromatom hervorgerufenen Radikalkettenmechanismus auch der in Nitrobenzol verlaufenden Stereomerisierung verliehen werden.

TABELLE I

MENGENVERHÄLTNISSE DER DURCH ADDITION DES BROMWASSERSTOFFS AUF DIE PHENYLPROPIOLSÄURE GEBILDETEN ISOMERE VON β-BROMSÄUREN*

| Lösungsmittel | Brenzkatechin | Verhältnis (*trans*/*cis*) |
|---|---|---|
| Nitrobenzol | − | 2.2 |
| Nitrobenzol | − | 2.3 |
| Anisol | − | 1.4 |
| Nitromethan | − | 2.4 |
| Benzol | + | 1.2 |
| Benzol | + | 1.0 |
| Nitrobenzol | + | 1.0 |

Genau beobachtet, wie später in der Beschreibung der Versuche erörtert, scheint die Menge der isolierten *cis*-Säure gegenüber derselben von der *trans*-Säure, beim Falle von Bildung der β-Bromsäuren durch Addition, einiges Abwechseln dadurch zu erfahren, dass das Brenzkatechin anwesend ist order nicht. Bei Gegenwart desselben bilden sich die beiden Säuren ungefähr um die gleiche Menge ohne Rücksicht auf die Verschiedenheit des

6) Y. Urushibara und O. Simamura, ebenda, **13**, 566 (1938); Y. Urushibara, *J. Chem. Soc. Japan, (Nippon Kwagaku Kwaisi)*, **60**, 717 (1938).

benutzten Lösungsmittels, aber beträgt die Menge des *trans*-Isomers bei Abwesenheit Brenzkatechins über doppelt so viel als dieselbe des *cis*-Isomers (Tabelle II).

TABELLE II

STEREOMERISIERUNG DER β-BROM*ALLO*ZIMTSÄURE DURCH EINWIRKUNG DES BROMWASSERSTOFFS*.

| Lösungsmittel | Brenzkatechin | Isomerisierter Teil der *cis*-Säure % |
|---|---|---|
| Benzol | – | 92 |
| Nitrobenzol | – | 47 |
| Benzol | + | 0 |
| Nitrobenzol | + | 0 |

* Umrechnet aus den Tabellen IV und V. Jeder Zahlenwert wird entsprechend der Reihenfolge in jenen Tabellen angeordnet.

Aus dieser Tatsache kann man ersehen, dass es in den Additionsprodukten der Phenylpropiolsäure selbst die beiden Formen der Isomere gäbe, die sich bei der Reaktion ungefähr um die gleiche Menge nebeneinander bilden, und ein Teil des *cis*-Isomers, das Wirken des Bromatoms erleidet, sich in den *trans*-Isomer isomerisieren könnte. Weil das Bromatom, der Radikalkettenträger, solange durch das „Antioxidant" nicht wirklos gemacht würde, sekundär eine partielle Isomerisierung verliefe, mag die erhaltene *trans*-Säure wahrscheinlich aus dem durch Addition unmittelbar gebildeten Teil und dem aus der *cis*-Säure durch ihre Isomerisierung nachher geformten Teil bestehen. Solange es sich um den reinen Ionenmechanismus handelt, fänden die beiden, *cis*- und *trans*-Addition ungefähr um den gleichen Grad statt[7].

Unter den aromatischen Flüssigkeiten, die man für Reaktionen als Lösungsmittel benutzt hat, um ihren Einfluss auf die Reaktion zu prüfen, kann man Benzol, Toluol, Brombenzol, Anisol und Nitrobenzol nennen. Die vorderen drei sind die α-Bromderivate gebenden, dagegen sind die letzteren zwei die β-Bromderivate gebenden Lösungsmittel. Deshalb gäbe es keinen Parallelismus zwischen den Einfluss des Substituenten aromatischer Verbindungen auf die Kernsubstitutionsreaktion und jener Wirkung dieser Verbindungen als Lösungsmittel bei der Addition von Bromwasserstoff. Selbst hat Michael, der sogenannten Lösungsmitteleffekt bei der Additionsreaktion annahm, geschlossen, dass derselbe Effekt mit den physikalischen Grössen, wie den Dissoziations- und Assoziationskonstanten der isomeren Säuren mit Rücksicht auf die Verschiedenheit der Lösungsmittel und den dielektrischen Konstanten von den letztgenannten usw. nicht in unmittelbaren Zusammenhang stände.

Wenn die Molekel des Lösungsmittels das Sauerstoffatom oder dergleichen enthält, durch dessen besondere Solvatationswirkung das Wasserstoffatom des Reagens sich in das Proton verwandelt und zur Molekel des ersteren herangezogen wird, so mag die normale Addition, die als Ionenreaktion anzusehen ist, durch diese Solvatation des Wasserstoffatoms vor sich gehen. Als Beispiele dieser Art vom Lösungsmittel mögen das Nitrobenzol und Anisol genannt werden.

In Lösungsmitteln, wie dem Benzol, den es an derartiger Solvatationswirkung fehlt, mag jetzt die Rolle, die Ionisierung des Reagens auszuführen, ausschliesslich von der eigentlichen ungesättigten Verbindung mit einem Carbonyle oder Carboxyle gespielt werden und die über diese Oxoniumbildung hinaus verlaufende Ionenreaktion mit der anomalen Addition gegenüberstellen lassen. Bei der Reaktion der Zimtsäure, würde Tendenz des Carbonylsauerstoffs, das Proton zu sich heranzuziehen, immer grösser, als die Folge der Verstärkung der Konjugierung der Kohlenstoffdoppelbindung mit dem Carboxyle durch Gegenwart von Benzolkern, und so würde die anomale Addition ganz und gar verzögert ohne Rücksicht auf die Verschiedenheit des Lösungsmittels. In den Fällen von α,β-ungesättigten Ketonen, wie dem Chalkon, verliefe die auf oben geschilderten Umstand zurückzuführende, normale Additionsreaktion allzu geschwind, als dass die anomale Addition damit konkurrieren könnte[8]. Im Gegensatz dazu, sei die Konjugierung der Dreifachbindung mit dem Carboxyle bei der Phenylpropiolsäure nicht so gross, deshalb bei der Reaktion, die in den an der Solvatationswirkung ärmeren oder fehlenden Lösungsmitteln ausgeführt wird, mag der Mechanismus von der anomalen Additionsreaktion, der die Vermöge des

7) Die Anlagerung des Chlorwasserstoffs an die Phenylpropiolsäure, in Eisessig vollgezogen, gibt hauptsächlich die *trans*-β-Chlorzimtsäure nebendem eine kleine Menge des *cis*-Isomers. R Stoermer und P. Heymann, loc. cit. Bezüglich der gleichen Reaktion der Tetrolsäure mit dem Bromwasserstoff, siehe A. Michael und G. H. Shadinger, loc. cit.; R. Mayo und C. Walling, *Chem. Revs.*, **27**, 351 (1940), S. 361, Anm. betreffs Untersuchung Grigorieffs.

8) H. Kasiwagi, Dieses Bulletin, **26**, 355 (1953).

TABELLE III

| Phenylpropiolsäure g | Lösungsmittel cc | Temp. °C | Reaktionsdauer Std | Produkt g: Rohes | Getrennter Isomer: α-Bromzimtsäure | Getrennter Isomer: α-Bromallozimtsäure | Unlösliches**** |
|---|---|---|---|---|---|---|---|
| 1.0 | Benzol 15 | 15 | 1, 24** | 1.35 | 1.22 | Spur | 0.02 |
| 7.0 | Benzol 200 | 10 | 1.5, 48 | 10.74 | 10.22 | Spur | 0.02 |
| 3.0 | Toluol* 80 | 8 | 3, 24 | 3.93 128～135*** | 3.85 | 0.00 | — |
| 4.0 | $CCl_4$ 80 | 8 | 1.5, 24 | 5.86 128.5～130*** | 5.01 | 0.00 | — |

* Toluol wurde unter vermindertem Druck abdestilliert.

** Die Lösung wird für durch die vordere Ziffer gezeigten Zeitverlauf von Bromwasserstoff durchströmt und lässt auf durch die letztere Ziffer gezeigte Dauer, mit Bromwasserstoff berührend, stehen.

*** Schmelzpunkt des aus Benzol-Ligroin oder Chloroform-Tetrachlorkohlenstoff umkristallisierten Exemplars. Die über das Bariumsalz getrennte α-Bromzimtsäure, mit demselben Lösungsmittel umkristallisiert, schmilzt bei 129～130°C.

**** Dieser Teil ist im Ammoniakwasser nicht gelöst worden.

TABELLE IV

| Phenylpropiolsäure g | Lösungsmittel cc | Brenzkatechin g | Temp. °C | Reaktionsdauer Std | Produkt g: Rohes | Getrennter Isomer: β-Bromzimtsäure | Getrennter Isomer: β-Bromallozimtsäure |
|---|---|---|---|---|---|---|---|
| 4.5 | Nitrobenzol* 140 | Unbenutzt | 8 | 3, 24 | 5.02 113～122*** | 3.33 | 1.54 |
| 5.5 | Nitrobenzol* 80 | Unbenutzt | 8 | 3, 24 | 6.46** 94～101*** | 3.55 | 1.85 |
| | | | | | 2.03** 124～129*** | 1.33 | 0.30 |
| | | | | sämtlich; | 8.49 | 4.88 | 2.15 |
| 3.5 | Anisol* 100 | Unbenutzt | 8 | 3, 24 | 3.57 110*** | 1.97 | 1.41 |
| 2.8 | Nitromethan 40 | Unbenutzt | 8 | 2, 24 | 3.35 | 2.19 | 0.91 |
| 7.0 | Benzol 200 | 0.18 | 8 | 1.5, 18 | 9.10 | 4.69 | 4.03 |
| 2.0 | Benzol 30 | 0.083 | 8 | 1.5, 18 | — | 1.25 | 1.22 |
| 5.0 | Nitrobenzol* 150 | 0.13 | 8 | 3, 24 | 4.85 113～128*** | 2.37 | 2.33 |

* Das Lösungsmittel wird mit Wasserdampf abdestilliert. Die Produkte, die sich von der zurückgebliebenen Wasserlösung beim Erkalten ausgeschieden sind, mit Äther aufgenommen, getrocknet, dann den Äther wegdampfen lassen.

** Der Niederschlag (6.46 g) wird gesondert von dem in Nitrobenzol aufgelösten Teil (2.03 g) behandelt. Man lässt den ersteren nach Durchschütteln mit Wasser sich sofort sein K-Salz bilden, während man zur Nitrobenzollösung eine grössere Menge von Äther hinzufügt und vereinigte Lösung, nach Waschen mit Wasser und Trocknen, zuerst den Äther, dann das Nitrobenzol unter vermindertem Druck abdestillieren lässt.

*** Schmelzpunkt.

TABELLE V

| β-Bromallozimtsäure g | Lösungsmittel cc | Brenzkatechin g | Produkt g: Rohes | β-Bromzimtsäure | Unveränderte β-Bromallozimtsäure |
|---|---|---|---|---|---|
| 0.20 | Benzol 10 | Unbenutzt | 0.19 | 0.16 | 0.015 |
| 0.20 | Nitrobenzol 7 | Unbenutzt | 0.16 | 0.07 | 0.08 |
| 0.30 | Benzol 15 | 0.047 | 0.27 | Spur | 0.25 |
| 0.30 | Nitrobenzol 10 | 0.049 | 0.25 | Spur | 0.23 |

minderen Grads der Konjugierung verlangsamte Protonbildung des Carbonyls übertrifft, die Hauptrolle spielen. Daraus folgt es, dass das Differenzieren des Reaktionsmechanismus durch die Verschidenheit des Lösungsmittels bei der Reaktion der Phenylpropiolsäure der ärmeren Fähigkeit ihrer Dreifachbindung, mit dem Carboxyle zu konjugieren, zuschreiben könnte. Dieser Umstand besteht auch zwischen der Krotonsäure und der Tetrolsäure und bei der letzteren wird das Differenzieren der Additionsprodukte durch die Art des Lösungsmittels beobachtet[7].

## Beschreibung der Versuche

**Bildung der α-Bromsäure.**—Man lässt die Phenylpropiolsäure (dargestellt und gereinigt, Schmelzpunkt: 136~137°C) in Lösungsmittel suspendieren, und den von Brom befreiten, getrockneten Bromwasserstoff darin einleiten. Während der Reaktion löst sich die Suspension einmal auf, aber bald danach scheidet der Niederschlag von Addukten ab. Nach Beendigung der Durchströmung lässt man die Reaktionsflüssigkeit auf erforderliche Zeit stehen, dann wäscht man dieselbe mit Wasser ab und filtriert den Niederschlag. Der Kristall des Addukten und das Waschwasser werden zusammen mit Äther aufgenommen. Die eigentliche Lösung, mit der Ätherlösung vereinigt, wird mit wasserfreiem Calciumchlorid getrocknet und lässt dann das Lösungsmittel abdestillieren. Zur Trennung beider Isomere, die sich im nachgebliebenen, gelblichen Rückstand vermengt befinden sollen, wird der letztgenannte nach der Methode von Sudborough und Thompson behandelt[9]. Neben dem wesentlichen Teil davon ist das zur Identifizierung beider Isomere angewandte Verfahren auf einer anderen Mitteilung schon erörtert worden[5]. Auf Tabelle III werden die Versuchsbedingungen und das Resultat angegeben.

**Bildung der β-Bromsäuren.**—Die Additionsreaktion von Bromwasserstoff an die Phenylpropiolsäure wird durch das im wesentlichen gleiche Verfahren mit Ausnahme von der Anwendung entweder des Brenzkatechins oder der alternierenden Lösungsmittel ausgeführt. Wenn man als Lösungsmittel das Benzol oder das Nitromethan benutzt, so werden die Reaktionsflüssigkeiten, getrocknet, auf Wasserbad abdestilliert. Zur Trennung der isomeren β-Bromsäuren hat man den Unterschied ihrer Löslichkeit in der konzentrierten Kaliumacetatlösung[10] ausgenutzt. Zur Identifizierung beider isomeren β-Bromsäuren hat man ihre Exemplar dargestellt, indem man die Phenylpropiolsäure in Wasser suspendieren und den Bromwasserstoff darin unter Erkaltung mit Eiswasser durchströmen liess und dann das erhaltene Säuregemisch durch das oben erwähnte Verfahren getrennt hat. Das mit Benzol oder Benzol-Ligroin umkristallisierte Exemplar der β-Bromzimtsäure schmilzt bei 134~135°C (Br: Beob. 34.9%. Ber. für $C_9H_7O_2Br$ 35.2%) und dasselbe der β-Brom*allo*zimtsäure bei 159~160°C (Br: Beob. 34.8%). Auf Tabelle IV werden die Versuchsbedingungen und die Zusammensetzung der Produkte angegeben.

***Cis-trans*-Isomerisierung der β-Brom*allo*zimtsäure.**—Die Reaktionen werden in Benzol und Nitrobenzol, worin man vorläufig den Bromwasserstoff eingeleitet hat, unter An- und Abwesenheit Brenzkatechins ausgeführt. Nach zweitägigem Stehen wäscht man die Reaktionsflüssigkeit mit Wasser und trocknet. Wenn man als Lösungsmittel das Nitrobenzol anwendet, fügt man das Wasser zum Waschen der Lösung hinzu und nimmt die ganze Flüssigkeit mit Äther auf. Man destilliert das Benzol auf Wasserbad, das Nitrobenzol unter 4 mmHg Druck ab. Der nachgebliebene Rückstand wird mit bezüglich der Additionsreaktionen schon erwähnten Verfahren in beiden Isomere getrennt. Tabelle V erklärt das Resultat.

## Zusammenfassung

Wenn man den Bromwasserstoff an die Phenylpropiolsäure addieren lässt, so erhält man nach Verschiedenheit benutzter Lösungsmittel bald die α-Bromsäure, bald die β-Bromsäuren. Die Bildung der α-Bromsäure läuft dem von Bromatom hervorgerufenen Radikalkettenmechanismus gemäss, wird durch Hinzufügen einer kleinsten Menge von Brenzkatechin stark verzögert und hat dabei die Bildung der β-Bromderivate zur Folge. Die erhaltene β-Bromderivate bestehen aus fast gleicher Menge von beiden Isomeren, d.h. β-Brom*allo*zimtsäure(*cis*) und β-Bromzimtsäure(*trans*). Dasselbe Resultat kann auch durch Austausch des Lösungsmittels mit anderem, z.B. mit Nitrobenzol (oder Anisol) erhalten werden, wenn das "Antioxidant" vorhanden ist. In diesem Falle vergrössert aber unter Abwesenheit desselben sich die Menge der *trans*-Säure in den Produkten gegenüber derselben der *cis*-Säure. Anderseits verliefe auch die Stereomerisierung der β-Brom*allo*zimtsäure in ihre *trans*-Isomer durch den Radikalkettenmechanismus. Deshalb unter den durch Hinzufügen Brenzkatechins dem Gang der Radikalreaktion schädlich gemachten Bedingungen, mag sich eine gleiche Menge von beiden Isomeren durch Anlagerung von Bromwasserstoff bilden und im Falle von der Anwendung Nitrobenzols oder Anisols als Lösungsmittel ein Teil der gebildeten β-Brom*allo*zimtsäure in den *trans*-Isomer umlagern. Dabei darf die gesamte Menge des letzteren das sekundär aus *cis*-Isomer verwandelte Produkt nicht angesehen werden.

Ferner dass nur die β-Bromsäuren bezüglich der Zimtsäure bei jedem Falle erhalten werden, mag erklärt werden dadurch, dass eine Ionenreaktion durch verstärkte Konjugierung der Doppelbindung mit dem Carboxyle Vermöge ihres

9) M. Sudborough und H. Thompson, *J. Chem. Soc.*, **83**, 686 (1903).
10) R. Stoermer und P. Heymann, loc. cit.

Benzolkerns beschleunigt würde, was die Verzögerung der damit gegenüberstellenden Radikalreaktion veranlassen hätte. Im Gegensatz dazu träte bei der Phenylpropiolsäure die Radikalreaktion als Folge der Verminderung der oben genannten Konjugierung durch Austausch der Doppelbindung mit Dreifachbindung auf, wenn die Reaktion in den an dem Solvatationseffekt ärmeren oder fehlenden Lösungsmitteln, wie Benzol, Toluol, Tetrachlorkohlenstoff usw. ausgeführt würde.

Also kann man ansehen das bei einer gewissen Klasse von Verbindungen mit Doppelbindung nicht befindliche Differenzieren der Orientation und des Mechanismus von der Anlagerung des Bromwasserstoffs in die zwei Richtungen als eigentümlich den entsprechend gebauten Verbindungen mit Dreifachbindung.

Zum Schluss möchte der Verfasser den Herren Professor Y. Urushibara und Professor O. Simamura an der Universität zu Tokyo für ihre freundlichen Leitungen und guten Räte den herzlichsten Dank aussprechen.

*Chemisches Laboratorium*
*Abteilung der allgemeinen Bildungen*
*Nagoya Universität*
*Mizuho-ku, Nagoya*

---

# *The Reaction of 1,8-Cineole with Acid Solutions*

By Tamon MATSUURA, Hisashi KOMAE and Kōzō SAITŌ

(Received April 16, 1958)

On the oxidation of 1,8-cineole with chromic acid in acetic acid[1] or with Beckmann's chromic acid mixture[2], terpin hydrate or $\alpha$-terpineol has been obtained in a poor yield together with the main reaction products such as homoterpenyl methyl ketone or terpenylic acid. As terpin hydrate and $\alpha$-terpineol are not oxidation products, it is of interest to clarify the effect of acid solutions on 1,8-cineole.

No work has been reported about the reaction of 1,8-cineole with an aqueous acetic acid solution and only a little attention has been paid to the reaction of cineole with sulfuric acid[3-6]. In 1887, Wallach observed that when cineole and sulfuric acid (sp. gr. 1.64) in alcohol were heated for 5 hours on a water bath, $\alpha$-terpinene and terpinolene were obtained[3]. Recently Lombard et al. treated this subject somewhat in detail[4]. They studied the problem at various concentrations of sulfuric acid (at 55 and 64% mainly) for various reaction times under stirring at 15°C, and obtained the following compounds: terpin hydrate, *trans*-terpin, $\alpha$-terpineol and hydrocarbons. Limonene, $\alpha$-terpineol and terpin hydrate were also studied. Before Lombard's observation, it was reported from this laboratory that when cineole and 21% aqueous sulfuric acid solution were heated at 70°C under stirring, terpin hydrate, $\alpha$-terpineol, $\alpha$-terpinene and *p*-cymene were obtained[5]. In this case, it was observed that as the time of contact increases, cineole gives progressively less terpene alcohols and more hydrocarbons.

In this investigation we intended to make clear the actions of acetic acid and sulfuric acid solutions on 1,8-cineole under conditions similar to those described in the foregoing papers[1,2], and to propose a reaction mechanism for the formation of terpins and $\alpha$-terpineol from 1,8-cineole.

## Results and Discussion

1,8-Cineole was treated with an aqueous acetic acid solution (60 wt. %) and an aqueous sulfuric acid solution (21 wt. %) and terpin hydrate was also treated with the same reagents. Further, the reaction of *trans*-terpin with 60% acetic acid solution and that of 1,8-cineole with 0.6% sulfuric acid solution were examined. The reaction conditions and the products

1) T. Matsuura and H. Matsuo, *J. Sci. Hiroshima Univ.*, **A16**, 153 (1952).
2) T. Matsuura and S. Yasuda, ibid., **15**, 273 (1952).
3) O. Wallach, *Ann.*, **239**, 22 (1887).
4) R. Lombard and E. Geiger, *Bull. soc. chim. France*, **1956**, 1564.
5) T. Matsuura and T. Furukawa, *J. Sci. Hiroshima Univ.*, **A18**, 447 (1956).
6) I. Ogura et al., *J. Pharm. Soc. Japan*, (*Yakugaku Zasshi*), **77**, 1355 (1957).

TABLE I

RESULTS OF THE REACTIONS OF CINEOLE AND TERPINS WITH ACID SOLUTIONS AT 70°C

| Expt. No. | Reaction condition | | Reaction time hr. | Yield of reaction products (wt. percentage to the charged sample) | | | |
|---|---|---|---|---|---|---|---|
| | Reagent | Sample | | Terpineol | Terpin hydrate | *trans*-Terpin | Hydrocarbons |
| 1 | 60% Acetic acid | Cineole | 10 | 0.12 | 0 | 0.03 | 0 |
| 2 | 64% Acetic acid | Terpin hydrate | 10 | 2.7 | — | trace | 0 |
| 3 | 60% Acetic acid | *trans*-Terpin | 10 | 1.8 | 0 | — | 0 |
| 4 | 21% Sulfuric acid | Cineole | 3 | 4.6 | 0.20 | 0.12 | small |
| 5 | 21% Sulfuric acid | Terpin hydrate | 0.25 | 17.8 | — | 0.20 | 11 |
| 6 | 0.6% Sulfuric acid | Cineole | 10 | 0.02 | 0 | 0.004 | 0 |

are shown in Table I. Among the reaction products, *α*-terpineol was identified as its phenylurethane and nitrosochloride. Fractional crystallization was employed for the separation of terpin hydrate and *trans*-terpin. For the identification of a small amount of the reaction products, strip-chromatography and I. R. and U. V. absorption spectra were used.

The reaction of cineole (1400 g.) with the acetic acid solution gave *dl*-*α*-terpineol (0.12% to cineole used) and *trans*-terpin (0.03% to cineole used). Under the same conditions terpin hydrate (90 g.) was converted into *trans*-terpin (trace) and *dl*-*α*-terpineol (2.7%) which was confirmed to be free from its acetate by the measurement of ester value. In order to compare the action of the acetic acid solution on *trans*-terpin with that on terpin hydrate, the former (4.0 g.) was treated under the same conditions as in the case of the latter. The reaction product was *dl*-*α*-terpineol (1.8%). The unsuccessful detection of terpin hydrate in the reaction product may result from the small scale of the experiment.

Cineole was attacked more easily by the aqueous sulfuric acid solution (21%) than by the aqueous acetic acid solution (60%), and converted into terpin hydrate, *trans*-terpin, *dl*-*α*-terpineol and monocyclic hydrocarbons consisting of *α*-terpinene and *p*-cymene*. In addition, the presence of $\Delta^{2,4(8)}$-*p*-methadiene was confirmed by the U. V. absorption maximum at 244 mμ[7]. The reaction of terpin hydrate with the sulfuric acid solution gave the following products: *dl*-*α*-terpineol, monocyclic hydrocarbons, *trans*-terpin and 1,8-cineole. The fact that terpin hydrate is attacked more easily than cineole shows that the cleavage of the ether ring in cineole is more difficult than the dehydration of terpin. A remarkable difference between the reaction of cineole with 60% acetic acid solution and that with 21% sulfuric acid solution lies in the point that the latter gives both *cis*- and *trans*-terpins in comparable amounts while the former gives *trans*-terpin predominantly. Since the reaction of cineole with a very dilute aqueous sulfuric acid solution (0.6%), having the same pH value as 60% aqueous acetic acid (pH 1), gives *trans*-terpin predominantly, it seems that the ratio of *cis*-terpin to *trans*-terpin is largely changed by the hydrogen ion concentration of the reagent.

From the above results, the mechanism of the reaction for the formation of the products obtained by the action of aqueous acid solutions on cineole is probably as shown in Fig. 1.

In this mechanism we consider that the main course of the reaction is as follows:

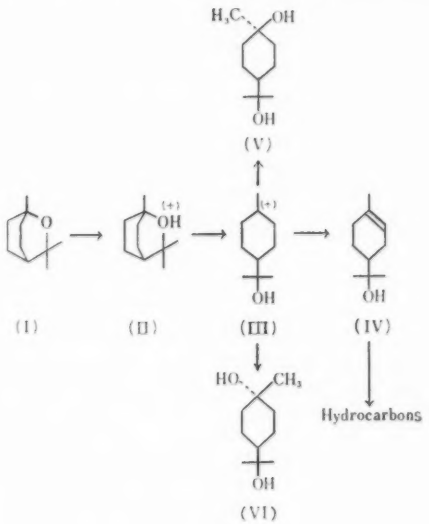


Fig. 1.

* cf. 5).

7) R. T. O'Connor and L. A. Goldblatt, *Anal. Chem.*, **26**, 1726 (1954).

cineole (I)→oxonium ion(II)→carbonium ion(III)→α-terpineol(IV)→hydrocarbons.

The main reaction product of cineole with the acid solutions is *dl*-α-terpineol under the above conditions (Expt. 1,4,6). We see, also, that *cis*- and *trans*-terpins (V and VI) are considerably stable to the action of 60% acetic acid (Expt. 2,3). If terpin were the intermediate in the main reaction course, a considerable amount of terpin should be accumulated as a reaction product. But the yield of terpin is very small in comparison with that of α-terpineol (Expt. 1,4,6). Furthermore, terpin hydrate is converted easily into hydrocarbons by the action of 21% sulfuric acid (Expt. 5), while in the case of cineole this is not true (Expt. 4). Therefore, one may probably assume that *cis*- and *trans*-terpins are not intermediates in the main reaction course but only by-products formed by the hydration of a carbonium ion(III) derived from an oxonium ion(II). The formation of the carbonium ion(III) may be considered on the basis of the presence of both *cis*- and *trans*-terpins in the reaction products.

In the cases of Expt. 1 and 6, where aqueous acetic acid and very dilute sulfuric acid solutions are the reagents, the terpin found in the reaction products is the only *trans* modification. This may be explained by taking into consideration that the stability of the carbonium ion (III) is decreased greatly in Expt. 1 and 6 as compared with in Expt. 4, owing to the difference of the hydrogen ion concentration. Thus in Expt. 1 and 6, the unstable carbonium ion(III) may react very rapidly with water while the departing group $\ddot{O}H-C(CH_3)_2-R$ in the formation of the carbonium ion(III) from the oxonium ion (II) is still partially screening one side of the planar carbonium ion (III).

(VII)

Although, Lombard et al. have proposed a carbonium ion(VII) as an intermediate in the hydrolysis of mono- and di-sulfates[5], the above obtained results can be explained by assuming the carbonium ion (III) instead of that of Lombard. In the reaction of 1,8-cineole with acid solutions, the transitory carbonium ion(III) which is derived from the oxonium ion(II) formed by the addition of the hydrogen ion to 1,8-cineole may react with a water molecule to form terpins ($S_N$ 1 type reaction), or may liberate a proton to form α-terpineol (E 1 type reaction). The above $S_N$ 1 and E 1 processes will be competed with each other, but in the E 1 reaction there will not be a steric hindrance which is possibly included in the $S_N$ 1 reaction. Thus it seems probable that the elimination process which results in the formation of α-terpineol is predominating.

If an $S_N$ 2 type reaction proceeded by the attack of an anion such as acetate on the oxonium ion(II) in Expt. 1, there would be a change of the configuration at $C_1$ atom resulting in a Walden inversion. In this case, however, an ester thus produced would give both *cis*- and *trans*-terpins by a successive hydrolysis*. Also, if the acetate were formed, it would be so stable that the hydrolysis could not occur under our conditions. Thus an $S_N$ 2 type reaction may be left out of consideration in our experiments.

Considering the results of this investigation, in the cases of the oxidation of 1,8-cineole with chromic acid in acetic acid[1] and with Beckmann's chromic acid mixture[2], the reaction seems to proceed in the intermediary formation of α-terpineol by the above mechanism. α-Terpineol thus formed is then oxidized to homoterpenyl methyl ketone (VIII) which in turn goes to terpenylic acid (IX).

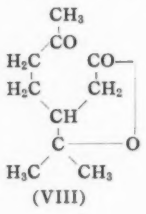

(VIII)

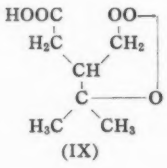

(IX)

## Experimental

**Reaction of Cineole with Acetic Acid Solution.**—Cineole (700 g.) isolated from a camphor white oil according to the method described before[6] (b. p. 173~173.5°C, $n_D^{25}$ 1.4540, $d_4^{25}$ 0.9195) and 60% aqueous acetic acid solution (1309 g.) were mixed in a flask. After the mixture was heated at 70°C for 10 hours under stirring, it separated into two parts, an oil and an aqueous solution, and they were neutralized with sodium

* It has been reported that hydrolysis of tertiary alkyl acetate by acid proceeds in alkyl-oxygen fission (C. K. Ingold et al., *Nature*, **166**, 680 (1950)).

8) S. Hayashi, T. Matsuura and B. Masumoto, *J. Sci. Hiroshima Univ.*, **A15**, 165 (1951).

carbonate. A large amount of sodium acetate was obtained from the aqueous solution. The oil was repeatedly washed with water and dried. The oil (1190 g.) obtained from two runs of the above treatment was distilled under a reduced pressure, b. p.$_{40}$ 80～85°C, $n_D^{25}$ 1.4532, $d_4^{25}$ 0.9196, yield 1173 g. Treatment of this fraction with *o*-cresol gave needle crystals, m. p. 55～56°C, which were identified as cresineol by the mixed melting point determination. Thus, it was confirmed that this fraction consisted of unchanged cineole.

The residue remaining in the flask was a pale yellow oil possessing a fragrant odor. After it was dissolved in ether and stood over night, white needle crystals (Crystal I), m. p. 155～156°C, deposited and were taken up by filtration. From the filtrate (the ether solution) a viscous oil (2.3 g.) was obtained, which on distillation gave the following fractions: (1) b. p.$_{20}$ 69～105°C, $n_D^{25}$ 1.4580, yield 0.1 g.; (2) b. p.$_{20}$ 105～135°C, $n_D^{25}$ 1.4730, $d_4^{25}$ 0.9444, yield 1.7 g.; (3) residue (0.4 g.). Fraction (2) was distilled and the main fraction, (b. p.$_{17.5}$ 103～107°C, $n_D^{25}$ 1.4742, $d_4^{25}$ 0.9388, yield 0.8g.), phenylurethane m. p. 112.5°C, and nitrosochloride m. p. 113～113.5°C, were obtained. This fraction was identified as *dl*-$\alpha$-terpineol by mixing its derivatives with authentic specimens. The residue (0.4 g.) was washed with a little ether and recrystallized from water-ethanol mixture twice. Colorless needle crystals (Crystal II), m. p. 156～156.5°C, were obtained. A large amount of sodium acetate which was produced by the neutralization of both the aqueous and the oily layers of the reaction mixture was extracted with ethanol. The ethanol extract was evaporated up to dryness and then repeatedly extracted with ether. From the ether extract colorless needle crystals (Crystal III), m. p. 152～154°C, were obtained. The aqueous layer separated from the precipitated sodium acetate was extracted with ether several times and crystals (Crystal IV), m.p. 155.5～156°C, were obtained from the ether extract. Crystals I, II, III and IV, which amounted to 0.427 g. in all, were identified as *trans*-terpin by the mixed melting point determination.

**Reaction of Terpin Hydrate with Acetic Acid Solution.** — Terpin hydrate, m. p. 119～121°C (90 g.), was heated with 64% aqueous acetic acid solution (132 g.)* at 70°C for 10 hours under stirring. Unchanged terpin hydrate was filtered off and washed with water until the odor of acetic acid vanished. The aqueous layer of the reaction mixture and the water washings were neutralized with sodium carbonate. The precipitated sodium acetate was filtered and washed with a small amount of ether in order to catch the oily product adhering to it and then extracted with ethyl acetate. The aqueous layer separated from sodium acetate was extracted with ether and then evaporated up to dryness. The non-volatile material thus obtained was again extracted with ethyl acetate. The ether extracts gave an oily matter (4.4 g.) which on distillation gave a main fraction, b. p.$_{18}$ 98～103°C, $n_D^{25}$ 1.4759, $d_4^{25}$ 0.9264, E. V. 16.26, yield 2.4 g. Phenylurethane and nitrosochloride of this fraction were identical with those of *dl*-$\alpha$-terpineol.

Unchanged terpin hydrate (71.6 g.) was recovered. On the other hand crystals, m. p. 154.5～155.5°C, which were identified as *trans*-terpin by the mixed melting point determination, were obtained in a very small amount from the ethyl acetate extracts mentioned above. Furthermore, strip-chromatography of these crystals was tried, and only one spot (Rf 0.45) corresponding to that of *trans*-terpin was found on the chromatogram developed with *n*-butanol-ethyl acetate (1 : 9) mixture[9].

**Reaction of *trans*-Terpin with Acetic Acid Solution.** — *trans*-Terpin[10], m. p. 156°C (4.0 g.), was heated with 60% aqueous acetic acid solution (6.9 g.) at 70°C for 10 hours under stirring. An oily product (0.07 g.) was separated according to the procedure described in the above section.

A strip-chromatogram of the oil gave one spot (Rf 0.24) corresponding to $\alpha$-terpineol when the oil was developed with 15% ethyl acetate in *n*-hexane[11].

Unchanged *trans*-terpin, m. p. 155～156°C (3.00 g.), was recovered.

**Reaction of Cineole with Sulfuric Acid Solution.**—Cineole (100 g.) was heated with 21% aqueous sulfuric acid solution (303 g.) at 70°C for 3 hours under stirring. After the neutralization with sodium carbonate, the reaction mixture was steam-distilled. The oily distillate (97.3 g.) was fractionated into the following fractions under reduced pressure. (1) b. p.$_{29}$ 74°C, $n_D^{25}$ 1.4546, $d_4^{25}$ 0.9175, yield 83.7 g.; (2) b. p.$_{29}$ 74～112°C, $n_D^{25}$ 1.4554, $d_4^{25}$ 0.9163, yield 2.4 g.; (3) b. p.$_{29}$ 112～113°C, $n_D^{25}$ 1.4769, $d_4^{25}$ 0.9276, yield 4.6 g.; (4) residue (1.1 g.). Fractions 1 and 2 were mainly unchanged cineole, because their odors and physical properties were close to those of cineole. But their U. V. absorption spectra (Fig. 2) showed absorption maxima at 244, 265 and 273 m$\mu$ corresponding to the characteristic absorption maxima for $\Delta^{2,4(9)}$-*p*-menthadiene, $\alpha$-terpinene and *p*-cymene, respectively. I. R. spectrum of fraction (3) is shown in Fig. 3. The absorption curve coincides with that of $\alpha$-terpineol and has no strong bands at 1643 and 885 cm$^{-1}$ such as are characteristic of the end methylene group presented in $\beta$-terpineol[12].

When the aqueous solution remained in a flask after the steam-distillation was evaporated up, a solid material including sodium sulfate was obtained. It was extracted thoroughly with ethyl

* In the case of terpin hydrate 64% acetic acid solution was employed under consideration of crystallization water in terpin hydrate.

9) K. Yamamoto and T. Furukawa, *Educational studies* (*J.* Faculty of Education), *Hiroshima Univ.* (2), **4**, 45 (1956).

10) *trans*-Terpin was prepared by the hydrolysis of *trans*-dipentene dihydrochloride with silver oxide and water (R. Lombard and E. Geiger, *Bull. soc. chim. France*, **1953**, 927).

11) J. G. Kirchner, J. M. Miller and G. J. Keller, *Anal. Chem.*, **23**, 420 (1951).

12) T. Aratani and T. Matsuura, *J. Sci. Hiroshima Univ.*, **A20**, 199 (1957).

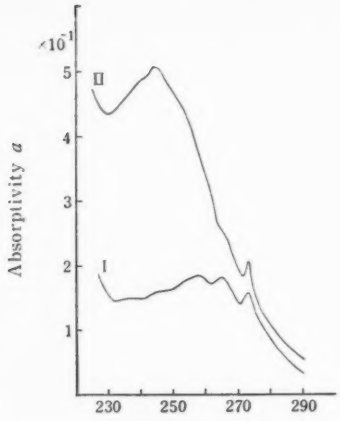


Fig. 2. Ultraviolet absorption spectra of hydrocarbon fractions: I fraction (1), II fraction (2) (in ethanol).

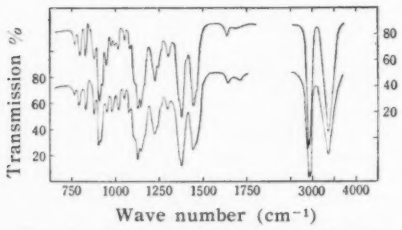


Fig. 3. Upper α-terpineol (liquid film). Lower fraction (3) (liquid film).

acetate. Colorless crystals (0.48 g.), which were obtained from the extract by evaporating the solvent, were recrystallized from water. The crystals, m. p. 117~119°C (0.20 g.), obtained by the repeated recrystallizations were identified as terpin hydrate by mixing with an authentic specimen. Evaporation of the mother liquor of the first recrystallization gave crystals possessing larger solubility in water than that of terpin hydrate. By recrystallization from ethyl acetate, the crystals were purified to colorless ones, m. p. 155~156°C (0.12 g.), which showed no depression of melting point on admixture with *trans*-terpin.

**Reaction of Terpin Hydrate with Sulfuric Acid Solution.** — Terpin hydrate (50 g.) was heated with 21% aqueous sulfuric acid solution (945 g.)* at 70°C for 15 minutes under stirring. Unlike the result in the case of acetic acid, terpin hydrate disappeared rapidly and was attacked easily. The reaction mixture which consisted of two layers, an oil and an aqueous solution, was neutralized with sodium carbonate under vigorous stirring, and then steam-distilled. The distillate was extracted with ether. After removal of the solvent, an oil (17.8 g.) was obtained, which was fractionated to the following fractions: (1) $b.p._{50}$ 80~90°C, $n_D^{25}$ 1.4600, $d_4^{25}$ 0.8818, yield 4.4 g.; (2) $b.p._{50}$ 90~103°C, $n_D^{25}$ 1.4773, $d_4^{25}$ 0.8661, yield 1.6 g.; (3) $b.p._{50}$ 125~130°C, $n_D^{25}$ 1.4789, $d_4^{25}$ 0.9296, yield 8.9 g.; (4) residue (1.6 g.).

Condensation of fraction (1) with maleic anhydride at 80°C for half an hour was carried out, and the reaction mixture was separated to an unchanged oil and an addition product by distillation. The adduct was treated with a dilute sodium carbonate solution and a dilute aqueous sulfuric acid successively. Thus there were obtained crystals, m. p. 133.5~134°C, undepressed with the free acid of α-terpinene maleic anhydride adduct by the mixed melting point determination. The U. V. absorption curve of fraction (1) shows a $\lambda_{max}^{alc}$ 265 mμ (*a*: 4.25), characteristic of α-terpinene (Fig. 4). The oil which remained unchanged by the maleic-anhydride treatment was extracted with a saturated resorcine solution. Steam-distillation of the extract gave an oil (0.3 g.) which was identified as 1,8-cineole by the formation of cresineol, m. p. 55~56°C, and by strip-chromatography (Rf 0.48)[11]. After the above treatment of fraction (1) there remained an oil consisting of dipentene and *p*-cymene. The former was characterized by its tetrabromide, m. p. 124~125°C, and the latter was confirmed by the absorption maxima at 258 and 273 mμ characteristic of *p*-cymene in a U. V. absorption spectrum (Fig. 4).

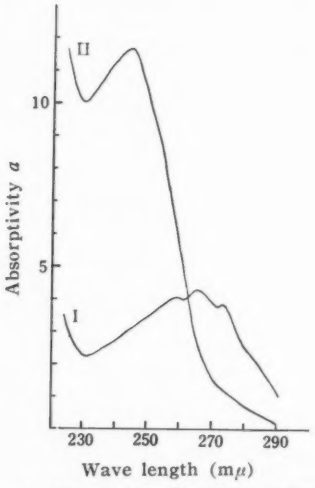


Fig. 4. Ultraviolet absorption spectra of hydrocarbon fractions: I fraction (1), II fraction (2) (in ethanol).

Fraction 2 consisted of dipentene (tetrabromide, m. p. 124~125°C) mainly and of a small amount of $\Delta^{2,4(8)}$-*p*-menthadiene ($\lambda_{max}^{alc}$ 244 mμ, *a*: 11.67, in U. V. absorption curve in Fig. 4).

Redistillation of fraction (3) gave a main fraction: $b.p._{20}$ 105~108°C, $n_D^{25}$ 1.4793, $d_4^{25}$ 0.9260,

* In this case the amount of crystallizaton water in terpin hydrate was so small that the concentraton of the acid was practically not changed.

phenylurethane m. p. 112~113°C characteristic of *dl*-α-terpineol.

The aqueous layer containing sodium sulfate was evaporated up on a water bath and the solid matter thus obtained was extracted with the same procedure described in the case of cineole. Unchanged terpin hydrate, m. p. 119.5~120°C (6.8 g. after repeated recrystallizations), was recovered, and *trans*-terpin, m. p. 156°C (0.1 g.), which was identified by mixing with an authentic specimen, was obtained.

**Reaction of Cineole with Dilute Sulfuric Acid Solution.** — Cineole (1000 g.) was heated with 0.6% aqueous sulfuric acid solution (706 g.) at 70°C for 10 hours under stirring. The acid solution used here showed the pH value (pH 1) equal to 60% aqueous acetic acid solution. After neutralization of the reaction mixture, and steam-distillation, a large amount of oil (952 g.) was obtained. Fractional distillation under reduced pressure gave a main fraction (935 g.) consisting of unchanged cineole and a higher boiling fraction (b. $p._{20}$ 71~96.5°C, $n_D^{25}$ 1.4783, yield 0.2 g.) whose I. R. spectrum agreed with that of α-terpineol.

Terpin was obtained from the aqueous layer according to the method mentioned above. Separation of *cis*- and *trans*-terpins by fractional crystallization was tried, and only *trans*-terpin, m.p. 154.5~155°C (0.04 g.), was obtained.

## Summary

The reaction of 1,8-cineole with 60% acetic acid at 70°C for 10 hours under stirring gave *dl*-α-terpineol (0.12%) and *trans*-terpin (0.03%). By the action of 21% sulfuric acid at 70°C for 3 hours, cineole yielded *dl*-α-terpineol (4.6%), terpin hydrate (0.20%), *trans*-terpin (0.12%) and monocyclic hydrocarbons (a small amount). On the other hand, the reaction of cineole with 0.6% sulfuric acid solution at 70°C for 10 hours gave *dl*-α-terpineol and *trans*-terpin in poor yields. In this case the reaction products are the same as in the case of 60% acetic acid.

Next, terpin hydrate was treated with 64% acetic acid at 70°C for 10 hours. The reaction products were *dl*-α-terpineol (2.7%) and *trans*-terpin (trace). By the action of 21% sulfuric acid at 70°C, terpin hydrate was attacked easily, and after 15 minutes it was converted to *dl*-α-terpineol (17.8%), *trans*-terpin (0.20%), 1,8-cineole and monocyclic hydrocarbons (11%). The monocyclic hydrocarbons consisted of α-terpinene, dipentene, $\Delta^{2,4(8)}$-*p*-menthadiene and *p*-cymene. *trans*-Terpin was, also, treated with 60% acetic acid at 70°C for 10 hours, the reaction product being *dl*-α-terpineol (1.8%).

On the basis of the above experiments a reaction mechanism for the action of acid solutions on 1,8-cineole was proposed.

The authors wish to thank Mrs. Michiko Satō for her assistance. This research was financed partly by the Scientific Research Grant of the Ministry of Education.

*Department of Chemistry*
*Faculty of Science*
*Hiroshima University*
*Hiroshima*

# SHORT COMMUNICATIONS

## *Optimum Sample Position in Radioactivation Analysis Using Radium-Beryllium Neutron Source in Paraffin Moderator*

By Fumio Aoki and Minoru Okada

(Received June 3, 1958)

It is known that in the radioactivation of samples by $(n, \gamma)$ reaction by use of a radium-beryllium neutron source surrounded by a paraffin moderator, the distance between the sample and the neutron source is an important factor affecting the intensity of the radioactivity induced in the sample. However, the optimum distance depends on the size of the sample and the neutron source. In spite of this fact, data for the optimum distance[1-4] have been given without the specification of the size of the sample and the neutron source.

We feel that the size of the sample and the neutron source has some influence on the optimum distance and that, in so far as the problem of the size effect is not solved, it is highly desirable for practical purpose to specify the size of the sample and the neutron source. Therefore, we report in this letter the optimum distance for specified experimental conditions as well as the effect of the orientation of sample surface on induced activity.

The optimum distance was determined on three samples by use of a radium-beryllium neutron source placed in a paraffin moderator. The neutron source had a cylindrical shape (2.2 cm. in diameter and 2.5 cm. in height) and was made of mixture of 1g. of radium and 5 g. of beryllium. The paraffin moderator had a shape of a rectangular parallelepiped, and the minimum distance from the neutron source to the external surface of the moderator was 11 cm. The samples were: a circular plate of silver and flat packages of rhodium and of vanadium powder, their diameter or corresponding size being less than that of the neutron source. The sample position was on the axis of the neutron source cylinder. The nuclides chosen for the measurement of a flux of neutrons which brought about the $(n, \gamma)$ reaction in the sample were 24.2 sec. $^{110}$Ag, 44 sec. $^{104}$Rh, and 3.76 min. $^{52}$V.

As is shown in Fig. 1, each of the three curves, obtained from the counting rates of the product nuclides, shows a maximum at the same distance of $1.7 \pm 0.1$ cm. Meanwhile, if the total cross-section curves given by Hughes and Harvey[5], were referred to, it would be difficult to suppose that the relation between the $(n, \gamma)$ reaction cross-section and the energy of neutrons for one of these elements was quite similar to the relation for the others. Nevertheless, the curves obtained showed very good agreement in the distance. The authors thus feeled that the distance may be valid for many other elements.

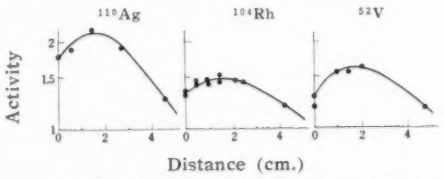


Fig. 1.. Activity induced vs. distance from radium-beryllium neutron source.

In the study of the effect of the orientation of sample surface on the induced activity, a strip of silver plate of 0.8 cm. in width was placed at a distance of 2.2 cm. from the same neutron source as above, on the axis of the neutron source cylinder, and irradiated in two orientations: (a) perpendicular to, and (b) parallel to the neutron source axis. The measurements of induced activity for the two cases showed no appreciable difference, the

1) J. E. Hudgens and L. C. Nelson, *Anal. Chem.*, **24**, 1473 (1952).
2) W. W. Meinke and R. E. Anderson, *Anal. Chem.*, **25**, 781 (1953).
3) Y. Kusaka, Report presented at the 10th Annual Meeting of the Chemical Society of Japan, held in Tokyo, April 1957.
4) T. Shiokawa, M. Yagi and N. Yamashiro, Report presented at the 1st Annual Symposium on Radiochemistry, held in Tokyo, Dec. 1957.
5) D. J. Hughes and J. A. Harvey, Neutron Cross Sections (U. S. Atomic Energy Commission) **BNL-325**, 1955.

standard deviation of the observed values of the activity being within ±1% of the absolute values. Thus, it may be said that the orientation of sample surface has no appreciable effect on induced activity, so far as the sample size is less than one-third of the neutron source diameter; although the sample position for this experiment was not at the optimum distance, the same statement will apply to the samples placed at the optimum distance.

We are greatly indebted to Dr. S. Uchida, Professor S. Makishima and Mr. H. Takahashi for their encouragement and helpful suggestions, and to Dr. T. Naito for permission to use laboratory facilities.

*Government Chemical Industrial Research Institute*
*Shibuya-ku, Tokyo*

---

## *Synthesis of Isoflavono(7′,8′ : 6, 5)-α-pyrones and Formylation of 2,4-Dihydroxyphenyl Benzyl Ketone*

By Yoshiyuki KAWASE, Tetsuya SEKIBA and Kenji FUKUI

(Received June 5, 1958)

In previous papers[1,2], the authors reported the preparation of furano(2′,3′ : 7, 8)-isoflavones. In connection with it, the present paper describes the preparation of isoflavono(7′,8′ : 6,5)-α-pyrones (IIa, b).

The synthesis of flavono(7′,8′ : 6,5)-α-pyrones has been carried out by two methods: that is, by α-pyrone-ring formation on 7-hydroxy-8-formyl-flavones[3], and by flavone-ring formation on 5-hydroxy-6-acyl-coumarins[4]. But, so far as the preparation of isoflavono(7′,8′ : 6,5)-α-pyrones is concerned, only the preparation of 2′,4-dimethyl-isoflavono-α-pyrone from 5-hydroxy-4-methyl-6-coumaryl benzyl ketone has been reported[5].

Here, isoflavono(7′,8′ : 6,5)-α-pyrone (IIa) and its 2′-methyl homologue (IIb) were prepared from 7-hydroxy-8-formyl-isoflavones (Ia, b) by the Perkin reaction in the usual way. IIa and IIb were hydrolyzed to a same acid, 2,6-dihydroxy-3-phenylacetyl-cinnamic acid (III) (not a lactone of it, namely a coumarin-derivative), which was re-derived into IIb by the action of acetic anhydride and sodium acetate.

It has been reported recently[6] that formylation of 2,4-dihydroxyphenyl benzyl ketone (resbenzylphenone) (IV) by the Hoesch reaction gives isoflavone through the compound formylated in α-methylene group.

In the present work, formylation of IV by the same reaction as above in the presence of anhydrous aluminum chloride gave 2,4-dihydroxy-3-formyl-phenyl benzyl ketone (V), the structure of which was confirmed by deriving it into IIb. (α-Acylresorcinols are usualy substituted in the 3-position in the Hoesch[7] or the

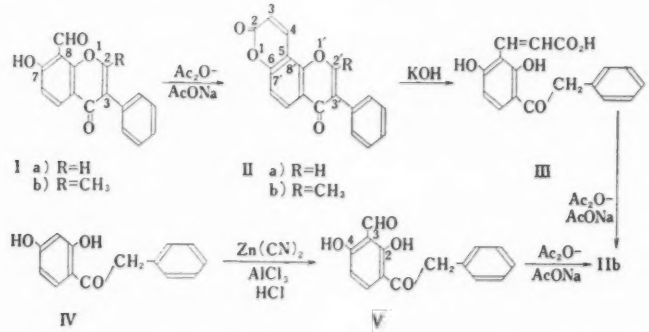


1) T. Matsumoto, Y. Kawase, M. Nanbu and K. Fukui, This Bulletin, **31**, 688 (1958).
2) K. Fukui and Y. Kawase, ibid., **31**, 693 (1958).
3) S. Rangaswami and T. R. Seshadri, *Proc. Indian Acad. Sci.*, **9A**, 7 (1939). [*Chem. Abstr.*, **33**, 4244 (1939)].
4) S. M. Sethna, N. M. Shah and R. C. Shah, *J. Chem. Soc.*, **1938**, 228.
5) C. V. Deliwala and N. M. Shah, ibid., **1939**, 1250.
6) L. Farkas, *Chem. Ber.*, **90**, 2940 (1957).
7) K. Nakazawa, *J. Pharm. Soc. Japan*, (*Yakugaku Zasshi*), **59**, 297 (1939); H. R. Shah and R. C. Shah, *J. Chem. Soc.*, **1939**, 132.
8) S. M. Sethna, N. M. Shah and R. C. Shah, *Current Sci.* (*India*), **6**, 93 (1937) [*Chem. Abstr.*, **32**, 549 (1938)].

Pechmann[4,5,8] reaction in the presence of anhydrous aluminum chloride.)

### Experimental[9]

*Isoflavono(7', 8' : 6, 5)-α-pyrone (IIa).*—A mixture of Ia[2] (0.6 g.) and anhydrous sodium acetate (0.7 g.) in acetic anhydride (4 cc.) was refluxed for 10 hr. The cooled mixture was poured into water, and the solid product was recrystallized from ethyl acetate, colorless needles, m.p. 200~200.5°C; yield 0.3 g. *Anal.* Found: C, 74.18; H, 3.55. Calcd. for $C_{19}H_{10}O_4$: C, 74.48; H, 3.47%.

*2, 4-Dihydroxy-3-formyl-phenyl benzyl ketone (V).*—A mixture of IV (5 g.), zinc cyanide (6 g.) and anhydrous aluminum chloride (5 g.) in anhydrous ether (100 cc.) was saturated with dry hydrogen chloride with stirring and cooling. By the usual treatment for the Hoesch reaction, the product was obtained in colorless microcrystals, m.p. 108~109°C (from dilute ethanol); yield 3.5 g. *Anal.* Found: C, 70.51; H, 4.85. Calcd. for $C_{15}H_{12}O_4$: C, 70.30; H, 4.72%.

*2'-Methyl-isoflavono(7', 8' : 6, 5)-α-pyrone (IIb).* (*a*) *From Ib.*—By the same procedure as described for IIa, starting from Ib[10] (1 g.), sodium acetate (1.1 g.) and acetic anhydride (6 cc.) the product IIb was obtained; m.p. 202~203.5°C (from ethyl acetate), yield 0.3 g. *Anal.* Found: C, 75.03; H, 4.05. Calcd. for $C_{19}H_{12}O_4$: C, 74.99; H, 3.97%.

(*b*) *From V.*—By the same treatment asd escribed for (a), starting from V (0.5 g.), sodium acetate (1 g.) and acetic anhyride (7 cc.) the product IIb (0.15 g.) was obtained; m.p. 202~203.5°C, identical with the sample from (a).

*Hydrolysis of IIa and IIb to 2, 6-dihydroxyl-3-phenyl-acetyl-cinnamic acid (III).*—(*a*) A mixture of IIa (0.1 g.) and 10% aqueous potassium hydroxide (5 cc.) was heated on a steam-bath for 4 hr. After being cooled, the solution was acidified with dilute hydrochloric acid, and the precipitates were collected and recrystallized from ethanol to give III, m.p. 210~211°C (decomp.), which was identical with the sample obtained from IIb. (*b*) A mixture of IIb (0.7 g.) and 10% aqueous potassium hydroxide (15 cc.) was treated similarly as described for a. Colorless microcrystals, m.p. 213~214°C (decomp.). III gave a brown ferric reaction in ethanol, and dissolved slowly in aqueous sodium bicarbonate. III was not converted into a lactone (coumarin-derivative) by heating with dilute hydrochloric acid. *Anal.* Found: C, 67.95; H, 4.73. Calcd. for $C_{17}H_{14}O_5$: C, 68.19; H, 4.74%. The mixture of III (0.1 g.), acetic anhydride (3 cc.) and sodium acetate (0.4 g), when refluxed for 10 hr., furnished IIb, m.p. 197~198°C (from ethyl acetate), which was identical with the sample described before.

An attempted preparation of IIa from III by the ethyl orthoformate-pyridine-piperidine method[11] was unsuccessful.

9) Melting points are uncorrect.
10) L. R. Row and T. R. Seshadri, *Proc. Indian Acad. Sci.*, **34A**, 187 (1951) [*Chem. Abstr.*, **47**, 12374 (1953)].
11) V. R. Sathe and K. Venkataraman, *Current Sci. (India)*, **18**, 378 (1949) [*Chem. Abstr.*, **44**, 8916 (1950)].

We are grateful to the Institute of Agricultural Chemistry, Faculty of Agriculture, Kyoto University for microanalyses.

*Faculty of Literature and Science*
*Toyama University*
*Hasumachi, Toyama*

---

## *A New Organic Reagent for the Colorimetric Determination of Iron(III) Ion : Phenothiazine Derivatives*

By Masao MARUYAMA, Tomonori MIKI and Shogo UEDA

(Received September 1, 1958)

During the course of examinations on interactions between 2-acetyl-10-(3-dimethylaminopropyl)phenothiazine maleate (I) or 2-chloro-10-(3-dimethylaminopropyl)-phenothiazine hydrochloride (II), and metal ions in aqueous solution, it was found that these phenothiazine derivatives reacted with iron (III) ions to form a

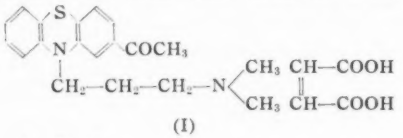

(I)

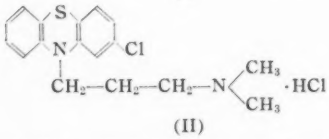

(II)

markedly colored solution. Both I and II react specifically with iron (III) ions and not with other ions such as iron (II), copper, nickel, cobalt, titanium and lead. Qualitatively, this reaction enables the detection of iron (III) ions in a concentration of 0.5 $\gamma$/cc., and a determination can be made for iron (III) ions of 1 to 8 $\gamma$/cc.

The compound I forms a yellow solution in water so that II is better suited for the determination than I. Aqueous solution of a mixture of iron (III) and the compound II exhibits an absorption spectrum in the visible region, with absorption maximum at 512 m$\mu$, as shown in Fig. 1, and the absorbance depends on the concentration of iron (III) ion and of the compound II. When the concentration

of II is above 0.2%, absorbance depends solely on the concentration of the iron ion.

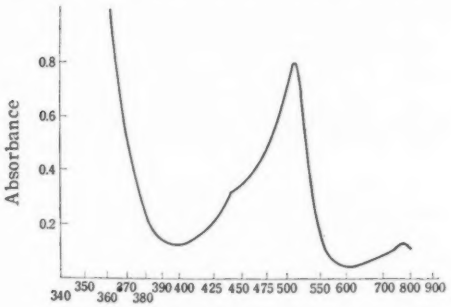


Fig. 1. Absorption spectrum of phenothiazine derivative with iron (III) ion in aqueous solution.
Contration of iron (III); $2.08\times10^{-4}$M/l.
Contration of the compound II; $4.82\times10^{-3}$ M/l.
pH, 1.0 ($H_2SO_4$·aq.)

An examination showed that a linearity was established with iron concentrations of 1 to 8 γ/cc.

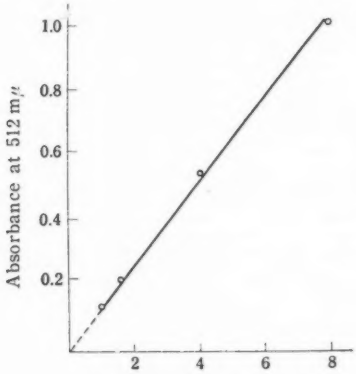


Fig. 2. Relation of iron (III) concentration to absorbance of colored solution.

As for the stability of the color developed, the color faded gradually with time but it was stable for 15 minutes after coloration.

In order to examine the effect of other metal ions, a sample solution containing iron (II), nickel, cobalt, copper, lead, titanium or chromium besides iron (III), in an amount 10 times that of iron (III) ion, was prepared, and caused to react with the compound II. It was found that the effect of these coexisting ions was negligible.

TABLE I
STABILITY OF COLORED SOLUTION
CONCENTRATION OF IRON (III): 4 γ/cc.
CONCENTRATION OF THE COMPOUND II: 2 mg./cc.

| Time after coloration (min.) | Absorbance at 512 mμ |
|---|---|
| 0 | 0.560 |
| 15 | 0.557 |
| 30 | 0.540 |
| 60 | 0.527 |

TABLE II.
EFFET OF OTHER ICNS
CONCENTRATION OF IRON (III): 4 γ/cc.
CONCENTRATION OF THE COMPOUND II: 2 mg./cc.

| Other ions (40 γ/cc.) | Absorbance at 512 mμ |
|---|---|
| — | 0.560 |
| Ni | 0.551 |
| Co | 0.560 |
| Cu | 0.550 |
| Cr | 0.545 |
| Ti | 0.555 |
| Pb | 0.558 |

The presence of ethylenediaminetetraacetate interfered with this reaction.

Examinations are now under way on the effect of anions and on various problems, as well as the structure of the reaction product.

*Shinagawa Plant, Sankyo Co., Ltd.*
*Nishi-shinagawa, Shinagawa-ku, Tokyo*

---

## *Isotope Effect of Boron in the Thermal Decomposition of the Boron Trifluoride-Calcium Fluoride Compound**

By Tatsuo MATSUURA
and Hisateru OKUNO

(Received October 8, 1958)

One of the purification methods of boron trifluoride gas for neutron counters involves the thermal decomposition of boron trifluoride-calcium fluoride addition compound[1,2]. In one of the papers describing

* Partly read at the 2nd Symposium of Atomic Energy in Japan, Feb. 1958.

1) A. C. Graves and D. K. Froman, "Miscellaneous Physical and Chemical Techniques of the Los Alamos Project", McGraw-Hill, New York (1952), p. 153.
2) F. Hudswell, J. S. Nairn and K. L. Wilkinson, AERE, C/R 651 (1951).

this process, Hudswell et al.[2] reported the unconfirmed, but apparently not erroneous result that at the earliest stage of the thermal decomposition of the boron trifluoride-calcium fluoride compound the fraction of the boron fluoride gas evolved might be enriched in $^{11}B$. The present authors attempted to make sure of this fact and found that there is a considerable isotopic fractionation effect in this reaction, to such an extent that this phenomenon might be of use for the isotope separation of boron-10.

The results obtained are shown in Figs. 1 and 2, in which the percentages of boron trifluoride gas evolved are taken at the abscissa in sequence as the gas was evolved, and the isotopic abundance ratios of boron in each fraction in terms of the ratio $^{11}B/^{10}B$ are taken at the ordinate. The latter was read directly from the height of the peaks of m/e 49 and 48 (due to $^{11}BF_2^+$ and $^{10}BF_2^+$, respectively) in the mass spectrogram.**,*** These ratios can also be estimated by the peaks of m/e 11 and 10, but these peaks are less sensitive than those of 48 and 49, and, as is shown in Fig. 2, the $^{11}B/^{10}B$ values from these lower m/e regions were smaller than those from the higher regions[3].

It is no doubt that a significant isotopic effect occurred in this reaction, and the separation factors calculated schematically reach 1.035 in Batch A and ca. 1.015 in Batch B. As this factor is considered to depend on the speed of evolution of the gas, it was kept as low as possible, i.e., in the case of Batch A, it was ca. $(2\,l.)_{STP}/hr$, the total gas content in the batch being 0.8 mol. Also, the boron trifluoride is so strongly adsorbed (chemisorbed) on calcium fluoride, that the sampling of the last fraction of the gas, which probably contains $^{10}B$ most enriched, was sometimes incomplete on account of cracking in the glass vessel by strong heating. Had these

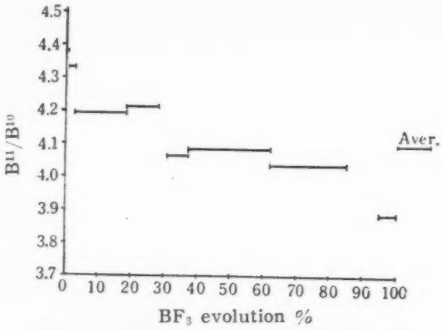


Fig. 1. Isotopic fractionation data for Batch A.†

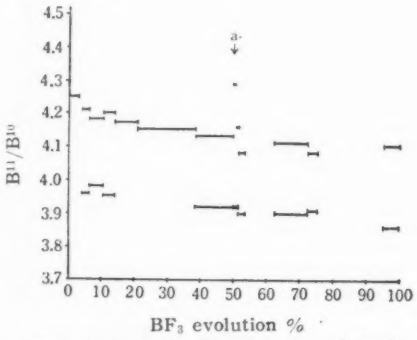


Fig. 2. Isotopic fractionation data for Batch B.†
(The lower group of the plots indicates the values from the peaks of m/e 11 and 10. The point a indicates the interruption of the gas evolution for several days.)

difficulties been avoided, the separation factor might have reached a greater value than this. Nevertheless, this observed separation factor in Batch A ($\alpha=1.035$) shows the largest value hitherto reported on the isotopic separation of $^{10}B$ using chemical exchange reactions[5].

The boron trifluoride-calcium fluoride compound was prepared by the method of Graves et al.[1] and the original boron trifluoride gas was prepared by Booth's method[6]. The thermal decomposition of

** The mass-spectroscopic measurements were done with a 21-103A Type Mass Spectrometer (Consolidated Electrodynamic Corp.) at the University of Tokyo or with a 103 Type Mass Spectrometer (Scientific Research Institute) at Nagoya University.

*** When the peak of m/e 47 was considerably large, correction was made on the observed values of peaks 48 and 49, on the basis that the whole peak of 47 is due to $^{28}SiF^+$, and that $^{29}SiF^+$ and $^{30}SiF^+$ did contribute to the peaks of 48 and 49 respectively, depending on the natural abundance ratio of $^{28}Si$, $^{29}Si$, and $^{30}Si$[3]. Lately, however, M. Yamane of Hitachi Co., in a personal communication, suggested that the peaks of 46 and 47 are due to $^{10}BF(OH)^+$ and $^{11}BF(OH)^+$. Although this is perhaps true, the tendency of the isotopic fractionation by this process and thus the separation factor do not deviate seriously from the data reported in this paper.

3) W. W. Watson, J. C. Buchanan and F. K. Elder, *Phys. Rev.*, **71**, 887 (1947).

† Batch A was prepared from purified (distilled) boron trifluoride etherate, $BF_3\cdot(C_2H_5)_2O$, and Batch B was from the residue of this etherate distillation. The fact that there is a difference between the average $^{11}B/^{10}B$ ratios of the two batches (Figs. 1 and 2 (upper group)) indicates that the isotopic fractionation effect occurred at the boron trifluoride etherate distillation[4,6].

4) R. Nakane, T. Watanabe and S. Isomura, *Report of Scientific Research Institute*, **33**, 330 (1957).

5) International Symposium on Isotope Separation, Amsterdam, 1957.

6) H. S. Booth and K. S. Willson, *J. Am. Chem. Soc.*, **57**, 2273 (1935).

the compound and the sampling of the gas were done in a closed, evacuated apparatus, in which the gas began to be evolved at about 200°C, and evolution did not completely cease even at about 350°C.

The authors believe that this effect is applicable to the practical separation of boron 10, the scheme of which and some fundamental data for which will be reported later.

In this connection, the authors wish to call attention to the expectation that, in regard to substances which contain the comparatively lighter atomic weight elements such as lithium[7] and boron, their isotopic abundance ratio may possibly change appreciably by a simple procedure, such as vaporization, recrystallization or adsorption. As for boron, its well known indefinite atomic weight due to various geological origins[8] has, without doubt, much connection with this inference.

The authors wish to express their hearty thanks to Dr. S. Araki of the Faculty of Engineering in the University of Tokyo, and to Mr. T. Matsuo of the Department of Earth Science in the University of Nagoya, for their labor and advice in the mass-spectroscopic measurements.

*College of Science*
*Rikkyo University*
*Toshima-ku, Tokyo*

7) A. E. Cameron, *J. Am. Chem. Soc.*, **77**, 2731 (1955); G. Wagner and A. Pelz, *Monatsh.*, **86**, 414 (1955) [*Chem., Abstr.* **50**, 692h (1956)], etc.
8) H. G. Thode, J. Macnamara, F. P. Lossing and C. B. Collins, *J. Am. Chem. Soc.*, **70**, 3008 (1948); H. V. A. Briscoe, P. L. Robinson and H. C. Smith, *J. Chem. Soc.*, **1927**, 282, etc.

## *The Variation of the Dielectric Constant of Phenol with Respect to Temperature*

By K. M. Somasundaram and C. V. Suryanarayana

(Received September 19, 1958)

For the temperature variation of dielectric constant Abegg and other workers[1-4] gave the relation

$$D = D_0 e^{-T/100}$$

Later work has shown, however, that the coefficient of $T$ in the exponent is, like $D_0$, specific for each liquid[5,6]. The equation

$$D = D_0 e^{-LT}$$

seems to hold with considerable accuracy for all the liquids hitherto examined. The second empirical constant $L$ is seen to have the dimension of the reciprocal of temperature.

The above relation is verified with phenol.

**Experimental procedure.** — "BDH. Analar" variety of phenol was distilled and the fraction boiling at 181.75°C was collected and used. Dielectric constant of phenol was determined at different temperatures ranging from 41.5 to 65.9°C. "Dekameter type DK03" of Wissenschaftlich Technische Werkstätten was used at a fixed frequency of 1.8 MC/sec., controlling the temperature of the cell with Hoppler's ultrathermostat. The results are given in the following table.

| | | | | | |
|---|---|---|---|---|---|
| $t$°C | 41.5 | 42.3 | 49.8 | 50.6 | 58.1 |
| $D$ | 11.78 | 11.72 | 11.10 | 11.03 | 10.48 |
| $t$°C | 60.7 | 64.8 | 65.4 | 65.5 | 65.9 |
| $D$ | 10.32 | 10.03 | 9.98 | 9.97 | 9.95 |

From the above data a plot of $\log_{10}D$ versus $T$ is a straight line and the variation of dielectric constant with temperature may be represented best by the relation

$$D = D_0^{-LT}$$

where $D_0 = 109.8$ and $L = 0.007094$.

It may be of interest that the data of Smyth and Hitchcock[7] for crystalline phenol has been tried by us to fit into the exponential equation. A plot of $\log_{10}D$ versus $T$ gives a curve tending towards a limiting value. The exponential equation, as pointed by Abegg, is valid only for liquids.

*Physico-Chemical Laboratory*
*Annamalai Universlty*
*Annamalainagar, South India*

1) Abegg, *Ann. Physik.*, **60**, 54 (1897).
2) Abegg and Seitz, *Z. physik. Chem.*, **29**, 242 (1899).
3) Walden, ibid., **70**, 569 (1909).
4) Tangl, *Ann. Physik.*, **26**, 59 (1908).
5) Lowry and Jessop, *Trans. Chem. Soc.*, 782 (1930).
6) Akerlöf, *J. Am. Chem. Soc.*, **54**, 4125 (1932).
7) Smyth and Hitchcock, ibid., **54**, 4631 (1932).

## *Synthesis of Antimycic Acid Methyl Ester Methyl Ether*

By Shigeo Okumura, Mitsuo Masumura, Tokunaru Horie and F. M. Strong*

(Received September 22, 1958)

The structure of antimycic acid was shown to be *N*-(3-aminosalicyloyl)-L-threonine by Strong and co-workers[1,2]. Dembro and Okumura have been trying to synthesize this acid without success[3].

Recently, the synthesis of both L- and DL-antimycic acid methyl ester methyl ether (VIb) has been achieved by us by the following process.

3-Nitrosalicylic acid methyl ether (I), m. p. 195~196°C[4], was prepared by hydrolysis with sodium hydroxide after methylation of 3-nitrosalicylic acid with diazomethane. I was refluxed with thionyl chloride to give the chloride (II) which was condensed with DL-threonine to obtain *N*-(3-nitro-2-methoxybenzoyl)-DL-threonine (IIIa) in 89% yield, m. p. 144.5~145.5°C. (*Anal.* Found: N, 9.38. Calcd. for $C_{12}H_{14}O_7N_2$: N, 9.39%). Prolonged methylation of IIIa with diazomethane gave 87% yield of methyl ester of IIIa, m.p. 92.5~93.5°C. (*Anal.* Found: N, 9.17. Calcd. for $C_{13}H_{16}O_7N_2$: N, 8.98%). IIIa was boild with in acetic anhydride to give 85% yield of *N*-(-3-nitro-2-methoxybenzoyl)-aminocrotonic azlactone (IV), m. p. 175~176°C. (*Anal.* Found: N, 10.70. Calcd. for $C_{12}H_{10}O_5N_2$: N, 10.68%). IIIa was catalyticaly reduced in methanol solution with palladium-carbon to obtaln *N*-(3-amino-2-methoxybenzoyl)-DL-threonine (Va), in 98% yield, m. p. 163~164°C. (*Anal.* Found: N, 10.53. Calcd. for $C_{12}H_{16}O_5N_2$: N, 10.45%). Prolonged methylation of this product with diazomethane gave *N*-(3-amino-2-methoxybenzoyl)-DL-threonine methyl ester (VIa), in 60% yield, m. p. 128.5~129.5°C. (*Anal.* Found: N, 9.92. Calcd. for $C_{13}H_{18}O_5N_2$: N, 9.93%), which was also prepared by catalytic reduction of the methyl ester of IIIa with palladium-carbon in methanol in 91% yield.

II was condensed with L-threonine to obtain the oily *N*-(3-nitro-2-methoxybenzoyl)-L-threonine (IIIb), which gave *N*-(3-amino-2-methoxybenzoyl)-L-threonine, (antimycic acid methyl ether) (Vb) by prolonged catalytic reduction in methanol with palladium-carbon, in 83% yield, m. p. 123.5~124.5°C, $[\alpha]_D^{28°}+14°$ (c 1.82, alcohol). (*Anal.* Found: N, 10.28. Calcd. for $C_{12}H_{16}O_5N_2$: N, 10.45%). Vb was methylated in methanol with diazomethane to obtain 78% yield of *N*-(3-amino-2-methoxybenzoyl)-L-threonine methyl ester, (Antimycic acid methyl ester methyl ether) (VIb) m. p. 155~156°C, $[\alpha]_D^{29°}+10°$ (c 2.05, alcohol). (*Anal.* Found: C, 55.27; H, 6.54; N, 10.09. Calcd. for $C_{13}H_{18}O_5N_2$: C, 55.32; H, 6.43; N, 9.93%).

A sample of antimycic acid methyl ester methyl ether, m. p. 155~156°C, obtained by methylation of natural antimycic acid in methanol with diazomethane, showed no depression of m. p. when mixed with VIb, and neither the infrared nor the ultraviolet spectra showed any significant difference between the two substances. Va or Vb was boiled in acetic anhydride with pyridine to give respectively 84% or 78% yield of *N*-(3-acetamino-2-methoxybenzoyl)-aminocrotonic azlactone (VII), m. p. 136.5~137.5°C. (*Anal.* Found: N, 10.45. Calcd. for $C_{14}H_{14}N_4O_2$: N, 10.22%), which gave by prolonged hydrolysis with 0.08 N sodium hydroxide 73% yield of *N*-(3-acetamino-2-methoxybenzoyl)-aminocrotonic acid (VIII), m. p. 195.5~196.5°C. (*Anal.* Found: N, 9.66. Calcd. for $C_{14}H_{16}O_5N_2$: N, 9.59%), as described previously for antimycic acid itself by Strong[1,2].

*Department of Applied Chemistry*
*Faculty of Engineering*
*University of Tokushima*
*Tokushima*

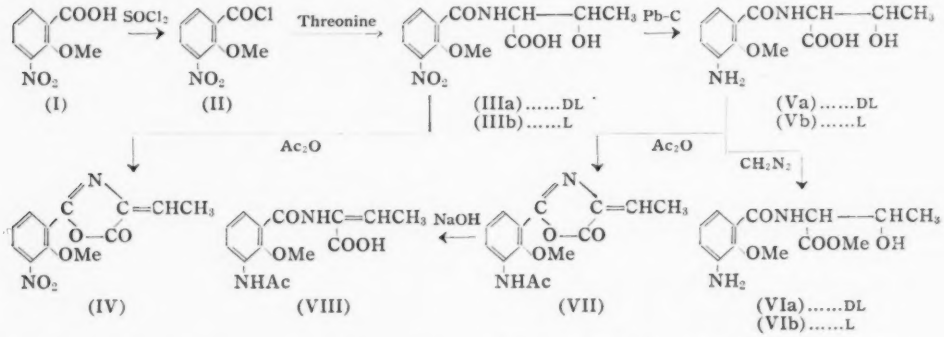


* Present Address, Department of Biochemistry, University of Wisconsin, Medison 6, Wisconsin, U. S. A.

1) G. M. Tener, F. M. Bumpus, B. R. Dunshee and F. M. Strong, *J. Am. Chem. Soc.*, **75**, 1100 (1953).

2) G. M. Tener, E. E. van Tamelen and F. M. Strong, ibid., **75**, 3623 (1953).

3) Unpublished work at Wisconsine University.

4) J. F. Simpnsen and M. G. Rau, *J. Chem. Soc.*, **111**, 220 (1917).

5) Eastman Organic Chemicals.